AD-A141 793 STATOR BLADE ROW GEOMETRY MODIFICATION INFLUENCE ON TWO-STAGE AXIAL-FLOW..(U) IOWA STATE UNIV AMES ENGINEERING RESEARCH INST D L TWEEDT ET AL. DEC 83 1/3

UNCLASSIFIED ISU-ERI-AMES-84179 AFOSR-TR-84-0418 F/G 21/5 NL

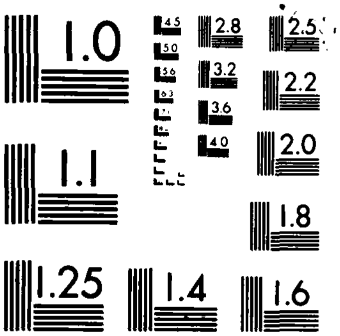


MICROCOPY RESOLUTION TEST CHART
NATIONAL BUREAU OF STANDARDS 1963-A

AFOSR-TR- 84-0418

AD-A141 793

DTIC FILE COPY

D. L. TWEEDT
T. H. OKIISHI

DECEMBER 1983

# STATOR BLADE ROW GEOMETRY MODIFICATION INFLUENCE ON TWO-STAGE, AXIAL-FLOW COMPRESSOR AERODYNAMIC PERFORMANCE

TURBOMACHINERY
COMPONENTS RESEARCH PROGRAM

ENGINEERING RESEARCH INSTITUTE
IOWA STATE UNIVERSITY
AMES IOWA USA

ISU-ERI-Ames-84179
TCRL-25
ERI Projects 1394, 1490, 1645



84 05 30 056

ENGINEERING
RESEARCH

ENGINEERING
RESEARCH

ENGINEERING
RESEARCH

ENGINEERING
RESEARCH

ENGINEERING
RESEARCH

TECHNICAL REPORT

# STATOR BLADE ROW GEOMETRY MODIFICATION INFLUENCE ON TWO-STAGE, AXIAL-FLOW COMPRESSOR AERODYNAMIC PERFORMANCE



Daniel L. Tweedt
Theodore H. Okiishi
December 1983

ISU-ERI-Ames-84179
TCRL-25
ERI Projects 1394, 1490, 1645

DEPARTMENT OF MECHANICAL ENGINEERING
ENGINEERING RESEARCH INSTITUTE
IOWA STATE UNIVERSITY, AMES

## REPORT DOCUMENTATION PAGE

READ INSTRUCTIONS BEFORE COMPLETING FORM

**1. REPORT NUMBER:** AFOSR-TR- 84-0418

**2. GOVT ACCESSION NO.:** AD-A141 793

**3. RECIPIENT'S CATALOG NUMBER:**

**4. TITLE (and Subtitle):** Stator Blade Row Geometry Modification Influence on Two-Stage, Axial-Flow Compressor Aerodynamic Performance

**5. TYPE OF REPORT & PERIOD COVERED:** Technical Report 1 October 1978 - 30 April 1983

**6. PERFORMING ORG. REPORT NUMBER:** TCRL-25

**7. AUTHOR(s):** Daniel L. Tweedt and Theodore H. Okiishi

**8. CONTRACT OR GRANT NUMBER(s):** F49620-83-K-0023

**9. PERFORMING ORGANIZATION NAME AND ADDRESS:** Engineering Research Institute/Mechanical Engineering Department Turbomachinery Components Research Laboratory, Iowa State University, Ames, Iowa 50011

**10. PROGRAM ELEMENT, PROJECT, TASK AREA & WORK UNIT NUMBERS:** 61102F 2307/A4

**11. CONTROLLING OFFICE NAME AND ADDRESS:** Air Force Office of Scientific Research Directorate of Aerospace Sciences (AFOSR/NA) Bldg. 410, Bolling AFB, D.C.

**12. REPORT DATE:** December 1983

**13. NUMBER OF PAGES:** 243

**14. MONITORING AGENCY NAME & ADDRESS (if different from Controlling Office):**

**15. SECURITY CLASS. (of this report):** Unclassified

**15a. DECLASSIFICATION/DOWNGRADING SCHEDULE:**

**16. DISTRIBUTION STATEMENT (of this Report):**

Approved for Public Release; Distribution Unlimited

**17. DISTRIBUTION STATEMENT (of the abstract entered in Block 20, if different from Report):**

**18. SUPPLEMENTARY NOTES:**

**19. KEY WORDS (Continue on reverse side if necessary and identify by block number):**

axial-flow turbomachinery
axial-flow compressor
stator

**20. ABSTRACT (Continue on reverse side if necessary and identify by block number):**

The influence of stator row geometry modification on the aerodynamic performance of a two-stage, low-speed, axial-flow research compressor was assessed in the experiments described in this project.

Stator geometry modifications tested included stator leading edge forward symmetrical sweep, large-radius blade/annulus wall corner fillets, and stator hub gap sealing (shrouding).

(continued)

20. Abstract. (continued)

Comparisons were made between detailed aerodynamic data associated with baseline and modified configurations. Substantial stator exit flow-field changes attributable to symmetrical sweeping of stator leading edges and to hub clearance sealing were observed with some evidence of corresponding near end wall loss reduction. The effects of large radii filleting were less clear.

Interesting conclusions about the off-design flow rate performance of the compressor also resulted from consideration of experimental data.

TABLE OF CONTENTS

# SYMBOLS AND NOTATION

| | |
|---|---|
| $A$ | compressor flow passage annulus area, $m^2$ |
| $A_v$ | venturi flow passage area, $m^2$ |
| $c$ | blade chord length, m |
| FCC | comparison of integrated and venturi flow coefficients (Eq. 10.34), percent |
| $g$ | local acceleration of gravity, $m/s^2$ |
| $H$ | total head with respect to barometric pressure (Eq. 10.5) N-m/kg |
| $h$ | static head with respect to barometric pressure, N-m/kg |
| $h_{hg}$ | barometric pressure, m of Hg |
| $h_w$ | casing static head with respect to barometric pressure (Eq. 10.9), N-m/kg |
| $i$ | incidence angle (Fig. 10.1), degrees |
| $P_{atm}$ | barometric pressure (Eq. 10.1), $N/m^2$ |
| $P_t$ | total pressure with respect to barometric pressure, m of water |
| $P_v$ | venturi static pressure with respect to barometric pressure, m of water |
| $P_w$ | casing static pressure with respect to barometric pressure, m of water |
| PHH | percent passage height from hub (Eq. 10.4), percent |
| $Q_a$ | integrated volumetric flow rate at probe-traversing measurement stations (Eq. 10.32), $m^3/s$ |
| $Q_v$ | venturi volumetric flow rate (Eq. 10.30), $m^3/s$ |
| $R$ | gas constant, N-m/(kg-°K) |
| $r$ | radius from compressor axis, m |
| RPM | rotor rotational speed, rpm |
| $S$ | circumferential space between blade camber lines, degrees |

| | |
|---|---|
| $T$ | compressor drive-shaft torque, N-m |
| $t$ | temperature, °K |
| $t_{baro}$ | barometer ambient temperature, °K |
| $t_{max}$ | blade section maximum thickness, m |
| $U$ | rotor blade velocity (Eq. 10.14), m/s |
| $V$ | absolute fluid velocity (Fig. 10.1; Eq. 10.12), m/s |
| $V'$ | relative fluid velocity (Eq. 10.21), m/s |
| $V_y$ | tangential component of absolute fluid velocity (Eq. 10.17), m/s |
| $V'_y$ | tangential component of relative fluid velocity (Eq. 10.19), m/s |
| $V_z$ | axial component of fluid velocity (Eq. 10.15), m/s |
| $Y$ | circumferential traversing position, degrees |
| $\beta_y$ | absolute flow angle with respect to axial direction (Fig. 10.1), degrees |
| $\beta'_y$ | relative flow angle with respect to axial direction (Fig. 10.1; Eq. 8.23), degrees |
| $\gamma_{H_2O}$ | specific weight of water manometer fluid (Eq. 10.3), $N/m^3$ |
| $\gamma_{hg}$ | specific weight of mercury, $N/m^3$ |
| $\Delta P_v$ | pressure differential across venturi, m of water |
| $\Delta Y_{fs}$ | freestream region in the circumferential space between blades, degrees |
| $\delta$ | deviation angle (Fig. 10.1), degrees |
| $\eta$ | hydraulic efficiency (Eqs. 10.42, 10.43, and 10.44) |
| $\eta_m$ | mechanical efficiency (Eq. 10.54) |
| $\kappa$ | blade angle, angle between tangent to blade camber line and axial direction (Fig. 10.1), degrees |
| $\rho$ | density of air (Eq. 10.2), $kg/m^3$ |

| | |
|---|---|
| $\sigma$ | blade row solidity |
| $\phi$ | venturi flow coefficient (Eq. 10.31) |
| $\bar{\phi}$ | circumferential-mean flow coefficient (Eq. 10.29) |
| $\phi_a$ | integrated flow coefficient at probe-traversing measurement stations (Eq. 8.33) |
| $\psi$ | head-rise coefficient (Eqs. 10.36 through 10.41 and 10.51, 10.52, 10.53) |
| $\omega$ | total-head loss coefficient (Eqs. 10.45 and 10.46) |

Subscripts

| | |
|---|---|
| h | annulus inner surface, hub |
| i | ideal |
| m | mechanical |
| overall | overall compressor |
| R | rotor |
| S | stator |
| stage | stage |
| t | annulus outer surface, tip |
| v | venturi |
| 1 | blade-row inlet |
| 2 | blade-row outlet |
| 1R | first rotor |
| 2R | second rotor |
| 1S | first stator |
| 2S | second stator |

## Superscripts

| | |
|---|---|
| $'$ | relative to rotor |
| $\bar{}$ | average; blade-to-blade circumferential-average |
| $\dot{\bar{}}$ | radial mass-average |
| $=$ | cross-section average |

# LIST OF FIGURES

# LIST OF TABLES

# 1. INTRODUCTION

The fluid flow viscous losses occurring in production axial-flow turbomachines continue to challenge designers. Even seemingly small gains in aerodynamic efficiency are vigorously sought by manufacturers to remain competitive. Better management of the complicated flows in end wall regions of the blade rows of a turbomachine is one example of a specific improvement goal.

A low speed research compressor can be a useful tool in this quest for improved performance. In particular, viscous phenomena may be ascertained in considerable detail, and a variety of builds designed to result in improved flows can be tried somewhat economically.

This report is about research initiated to provide a clearer understanding of the potential for better managing the end-wall flows in an axial-flow compressor. More specifically, the use of stator geometry modification (blade shape and end-wall fillets and/or sealing) to improve stage performance was explored.

Two kinds of stator blades were used. A baseline stator, conventional in geometry, provided baseline data against which to compare data for other stator geometries. A modified stator featuring forward symmetrical sweep of the leading edge from mid-span to the inner and outer annulus walls was also utilized.

Both large and small blade/end-wall corner fillets were tested in the second stage stator row of the compressor with the modified stator blades. This investigation into the influence of large corner-fillets on end-wall flows also supplied data on the effects of sealing a stator/stationary end-wall clearance gap. These sealing effects were further investigated with the baseline stators.

# 2. RESEARCH COMPRESSOR EXPERIMENTAL FACILITY

The axial-flow research compressor and data acquisition system of the Iowa State University Engineering Research Institute/Mechanical Engineering Department Turbomachinery Components Research Laboratory that were used to accomplish the experimental research outlined in this report are briefly described in this section. More comprehensive and detailed information about this equipment is provided by Hathaway and Okiishi [1].

## 2.1. Axial-Flow Research Compressor

The two-stage axial-flow research compressor rig (see Figure 2.1) of the Turbomachinery Components Research Laboratory was used in the aerodynamic performance testing of four different compressor builds. These builds consisted of the same rotor blade rows and two kinds of stator blade rows, namely, baseline and modified. The rotor and baseline stator blades were designed to be representative of typical transonic compressor blades in terms of high reaction stages, axially discharging stators, and the absence of inlet guide vanes. A uniform spanwise distribution of total pressure was prescribed for each rotor exit. The blade section profiles used for all blades were double circular arc, and were considered conventional and appropriate for the low-speed testing involved. The two-stage compressor design data are summarized in Table 2.1.

The modified stator blades, as already mentioned, featured forward symmetrical sweep of each stator leading edge from mid-span

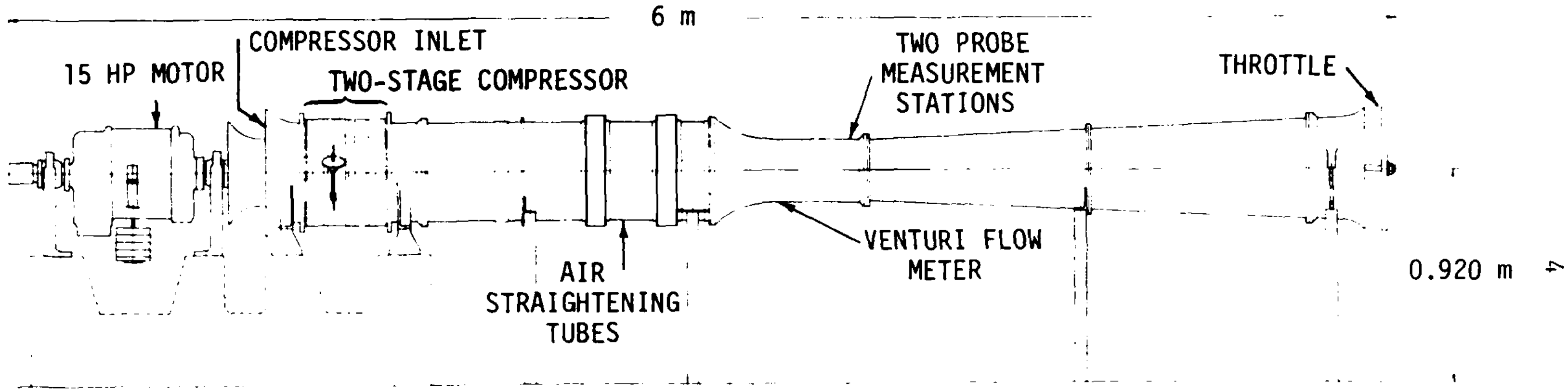


Figure 2.1 Schematic of research compressor.

Table 2.1. Summary of two-stage compressor design data.

| | |
|---|---|
| Rotor speed | 2400 rpm |
| Flow rate | 5.25 $lb_m$/s (2/38 kg/s) |
| Pressure ratio | 1.019 |
| Number of blades | |
| Rotor | 21 |
| Stator | 30 |
| Blade material | fiberglass with steel trunnion and spine |
| Blade aerodynamic chord | 2.30 in. (6.07 cm) constant for rotor and baseline stator |
| | 2.38 in. to 3.03 in. (6.04 to 7.70 cm) for modified stator |
| Blade section profile | double circular arc |
| Blade stacking axis location | radial line through center of gravity of blade sections for rotor and baseline stator blades |
| | radial line through blade section trailing edge circle centers for modified stator blade |
| Leading and trailing edge radius to aerodynamic chord ratio | 0.01 constant |
| Maximum thickness to aerodynamic chord ratio | 0.10 to 0.06 linear variation from blade root to other end of blade span |
| Annulus flow path | |
| Hub radius | 5.60 in. (14.22 cm) constant |
| Tip radius | 8.00 in. (20.32 cm) constant |

to the inner and outer annulus walls. The baseline and modified stator blade geometries are compared in Table 2.2, and some representative blade section profiles for the baseline and modified rotor and stator blades are shown in Figures 2.2, 2.3, and 2.4, respectively. The baseline rotor and stator blade designs are discussed in more detail by Hathaway and Okiishi [1]. The modified stator blade design details are summarized in Appendices A and B. All blades were manufactured as described by Hathaway and Okiishi [1], with clearances between blade extremities and the casing (for rotor blades) and hub (for stator blades) kept constant at 0.034 inches (0.864 mm) (1.4 percent span) by precision grinding of blade tips to appropriate radii with the blades mounted in place.

The four different compressor builds consisted of two baseline stator builds, namely, baseline 1 and baseline 2, and two modified stator builds, modified 1 and modified 2. The two builds with each kind of stator blade geometry (baseline and modified) differed only in the second stage stator row, as indicated in Table 2.3. A meridional plane view of the compressor blading with build features summarized in note form is provided in Figure 2.5. The large corner fillets used in the second stage stator row of the modified 2 build involved a radius of 0.25 inches. All small corner fillets were made as small as was practical.

Table 2.2. Comparison of stator blade geometries.

Similarities between Baseline and Modified Stator Blades

- Number of blades per row
- Blade surface finish
- Mid-span chord length
- Spanwise distribution of maximum thickness to chord ratios

Differences between Baseline and Modified Stator Blades

| Baseline | Modified |
|---|---|
| Stacking point at center of gravity | Stacking point at trailing edge circle center |
| No leading edge sweep | Symmetrical leading edge forward sweep |
| Constant spanwise distribution of chord length | Varying spanwise distribution of chord length |

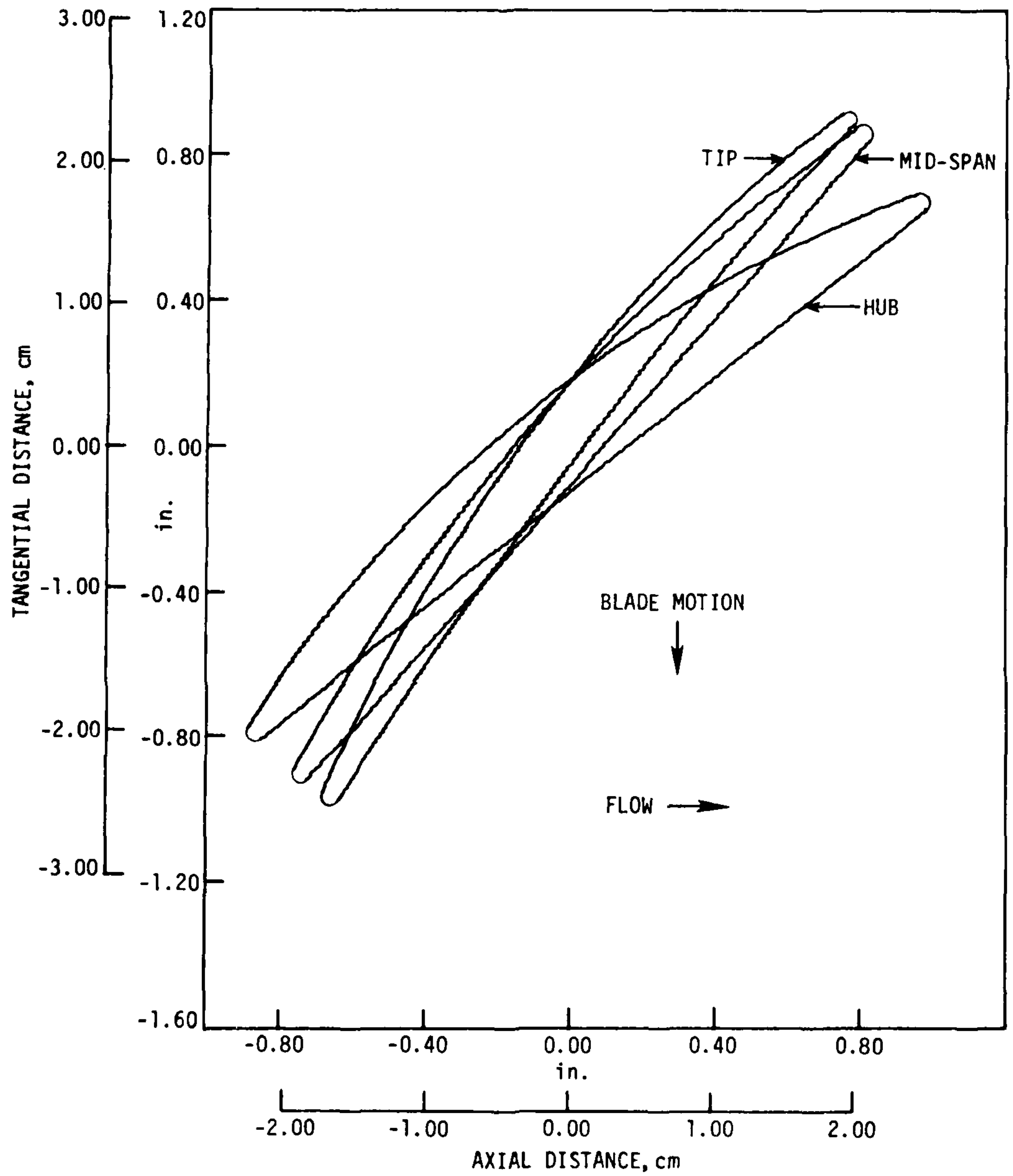


**Figure 2.2.** Representative compressor rotor blade sections (same for baseline and modified builds).

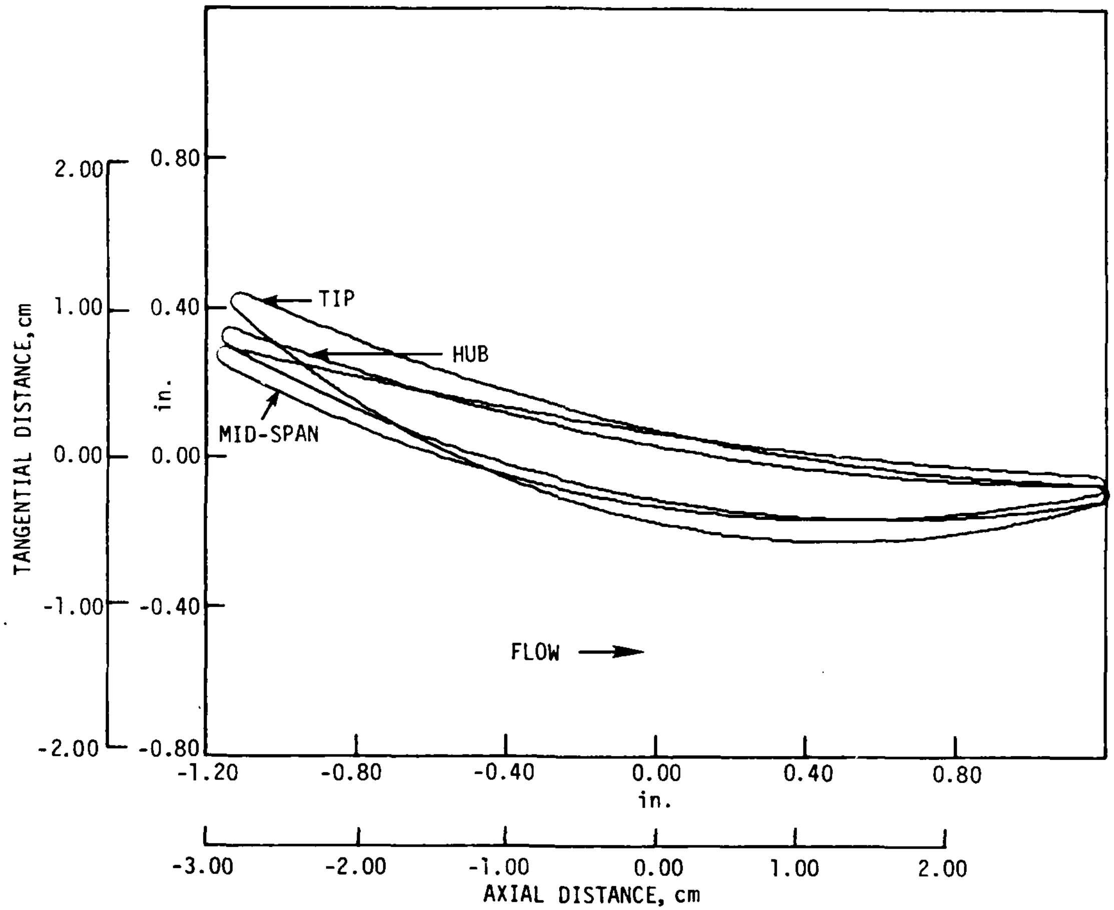


**Figure 2.3** Representative baseline stator blade sections.

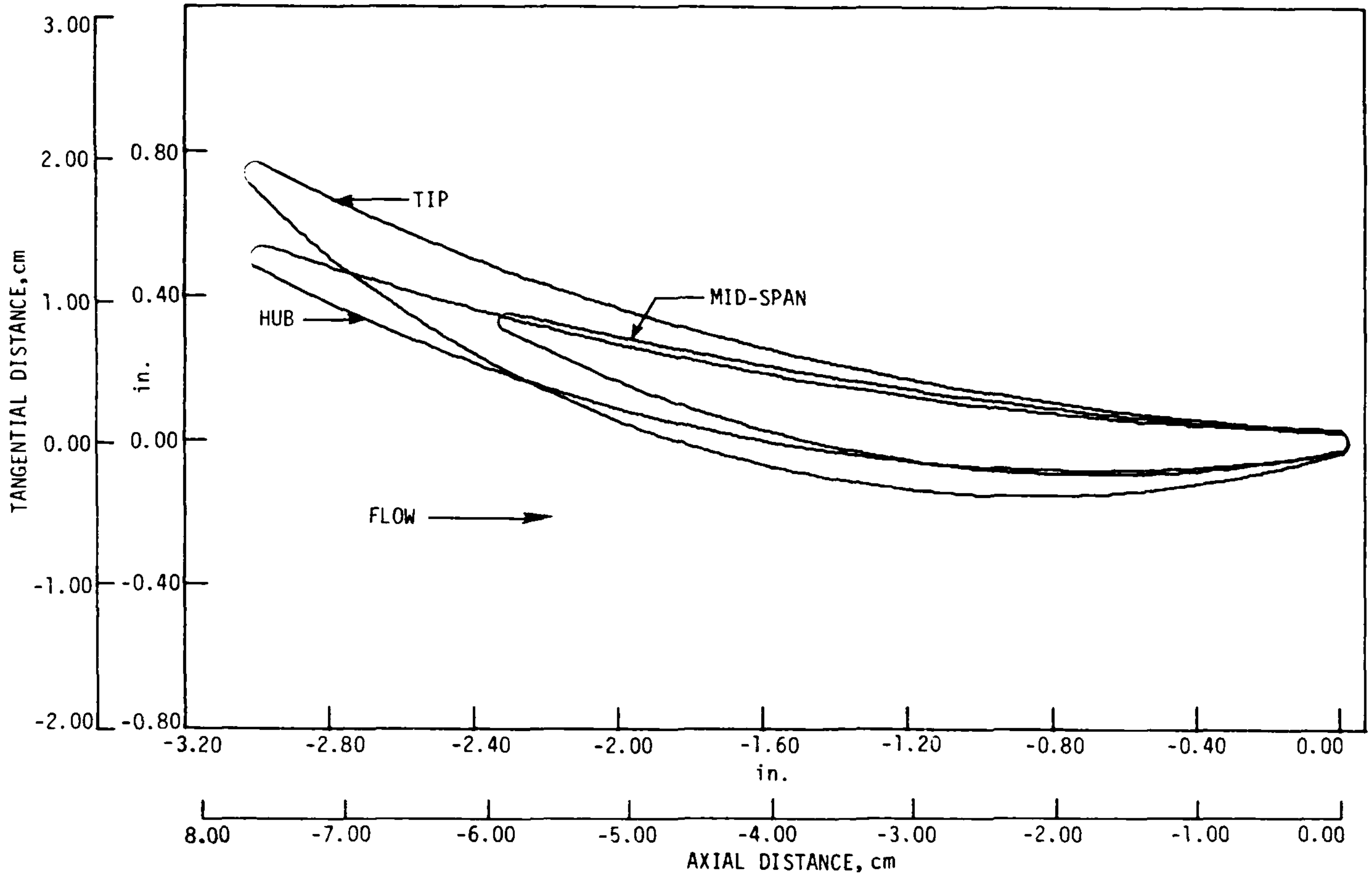


Figure 2.4 Representative modified stator blade sections.

Table 2.3. Comparison of compressor builds.

| Baseline 1 | Baseline 2 | Modified 1 | Modified 2 |
|---|---|---|---|
| baseline rotor blade rows | baseline rotor blade rows | baseline rotor blade rows | baseline rotor blade rows |
| small corner fillets at inner endwall for first and second stage rotor blade rows | small corner fillets at inner endwall for first and second stage rotor blade rows | small corner fillets at inner endwall for first and second stage rotor blade rows | small corner fillets at inner endwall for first and second stage rotor blade rows |
| clearance between first stage stator blade tips and rotating inner endwall | clearance between first stage stator blade tips and rotating inner endwall | clearance between first stage stator blade tips and rotating inner endwall | clearance between first stage stator blade tips and rotating inner endwall |
| clearance between second stage stator blade tips and stationary inner endwall | shrouded second stage stator--small corner fillets at inner endwall | clearance between second stage stator blade tips and stationary inner endwall | shrouded second stage stator--large corner fillets at inner endwall |

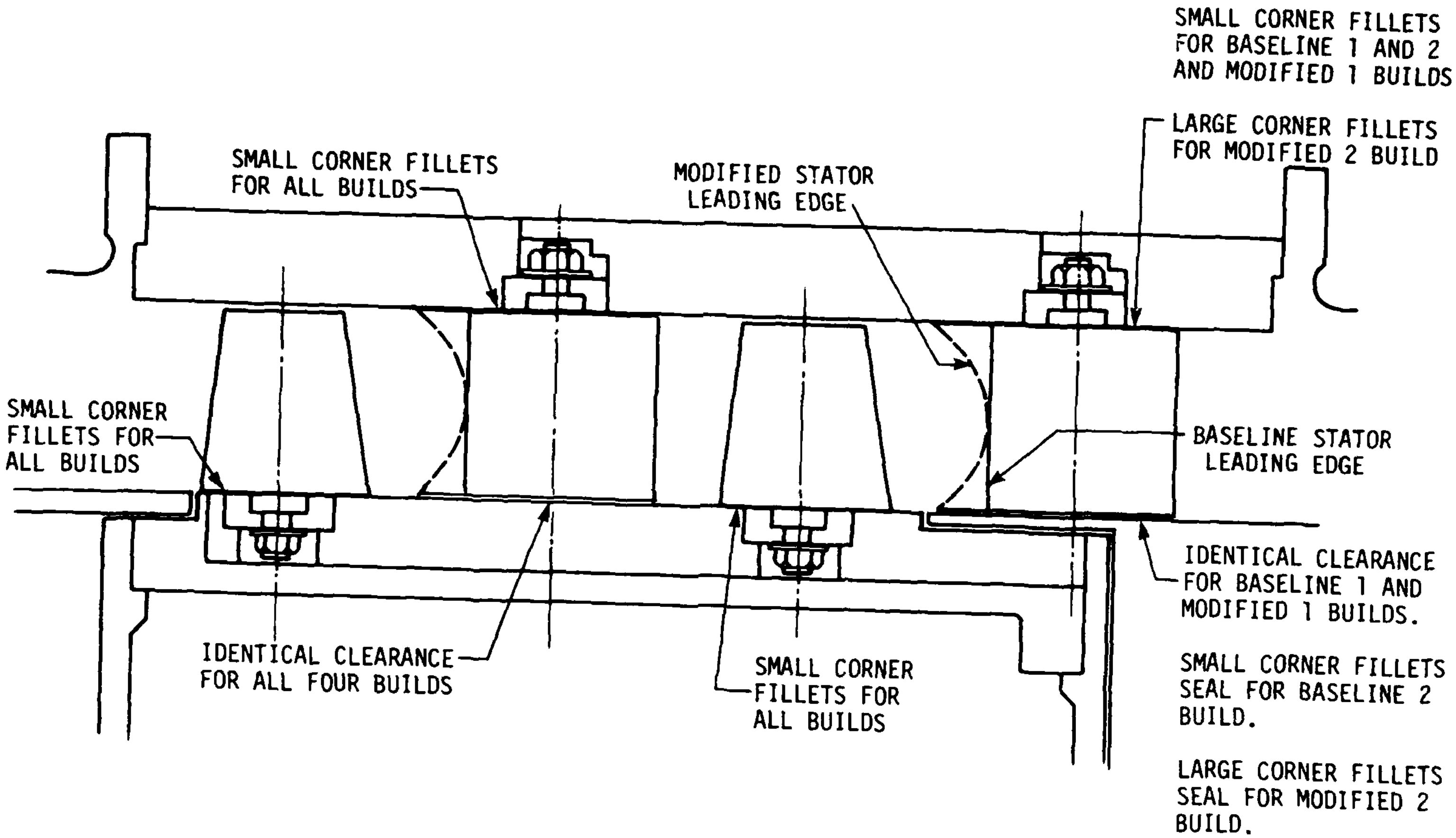


Figure 2.5 Meridional plane view of compressor blading.

## 2.2. Data Acquisition System

The data acquisition system included the following basic items:

- Slow-response pressure instrumentation
- Probe and stator blade row actuators
- Scanivalve system
- Venturi flow meter
- Temperature instrumentation
- Compressor drive-shaft torque measurement device
- Computer control system
- Oscilloscope (Tektronix type R546B with type 3A7 Differential Comparator and type 3A1 Dual-Trace Amplifier)

The slow-response pressure instrumentation included a cobra probe (United Sensor type CA-120-24-F-18-CD), a Kiel probe (United Sensor type KBC-24-L-22-W), casing static pressure taps, and a mercury-in-glass barometer (Princo Instruments model B-222). The probes were immersed and yawed with a probe actuator (L. C. Smith Company model BBS-3180) controlled by a control indicator (L. C. Smith Company model DI-3R) and switchbox (L. C. Smith Company model DI-3R-SB4). The measurement station locations are shown in Figure 2.6.

A scanivalve pressure-port selector system (Scanivalve Company model 48D3-1016) including a strain-gauge pressure transducer (Scanivalve Company model PDCR22), solenoid drive (Scanivalve Company model DS3-48) and control (Scanivalve Company model CTLR2/S2-S6), a signal conditioner (Endevco model 4470), and an amplified bridge

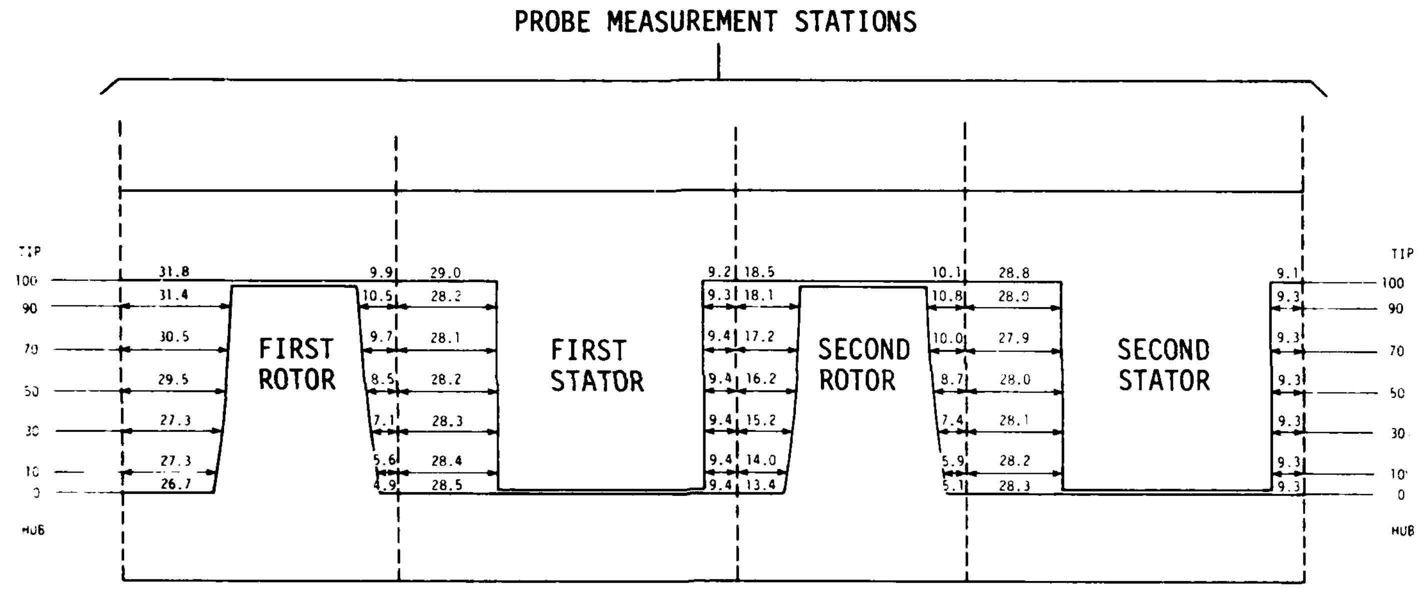


Figure 2.6 Schematic showing axial location of probe measurement stations relative to adjacent blade rows (dimensions in mm).

circuit conditioner (Endevco model 4476.2A) were used to acquire all pressure measurements.

Temperature measurements were acquired using a solid-state thermocouple reference junction (Pace Engineering Company model LRJ49-8TT) with copper-constantan thermocouples.

A desk top computer (Commodore PET model 2001-32) and digital voltmeter (Hewlett Packard model 3455A) were used in combination with a multiple channel voltage scanner (Hewlett Packard model 3495A) to control the data acquisition process.

A schematic illustrating how these components interacted with each other appears in Figure 2.7.

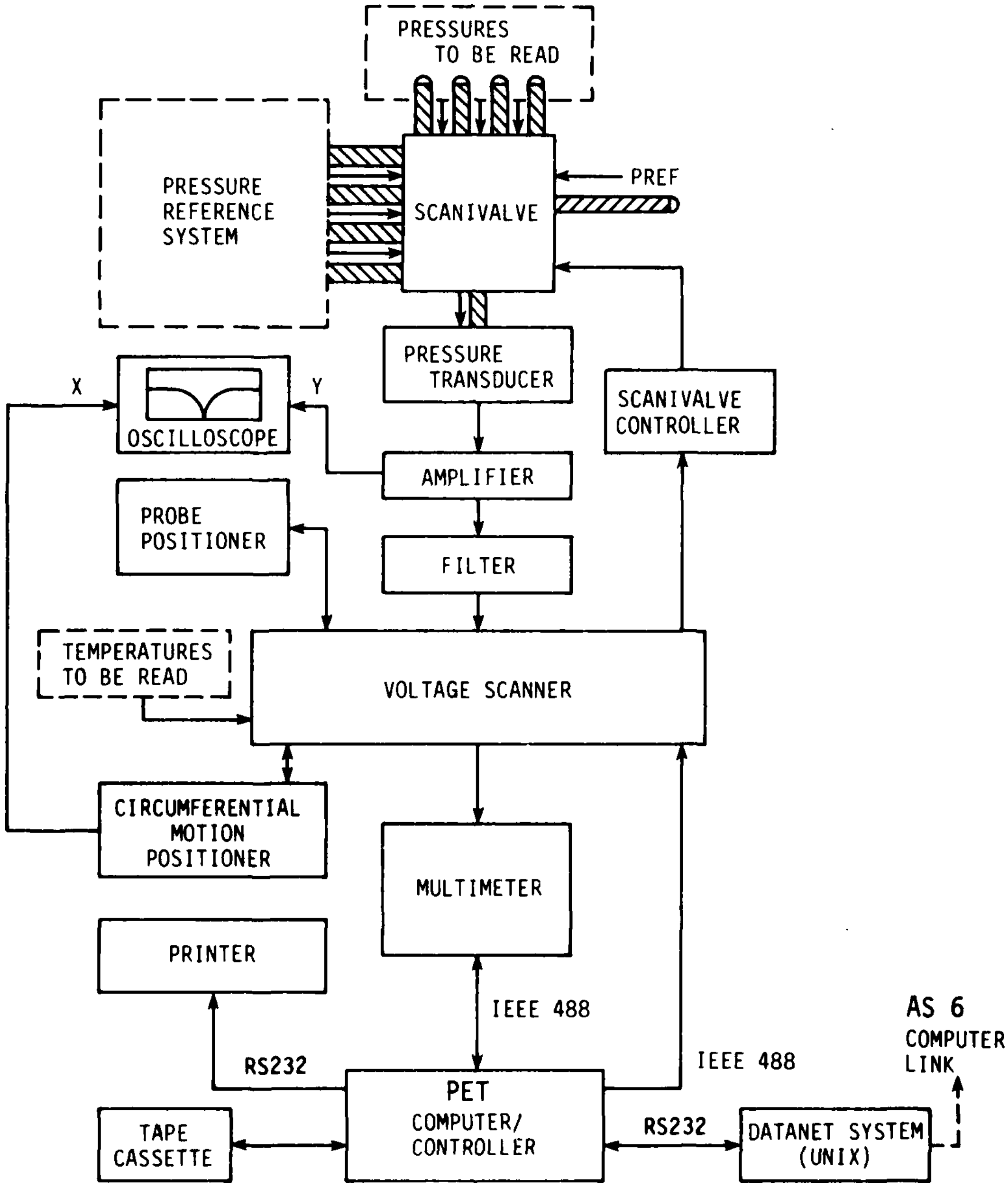


Figure 2.7 Schematic of data acquisition system.

# 3. EXPERIMENTAL PROCEDURE AND DATA REDUCTION

Involved with the present experiment were the following specific goals:

- Construct overall performance maps for the baseline 1 and modified 1 compressor builds
- Establish from these performance maps a flow rate at which to obtain detailed flow-field data for the four different compressor builds
- Test the four compressor builds at the selected flow rate (operating point) in order to obtain detailed time-average total-pressure and flow angle data at each blade row inlet and exit station
- Track the first stage stator wake flow through the second stage rotor

Details involved in attaining these goals are summarized below. More complete information about the calibration procedures involved is provided in Reference 1.

## 3.1. Calibration

The equipment calibrations necessary before and during data acquisition were as follows:

- Probe and stator blade row actuator position/potentiometer voltage calibrations (probe yaw angle and immersion position and stator blade row circumferential position)

- Pressure-transducer calibrations (on-line using the pressure reference system described in Reference 2)
- Shaft torque measurement device (torque meter) calibrations
- Thermocouple calibrations using a mercury-in-glass thermometer

The Kiel and cobra probes were positioned immersion-wise relative to their respective actuators with a depth micrometer. The cobra probe zero yaw angle position was ascertained by "nulling" the probe side port pressures with the probe immersed in a stream of air from a flow nozzle, with the actuator mounted at right angles to the nozzle flow direction. The Kiel probe was also tested in the nozzle flow where it could accurately measure total pressure within an angular range of as much as ±45 degrees from the actual flow direction. After these probes were adjusted and calibrated, appropriate constants were entered into the data acquisition computer programs [1].

On-line pressure-transducer calibration was accomplished using a pressure reference system [2] consisting of several water columns of differing heights and triple-beam balances. This system provided four reference pressures against which the pressure transducer could be calibrated. Calibration of the pressure transducer consisted of a linear least-squares correlation of transducer output voltage versus the known reference column pressures. The reference column pressures were determined with a resolution of 0.003 inches (0.076 mm) of water or better from linear least-squares correlation equations which were determined from a periodic (about three month intervals) calibration of column pressure versus column weight. Therefore, it was necessary to only weigh each column prior to testing in order to determine the reference column pressures. Each column pressure and transducer voltage recorded was referenced to one of the columns, the same column each time. This was done to reduce errors due to thermal drift and other transient errors between successive readings, as well as to insure that the linear transducer correlation went through zero as it should. The above procedure consistently provided a transducer linear correlation coefficient of transducer voltage versus column pressure of 0.99999 or better. The calibration was repeated if this correlation criterion was not met. The pressure trnsducer was repeatedly checked in this manner prior to making any pressure measurements.

An additional water column was used to provide a base pressure to one side of the scanivalve transducer in order to insure that the pressure transducer was always displaced from zero. This eliminated errors from having the transducer pressure fluctuate around zero.

Thermocouples were calibrated against a precise mercury-in-glass thermometer. Since the flow was virtually incompressible, this procedure was sufficiently accurate for the situation involved.

Torque measurements were obtained by floating the drive motor on air bearings and applying a torque counter to the drive-motor torque. The balancing torque was applied by adding discrete weights to a torque arm, with a so-called torque meter being used to resolve the torque arm loads. This meter, employing a load transducer (strain gauge on a cantilevered beam) and accompanying circuitry, was subject to considerable transient drifting, and as such needed periodic recalibration during any measurement sequence. A built-in calibration circuit was used to accomplish this, allowing adjustment to the correct 0 to 1 kg full-scale meter deflection.

## 3.2. Data Acquisition

All measurements were made with slow-response (time-averaging) instrumentation. Testing was done at the design rotor speed of 2400 rpm only, which was maintained with a feed-back electronic control system to within ±1 rpm. Four general measurement procedures were used. The first involved acquisition of overall performance data from which overall performance maps were constructed. With these overall performance data, a single operating point could be selected at which to obtain detailed aerodynamic performance data for the different compressor builds. This detailed performance testing required another two measurement procedures, one associated with the Kiel probe (total pressure) another with the cobra probe (flow angle). The fourth procedure was associated with the first stage stator wake tracking experiment.

As mentioned earlier, the data acquisition system was controlled by a desk-top computer. A separate "data acquisition program" was constructed for each of the first three general measurement procedures mentioned above. Logic diagrams (Figure 3.1) for these are included with the following discussion.

### 3.2.1. Overall Performance Data Acquisition

Three basic types of measurement were involved in this procedure; namely, casing static-pressure, fluid temperature, and drive-shaft

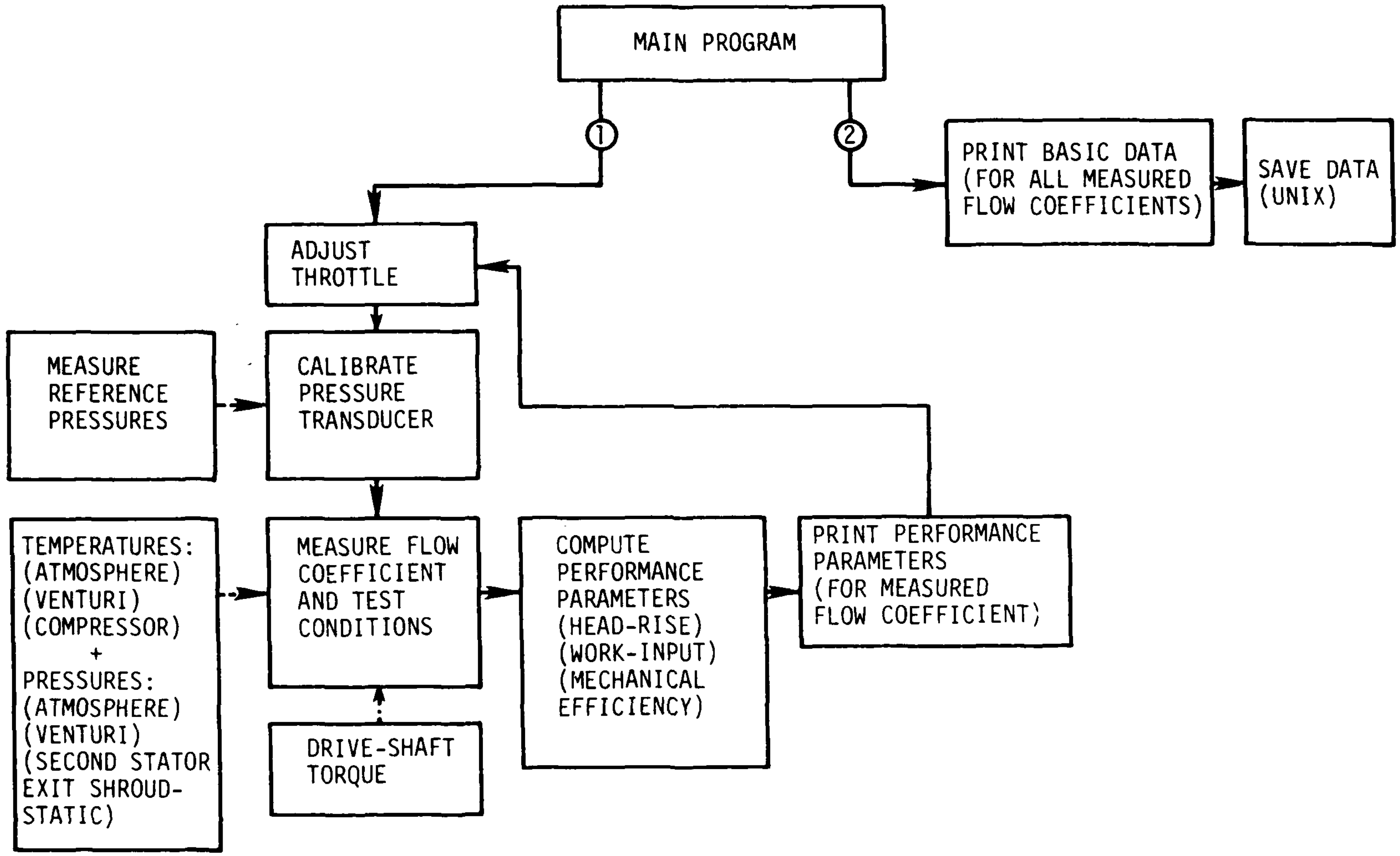


(a) OVERALL PERFORMANCE MEASUREMENT

**Figure 3.1 Logic diagrams for data acquisition.**

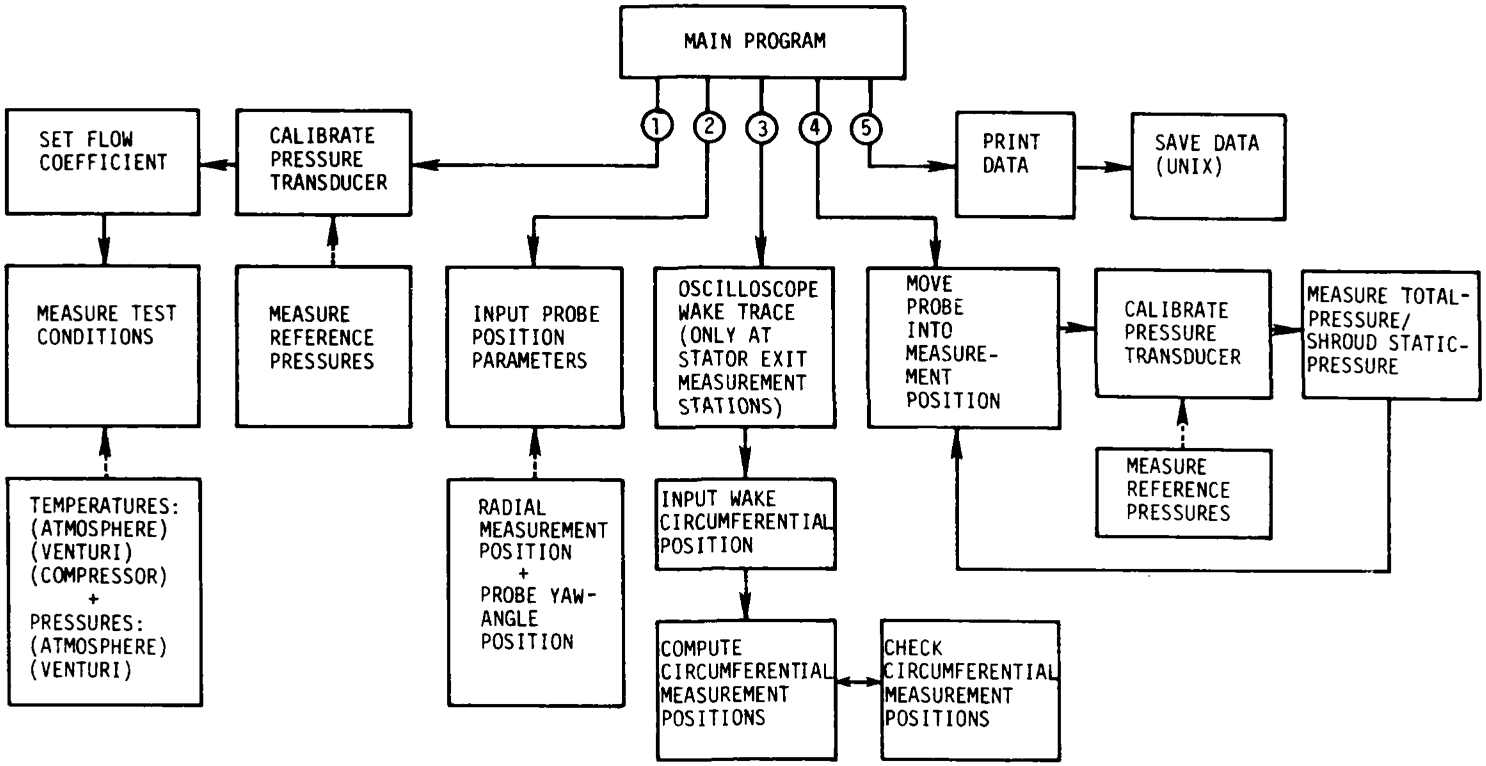


(b) KIEL PROBE (TOTAL PRESSURE) MEASUREMENT

Figure 3.1 continued.

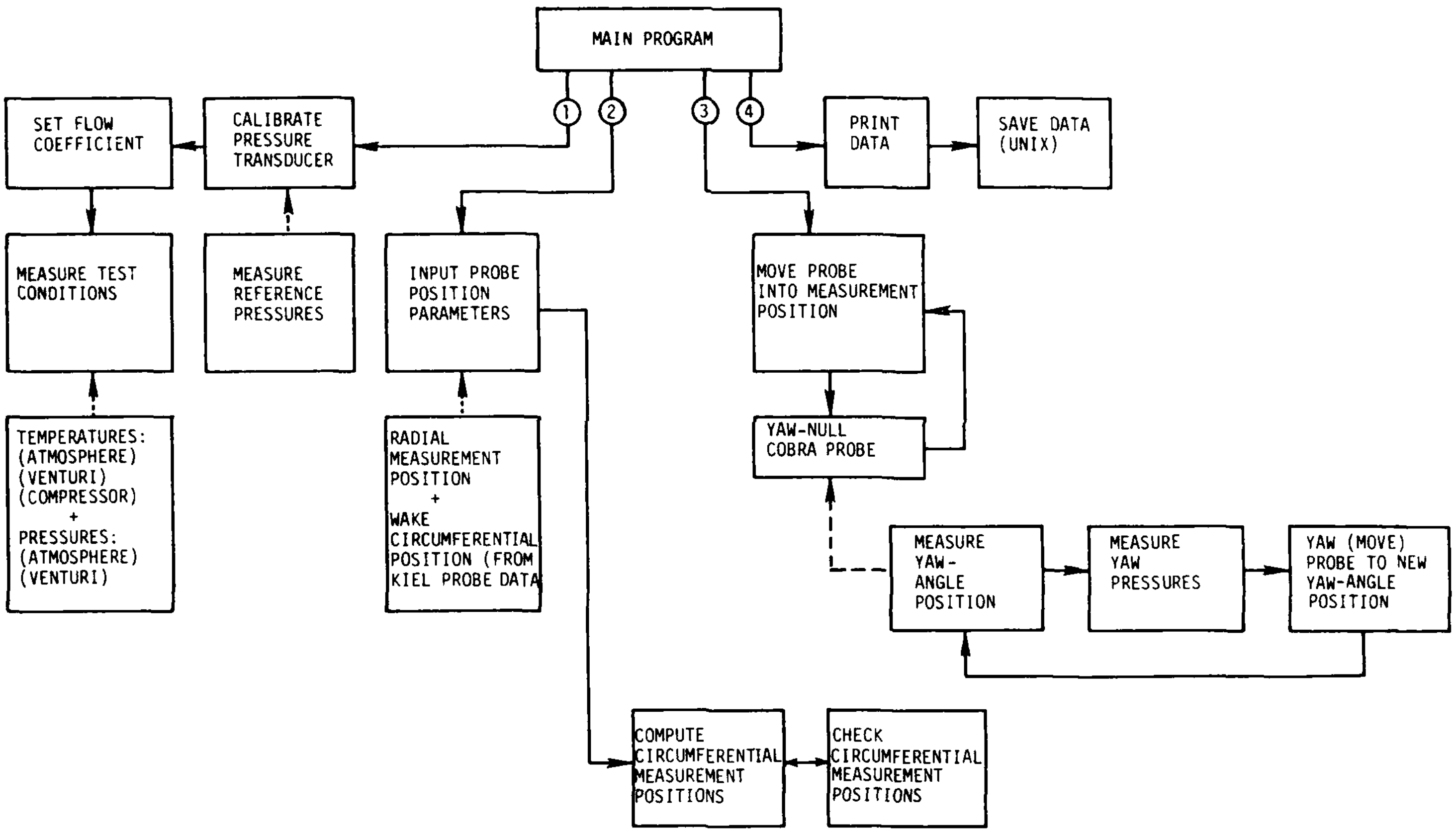


(c) COBRA PROBE (ABSOLUTE FLOW ANGLE) MEASUREMENT

**Figure 3.1 concluded.**

torque. Casing static pressures were obtained both at the venturi meter throat and the second stator exit station. Fluid temperature was measured in the lab, near the compressor inlet and at the venturi throat. The logic diagram for the data acquisition program used to automate this procedure is presented in Figure 3.1(a).

### 3.2.2. Detailed Data Acquisition

Sets of detailed data were acquired at a fixed operating point of the compressor (shaft speed = 2400 rpm and flow coefficient = 0.500). The measurements involved in obtaining these data were total pressure, casing static pressure, and absolute flow angle. Total pressure was measured with a Kiel probe, and absolute flow angle was measured with a cobra probe.

The Kiel probe was set at a fixed yaw angle for any given axial measurement station. This angular setting was not critical since the Kiel probe was capable of measuring total pressure accurately to within ±45 degrees of the actual flow angle. At the compressor inlet and stator exit stations, this setting was approximately 0 degrees while at the rotor exit stations a setting of 25 degrees was used. Qualitative oscilloscope traces of the circumferential variation of total pressure at various span locations were made at the stator exit stations to reveal the stator wake location. This information was used to pack total-pressure data within the stator wake for better wake definition.

At each stator exit measurement station, absolute flow angles could be measured only in the free-stream regions. This was because flow angles could not be measured accurately with a cobra probe in the stator wake because of the large total-pressure gradients there. The logic diagrams for the total-pressure and absolute flow angle data acquisitions programs are presented in Figure 3.1(b) and (c), respectively.

Figure 3.2 depicts, to scale, a cascade representation of the compressor blade rows showing locations of the five axial measurement stations and the circumferential extent of the measurement window at each station. Data were acquired at all five axial stations for a complete set of measurements. Circumferential surveys were made by moving the stator rows circumferentially past the stationary probe. It should be noted that the stator blades of both stator rows were "in line" when viewed along the compressor axis for all measurements.

At all axial stations, data were generally obtained at eight annulus passage height (spanwise) locations, specifically, at 5%, 10%, 30%, 50%, 70%, 80%, 90%, and 95% span from the hub. Circumferential surveys were made over one stator pitch at each spanwise location, with the number of circumferential data points depending on the measurement type (total pressure or flow angle) and the axial station involved. Also, a casing static-pressure data point was taken with each total-pressure data set. The number of circumferential data points per stator pitch were as follows:

- STATION 1: 10 total pressure / 6 flow angle
- STATION 2: 10 total pressure / 6 flow angle
- STATION 3: 25 total pressure / 10 flow angle (free-stream only)
- STATION 4: 20 total pressure / 10 flow angle

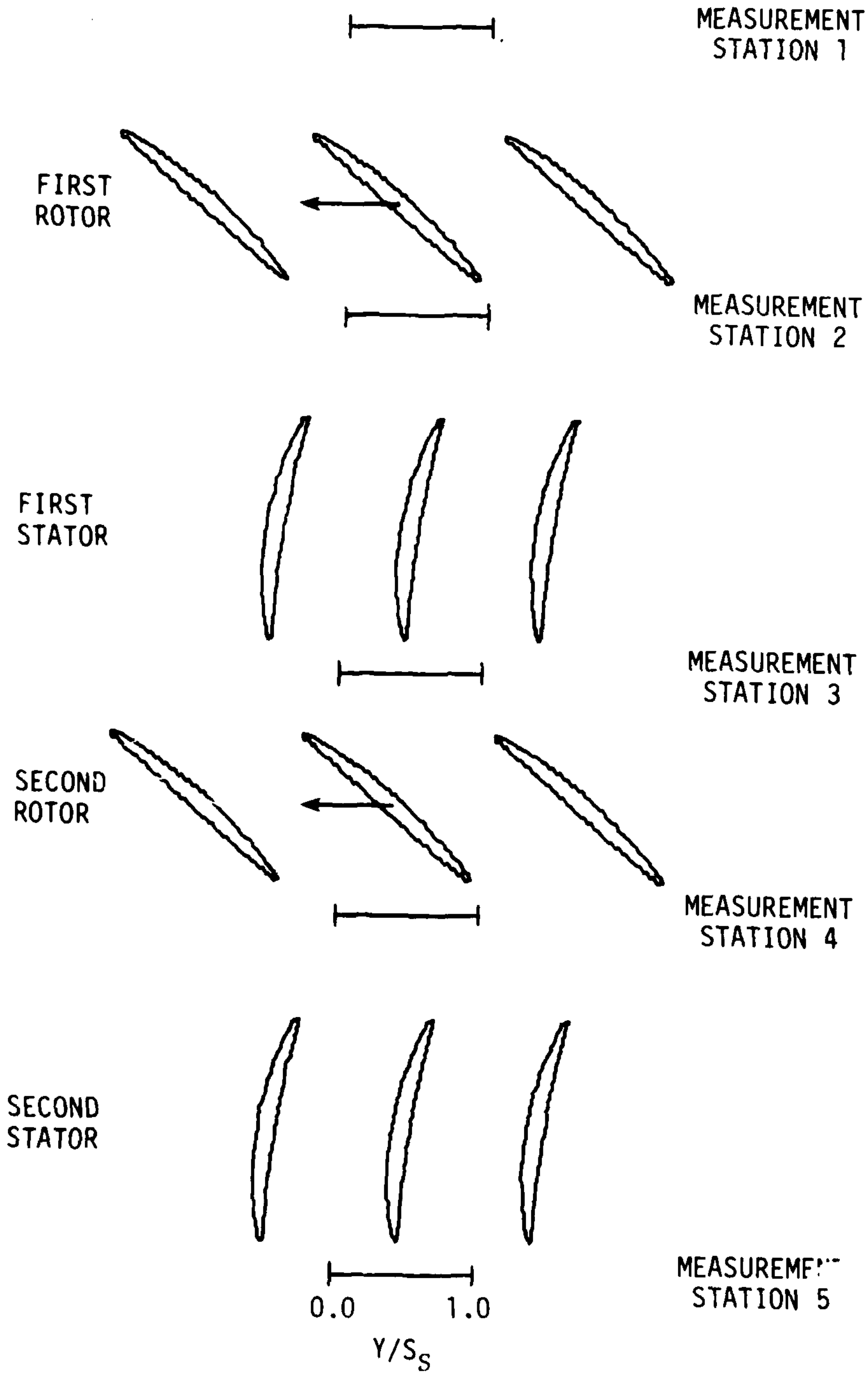


Figure 3.2 Blade cascade showing circumferential measurement window.

- STATION 5: 25 total pressure / 10 flow angle (free-stream only)

Complete sets of data were obtained for the baseline 1 and modified 1 compressor builds. For the baseline 2 and modified 2 builds, total-pressure data were acquired only at axial stations 3, 4, and 5, with flow angle data also acquired at these three stations for the modified 2 build only.

3.2.3. First Stator Wake Tracking Through the Second Rotor

A special series of tests was conducted on the modified 2 compressor build to determine first stator wake movement and dispersion through the second rotor blade row. These tests involved a specially constructed first stator blade with a heating wire wound to form a hot coil over the span of the blade near the trailing edge. In Figure 3.3 is a sketch of this heated stator blade and its location with respect to the circumferential measurement window. Data were obtained with the blade mounted in two different locations, referred to as position I and position II.

The stator wake tracking procedure consisted of activating the heating coil with a 3 amp current using a 120 volt variable transformer, and measuring air flow temperature at the second rotor exit with a thermocouple. This procedure was partially automated by modifying the Kiel probe data acquisition program discussed earlier. For two flow rates (flow coefficient = 0.575 and flow coefficient = 0.500), circumferential temperature surveys (position II) were made at five spanwise locations, specifically, at 10%, 30%, 50%, 70%, and 90% span from the hub. Circumferential temperature surveys at these

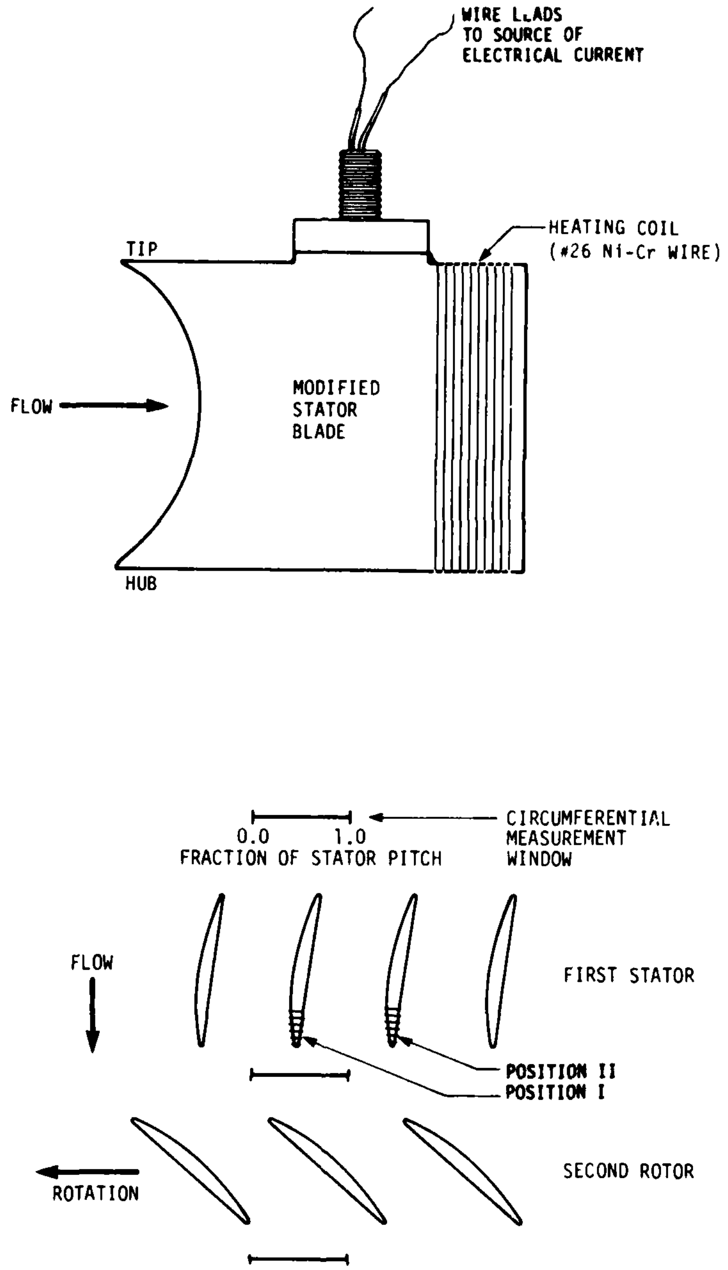


**Figure 3.3** Meridional plane view of the modified stator blade equipped with heating coil, and blade cascade view illustrating the position I and position II heated blade locations.

radii were also made for the position I heating coil location at the flow coefficient of 0.575 only. A single circumferential temperature survey (position II) was made at mid-span for the flow coefficient of 0.425. The number of temperature data points for all circumferential surveys was 25 per stator pitch.

The stator wake tracking temperature data were supplemented with a few second rotor exit circumferential surveys of total pressure. The surveys of 20 data points each per stator pitch were made at mid-span only and were used to assess wake avenue distortion caused by the heating coil.

## 3.3. Data Reduction

Preliminary reduction of the data was performed during acquisition and consisted of determining a primary quantity values of total head, static head, and absolute flow angle. These primary values were subsequently stored on magnetic disk (UNIX). Completion of data reduction generally occurred on the mainframe computer (NAS AS6). For all calculations, the flow was assumed incompressible since velocities involved Mach number levels less than 0.2. Integrals were evaluated using a spline-fit integration scheme [3]. A complete list of all quantities and equations used in reducing the data is presented in Appendix C.

### 3.3.1. Overall Performance Parameters

All overall performance parameters were computed during acquisition and then transferred to the mainframe computer for plotting (performance maps). The equations used to compute these parameters (see list below) are presented in Appendix C.

- Overall head-rise coefficient (venturi based, Eq. 10.52)
- Overall head-rise coefficient (second stator exit shroud static-pressure based, Eq. 10.51)
- Mechanical work-input coefficient (shaft torque based, Eq. 10.53)
- Mechanical efficiency (second stator exit shroud static-pressure/shaft torque based, Eq. 10.54)

3.3.2. Flow-Field and Performance Parameters (Detailed Data)

The total head was determined at each flow-field measurement point from the Kiel probe measured total pressure. Circumferential-mean values of total head and absolute flow angle were determined for each spanwise position at every axial measurement station. All circumferential averages, except for flow angle averages at the stator blade row exits, were determined by integrating over one stator blade pitch. Circumferential-mean absolute flow angles at the stator blade row exits were obtained by integrating over the free-stream portion of the flow only.

The static head was assumed to be circumferentially constant, and the spanwise distribution of static head was determined for each spanwise location at every axial measurement station by solving the radial equilibrium equation (Eq. 10.11) using the Runge-Kutta numerical technique [4]. The circumferential-mean casing static head was used as a boundary value. The pressure distribution was obtained by marching radially toward the hub at increments of 5% of passage height. The circumferential-mean values of total head and absolute flow angle required at each step of the Runge-Kutta solution were obtained with a second-order Lagrange interpolation of their measured spanwise distributions.

From the radial distributions of total head, absolute flow angle, and static head, the circumferential-mean absolute velocities were determined for each spanwise location of every axial measurement station. With the circumferential-mean absolute velocities and flow angles determined, the following circumferential-mean flow values were computed for each spanwise location of every axial measurement station.

- Axial velocity, m/s (Eq. 10.16)
- Absolute tangential velocity, m/s (Eq. 10.18)
- Relative tangential velocity, m/s (Eq. 10.20)
- Relative velocity, m/s (Eq. 10.22)
- Relative flow angle, degrees (Eq. 10.24)
- Blade incidence angle, degrees (Eqs. 10.25 and 10.27)
- Blade deviation angle, degrees (Eqs. 10.26 and 10.28)
- Flow coefficient (Eq. 10.29)

In addition, for each axial measurement station an annulus cross-section integrated flow coefficient was calculated and compared with the flow coefficient determined from the venturi flow meter. In determining the annulus cross-section flow rate and corresponding flow coefficient, the axial velocities at the hub and casing end walls were assumed equal to zero.

The performance parameters were computed using the above circumferential-mean data. The actual and ideal (Euler turbine equation based) head-rise coefficients and hydraulic efficiency were determined for each of the eight spanwise locations for both rotor rows, stages, and the entire compressor. Total-head loss coefficients were also determined for each rotor and stator blade row. Also, radially mass-averaged values of each of the above performance parameters were determined for both rotor rows, stages, and the entire compressor (see Appendix C).

### 3.3.3. First Stator Wake Tracking Data

All heat stator wake temperature data obtained at the second rotor exit were normalized before plotting as described below. The so-called relative temperatures were computed by subtracting the venturi meter throat fluid temperature from all temperature values. These relative temperature data were then graphed by the mainframe computer.

### 3.3.4. General Graph Types

Most reduced data were graphed by the mainframe computer to aid in analysis. Four general types of graphs were used:

- Performance maps--for point data (versus flow coefficient)
- Graphs with circumferential extent--for point data
- Contour maps--for point data
- Spanwise graphs--for circumferential-mean data

It should be noted that for contour mapping, the data acquired over a single stator blade pitch were repeated circumferentially over two stator blade pitches in order to provide better visualization of the flow pattern.

# 4. RESULTS AND DISCUSSION

Experimental results obtained from aerodynamic performance testing of the two-stage axial-flow compressor are presented and discussed in this section. The sequence of presentation is as follows:

4.1. Uncertainty Analysis

4.2. Overall Compressor Performance

4.3. Baseline 1 Compressor Build--Different Flow Rates

4.4. Comparison of Compressor Builds

A detailed comparison of design code predictions with experimental results for the baseline 1 compressor build at design flow is provided in Reference 1.

## 4.1. Uncertainty Analysis

Uncertainty estimates associated with the experimental results are presented in this section and the methods used to obtain these estimates are discussed. Primary measurement uncertainty intervals are provided first, followed by a discussion and presentation of the uncertainty intervals in calculated quantities.

Estimated uncertainty intervals for the primary measurement quantities are listed in Table 4.1. Also included in Table 4.1 are typical quantity values. The estimates for transducer pressure and absolute flow angle uncertainty were statistically determined from several sets of repeatability tests. Some actual test data

Table 4.1. Estimated uncertainty intervals for primary measurement quantities.

| Quantity | Symbol | Typical Value | Uncertainty Interval (20:1 odds) | |
|---|---|---|---|---|
| Barometric pressure | $h_{hg}$ | 735.0 mm Hg | ±0.3 | (0.04%) |
| Transducer pressure | P | 60.00 mm $H_2O$ | ±0.58 | (0.97%) |
| Temperature | t | 300.0 deg. K | ±0.5 | (0.17%) |
| Shaft torque | T | 11.000 N·m | ±0.125 | (1.14%) |
| Absolute flow angle | $\beta_y$ | | | |
| Station 1 | | 0.0 deg. | ±1.25 | |
| Station 2 | | 30.0 deg. | ±0.90 | |
| Station 3 | | 0.0 deg. | ±0.70 | |
| Station 4 | | 30.0 deg. | ±0.65 | |
| Station 5 | | 0.0 deg. | ±0.70 | |

sets were also replicated to provide repeatability information. An attempt was made to assess fixed errors in these results.

The estimated uncertainty intervals for so-called "primary computed quantities" are presented in Table 4.2. Primary computed quantities are those data closely associated with primary measurement data and from which the flow-field and performance parameters are directly calculated. Several points should be noted about the information in Table 4.2:

- Most of the uncertainty intervals are for circumferetial-mean quantities.
- The uncertainty intervals for a given quantity depend on the measurement station.
- The uncertainty intervals for circumferential-mean total-head data are smaller than those for individual total-head data.
- The uncertainty intervals for circumferential-mean/radial equilibrium static-head data at stations 3 and 5 are relatively large (compared with the intervals for total-head data).
- Two sets of uncertainty intervals are listed for circumferential-mean absolute flow angle data, one includes a suspected fixed-error uncertainty and the other excludes it.

Some of these observations are discussed further.

The uncertainty intervals for circumferential-mean quantities are smaller than those for the individual quantities used to calculate them, as pointed out above for total head. Similarly, radially mass-averaged quantities have smaller uncertainty intervals than the circumferential-mean quantities from which they are computed. This

Table 4.2. Estimated uncertainty intervals for primary computed quantities.

ESTIMATED UNCERTAINTY INTERVALS (20:1 ODDS)

| Station | Total Head $H$(N-m/kg) | Circumferential-Mean Total Head $\bar{H}$(N-m/kg) | Circumferential-Mean/Radial Equilibrium Static Head $\bar{h}$(N-m/kg) | Circumferential Mean Absolute Flow Angle $\beta_y$ (deg.) | Circumferential-Mean Absolute Flow Angle (No Fixed Error) $\bar{\beta}_y$ (deg. |
|---|---|---|---|---|---|
| 1 | ±5.0 | ±2.0 | ±5.0 | ±0.85 | ±0.50 |
| 2 | ±5.0 | ±3.0 | ±5.0 | ±0.65 | ±0.30 |
| 3 | ±5.0 | ±3.0 | ±15.0 | ±0.70 | ±0.35 |
| 4 | ±5.0 | ±3.0 | ±5.0 | ±0.50 | ±0.15 |
| 5 | ±5.0 | ±3.0 | ±25.0 | ±0.70 | ±0.35 |

is reasonable since an average (mean) datum has less random error uncertainty associated with it than the individual data (normally distributed) from which it is calculated.

The absolute flow angle data have two sets of uncertainty intervals associated with them because the suspected fixed-error uncertainty need not be included when estimating the uncertainty intervals of many calculated results. Most calculated results are practically unaffected by a small systematic error in measured angles because they involve angle difference, e.g., ideal head rise, hydraulic efficiency, and rotor loss. Only the uncertainty intervals for incidence and deviation angles include this fixed-error uncertainty.

Some additional uncertainty in stator exit circumferential-mean absolute flow angle data exists. This uncertainty is due to the fact that different estimates of free-stream extent (flow angles cannot be measured in the wake with a cobra probe) result in different circumferential-mean angles.

The uncertainty intervals for circumferential-mean/radial equilibrium static-head data are relatively large at the stator exits because the predicted values of static head over the blade span (by radial equilibrium using casing static head) are evidently inaccurate. This can be seen from the comparisons of venturi and station integrated flow coefficients presented in Table 4.3. The relatively large error in the stator exit integrated flow coefficients can be traced to static head, since the total-head data are considered accurate. Further, the uncertainty intervals for the static-head data

Table 4.3. Comparison of venturi and axial measurement station integrated flow coefficients for the different compressor builds ($\phi$ = 0.500).

| Station | Venturi Flow Coefficient $\phi$ | Integrated Flow Coefficient $\phi_a$ | Flow Coefficient Comparison (Percent) FCC |
|---|---|---|---|
| **Baseline 1** | | | |
| 1 | 0.5001 | 0.5051 | 1.0112 |
| 2 | 0.5001 | 0 4980 | -0.4274 |
| 3 | 0.5001 | 0.4964 | -0.7409 |
| 4 | 0.5001 | 0.5016 | 0.2989 |
| 5 | 0.5000 | 0.4876 | -2.4900 |
| **Baseline 2** | | | |
| 1 | 0.5001 | 0.5051 | 1.0112 |
| 2 | 0.5001 | 0.4980 | -0.4274 |
| 3 | 0.5001 | 0.4960 | -0.8260 |
| 4 | 0.5000 | 0.5034 | 0.6778 |
| 5 | 0.5002 | 0.4910 | -1.8412 |
| **Modified 1** | | | |
| 1 | 0.5001 | 0.5038 | 0.7433 |
| 2 | 0.5001 | 0.4961 | -0.8002 |
| 3 | 0.5001 | 0.4911 | -1.7991 |
| 4 | 0.5001 | 0.4981 | -0.3997 |
| 5 | 0.5002 | 0.4863 | -2.7780 |
| **Modified 2** | | | |
| 1 | 0.5001 | 0.5038 | 0.7433 |
| 2 | 0.5001 | 0.4961 | -0.8002 |
| 3 | 0.5000 | 0.4918 | -1.6527 |
| 4 | 0.4999 | 0.5021 | 0.4272 |
| 5 | 0.5000 | 0.4869 | -2.6118 |

were estimated by using the flow rate comparison values and assuming that, the stator exit flow rate discrepancies were due solely to static-head error.

The uncertainty intervals for flow-field quantities and performance parameters were estimated from those of the "primary computed quantities" using the uncertainty propagation methods of Kline and McClintock [5]. The second-power equation was solved analytically to estimate the uncertainty intervals for overall performance parameters. These are listed in Table 4.4. Uncertainty intervals for circumferential-mean quantities were estimated by solving the second-power equation numerically. To this end, a so-called "Jitter Program" discussed by Moffat [6] was employed. The uncertainty intervals estimated for circumferential-mean flow-field quantities are listed in Tables 4.5 and 4.6. The uncertainty intervals estimated for circumferential-mean performance parameters are presented in Table 4.7. Some of these uncertainty intervals are graphed in Figure 4.1.

## 4.2. Overall Compressor Performance

Results for overall compressor aerodynamic performance are presented and discussed in this section. Performance curves for the baseline 1 and modified 2 compressor builds are contained in Figure 4.2. Figure 4.2(a) and (b) involve overall head-rise variation with flow coefficient, while in Figure 4.2(c) overall work-input (shaft torque based) is presented. Lastly, an overall efficiency map of the compressor is shown in Figure 4.2(d). Each

Table 4.4. Estimated uncertainty intervals for overall performance parameters.

ESTIMATED UNCERTAINTY INTERVALS (20:1 ODDS).

| Venturi Flow Coefficient (Value) $\phi$ | Venturi Flow Coefficient (Uncertainty) $\phi$ | Overall Head-Rise Coefficient (Based on Second Stator Exit Shroud Static-Pressure) $\psi_{overall,2,2S}$ | Overall Head-Rise Coefficient (Based on Venturi Static-Pressure) $\psi_{overall,v}$ | Overall Work-Input Coefficient (Based on Shaft Torque) $\psi_{i,overall,m}$ | Overall Efficiency $\eta_{m,overall,2,2S}$ |
|---|---|---|---|---|---|
| 0.400 | ±0.0042 (1.1%) | ±0.0097 (2.0%) | ±0.0034 (0.7%) | ±0.0108 (1.5%) | ±0.018 (2.5%) |
| 0.500 | ±0.0034 (0.7%) | ±0.0097 (2.4%) | ±0.0034 (0.9%) | ±0.0072 (1.3%) | ±0.021 (2.7%) |
| 0.600 | ±0.0028 (0.5%) | ±0.0097 (3.5%) | ±0.0034 (1.5%) | ±0.0055 (1.4%) | ±0.026 (3.7%) |

Table 4.5 Uncertainty estimates (20:1 odds) for circumferential-mean flow-field quantities ($\phi$ = 0.500).

STATION 1 : ROTOR 1 INLET

| PHH | HT N*M/KG | HS N*M/KG | BETA Y DEG. | V M/S | VZ M/S | VY M/S | BETA R DEG. | VR M/S | VYR M/S | FC |
|---|---|---|---|---|---|---|---|---|---|---|
| 5.00 | 2.0000 | 5.0000 | 0.5000 | 0.1976 | 0.1977 | 0.2376 | 0.2701 | 0.2250 | 0.2376 | 0.0039 |
| 10.00 | 2.0000 | 5.0000 | 0.5000 | 0.1976 | 0.1976 | 0.2379 | 0.2664 | 0.2254 | 0.2379 | 0.0039 |
| 30.00 | 2.0000 | 5.0000 | 0.5000 | 0.1975 | 0.1975 | 0.2380 | 0.2502 | 0.2266 | 0.2380 | 0.0039 |
| 50.00 | 2.0000 | 5.0000 | 0.5000 | 0.1973 | 0.1973 | 0.2381 | 0.2359 | 0.2278 | 0.2381 | 0.0039 |
| 70.00 | 2.0000 | 5.0000 | 0.5000 | 0.1974 | 0.1974 | 0.2380 | 0.2229 | 0.2287 | 0.2381 | 0.0039 |
| 80.00 | 2.0000 | 5.0000 | 0.5000 | 0.1974 | 0.1974 | 0.2380 | 0.2154 | 0.2285 | 0.2380 | 0.0039 |
| 90.00 | 2.0000 | 5.0000 | 0.5000 | 0.1981 | 0.1981 | 0.2373 | 0.2102 | 0.2286 | 0.2373 | 0.0039 |
| 95.00 | 2.0000 | 5.0000 | 0.5000 | 0.1994 | 0.1993 | 0.2357 | 0.2081 | 0.2279 | 0.2357 | 0.0039 |

STATION 2 : ROTOR 1 EXIT / STATOR 1 INLET

| PHH | HT N*M/KG | HS N*M/KG | BETA Y DEG. | V M/S | VZ M/S | VY M/S | BETA R DEG. | VR M/S | VYR M/S | FC |
|---|---|---|---|---|---|---|---|---|---|---|
| 5.00 | 3.0000 | 5.0000 | 0.3000 | 0.1813 | 0.1774 | 0.1727 | 0.3187 | 0.1703 | 0.1727 | 0.0035 |
| 10.00 | 3.0000 | 5.0000 | 0.3000 | 0.1842 | 0.1789 | 0.1715 | 0.3147 | 0.1679 | 0.1715 | 0.0035 |
| 30.00 | 3.0000 | 5.0000 | 0.3000 | 0.1867 | 0.1805 | 0.1703 | 0.2969 | 0.1653 | 0.1703 | 0.0035 |
| 50.00 | 3.0000 | 5.0000 | 0.3000 | 0.1872 | 0.1815 | 0.1695 | 0.2750 | 0.1648 | 0.1695 | 0.0036 |
| 70.00 | 3.0000 | 5.0000 | 0.3000 | 0.1857 | 0.1813 | 0.1693 | 0.2505 | 0.1655 | 0.1694 | 0.0036 |
| 80.00 | 3.0000 | 5.0000 | 0.3000 | 0.1828 | 0.1798 | 0.1704 | 0.2352 | 0.1682 | 0.1703 | 0.0035 |
| 90.00 | 3.0000 | 5.0000 | 0.3000 | 0.1865 | 0.1809 | 0.1699 | 0.2477 | 0.1642 | 0.1700 | 0.0035 |
| 95.00 | 3.0000 | 5.0000 | 0.3000 | 0.2109 | 0.1896 | 0.1718 | 0.3002 | 0.1450 | 0.1718 | 0.0037 |

STATION 3 : STATOR 1 EXIT / ROTOR 2 INLET

| PHH | HT N*M/KG | HS N*M/KG | BETA Y DEG. | V M/S | VZ M/S | VY M/S | BETA R DEG. | VR M/S | VYR M/S | FC |
|---|---|---|---|---|---|---|---|---|---|---|
| 5.00 | 3.0000 | 15.0000 | 0.3500 | 0.6353 | 0.6336 | 0.1541 | 0.7506 | 0.3454 | 0.1541 | 0.0124 |
| 10.00 | 3.0000 | 15.0000 | 0.3500 | 0.5824 | 0.5824 | 0.1606 | 0.6033 | 0.3633 | 0.1606 | 0.0114 |
| 30.00 | 3.0000 | 15.0000 | 0.3500 | 0.5734 | 0.5734 | 0.1630 | 0.5739 | 0.3457 | 0.1629 | 0.0112 |
| 50.00 | 3.0000 | 15.0000 | 0.3500 | 0.5630 | 0.5629 | 0.1660 | 0.5474 | 0.3273 | 0.1660 | 0.0110 |
| 70.00 | 3.0000 | 15.0000 | 0.3500 | 0.5536 | 0.5532 | 0.1699 | 0.5285 | 0.3073 | 0.1699 | 0.0108 |
| 80.00 | 3.0000 | 15.0000 | 0.3500 | 0.5494 | 0.5482 | 0.1740 | 0.5276 | 0.2926 | 0.1739 | 0.0107 |
| 90.00 | 3.0000 | 15.0000 | 0.3500 | 0.5922 | 0.5907 | 0.1634 | 0.5760 | 0.2821 | 0.1634 | 0.0116 |
| 95.00 | 3.0000 | 15.0000 | 0.3500 | 0.6515 | 0.6514 | 0.1435 | 0.6148 | 0.3024 | 0.1435 | 0.0128 |

Table 4.5 concluded.

STATION 4 : ROTOR 2 EXIT / STATOR 2 INLET

| PHH | HT N*M/KG | HS N*M/KG | BETA Y DEG. | V M/S | VZ M/S | VY M/S | BETA R DEG. | VR M/S | VYR M/S | FC |
|---|---|---|---|---|---|---|---|---|---|---|
| 5.00 | 3.0000 | 5.0000 | 0.1500 | 0.1835 | 0.1442 | 0.1407 | 0.3798 | 0.0918 | 0.1407 | 0.0028 |
| 10.00 | 3.0000 | 5.0000 | 0.1500 | 0.1881 | 0.1641 | 0.1226 | 0.3105 | 0.0983 | 0.1226 | 0.0032 |
| 30.00 | 3.0000 | 5.0000 | 0.1500 | 0.1874 | 0.1677 | 0.1169 | 0.2817 | 0.0960 | 0.1169 | 0.0033 |
| 50.00 | 3.0000 | 5.0000 | 0.1500 | 0.1859 | 0.1685 | 0.1136 | 0.2590 | 0.0939 | 0.1136 | 0.0033 |
| 70.00 | 3.0000 | 5.0000 | 0.1500 | 0.1828 | 0.1658 | 0.1135 | 0.2432 | 0.0919 | 0.1135 | 0.0032 |
| 80.00 | 3.0000 | 5.0000 | 0.1500 | 0.1793 | 0.1615 | 0.1154 | 0.2368 | 0.0912 | 0.1154 | 0.0032 |
| 90.00 | 3.0000 | 5.0000 | 0.1500 | 0.1888 | 0.1661 | 0.1207 | 0.2534 | 0.0832 | 0.1207 | 0.0033 |
| 95.00 | 3.0000 | 5.0000 | 0.1500 | 0.2133 | 0.1759 | 0.1403 | 0.3023 | 0.0731 | 0.1403 | 0.0034 |

STATION 5 : STATOR 2 EXIT

| PHH | HT N*M/KG | HS N*M/KG | BETA Y DEG. | V M/S | VZ M/S | VY M/S | BETA R DEG. | VR M/S | VYR M/S | FC |
|---|---|---|---|---|---|---|---|---|---|---|
| 5.00 | 3.0000 | 25.0000 | 0.3500 | 1.1860 | 1.1839 | 0.1472 | 1.4660 | 0.5618 | 0.1473 | 0.0232 |
| 10.00 | 3.0000 | 25.0000 | 0.3500 | 1.0593 | 1.0587 | 0.1497 | 1.1988 | 0.5609 | 0.1498 | 0.0207 |
| 30.00 | 3.0000 | 25.0000 | 0.3500 | 0.9775 | 0.9773 | 0.1586 | 0.9732 | 0.5539 | 0.1586 | 0.0191 |
| 50.00 | 3.0000 | 25.0000 | 0.3500 | 0.9269 | 0.9269 | 0.1660 | 0.8848 | 0.5113 | 0.1659 | 0.0181 |
| 70.00 | 3.0000 | 25.0000 | 0.3500 | 0.9059 | 0.9048 | 0.1750 | 0.8623 | 0.4620 | 0.1750 | 0.0177 |
| 80.00 | 3.0000 | 25.0000 | 0.3500 | 0.9063 | 0.9038 | 0.1827 | 0.8687 | 0.4353 | 0.1827 | 0.0177 |
| 90.00 | 3.0000 | 25.0000 | 0.3500 | 0.9676 | 0.9661 | 0.1676 | 0.9204 | 0.4362 | 0.1677 | 0.0189 |
| 95.00 | 3.0000 | 25.0000 | 0.3500 | 1.0432 | 1.0432 | 0.1474 | 0.9673 | 0.4711 | 0.1475 | 0.0204 |

Table 4.6 Uncertainty estimates (20:1 odds) for circumferential-mean incidence and deviation angles ($\phi$ = 0.500).

INCIDENCE ANGLES (DEG.)

| PHH | STATION 1 (ROTOR 1) | STATION 2 (STATOR 1) | STATION 3 (ROTOR 2) | STATION 4 (STATOR 2) |
|---|---|---|---|---|
| 5.00 | 0.3635 | 0.6500 | 0.7708 | 0.5000 |
| 10.00 | 0.3564 | 0.6500 | 0.6362 | 0.5000 |
| 30.00 | 0.3285 | 0.6500 | 0.6030 | 0.5000 |
| 50.00 | 0.3041 | 0.6500 | 0.5730 | 0.5000 |
| 70.00 | 0.2830 | 0.6500 | 0.5503 | 0.5000 |
| 80.00 | 0.2735 | 0.6500 | 0.5466 | 0.5000 |
| 90.00 | 0.2643 | 0.6500 | 0.5881 | 0.5000 |
| 95.00 | 0.2595 | 0.6500 | 0.6241 | 0.5000 |

DEVIATION ANGLES (DEG.)

| PHH | STATION 2 (ROTOR 1) | STATION 3 (STATOR 1) | STATION 4 (ROTOR 2) | STATION 5 (STATOR 2) |
|---|---|---|---|---|
| 5.00 | 0.3795 | 0.7000 | 0.4024 | 0.7000 |
| 10.00 | 0.3659 | 0.7000 | 0.3429 | 0.7000 |
| 30.00 | 0.3285 | 0.7000 | 0.3068 | 0.7000 |
| 50.00 | 0.2972 | 0.7000 | 0.2788 | 0.7000 |
| 70.00 | 0.2691 | 0.7000 | 0.2576 | 0.7000 |
| 80.00 | 0.2554 | 0.7000 | 0.2484 | 0.7000 |
| 90.00 | 0.2545 | 0.7000 | 0.2565 | 0.7000 |
| 95.00 | 0.3014 | 0.7000 | 0.3032 | 0.7000 |

Table 4.7 Uncertainty estimates (20:1 odds) for circumferential-mean performance parameters ($\phi$ = 0.500).

*** FIRST STAGE ***

| | HEAD RISE ---COEFFICIENT---- | | LOSS ---COEFFICIENT---- | | ----EFFICIENCY---- | |
|---|---|---|---|---|---|---|
| PHH | ROTOR | IDEAL | ROTOR | STATOR | ROTOR | STAGE |
| 5.00 | 0.0014 | 0.0041 | 0.0104 | 0.0077 | 0.0159 | 0.0144 |
| 10.00 | 0.0014 | 0.0042 | 0.0104 | 0.0082 | 0.0170 | 0.0169 |
| 30.00 | 0.0014 | 0.0045 | 0.0099 | 0.0085 | 0.0173 | 0.0173 |
| 50.00 | 0.0014 | 0.0049 | 0.0096 | 0.0085 | 0.0182 | 0.0180 |
| 70.00 | 0.0014 | 0.0052 | 0.0093 | 0.0083 | 0.0196 | 0.0190 |
| 80.00 | 0.0014 | 0.0054 | 0.0091 | 0.0079 | 0.0196 | 0.0185 |
| 90.00 | 0.0014 | 0.0055 | 0.0084 | 0.0081 | 0.0148 | 0.0133 |
| 95.00 | 0.0014 | 0.0056 | 0.0077 | 0.0105 | 0.0111 | 0.0109 |

*** SECOND STAGE ***

| | HEAD RISE ---COEFFICIENT---- | | LOSS ---COEFFICIENT---- | | ----EFFICIENCY---- | |
|---|---|---|---|---|---|---|
| PHH | ROTOR | IDEAL | ROTOR | STATOR | ROTOR | STAGE |
| 5.00 | 0.0016 | 0.0029 | 0.0087 | 0.0078 | 0.0092 | 0.0087 |
| 10.00 | 0.0016 | 0.0029 | 0.0072 | 0.0083 | 0.0113 | 0.0112 |
| 30.00 | 0.0016 | 0.0031 | 0.0070 | 0.0084 | 0.0125 | 0.0126 |
| 50.00 | 0.0016 | 0.0033 | 0.0068 | 0.0083 | 0.0135 | 0.0137 |
| 70.00 | 0.0016 | 0.0036 | 0.0067 | 0.0080 | 0.0138 | 0.0137 |
| 80.00 | 0.0016 | 0.0038 | 0.0069 | 0.0076 | 0.0138 | 0.0133 |
| 90.00 | 0.0016 | 0.0039 | 0.0068 | 0.0084 | 0.0128 | 0.0124 |
| 95.00 | 0.0016 | 0.0039 | 0.0061 | 0.0109 | 0.0092 | 0.0098 |

*** OVERALL ***

| PHH | HEAD RISE COEFFICIENT | EFFICIENCY |
|---|---|---|
| 5.00 | 0.0014 | 0.0073 |
| 10.00 | 0.0014 | 0.0092 |
| 30.00 | 0.0014 | 0.0100 |
| 50.00 | 0.0014 | 0.0109 |
| 70.00 | 0.0014 | 0.0112 |
| 80.00 | 0.0014 | 0.0109 |
| 90.00 | 0.0014 | 0.0089 |
| 95.00 | 0.0014 | 0.0071 |

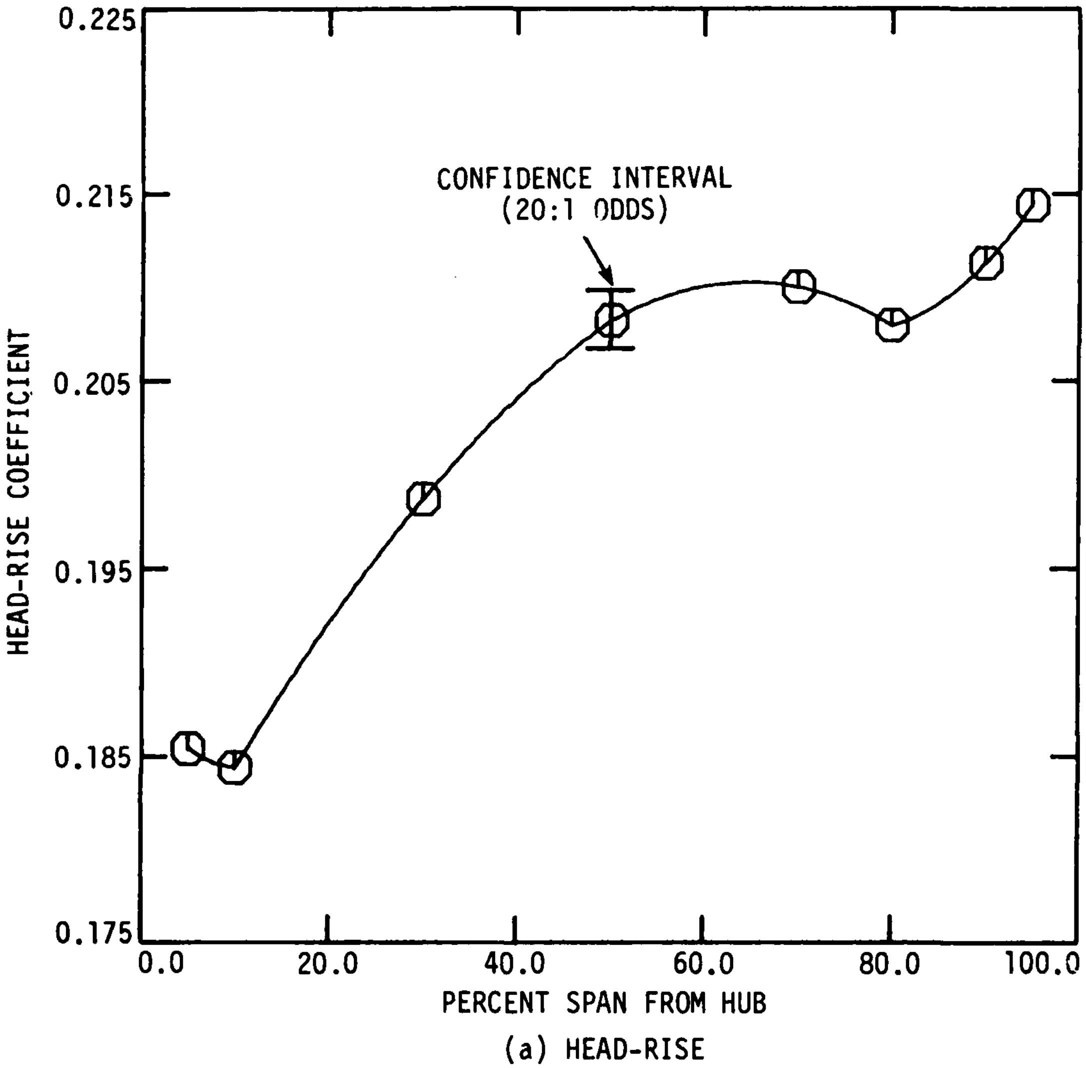


Figure 4.1 Confidence intervals (20:1 odds) for circumferential-mean performance parameters ($\phi$ = 0.500).

Note: The curves drawn through the data in this and other Figures were generated by a computer plotting routine based on a second order fit. As such, these curves should be interpreted with caution.

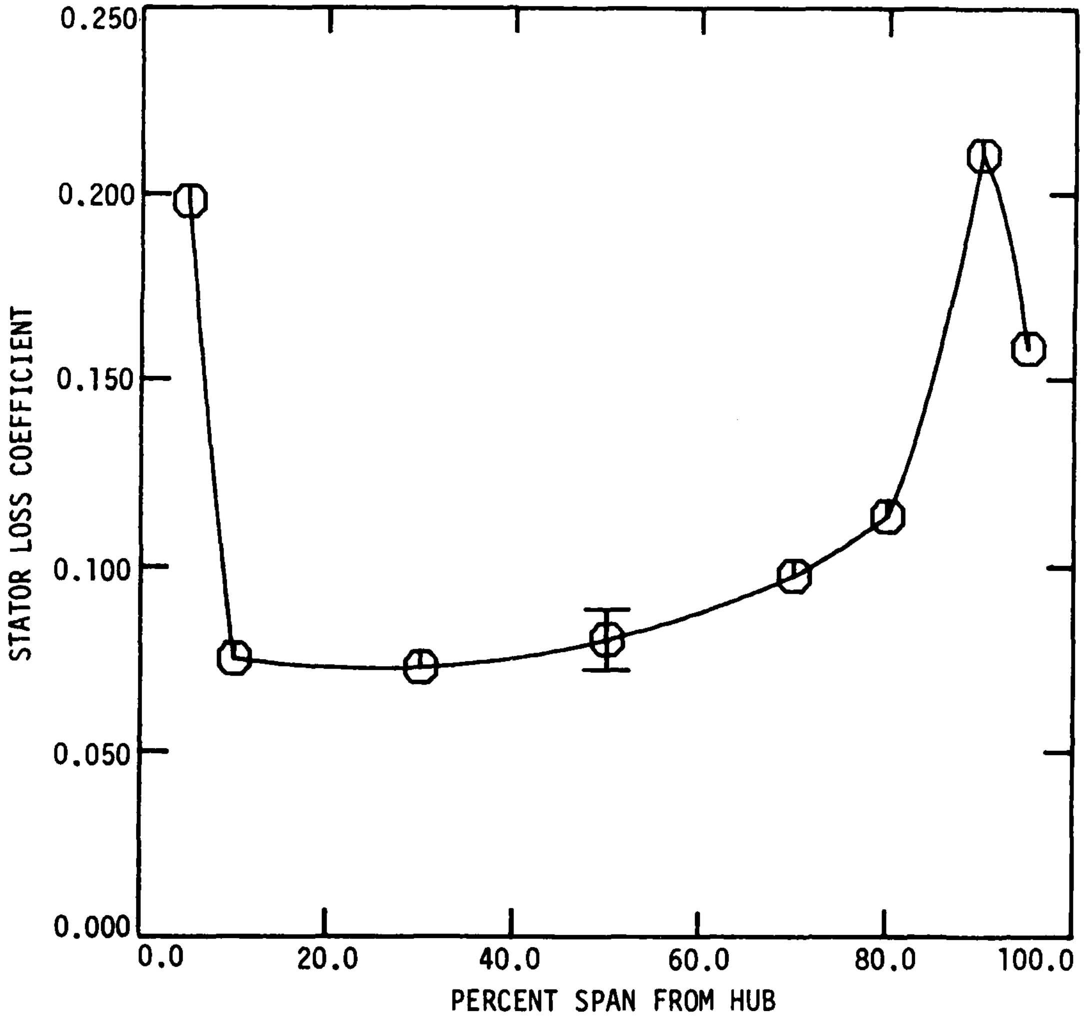


(b) STATOR LOSS

**Figure 4.1 continued.**

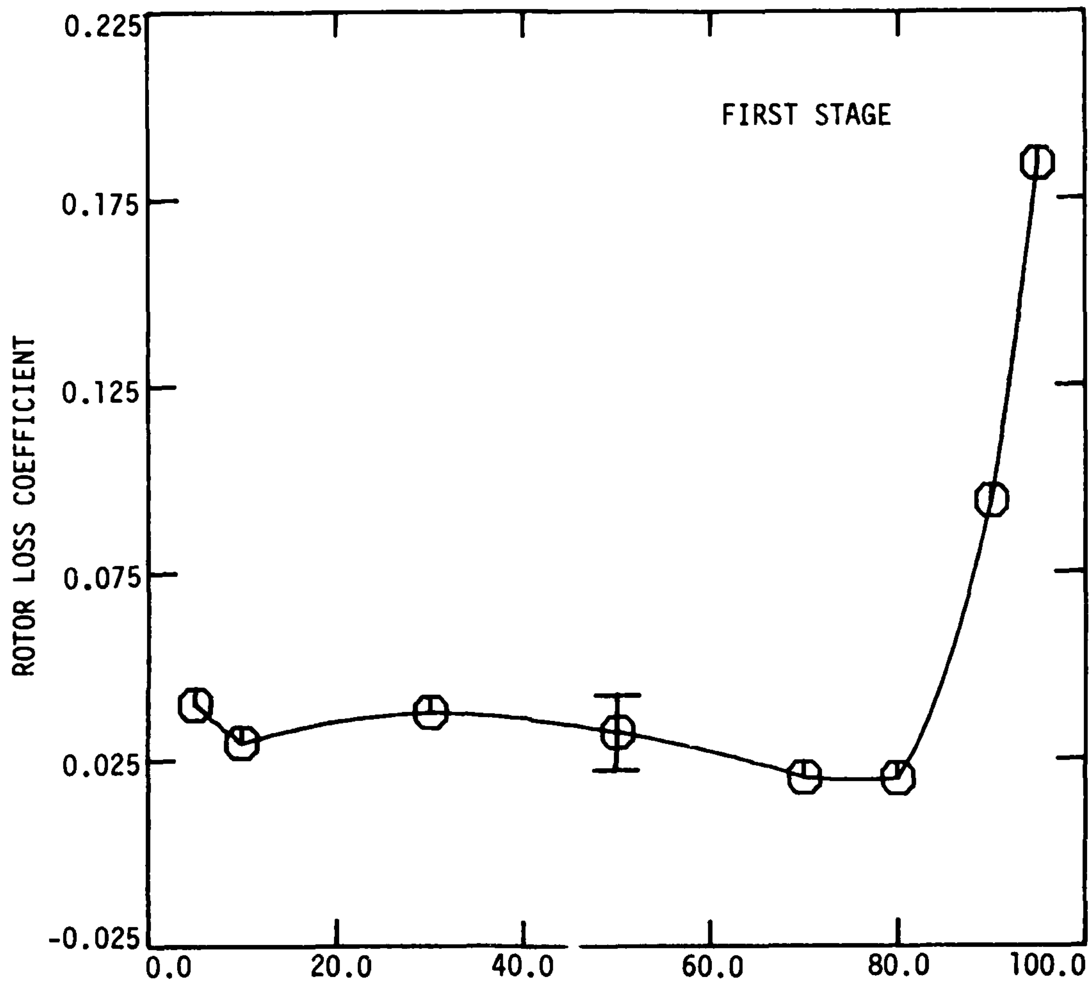

(c) FIRST STAGE ROTOR LOSS

**Figure 4.1** continued.

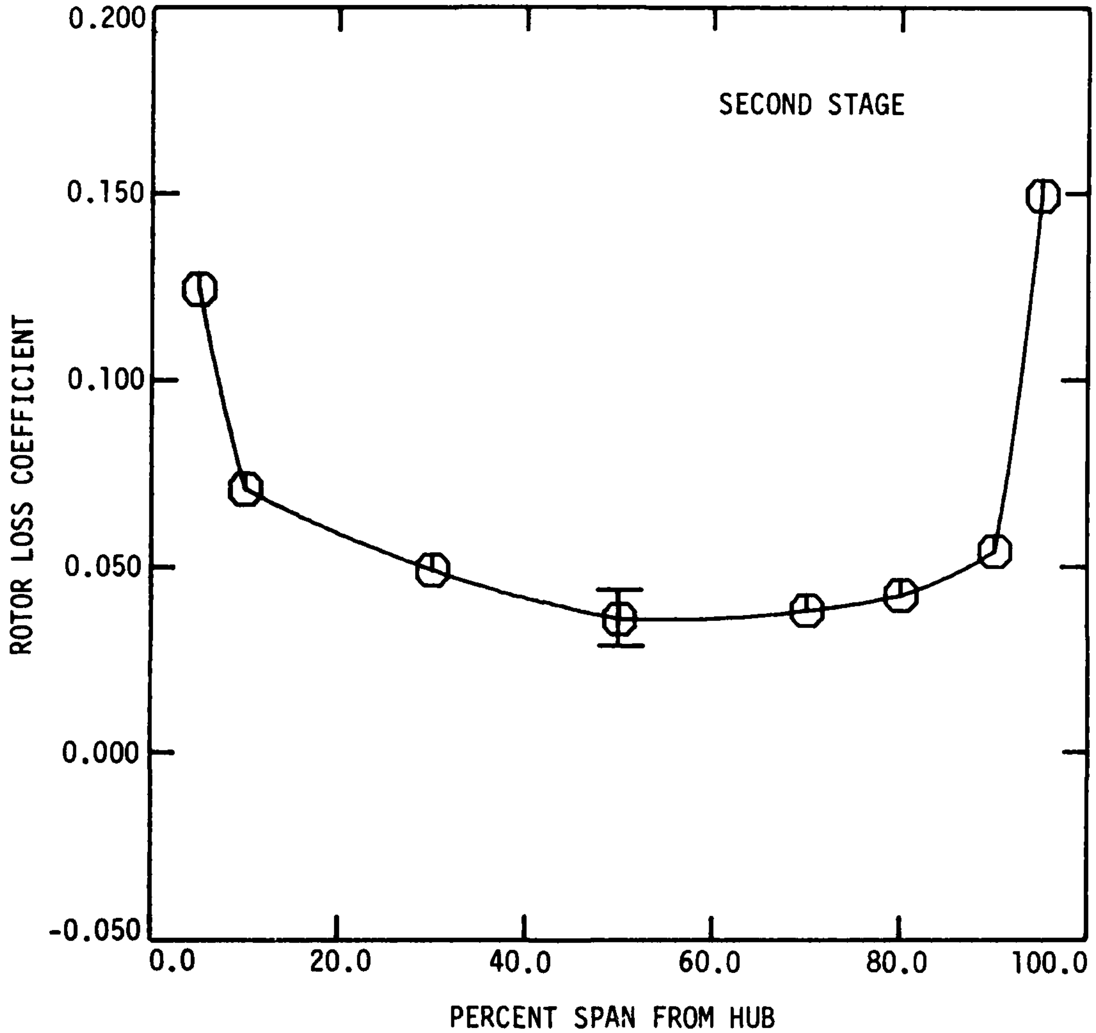


(d) SECOND STAGE ROTOR LOSS

**Figure 4.1 continued.**

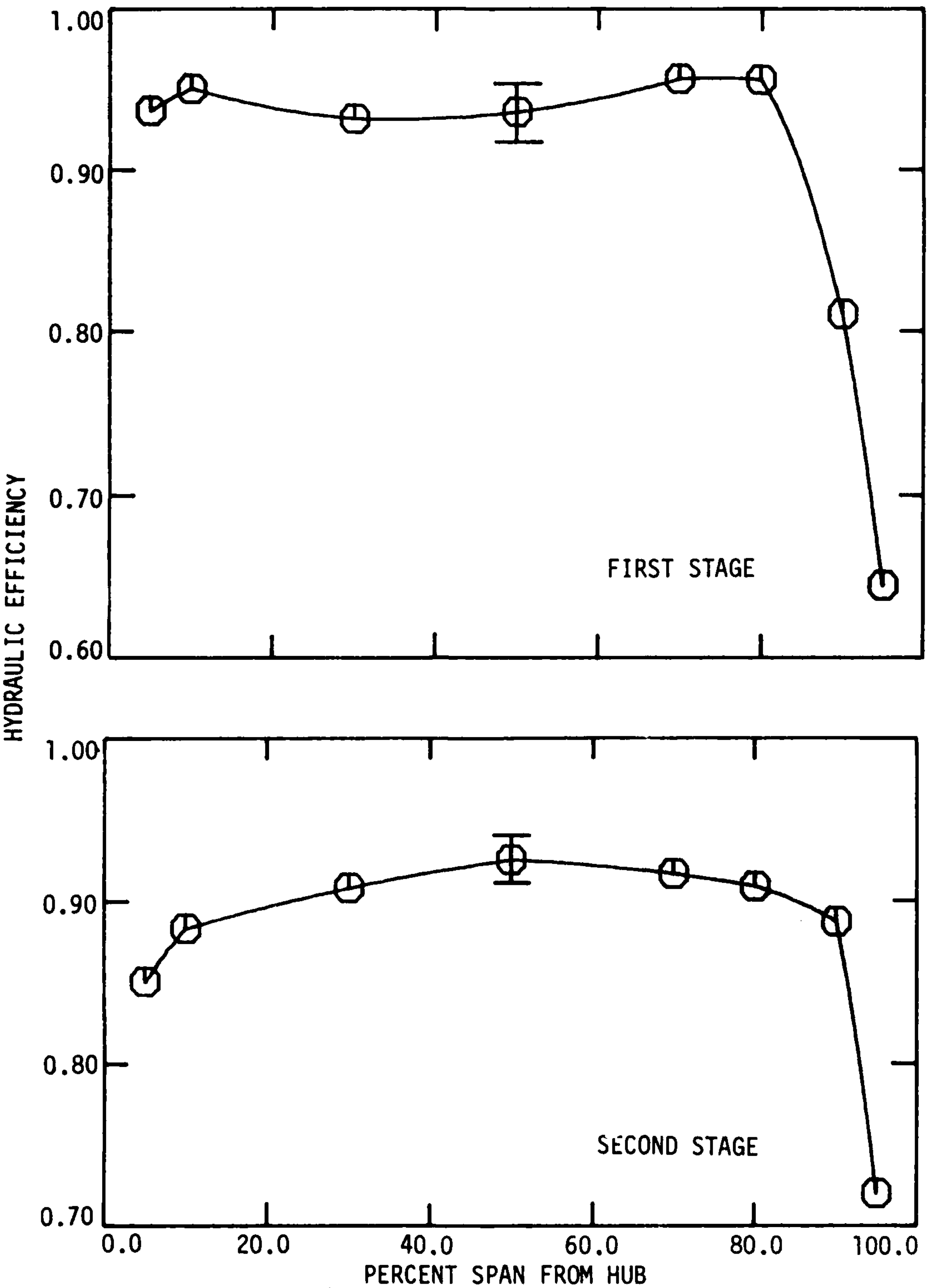


(e) ROTOR AND STAGE EFFICIENCY

Figure 4.1 continued.

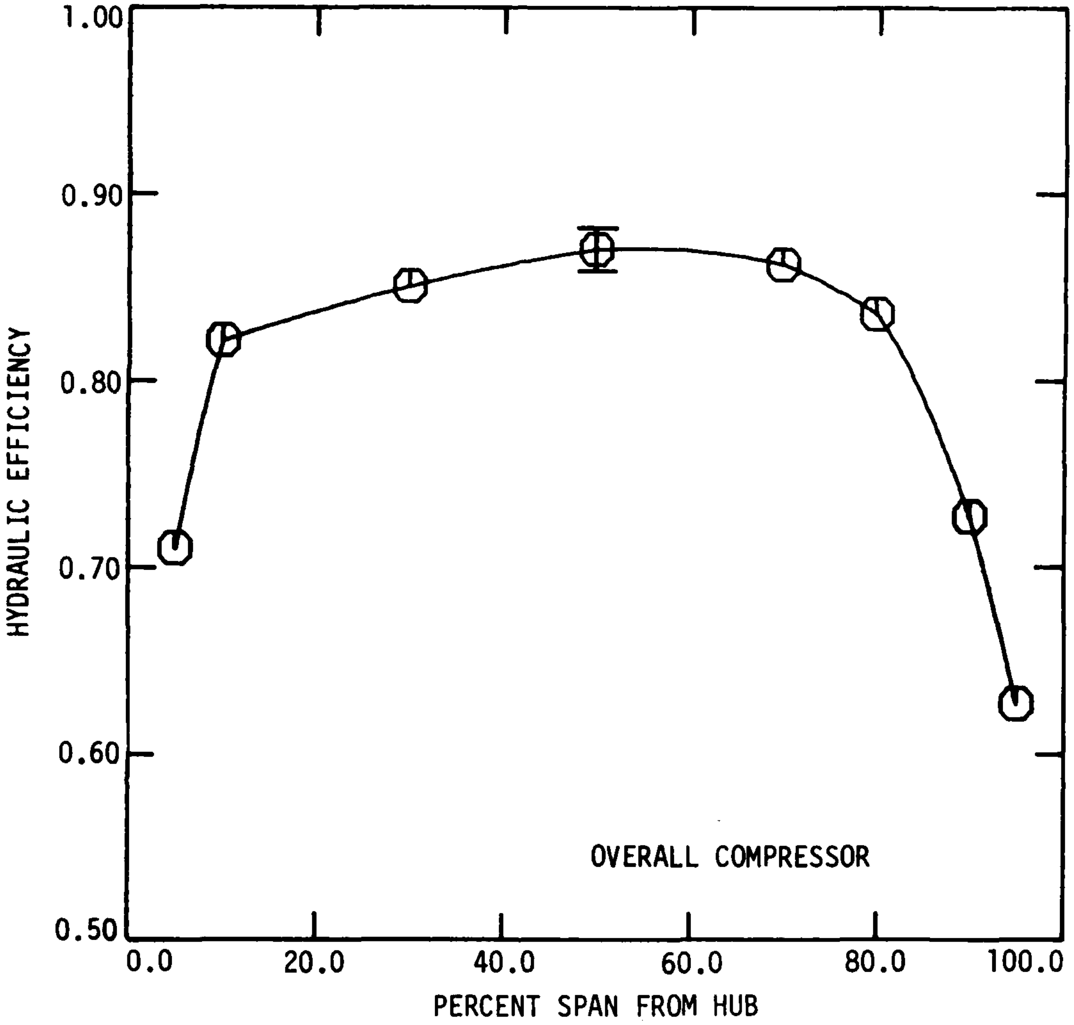


(f) EFFICIENCY FOR OVERALL COMPRESSOR

Figure 4.1 continued.

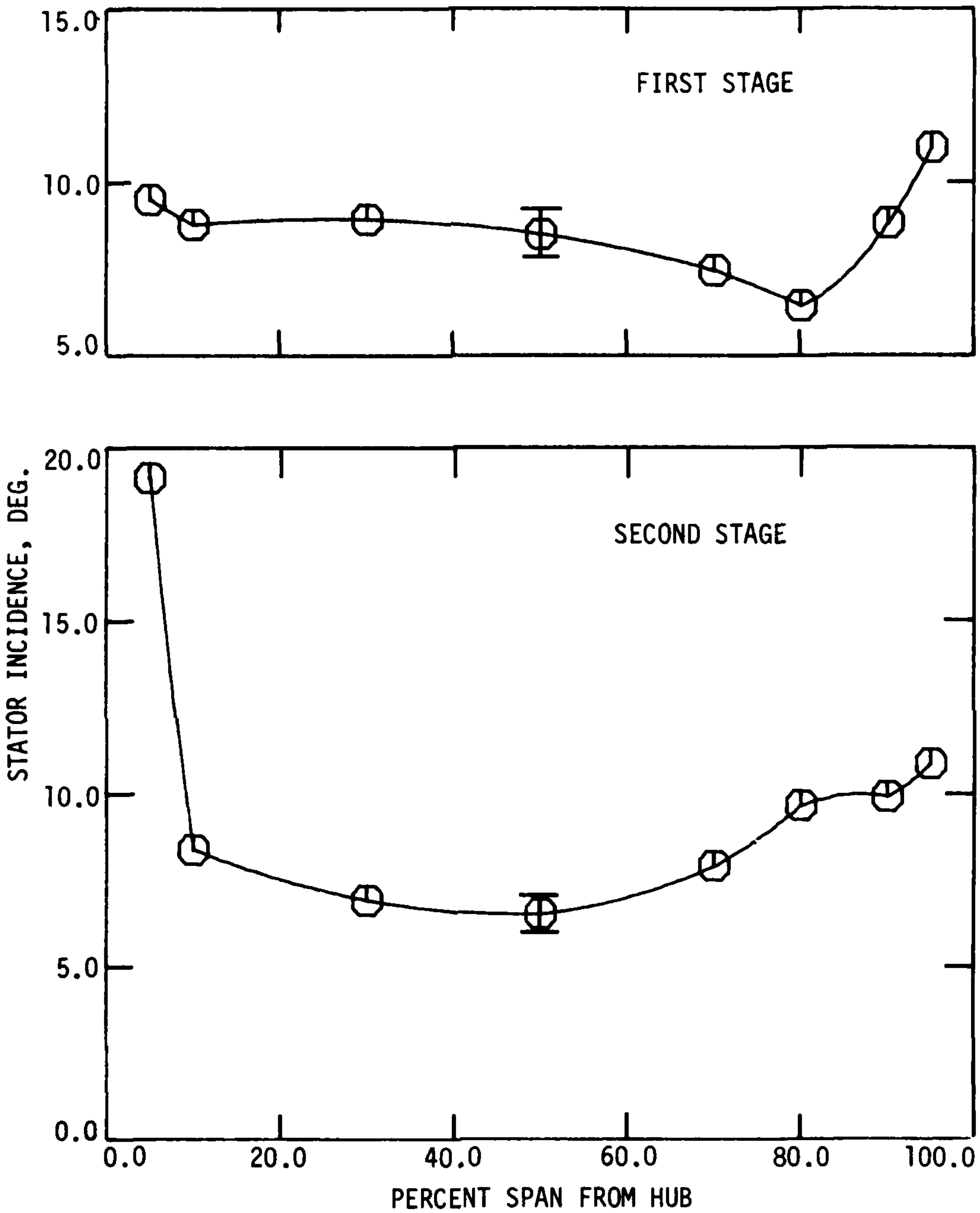


(g) STATOR INCIDENCE

Figure 4.1 continued.

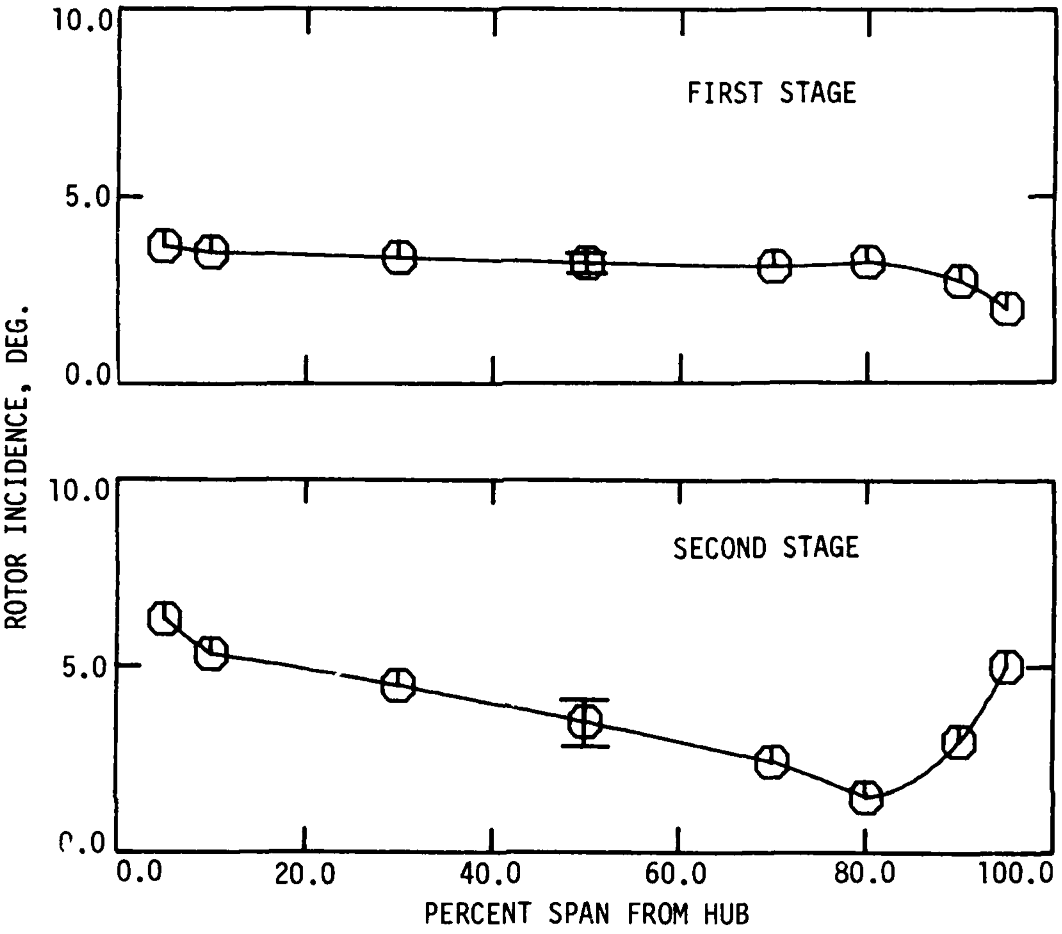


(h) ROTOR INCIDENCE

Figure 4.1 continued.

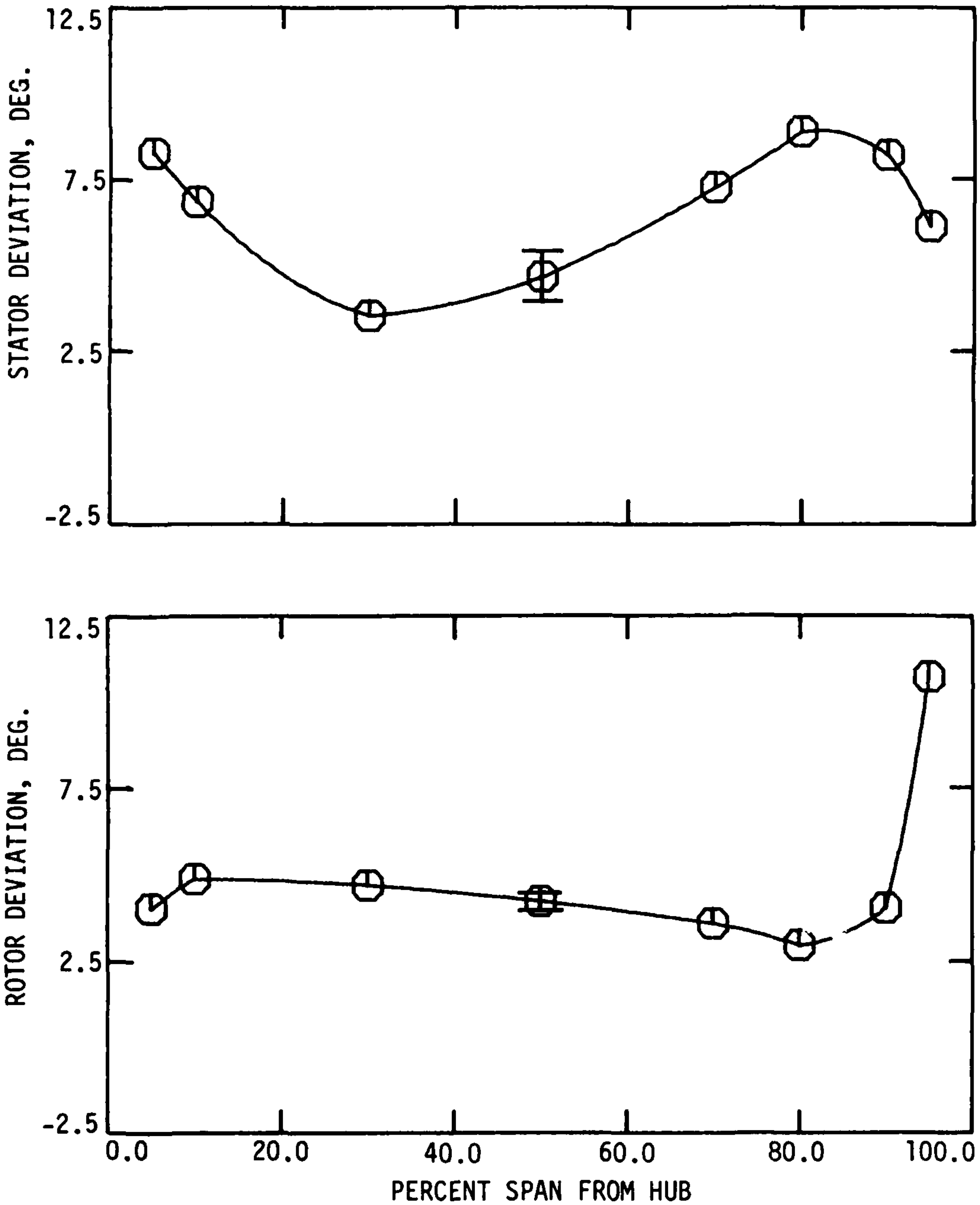


(i) STATOR AND ROTOR DEVIATION

**Figure 4.1 concluded.**

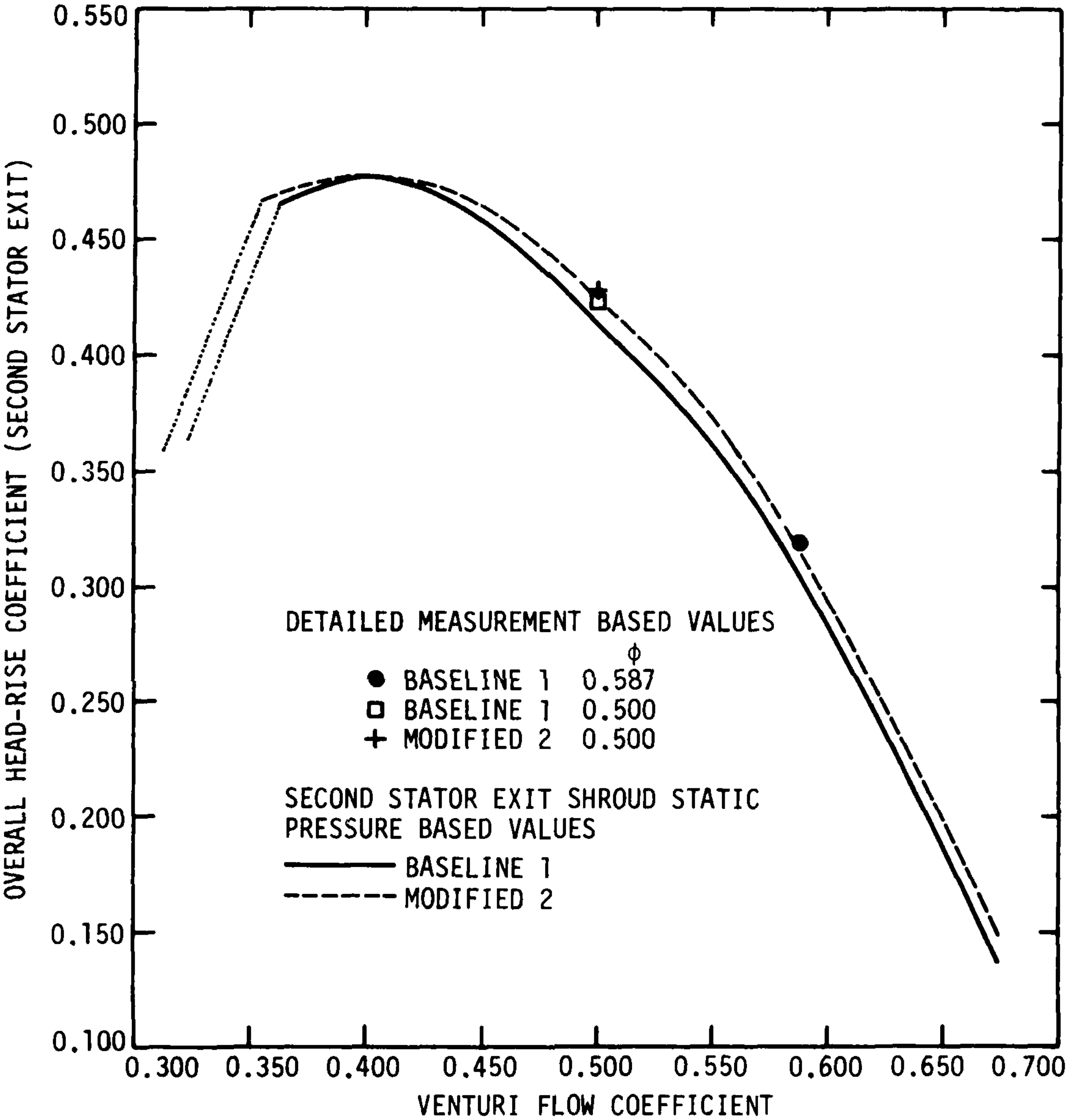


(a) OVERALL HEAD-RISE (SECOND STATOR EXIT)

Figure 4.2 Overall performance parameter variation with flow coefficient.

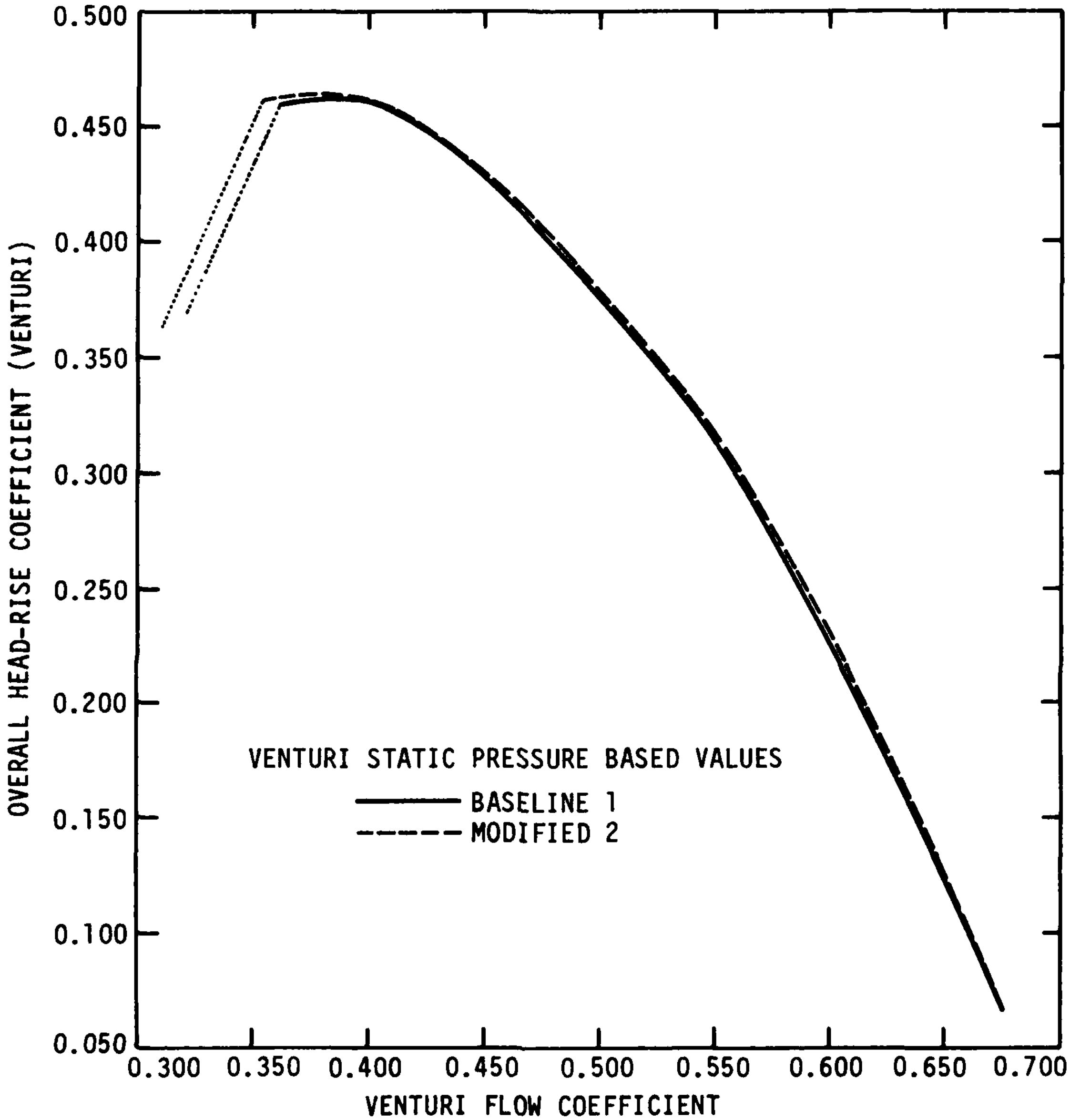


(b) OVERALL HEAD-RISE (VENTURI)

**Figure** 4.2 continued.

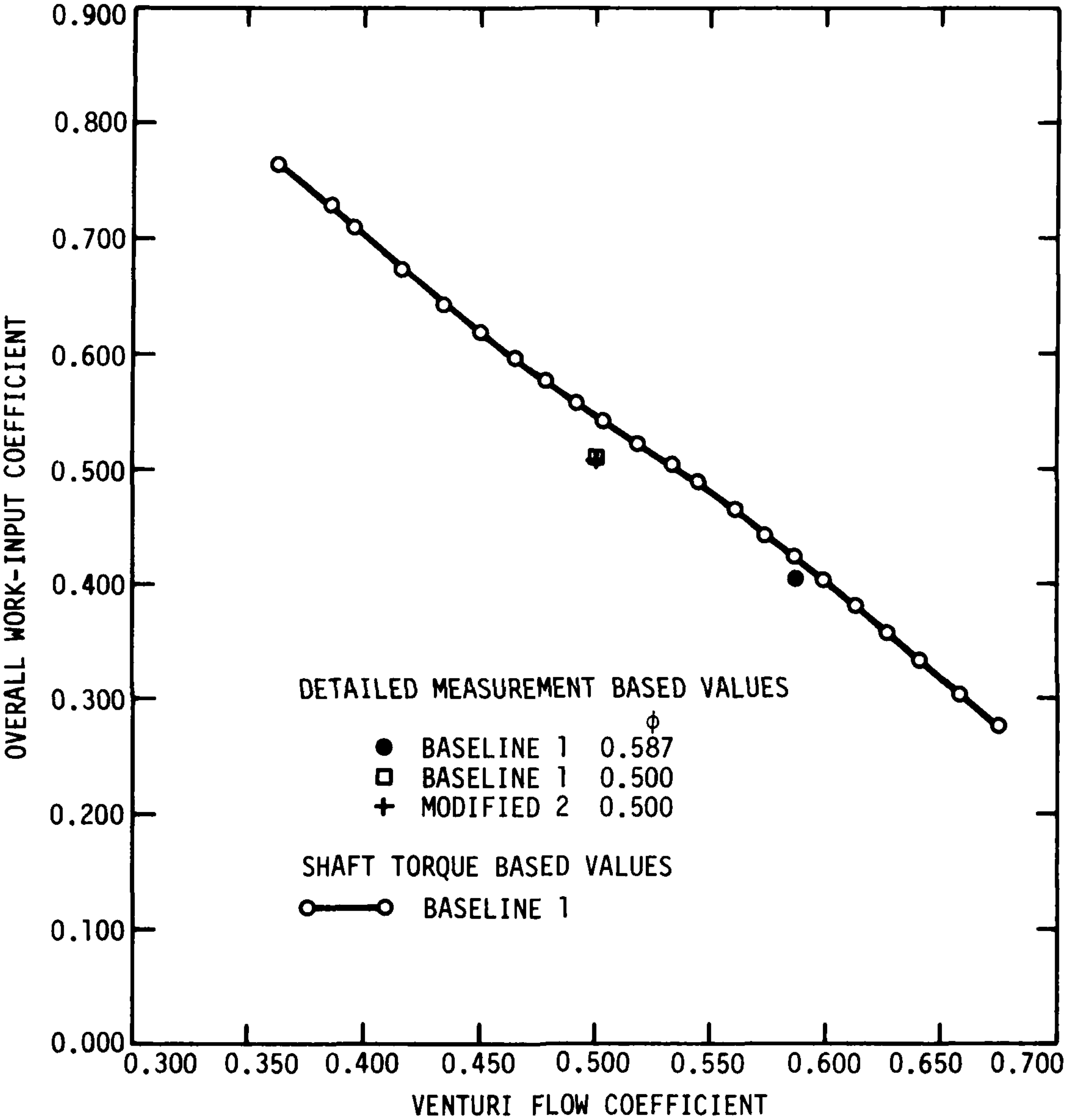

(c) OVERALL WORK-INPUT

Figure 4.2 continued.

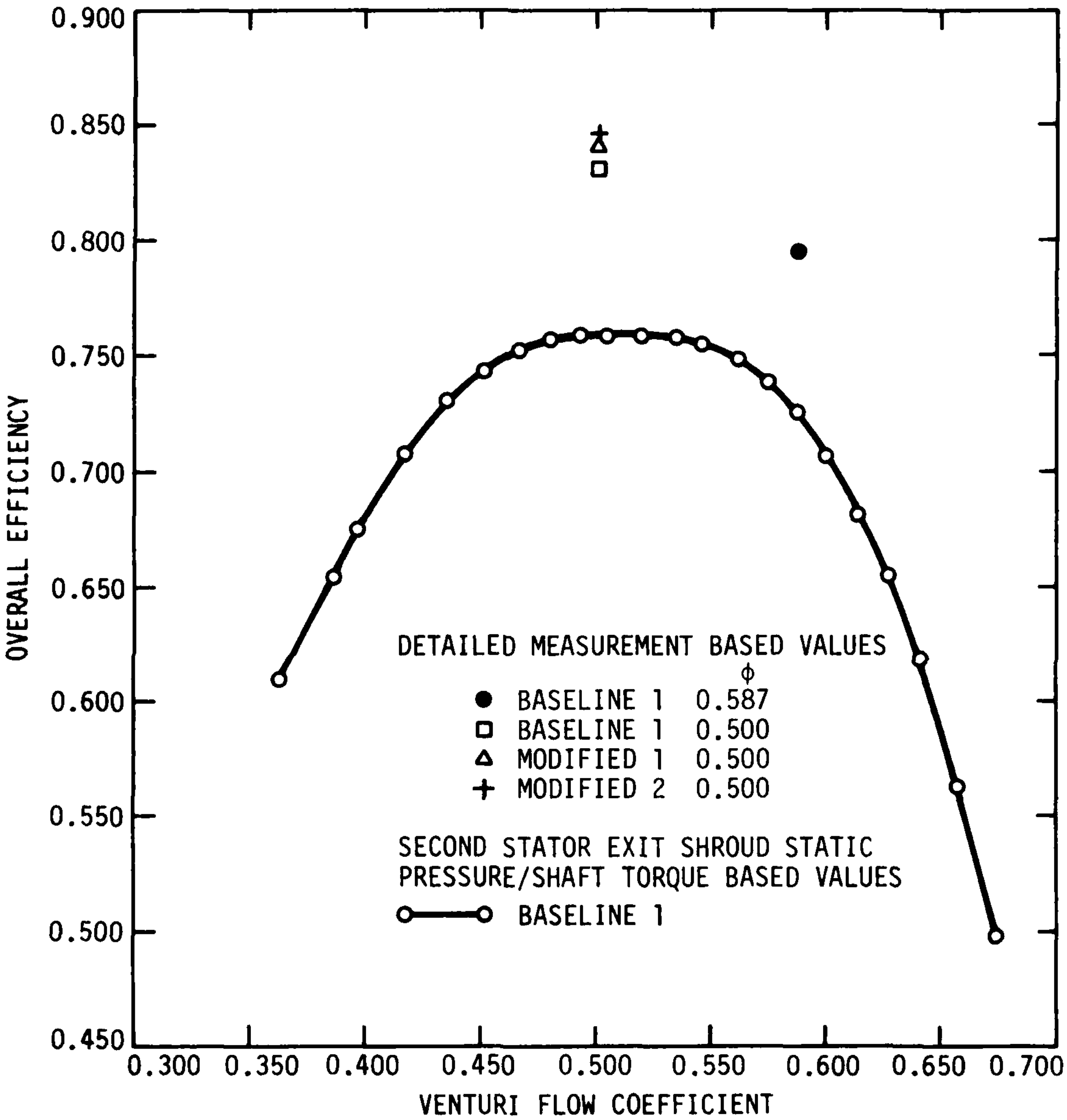


(d) OVERALL EFFICIENCY

**Figure** 4.2 concluded.

figure also includes data based on detailed measurements. Detailed measurement-based values are those radially mass-averaged overall performance quantities computed from the more extensive Kiel/cobra probe data acquired at selected flow rates.

The overall head-rise curves (Figure 4.2(a) and (b)) are based on data which could be rapidly measured over the entire operating range of the compressor (shaft speed = 2400 rpm). In particular, casing static-pressure measurements were obtained at the second stator exit and at the venturi meter throat for various flow rates and from these data the second stator-exit and venturi overall head-rise coefficients were calculated (Eqs. 8.51 and 8.52, respectively).

The second stator exit shroud static-pressure based head-rise curves in Figure 4.2(a) are only fair approximations to "actual" overall head-rise curves; the detailed measurement-based values included on the map are not coincident with any of the curves. The main reason for the discrepancy is that the measured shroud static-pressure is not sufficiently representative of the actual passage static pressure. These curves must, thus, be used with caution when comparing head-rise performance between different compressor builds. The curves in Figure 4.2(a) indicate differences in head-rise performance between the baseline 1 and modified 2 builds which are similar in magnitude to the discrepancy between the curves and their respective detailed measurement-based values at flow coefficient = 0.500. Further, the detailed measurement values show that the accepted difference in head-rise performance between the baseline 1 and modified 2 builds is smaller than the two curves might imply.

The venturi throat static-pressure based head-rise curves in Figure 4.2(b) seem to provide a better comparison of head-rise performance of the different compressor builds. The venturi flow is well "mixed out," with the measured throat wall static pressure being representative of the passage static pressure. However, since these curves include losses between the compressor exit and the venturi meter throat, they involve substantially lower head-rise values.

Several conclusions regarding the head-rise performance maps in Figure 4.2(a) and (b) follow:

- The second stator exit shroud static-pressure based head-rise curves (Figure 4.2(a)) are approximate indicators of overall head-rise performance for the compressor. These curves should be used with great caution only for comparing the different compressor builds.
- The venturi static-pressure based head-rise curves (Figure 4.2(b)) provide a better comparison of overall head-rise performance for the different compressor builds. The observed differences, however, are small. The curves for all four compressor builds are not shown because they would be difficult to sort out at the graph scale used.
- The overall and detailed performance data indicate a head-rise benefit associated with the modified stator configuration.

- The stall-limit flow coefficient is significantly different between the baseline 1 and the modified 2 builds. (The baseline 2, modified 1, and modified 2 builds have a similar stall-limit flow coefficient). This difference, although significant, should not be used to establish definite conclusions presently since other unaccounted factors might be involved.

The overall work-input performance map (Figure 4.2(c)) provides a comparison of two types of data. The single curve is based on compressor drive-shaft torque data, and thus shows the overall work-input requirement of the baseline 1 compressor build with mechanical losses included. The detailed measurement-based data show the aerodynamic overall work-input (conventional "ideal" head-rise) of two different compressor builds at fixed operating points. These data indicate that the aerodynamic overall work-input is considerably less than the shaft overall work-input. This is, of course, the expected qualitative result. Quantitatively, the aerodynamic overall work-input is approximately 90% to 95% of the shaft overall work-input. About 5% to 10% of the shaft overall work-input is due to mechanical losses, i.e., bearing friction. Because bearing friction is substantial, the shaft overall work-input curves were unacceptable for comparison of compressor builds. The day-to-day shifts in the shaft overall work-input curves for a single build were as large as the differences between builds. The curve trends for each specific build are, however, very similar. This consistency in curve trend is useful for establishing a representative overall efficiency curve for the compressor.

The shaft overall efficiency curve for the baseline 1 compressor build is presented in Figure 4.2(d). This curve is based on second stator-exit shroud static pressure and shaft torque measurements, and like the shaft overall work-input curve, is not useful for comparing builds. The curve is fairly accurate in trend, however, and therefore, indicates the approximate operating range for peak overall efficiency. Because they involve aerodynamic performance only, the detailed measurement-based efficiencies (aerodynamic overall efficiencies) are suitable for build comparisons. The apparent large gain in aerodynamic overall efficiency associated with using the modified stator configuration will be discussed later.

In Figure 4.3 is shown the variation of first rotor and first stator incidence with flow coefficient at mid-span. These data can be useful in combination with the overall efficiency data (Figure 4.2(d)) for estimating the peak aerodynamic efficiency operating point for the baseline 1 compressor build. In this case, peak aerodynamic efficiency is expected at a flow coefficient between 0.5 and 0.587. The shaft overall efficiency begins to drop slightly at flow coefficient = 0.55. However, this shaft overall efficiency curve is distorted relative to that of the anticipated aerodynamic overall efficiency curve, which would have had its peak shifted somewhat to the right of that shown in Figure 4.2(d) because mechanical losses become proportionately larger relative to the overall work-input as flow coefficient increases. Considering the above, an estimated flow coefficient of 0.550 (rotor incidence = 1 deg and stator incidence = 3 deg) is probably close to the peak aerodynamic efficiency operating point of the baseline 1 build.

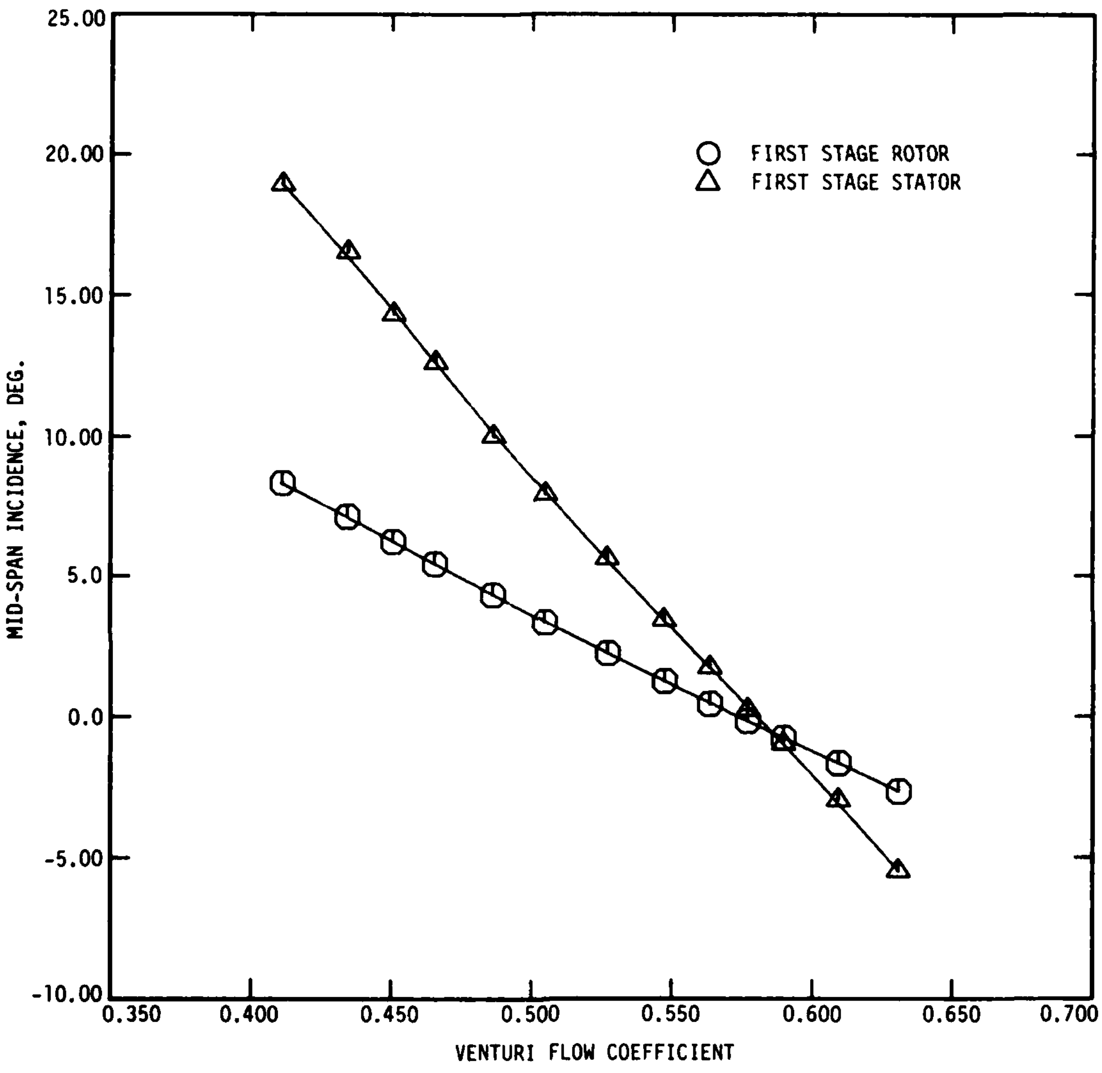


**Figure 4.3** **First stage incidence angle variation with flow coefficient at mid-span.**

Some remarks concerning the decision to test the different compressor builds at a flow coefficient of 0.500 rather than 0.550 seem appropriate at this time. The primary consideration in selecting this flow coefficient was to test at a flow rate which would result in distinct and observable variation in the performance (head-rise) of the different builds while at a reasonably high (near peak) aerodynamic efficiency. Preliminary overall head-rise performance data for the baseline 1 and the modified 1 compressor builds available at the time the flow coefficient selection was made indicated that 0.5 was a good choice. At this flow coefficient the approximate overall head-rise curves indicated a significant head-rise difference associated with the two kinds of stator blades and overall efficiency values within the "flat" peak efficiency ranges involved.

## 4.3. Baseline 1 Compressor Build--Different Flow Rates

### 4.3.1. Design/Off-Design Performance Comparison

Results obtained for two operating points of the baseline 1 compressor build, design (venturi flow coefficient = 0.587) and off-design (venturi flow coefficient = 0.500), are presented and compared in this section. The sequence of presentation is as follows:

- rotor, stage, and overall head-rise
- stator loss
- stator incidence and deviation

- ideal head-rise, rotor loss, and rotor incidence and deviation
- rotor, stage, and overall hydraulic efficiencies
- mass-averaged performance

4.3.1.1. Head Rise

Spanwise variations of circumferential-mean head-rise performance are presented in Figure 4.4. Conventional rotor, stage, and overall head-rise curves are shown in Figure 4.4(a), (b), and (c), respectively. In Figure 4.5 are shown rotor exit total-head values, normalized by a single mass-averaged total-head value at the rotor inlet. Figure 4.5 thus provides a comparison of the first and second rotor exit total-head distributions on a common (constant inlet total-head) basis.

The rotor head-rise data are discussed first. The following trends can be noted:

- At design flow, the first and second rotors have different spanwise trends in head rise.
- At off-design flow, both rotors have similar spanwise trends in head rise.
- At both flow rates, the first rotor involves more head rise than the second rotor over most of the span.
- The spanwise trends in first rotor head rise are different for the two flow rates.
- The spanwise trends in second rotor head rise are similar for the two flow rates.
- Near the hub and tip, head-rise values can change abruptly.

The dissimilarity in spanwise trends in head rise for the first and second rotors at design flow is in contrast to the similarity in

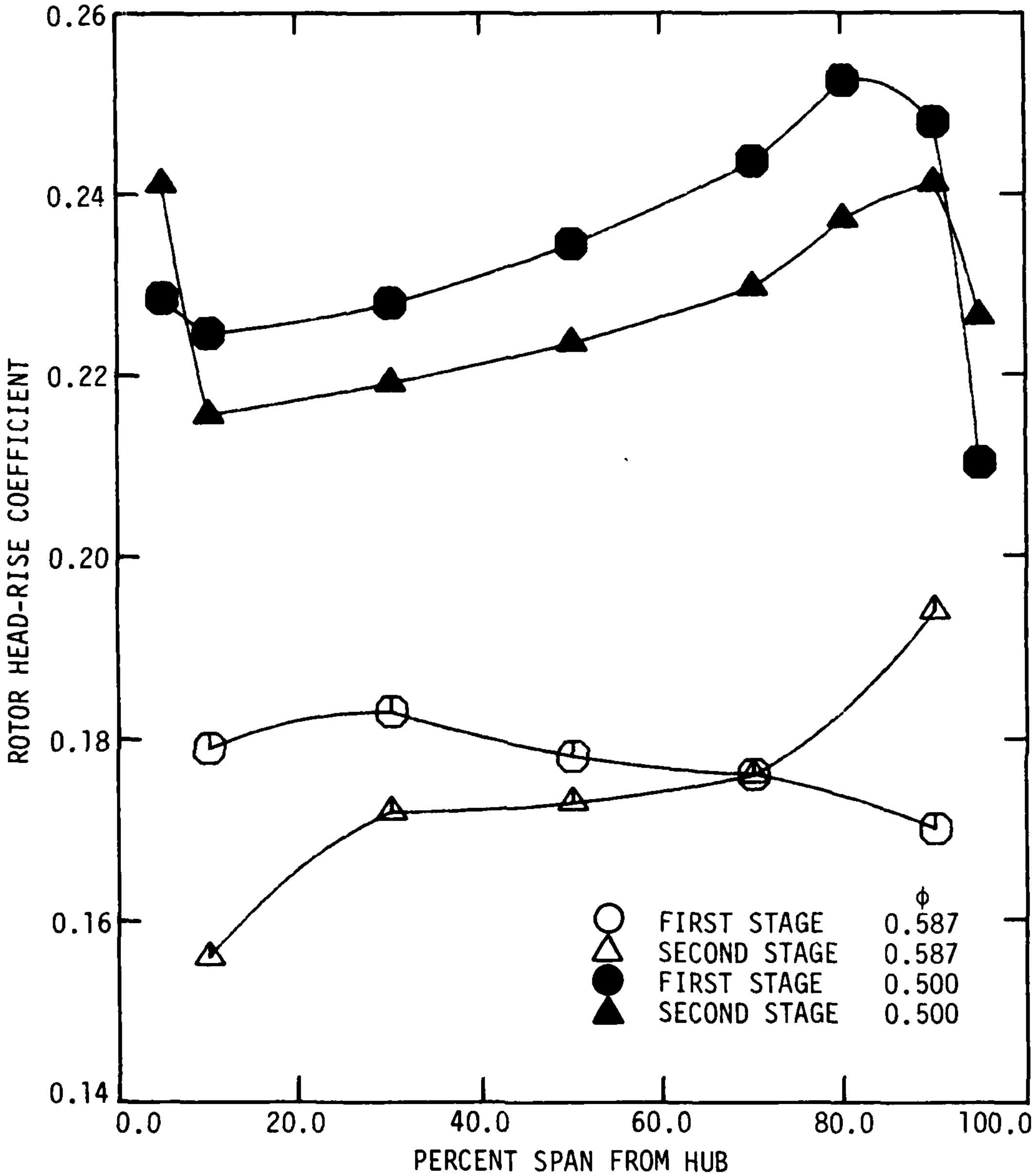


(a) ROTOR

Figure 4.4 Spanwise distribution of circumferential-mean head-rise coefficients for the baseline 1 compressor build at the design ($\phi$ = 0.587) and the off-design ($\phi$ = 0.500) operating points.

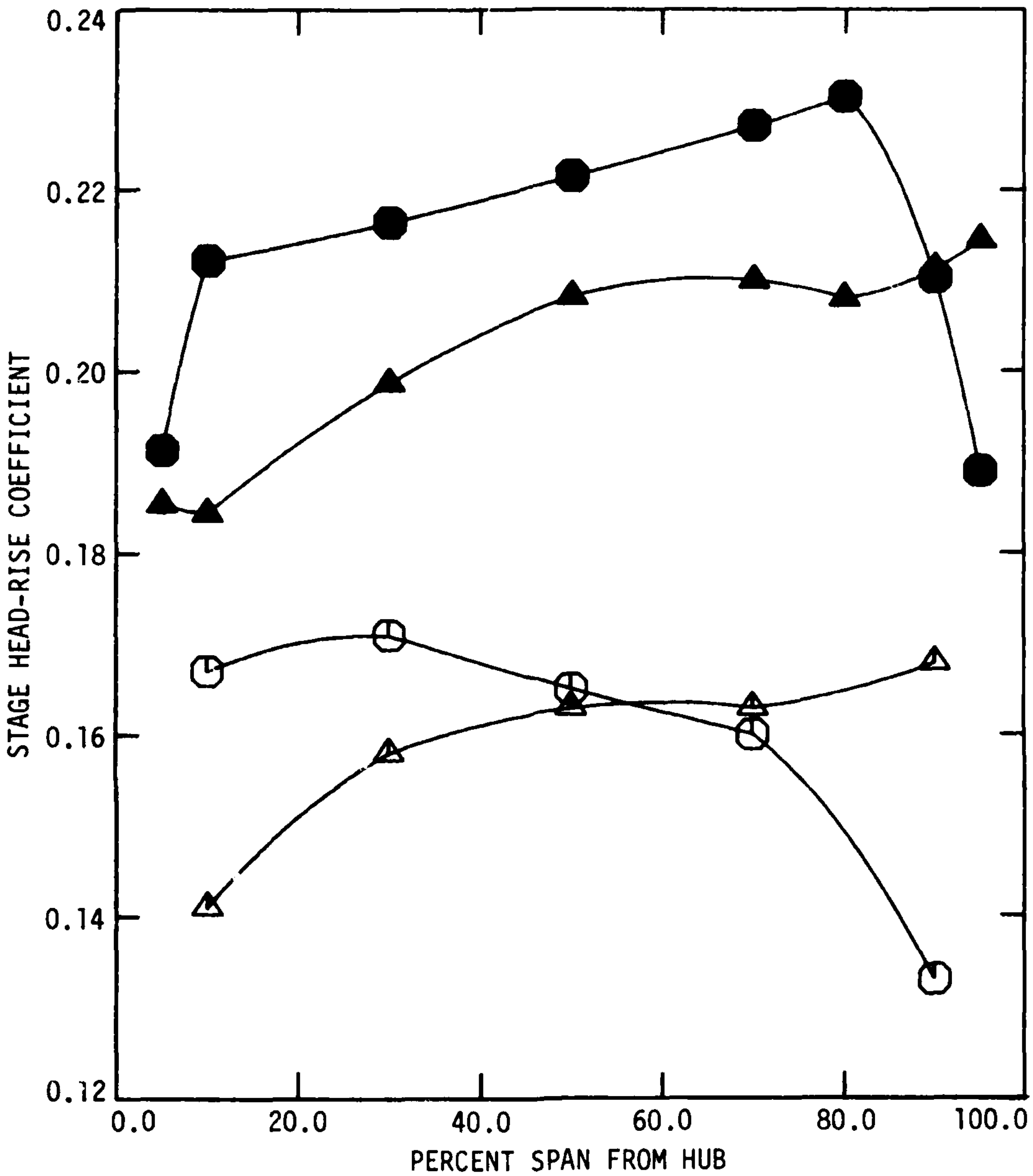

(b) STAGE

Figure 4.4 continued.

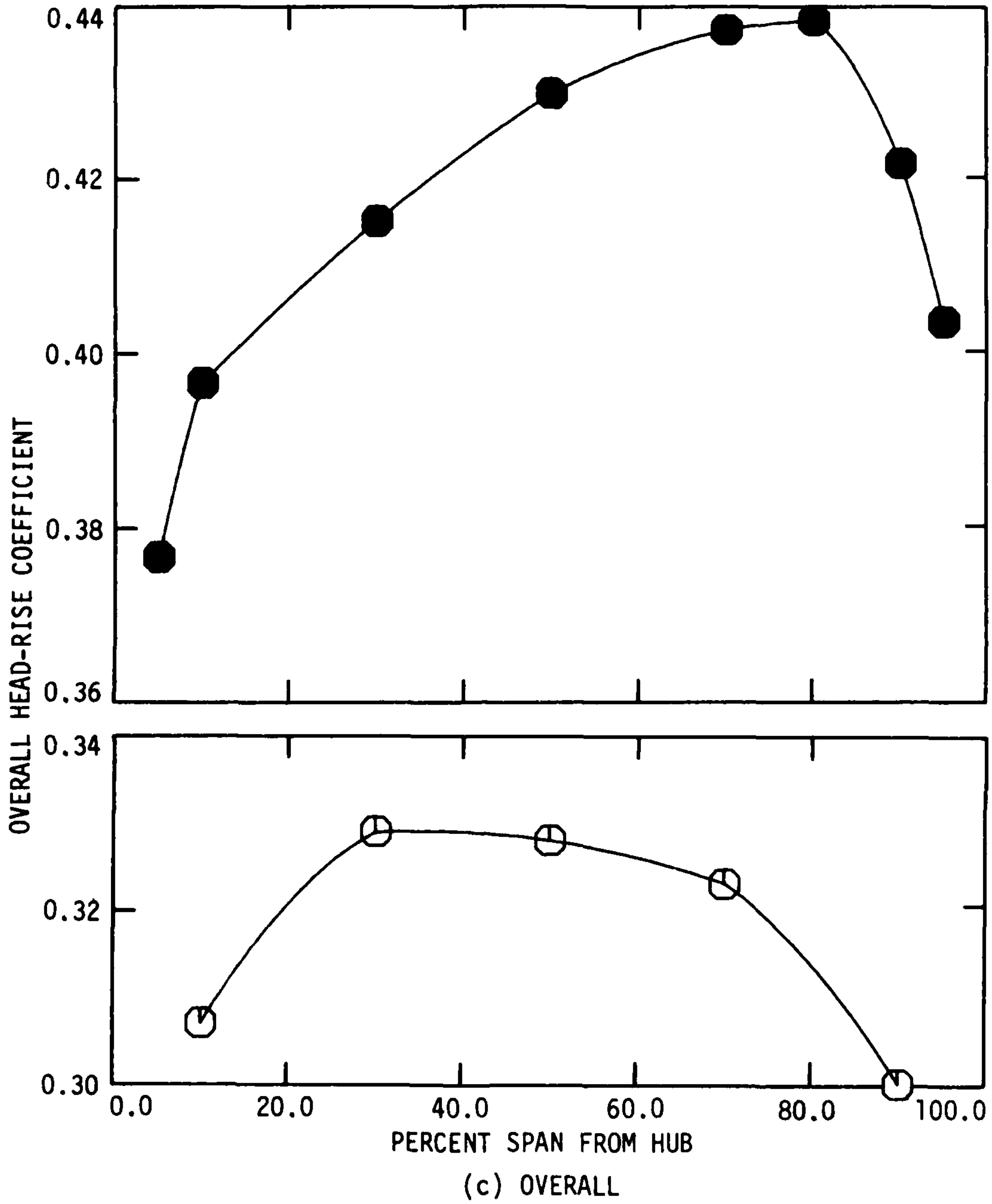


Figure 4.4 concluded.

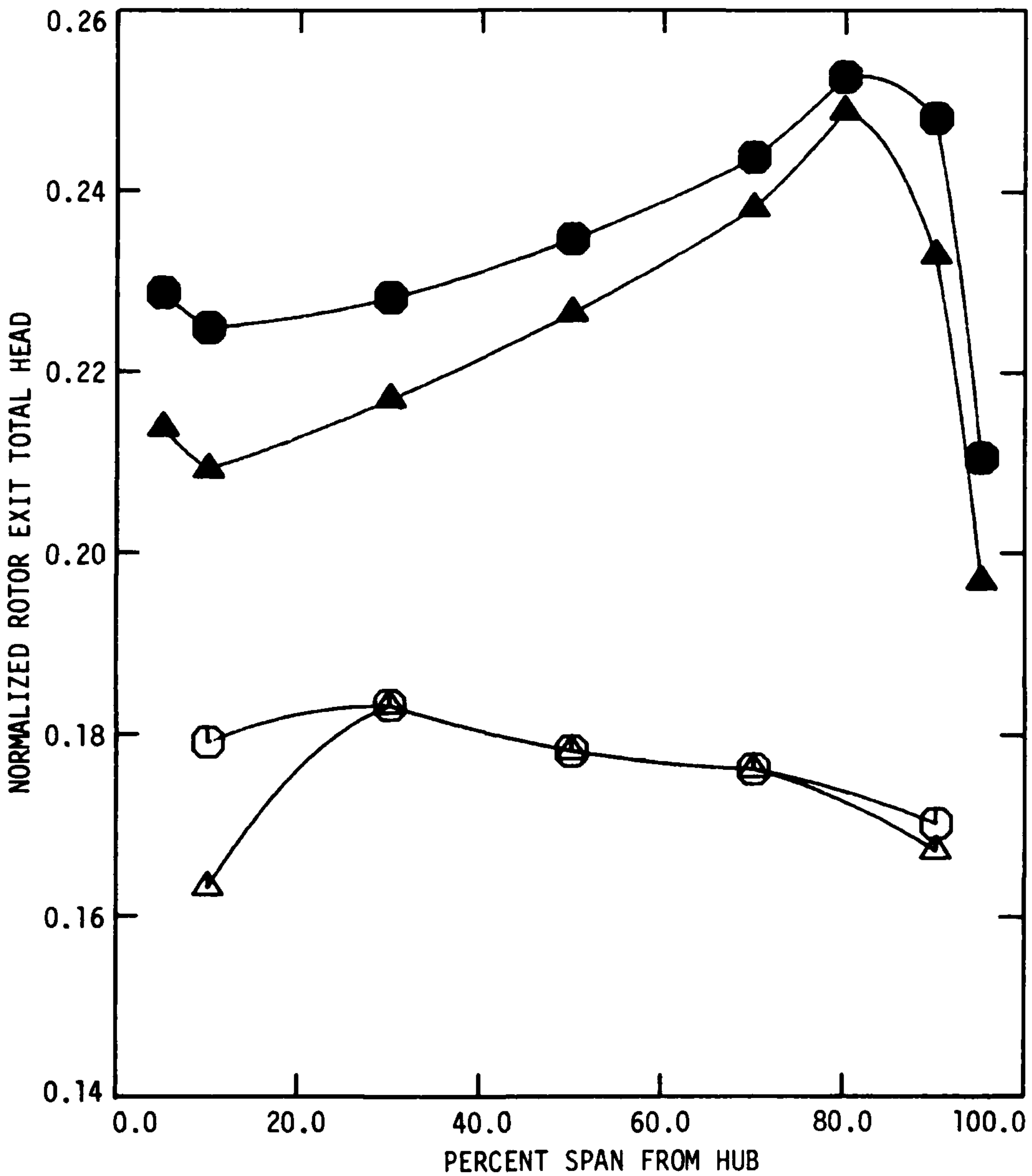


Figure 4.5 Spanwise distribution of normalized circumferential-mean rotor exit total-head values for the baseline 1 compressor build at the design ($\phi$ = 0.587) and the off-design ($\phi$ = 0.500) operating points.

these trends at off-design flow. This deserves further comment. Figure 4.5 demonstrates how the first and second rotor exit total-head distributions over the span of the blades are similar even though the head-rise distributions may not be. Thus, the spanwise trends in second rotor conventional head-rise (Figure 4.4(a)) are appproximately similar to the spanwise trends in first stator loss. This conclusion is best demonstrated in equation form using the definitions of the rotor head-rise and the stator loss coefficients. The second rotor head-rise coefficient can be written as follows:

$$\psi_{2R} = \frac{\omega_{1S}\bar{V}^2_{1,1S}}{2U_t^2} + \frac{\left(\bar{H}_{2,2R} - \bar{H}_{2,1R}\right)}{U_t^2} \qquad 4.1$$

For similar trends in the distributions of first and second rotor exit total-head values, the second term on the right-hand side of this equation is approximately constant over the blade span. This being the case, the second rotor head-rise will vary spanwise as the first stator loss does. Exact proportionality does not exist because the first stator inlet velocity varies over the blade span, especially near the hub and tip where the second rotor head-rise and first stator loss trends become most dissimilar.

These observations on rotor performance can be summarized:

- The spanwise trends in rotor exit total-head are similar between stages for a given operating point.
- These trends differ with flow rate variation.

- The rotor tends to compensate for variations in the spanwise distribution of total head at its inlet. That is, the rotor exit-flow similarity between stages exists despite the differences between the first and second rotor inlet conditions.
- There is an approximate relationship between the spanwise trend in second rotor head-rise and the spanwise trend in first stator loss, except near the hub and tip.

Some of these results lend support to the so-called "repeating stage" concept as discussed, for example, by Smith [7]. Further, the relationship between the spanwise distributions of second rotor head-rise and first stator loss is not unreasonable. The spanwise distribution of stator loss is related to the stator blade wake distribution. Larger stator losses are associated with larger blade wakes. Thus, larger head rise through the second rotor is relatable to larger stator wakes, the implication being that larger stator wakes can experience more energy addition within the rotor since wake fluid resides longer in the rotor than does free-stream fluid. More data supporting this line of reasoning is presented in section 4.4 of this report.

The stage and overall head-rise performance data (Figure 4.4(b) and (c)) are discussed next. The stage head-rise distributions are similar to their corresponding rotor head-rise distributions, but also reflect the spanwise distribution of stator loss as expected.

The overall head-rise distributions also have a rotor basis for comparing spanwise trend. The spanwise trends in second rotor exit total-head (Figure 4.5) are similar to the spanwise trends of overall head rise. Each represent the exit conditions for the second rotor and the second stator, respectively. Any difference in shape of the second rotor exit total-head distributions and the overall head-rise distributions represents the influence of second stator losses.

Some general conclusions regarding the head-rise performance of the baseline 1 compressor operating at two different flow rates are now apparent:

- The spanwise trend in total head, as set up by the first rotor, does not change significantly for the fluid as it moves axially through the compressor.
- At design flow this trend is generally decreasing from hub to tip with a peak at 30% span from the hub.
- At off-design flow this trend is generally increasing from hub to tip with a peak at 80% span from the hub.

These general conclusions can also be drawn from the total-head contour maps for each blade row exit of the baseline 1 compressor as presented in Figures 4.6 and 4.7 for the design and off-design flows, respectively. A peculiar result can be noted at this time. In Figure 4.6 (design flow), the second rotor exit total-head contour map indicates two regions of lower total-head within one stator pitch over most of the span. This is surprising because only one lower total-head region was expected. This behavior was further investigated and the results are presented and discussed in section 4.3.2.

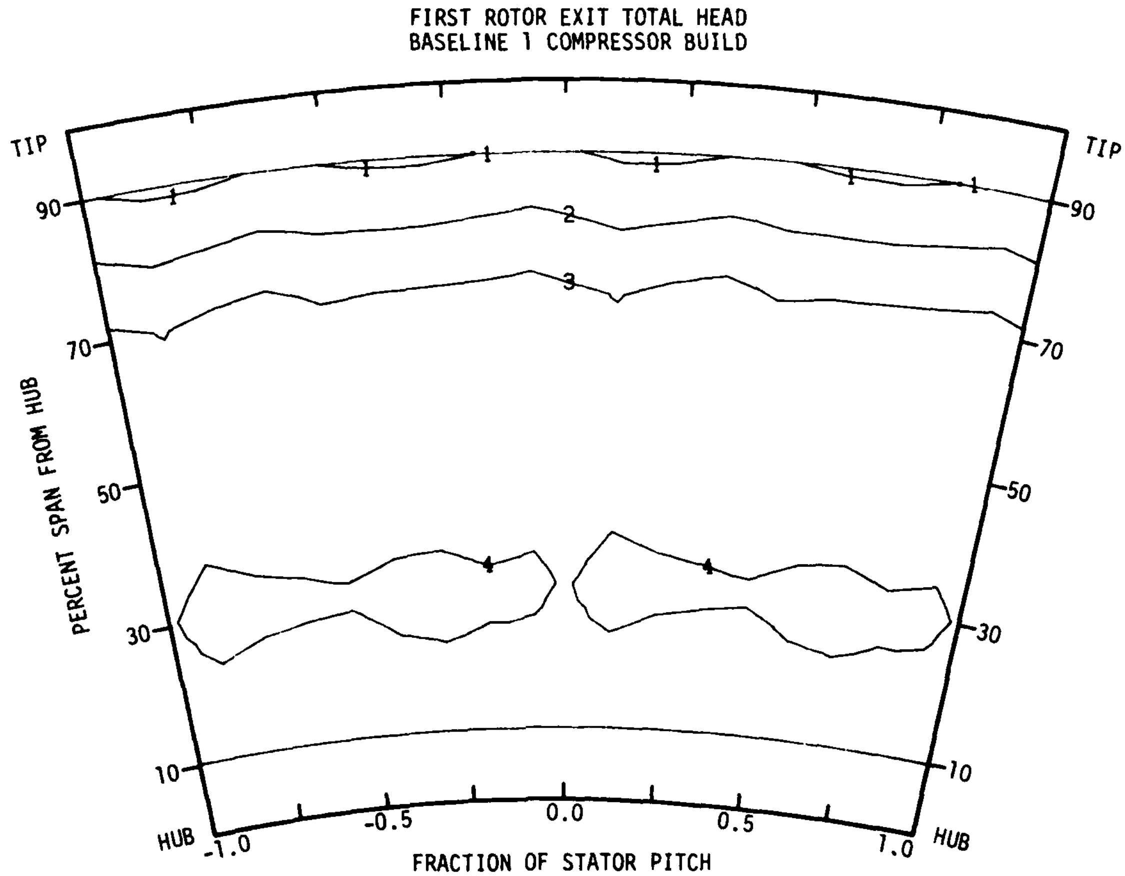


| CURVE LABEL | CURVE VALUE (N-M/KG) |
|---|---|
| 1 | 415 |
| 2 | 435 |
| 3 | 455 |
| 4 | 475 |

**Figure 4.6** Total-head contour maps for each blade row exit of the baseline 1 compressor build at the design operating point ($\phi = 0.587$).

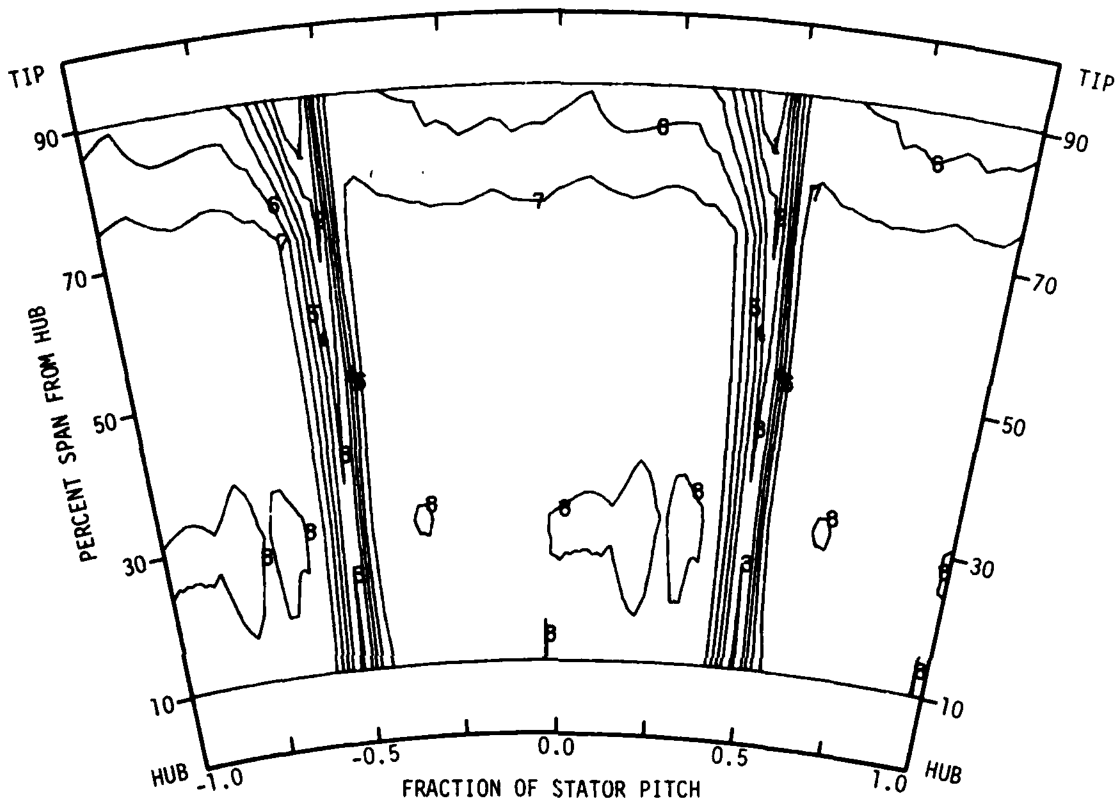


| CURVE LABEL | CURVE VALUE (N-M/KG) |
|---|---|
| 1 | 115 |
| 2 | 165 |
| 3 | 215 |
| 4 | 265 |
| 5 | 315 |
| 6 | 365 |
| 7 | 415 |
| 8 | 465 |

Figure 4.6 continued.

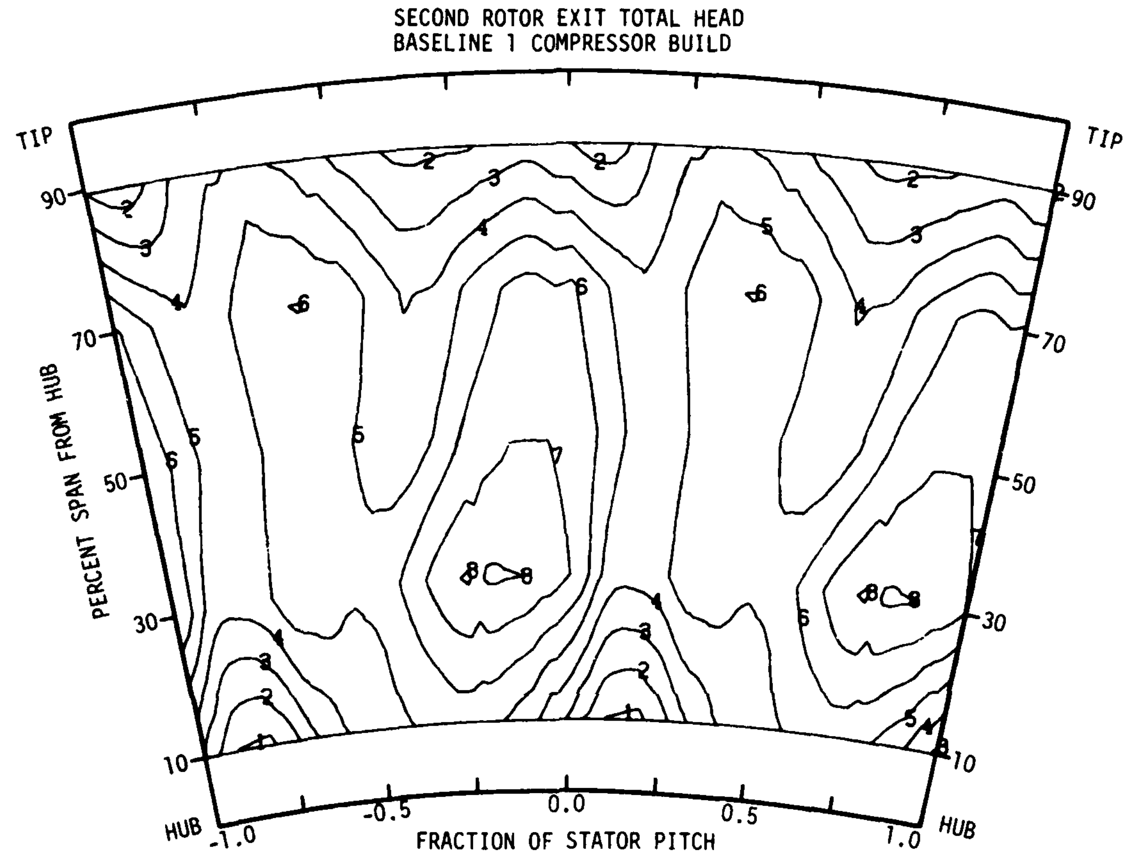


| CURVE LABEL | CURVE VALUE (N-M/KG) |
|---|---|
| 1 | 790 |
| 2 | 810 |
| 3 | 830 |
| 4 | 850 |
| 5 | 870 |
| 6 | 890 |
| 7 | 910 |
| 8 | 930 |

Figure 4.6 continued.

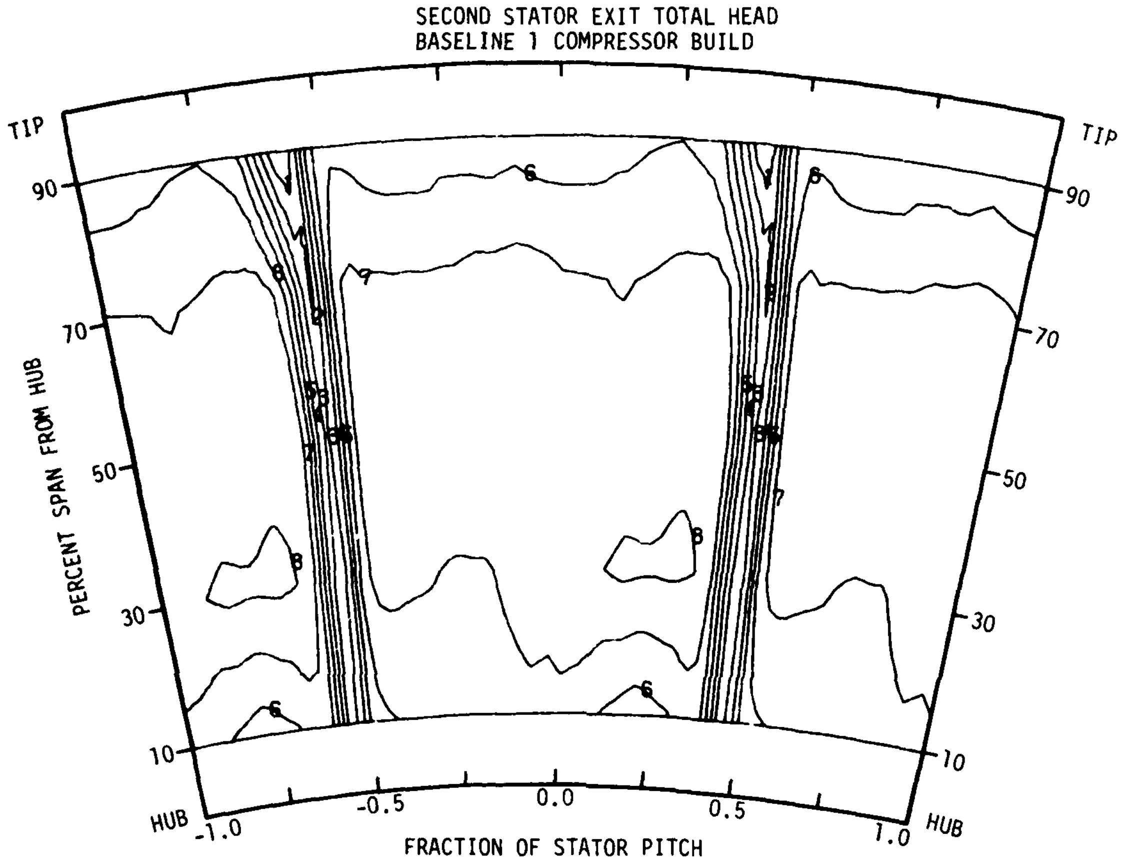


| CURVE LABEL | CURVE VALUE (N-M/KG) |
|---|---|
| 1 | 550 |
| 2 | 600 |
| 3 | 650 |
| 4 | 700 |
| 5 | 750 |
| 6 | 800 |
| 7 | 850 |
| 8 | 900 |

Figure 4.6 concluded.

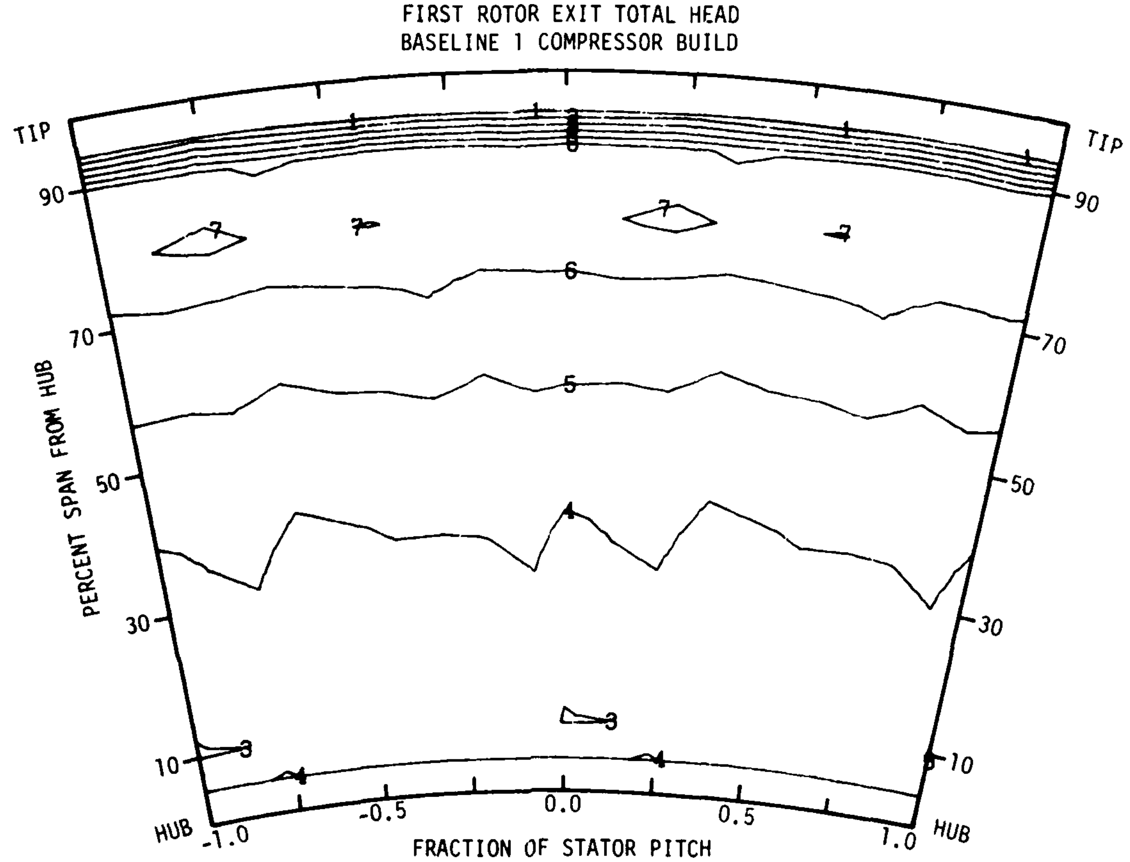


| CURVE LABEL | CURVE VALUE (N-M/KG) |
|---|---|
| 1 | 540 |
| 2 | 560 |
| 3 | 580 |
| 4 | 600 |
| 5 | 620 |
| 6 | 640 |
| 7 | 660 |

Figure 4.7 Total-head contour maps for each blade row exit of the baseline 1 compressor build at the off-design operating point ($\phi = 0.500$).

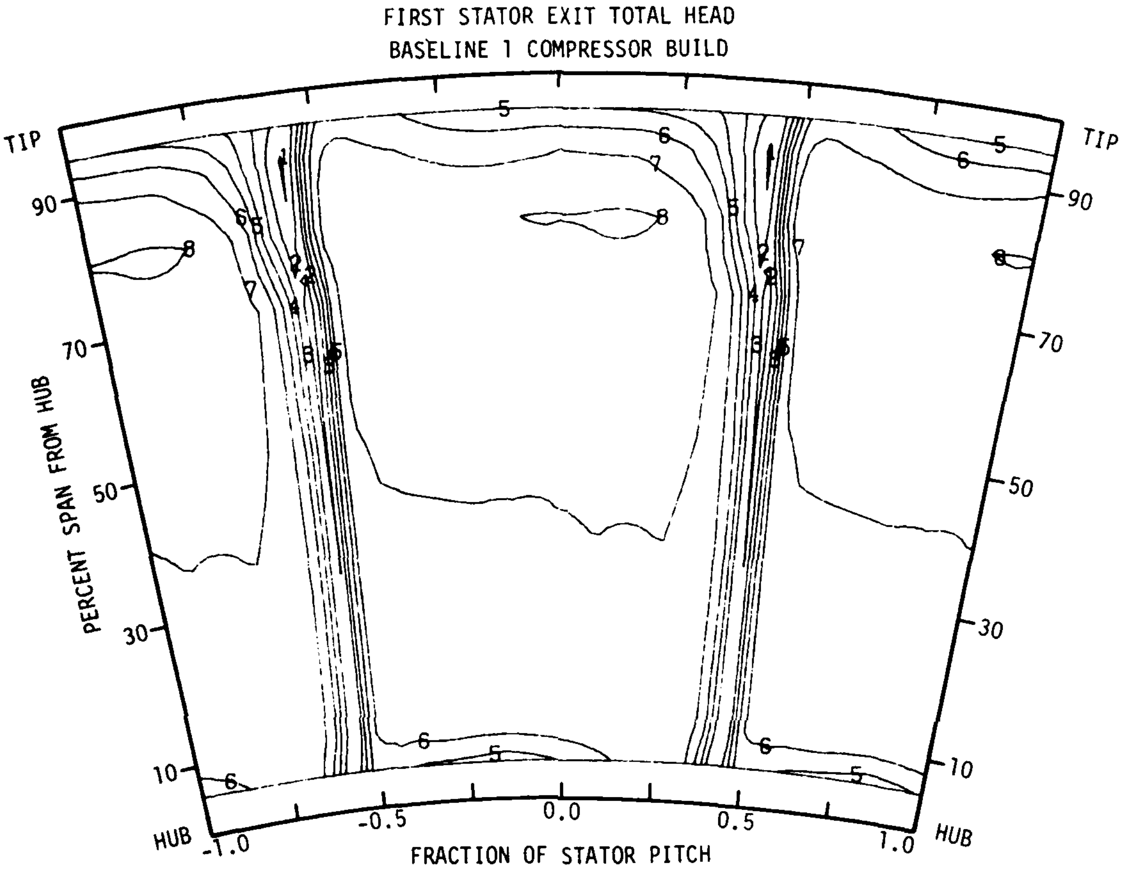


| CURVE LABEL | CURVE VALUE (N-M/KG) |
|---|---|
| 1 | 290 |
| 2 | 340 |
| 3 | 390 |
| 4 | 440 |
| 5 | 490 |
| 6 | 540 |
| 7 | 590 |
| 8 | 640 |

Figure 4.7 continued.

SECOND ROTOR EXIT TOTAL HEAD

BASELINE 1 COMPRESSOR BUILD

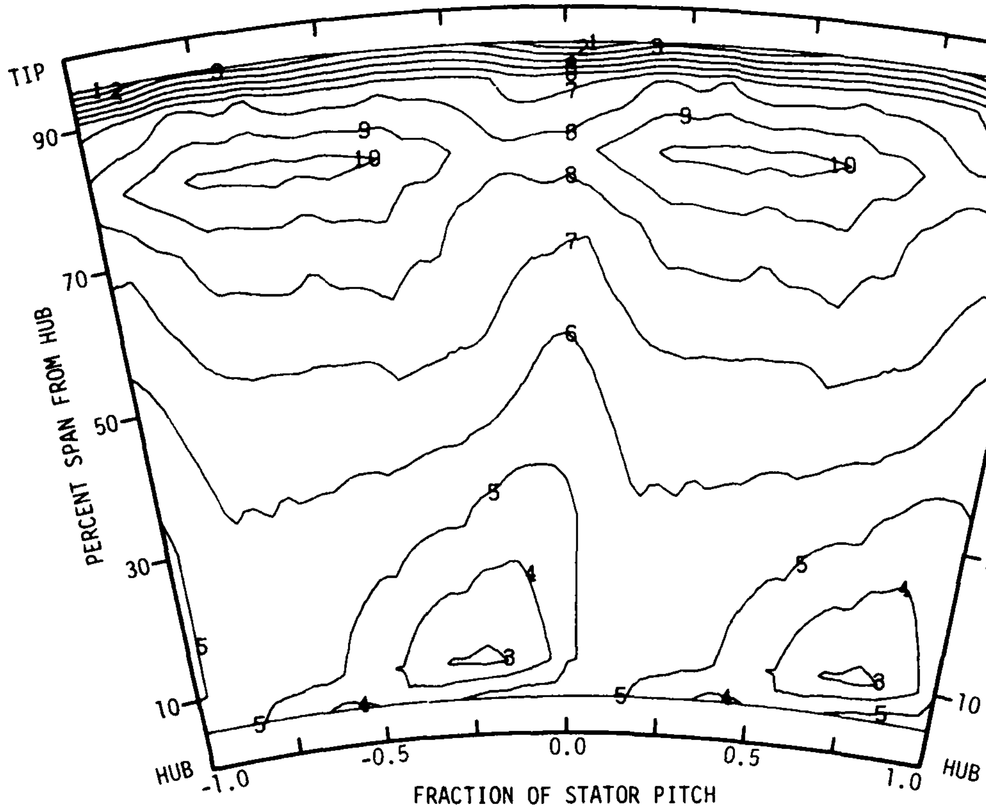


| CURVE LABEL | CURVE VALUE (N-M/KG) |
|---|---|
| 1 | 1050 |
| 2 | 1070 |
| 3 | 1090 |
| 4 | 1110 |
| 5 | 1130 |
| 6 | 1150 |
| 7 | 1170 |
| 8 | 1190 |
| 9 | 1210 |
| 10 | 1230 |

Figure 4.7 continued.

SECOND STATOR EXIT TOTAL HEAD
BASELINE 1 COMPRESSOR BUILD

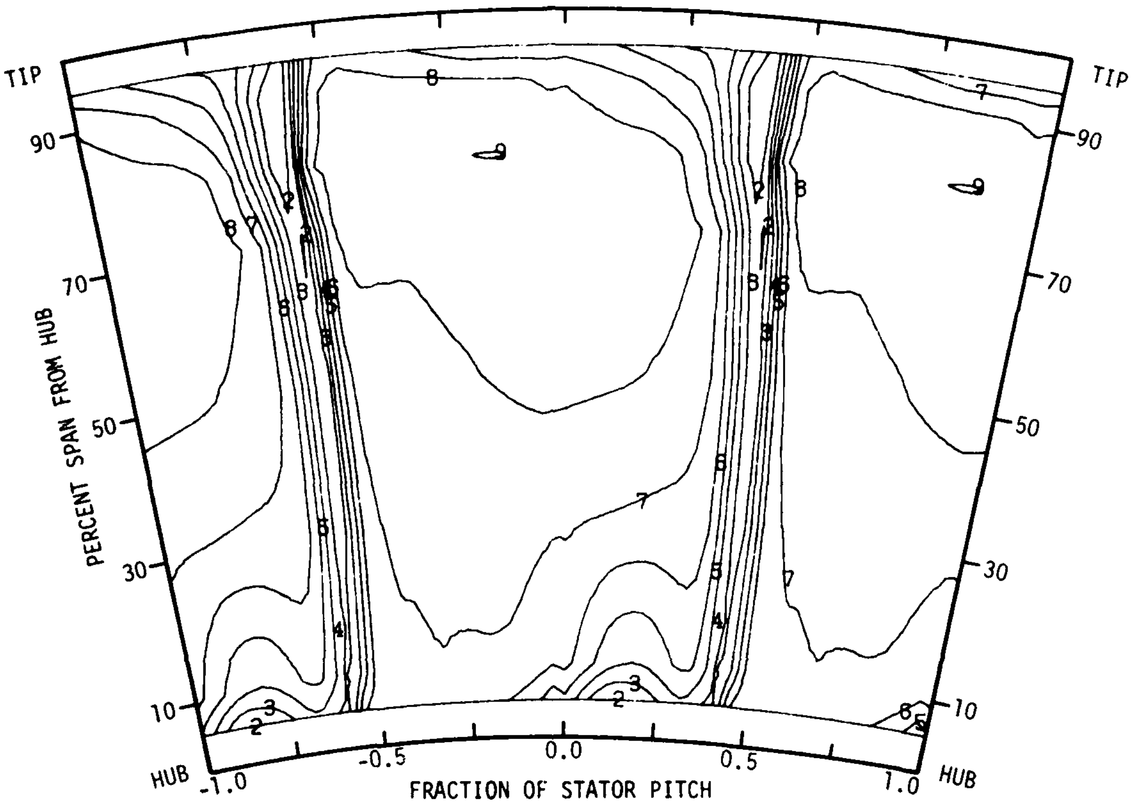


| CURVE LABEL | CURVE VALUE (N-M/KG) |
|---|---|
| 2 | 850 |
| 3 | 900 |
| 4 | 950 |
| 5 | 1000 |
| 6 | 1050 |
| 7 | 1100 |
| 8 | 1150 |
| 9 | 1200 |

Figure 4.7 concluded.

AD-A141 793 STATOR BLADE ROW GEOMETRY MODIFICATION INFLUENCE ON TWO-STAGE AXIAL-FLOW..(U) IOWA STATE UNIV AMES ENGINEERING RESEARCH INST D L TWEEDT ET AL. DEC 83 2/3

UNCLASSIFIED ISU-ERI-AMES-84179 AFOSR-TR-84-0418 F/G 21/5 NL

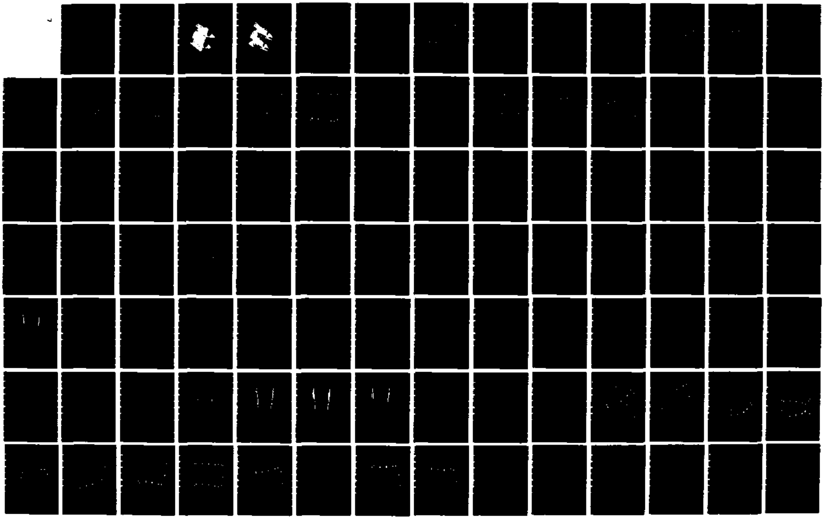

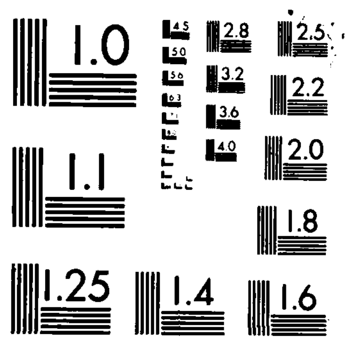


MICROCOPY RESOLUTION TEST CHART
NATIONAL BUREAU OF STANDARDS 1963 A

In Figure 4.8, immediately following the contour maps, are shown two total-head topographic (3-D) maps for the first and second stator exits at off-design flow. These maps may serve to help the reader better visualize the stator exit contour maps.

4.3.1.2. Stator Loss

Spanwise variations of circumferential-mean stator loss coefficients are presented in Figure 4.9. The first and second stator loss data are presented separately in Figure 4.9(a) and (b), respectively. In Figure 4.9(c), data for both stages are presented together for stage-to-stage comparison purposes.

An analysis of these graphs reveals several aspects of the baseline 1 build stator loss performance:

- For each stage, the spanwise trends in stator loss are similar for design and off-design flows.
- For each stage, the off-design flow stator losses are greater than the design flow stator losses.
- In all cases, the stator loss increases from mid-span to near-tip (90% span from the hub).
- The second stator loss increases from mid-span to the hub at both flow rates, but more so for the off-design flow rate. This is in contrast to the first stator loss behavior.
- Near the hub and tip, stator loss can change abruptly, increasing near the hub and decreasing near the tip.
- At design flow, the first stator loss is greater than the second stator loss over most of the span, except near the hub.

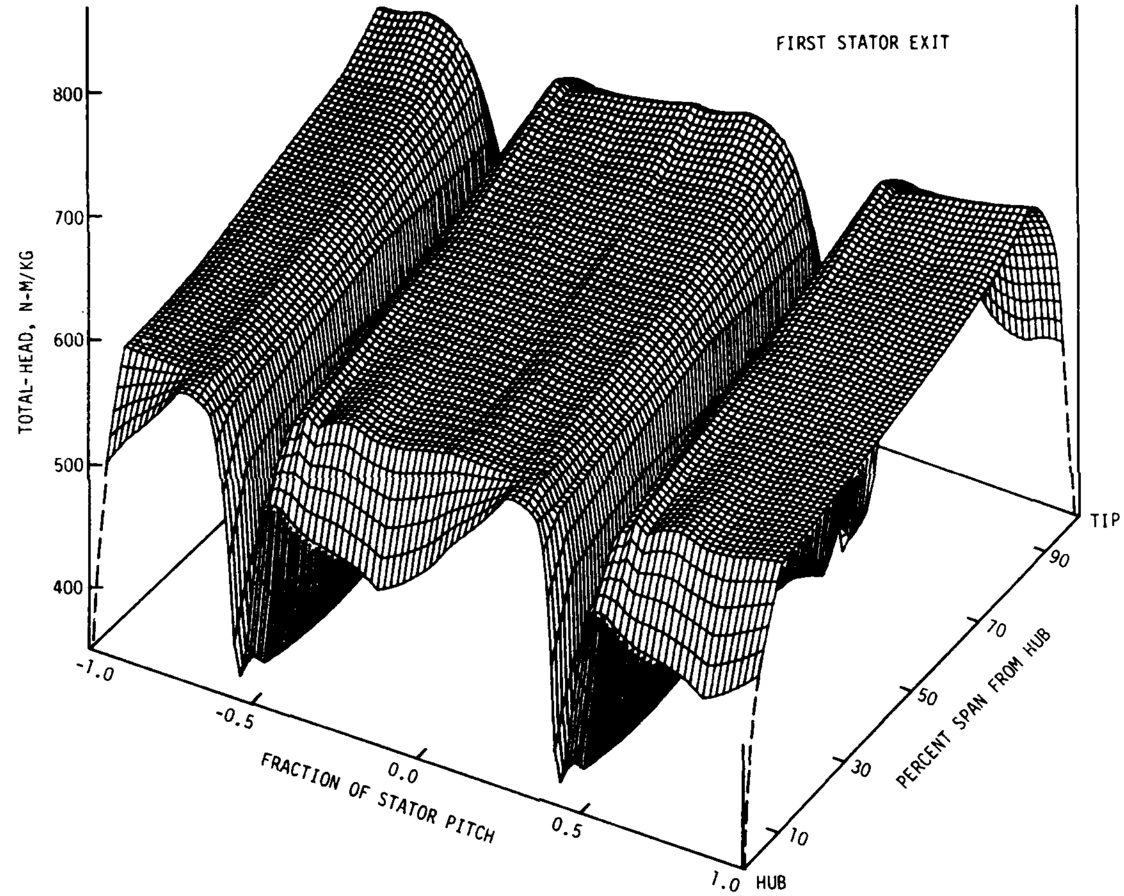


Figure 4.8 Total-head topographic maps for each stator row exit of the baseline 1 compressor build at the off-design operating point ($\phi$ = 0.500).

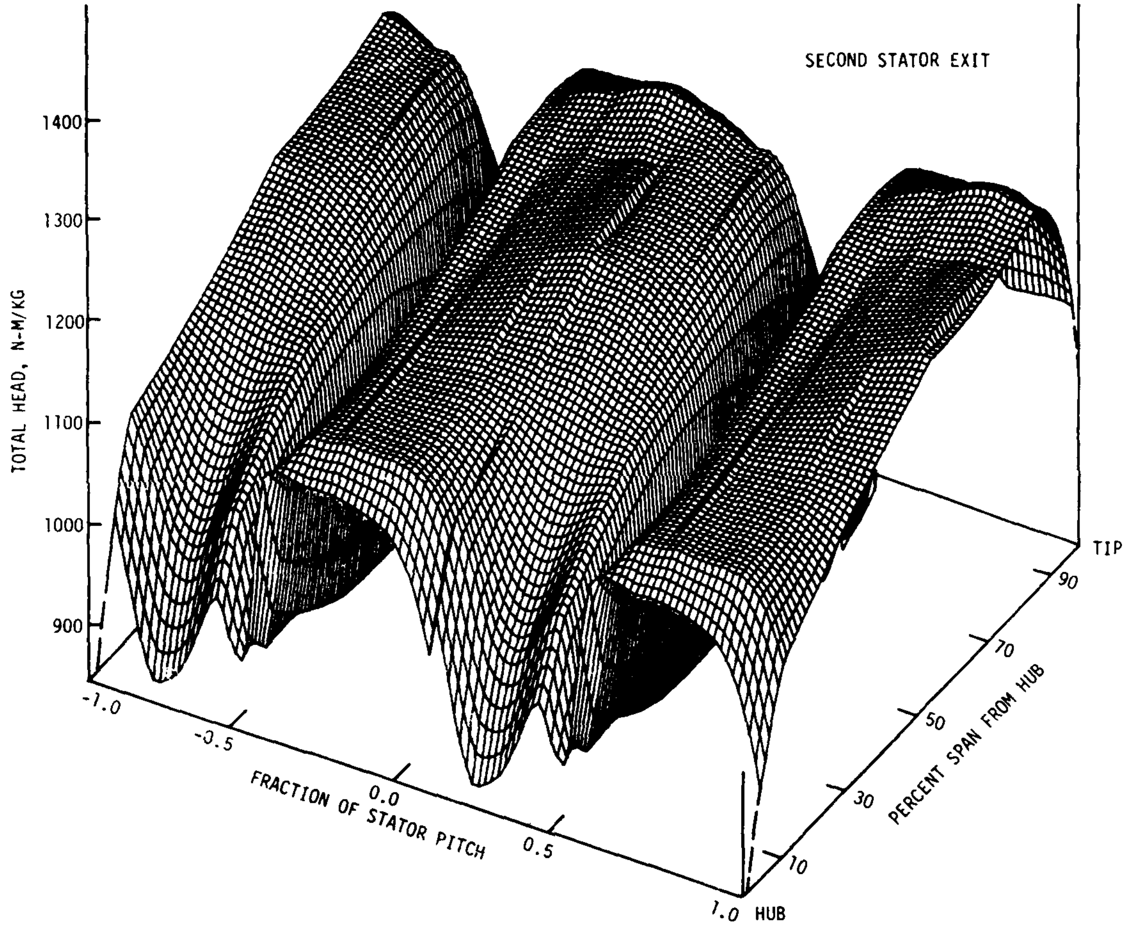


**Figure 4.8 concluded.**

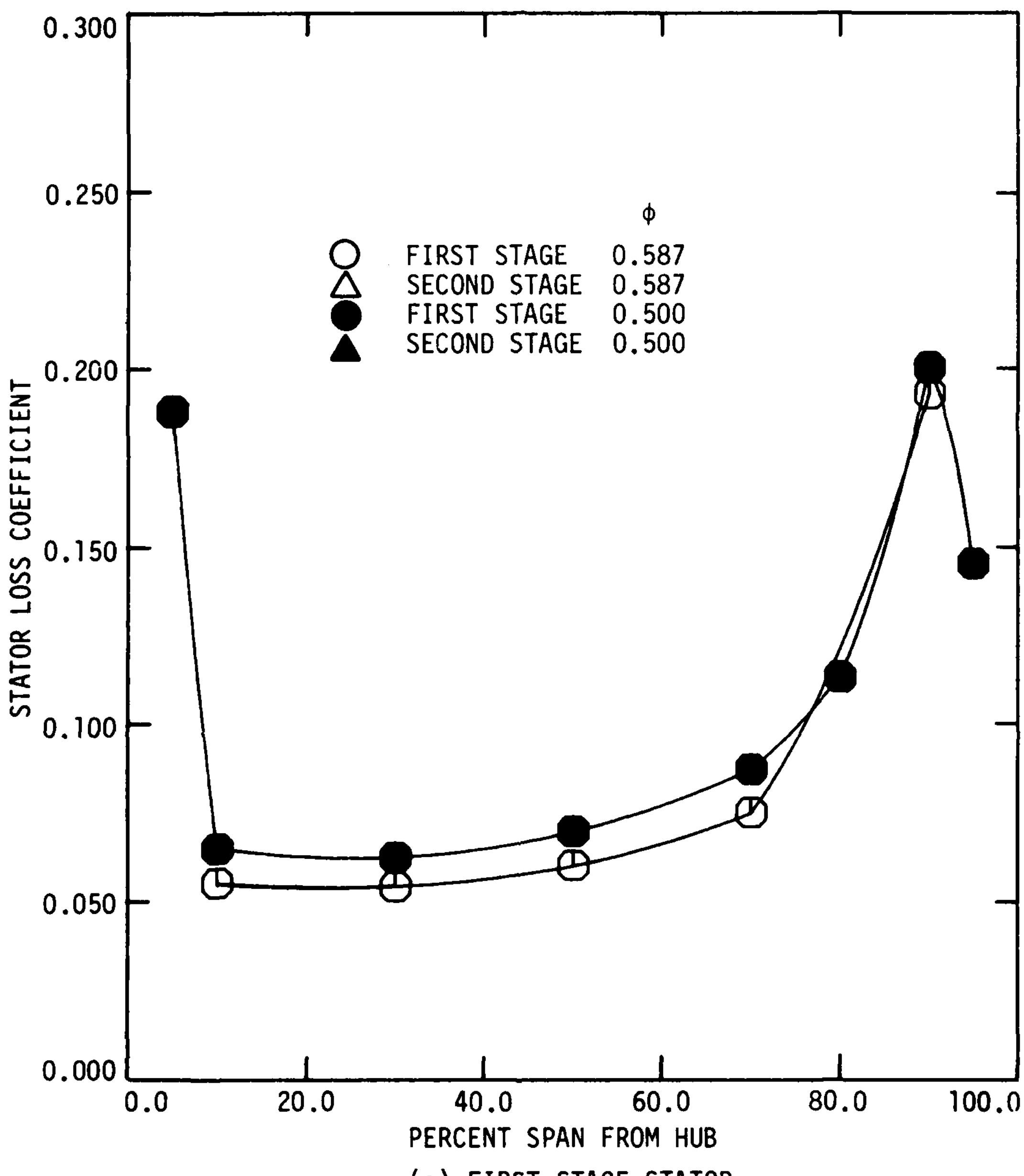


(a) FIRST STAGE STATOR

**Figure 4.9** Spanwise distribution of circumferential-mean stator loss coefficients for the baseline 1 compressor build at the design ($\phi$ = 0.587) and the off-design ($\phi$ = 0.500) operating points.

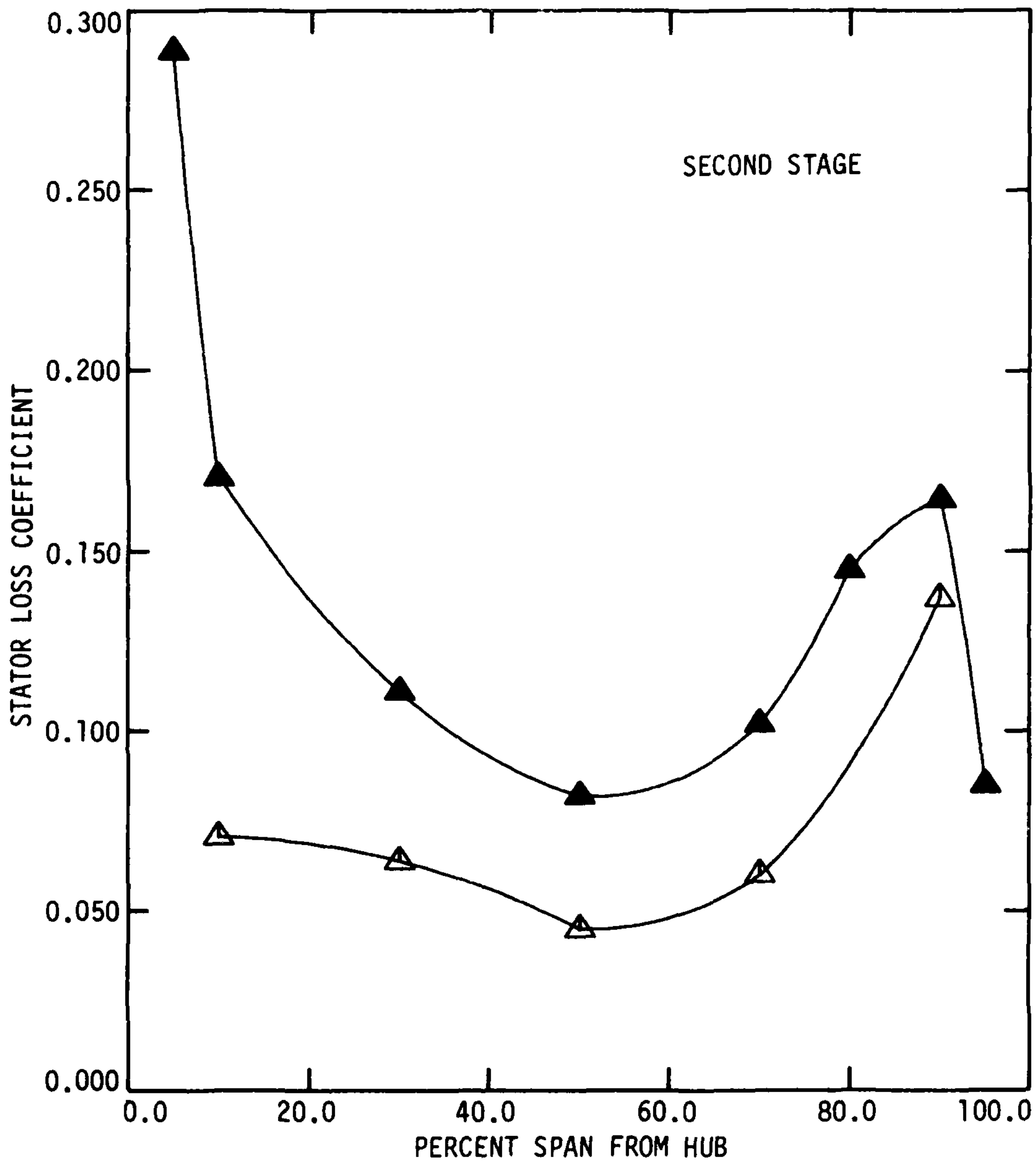


(b) SECOND STAGE STATOR

Figure 4.9 continued.

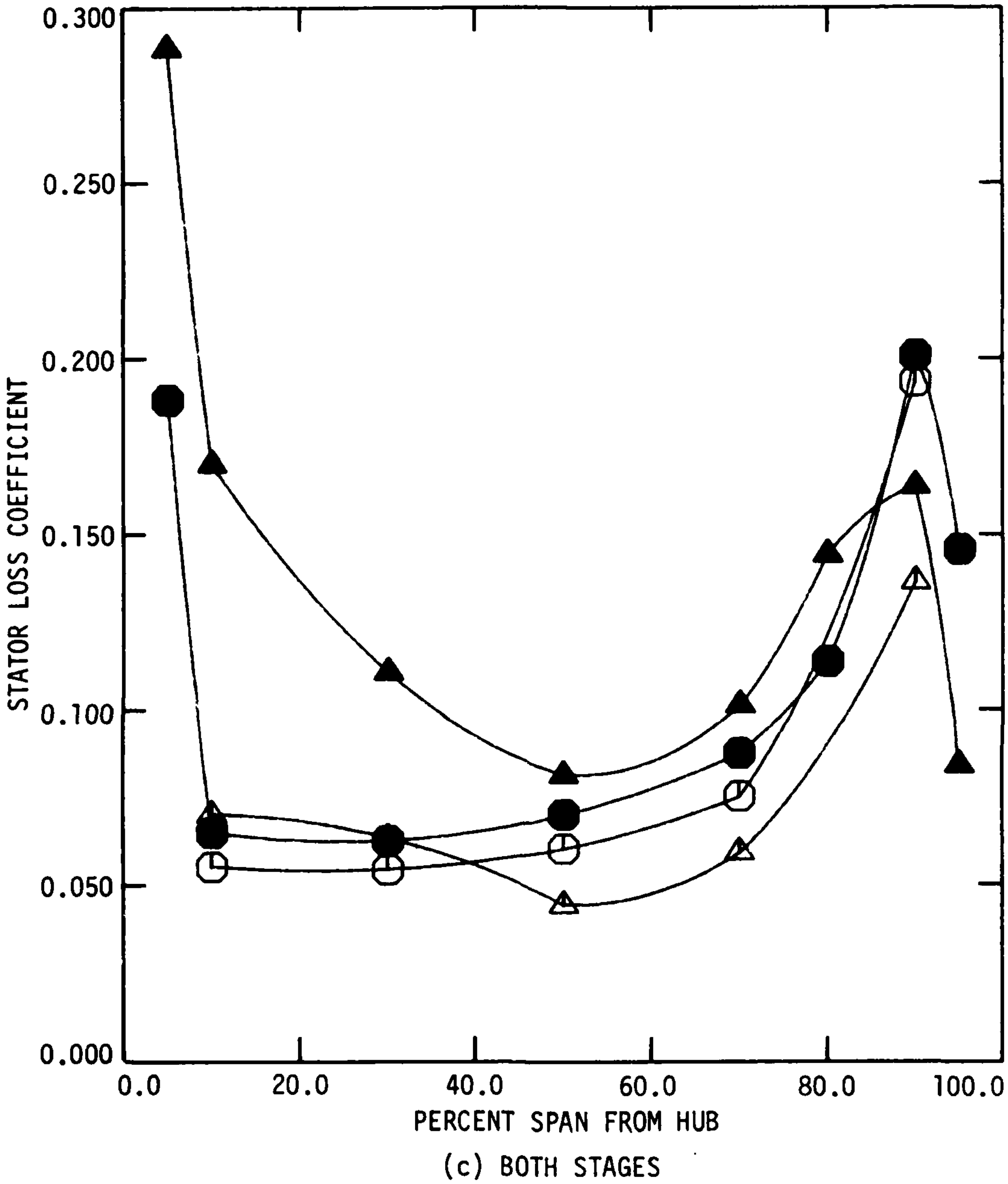


Figure 4.9 concluded.

- At off-design flow, the first stator loss is less than the second stator loss over most of the span, except near the tip.

In the following discussion, much reference is made to the total-head contour maps presented in Figures 4.6 and 4.7, particularly those for the stator exits. The stator exit maps are useful for analyzing the spanwise trends in stator loss. As will become evident, the spanwise graphs of circumferential-mean stator loss summarize much of the wake and end-wall flow behavior apparent from these contour maps. It should be noted regarding the maps, however, that only the gradients in total head are important. Also, only the spanwise trends in stator loss, not the magnitudes of stator loss, are reflected in the spanwise wake behavior.

Several observations about first stage stator performance can be pointed out. First, for both flow rates the stator wake has a fairly uniform width, and a slight increase in depth, from 10% to 70% span from the hub. This slight increase in wake depth shows up in the stator loss graphs as a gradual increase in loss. The wakes flare out into a combined wake/end-wall flow from 70% span to the tip. This results in a corresponding increase in stator loss. The abrupt increase in stator loss very near the hub (data at 5% span for off-design flow only) is associated with a "piling-up" of lower-momentum fluid on the pressure side of the stator blade. Excess lower-momentum fluid is expected in this region from the hub boundary layer. The "piling-up" is caused by hub rotation, where the hub is moving to the left as viewed on the stator exit contour maps.

The abrupt decrease in stator loss very near the tip (data at 95% span for off-design flow only) is somewhat difficult to interpret. Actually, a continued increase in stator loss is expected as the tip is approached. This unexpected behavior is probably due mainly to radial mixing of the flow near the tip. The first rotor head-rise curves in Figure 4.4(a) show a rapid decrease in rotor head-rise near the tip (95% span). The first stage head-rise curves, however, indicate that this lower head-rise region has expanded towards the "core" flow to include 90% span at the stator exit. This implies a mixing of the lower- and higher-momentum fluids at 95% and 90% span, respectively, as the fluid moves through the stator. Since the stator loss coefficient parameter does not take into account this radial mixing, the loss computed at the tip is too low, while that near the tip (90% span) is too high.

The second stator loss performance is qualitatively similar to that of the first stator for the outer half of the span. However, from mid-span to hub the loss performance is considerably different between the stages, especially for the off-design flow. This difference between stages is attributed to the second stator hub being stationary, whereas the first stator hub, as mentioned before, is rotating.

The second stator exit total-head contour maps (Figures 4.6 and 4.7) show a substantial region of lower-momentum fluid adjacent to that stator suction surface near the hub, particularly for the off-design flow. On the maps the region appears as a group of concentric half-circles with the center located somewhere very near the hub.

This region is evidence of a "leakage vortex," the likes of which have also been observed by others in conjunction with a stationary-blade/ stationary-hub gap (for example, see Leboeuf et al. [8]). A leakage vortex, with its large static-pressure gradient, pulls local lower-momentum fluid toward its center, resulting in the so-called "solid body" image on the total-head contour maps [8]. This region of lower-momentum fluid is, as expected, associated with an increase in the second stator loss near the hub. The off-design losses are considerably greater than those at design, and this is consistent with the size and strength of the lower-momentum regions on the contour maps. That is, the leakage vortex at off-design is larger in size and involves a steeper total-head gradient than the one at design.

The "vortex" size comparison between the design and off-design flows tends to support the contention that the lower-momentum region is indeed a leakage vortex. The off-design flow--being lower than the design flow--produces a higher loading on the stator blades. Thus, one expects a stronger leakage at the hub since the flow through the clearance is driven by the static pressure differences (loading) between hub blade-section pressure and suction surfaces.

4.3.1.3. Stator Incidence and Deviation

Spanwise variations of circumferential-mean stator incidence and deviation angles are presented in Figure 4.10(a) and (b), respectively. These results are discussed primarily as they relate to corresponding stator loss performance. The main points are as follows:

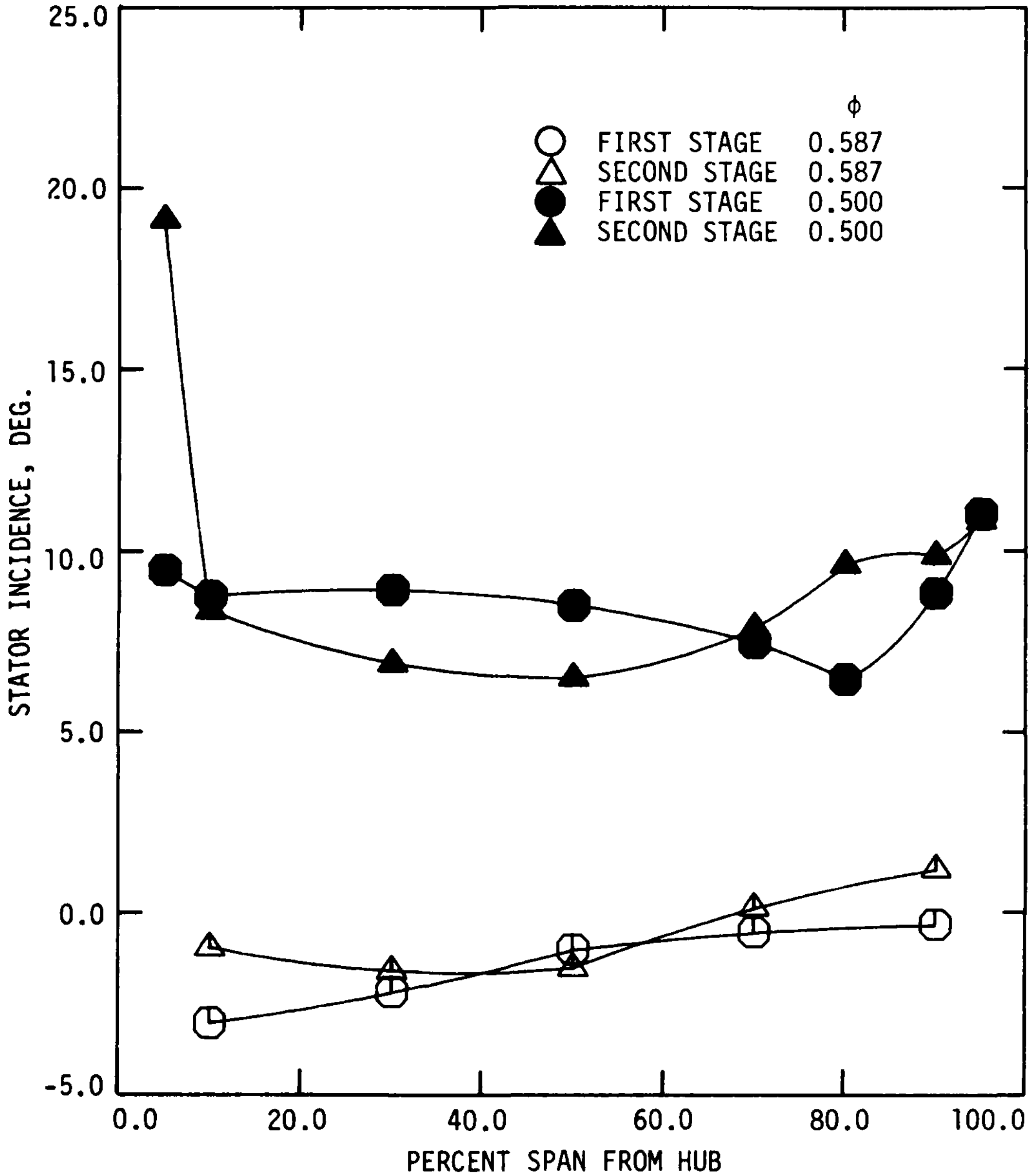


(a) STATOR INCIDENCE

Figure 4.10 Spanwise distribution of circumferential-mean stator incidence and deviation angles for the baseline 1 compressor build at the design ($\phi$ = 0.587) and the off-design ($\phi$ = 0.500) operating points.

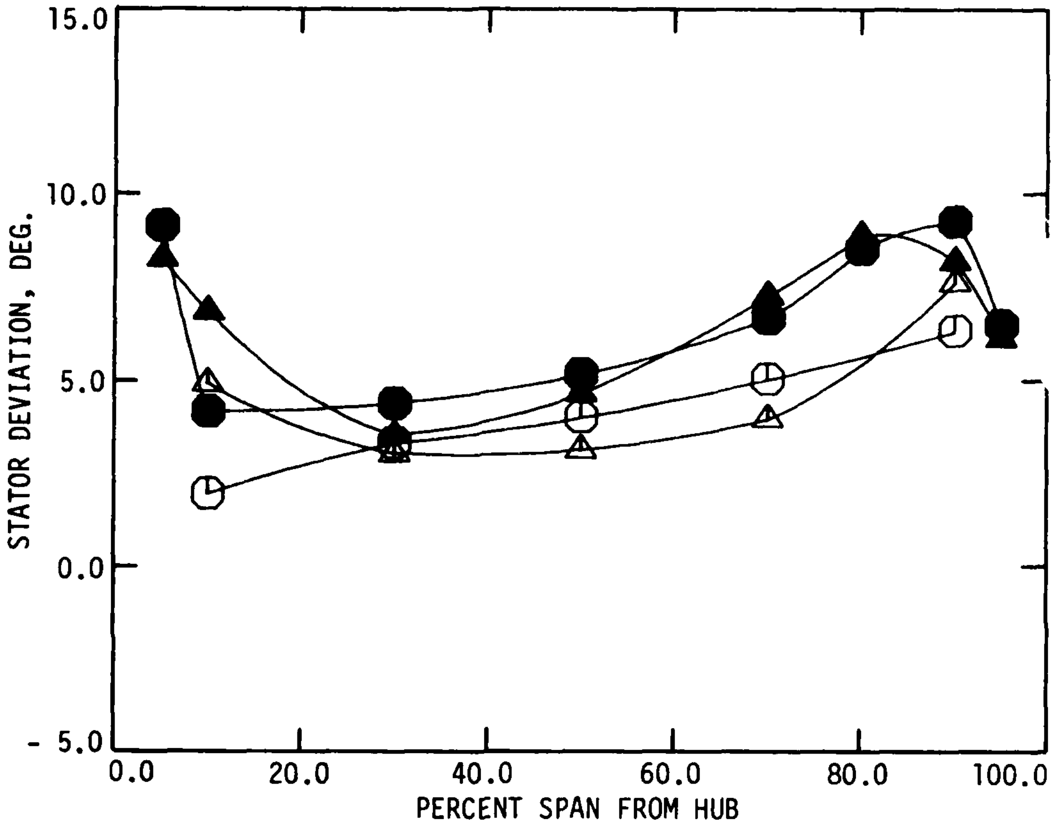


(b) STATOR DEVIATION

Figure 4.10 concluded.

- The stator incidence angle at off-design flow (approximately 8 deg) is much larger than the incidence angle at design flow (approximately -1 deg).
- There is no definite relationship between the spanwise trends in stator incidence angle and those in stator loss.
- Higher stator loss levels can be associated with larger positive incidence angle values.
- There is an approximate correlation between the spanwise trends in stator deviation angle and those in stator loss.

The stator incidence angle at off-design flow is expected to be larger than the incidence angle at design flow because the off-design flow rate is lower than the design value. The larger stator incidence angle at off-design flow is also expected to result in a higher stator loss level (Figure 4.9), since, for the kind of blading design involved [1,9], an 8 degree incidence angle would tend to produce a higher loss than would a -1 degree incidence angle.

#### 4.3.1.4. Rotor Performance

Spanwise variations of circumferential-mean rotor performance data are presented in this subsection. Rotor head-rise is not included here since it has already been discussed. Conventional ideal head-rise (Euler turbine equation based) and rotor loss curves are shown in Figures 4.11 and 4.12, respectively. Rotor incidence and deviation angles are presented in Figure 4.13. These data are only briefly discussed and are included for completeness and possible future reference.

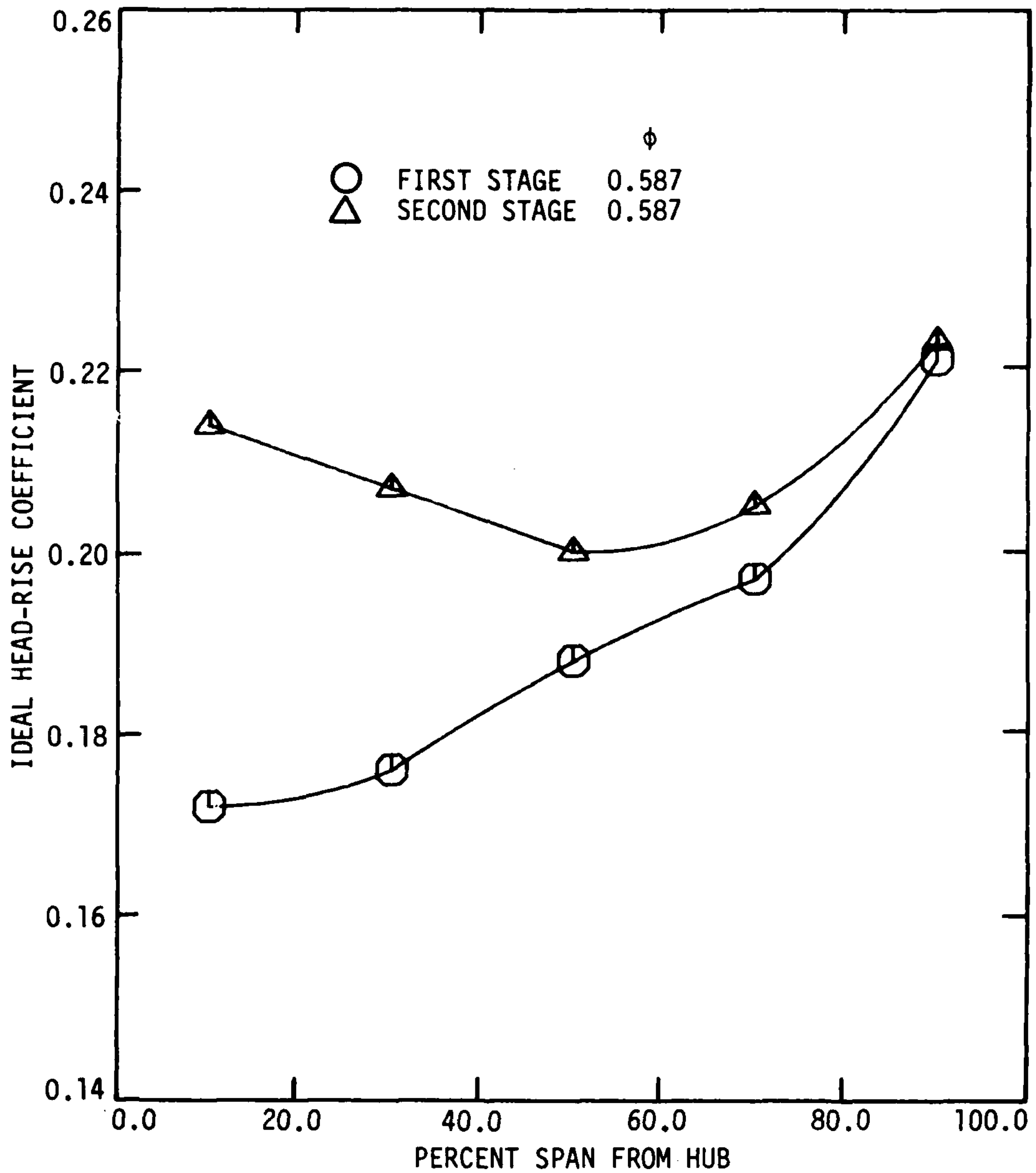


(a) DESIGN ($\phi$ = 0.587)

Figure 4.11 Spanwise distribution of circumferential-mean ideal head-rise coefficients for the baseline 1 compressor build at the design ($\phi$ = 0.587) and the off-design ($\phi$ = 0.500) operating points.

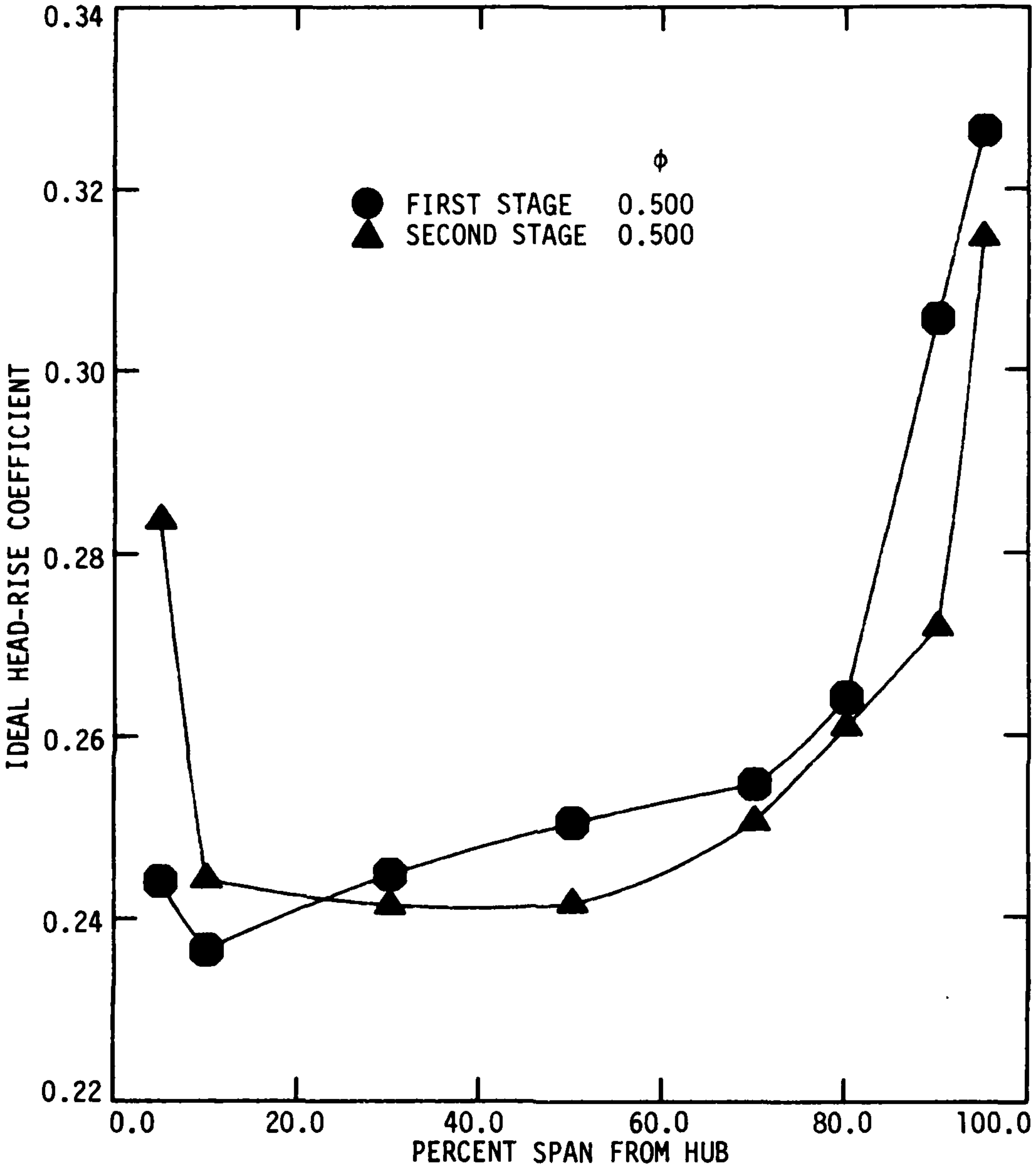


(b) OFF-DESIGN ($\phi$ = 0.500)

**Figure 4.11 concluded.**

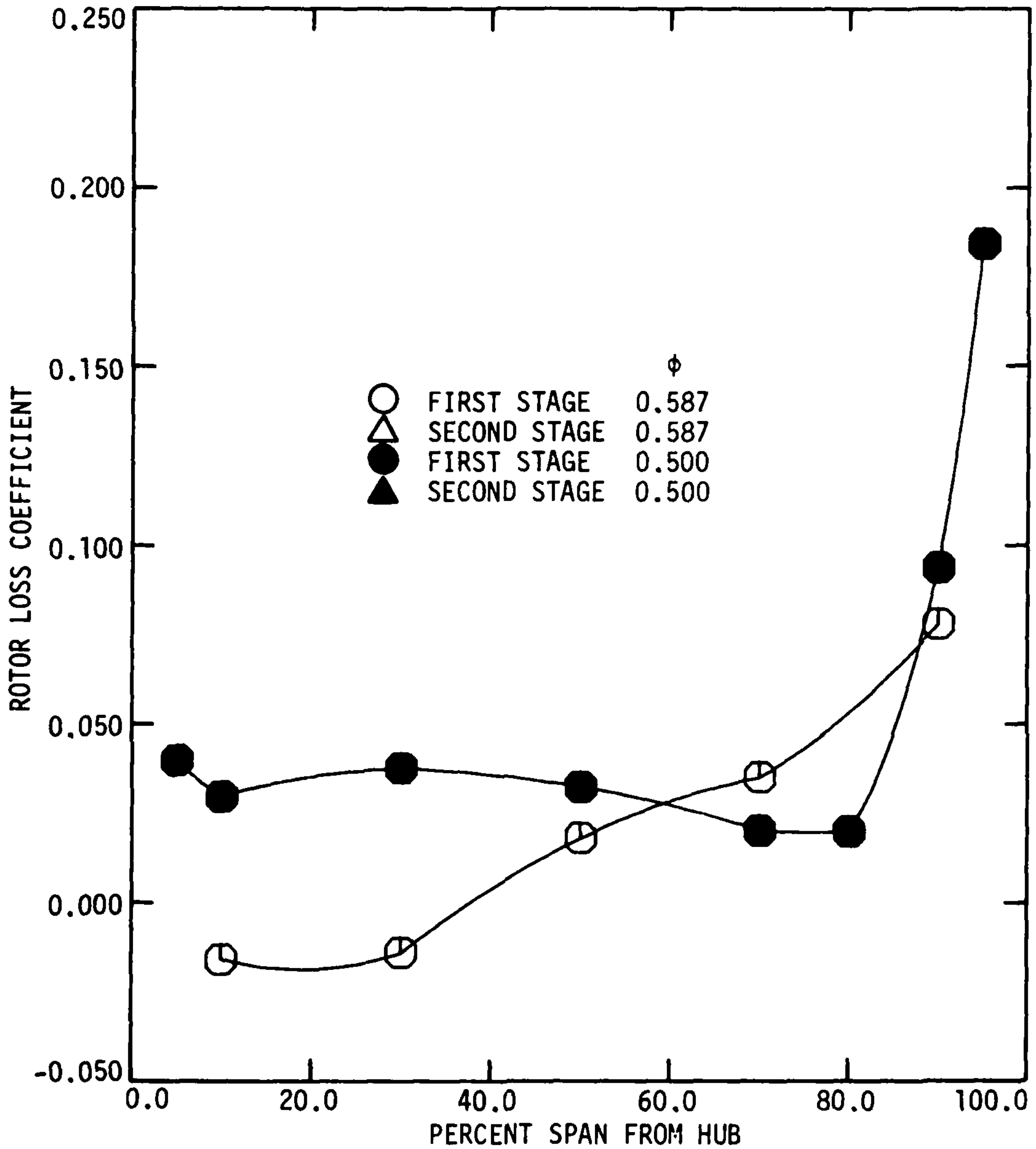


(a) FIRST STAGE ROTOR

**Figure 4.12** Spanwise distribution of circumferential-mean rotor loss coefficients for the baseline 1 compressor build at the design ($\phi$ = 0.587 ) and the off-design ($\phi$ = 0.500) operating points.

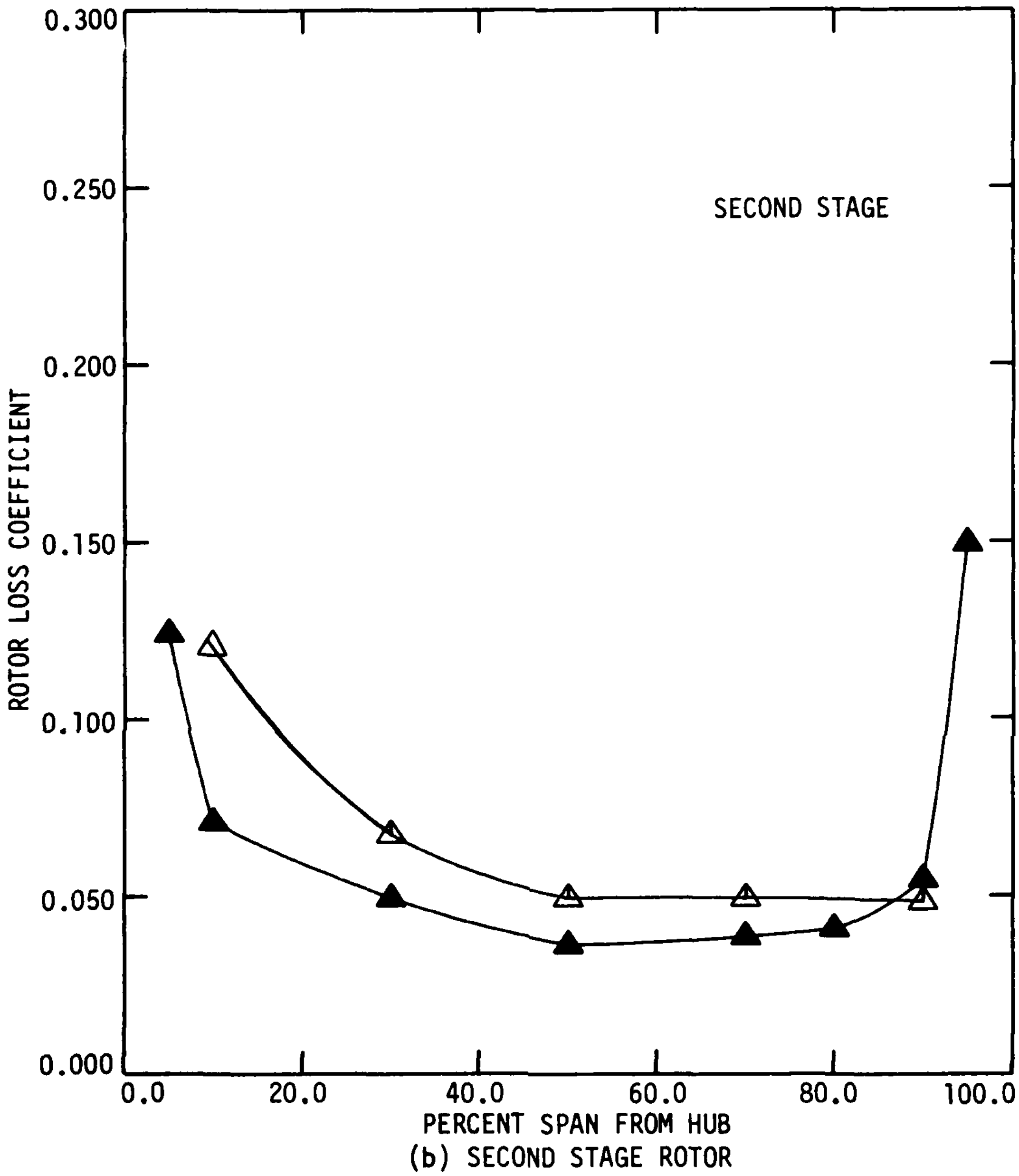


Figure 4.12 continued.

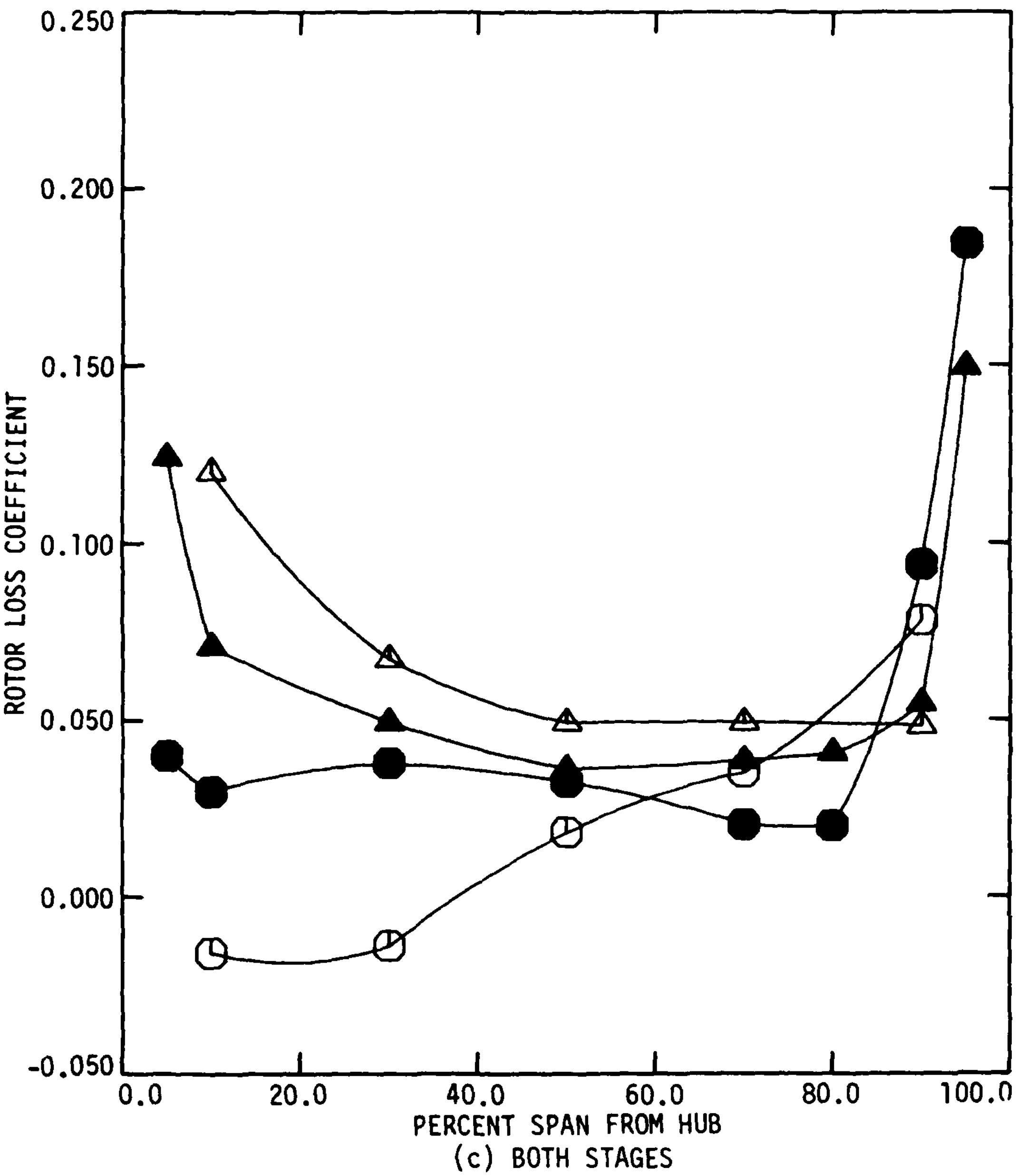


Figure 4.12 concluded.

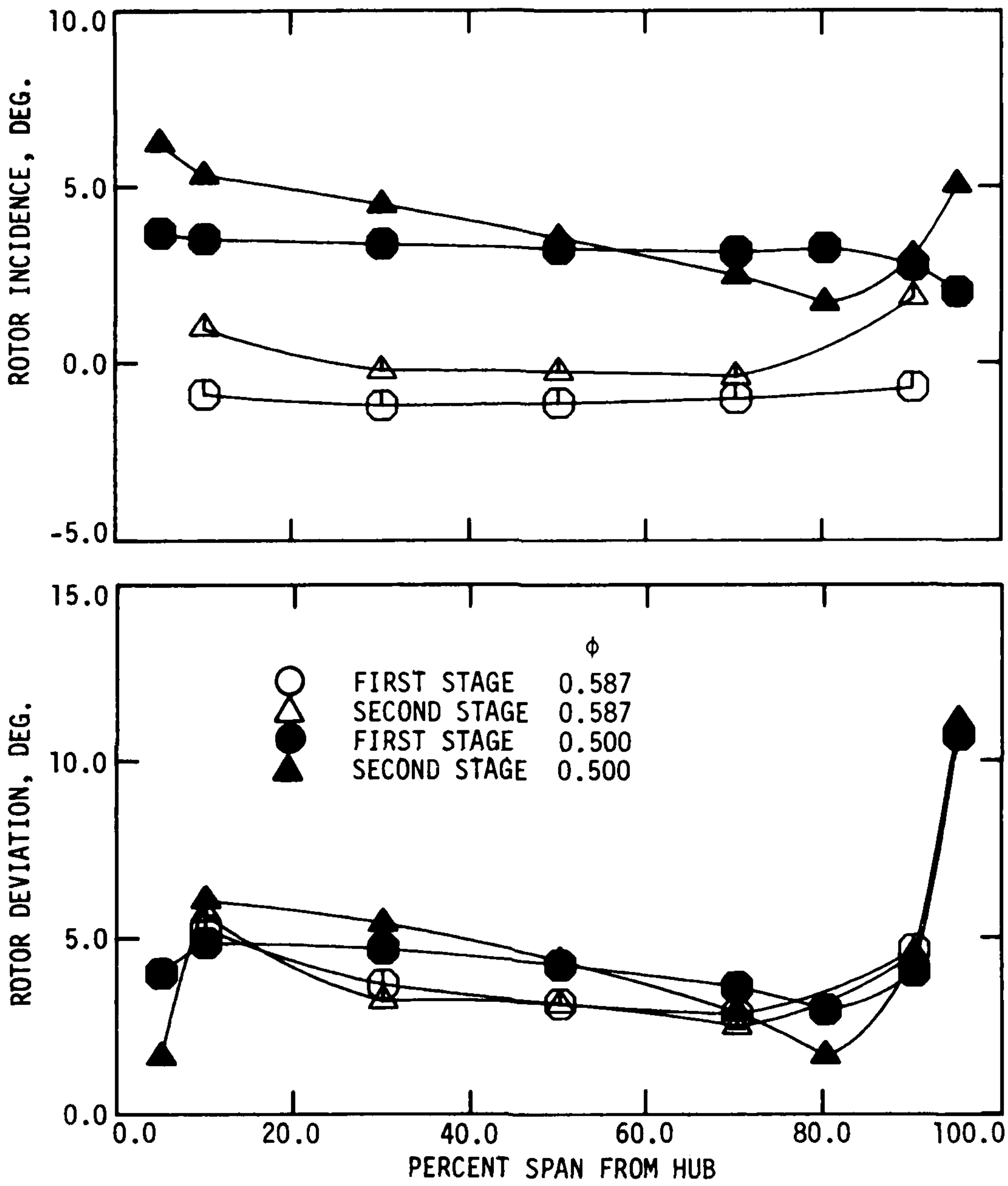


Figure 4.13 Spanwise distribution of circumferential-mean rotor incidence and deviation angles for the baseline 1 compressor build at the design ($\phi$ = 0.587) and the off-design ($\phi$ = 0.500) operating points.

Several characteristics of the ideal head-rise performance (Figure 4.11) are noteworthy:

- The first stage spanwise trend in ideal head-rise at design flow is similar to that at the off-design flow.
- The second stage spanwise trend in ideal head-rise at design flow is similar to that at the off-design flow.
- At off-design flow, the second stage spanwise distribution of ideal head-rise is similar to that of the first stage.
- At design flow, the second stage ideal head-rise is substantially higher than that of the first stage.

Some conclusions regarding rotor loss, incidence, and deviation follow:

- The first rotor loss curve for design flow is suspect because it indicates a negative rotor loss. This is probably due to calculated ideal head-rise, based on measured absolute flow angles, which was too low in the hub region.
- The spanwise trends in second rotor loss at design flow are similar to those at the off-design flow.
- At off-design flow, the spanwise distribution of second rotor loss is similar to that of the first rotor.
- There is no definite relationship between the spanwise trends in rotor incidence angle and those in rotor loss.
- There is no definite relationship between the spanwise trends in rotor deviation angle and those in rotor loss.

4.3.1.5. Hydraulic Efficiency

Spanwise variations in circumferential-mean hydraulic efficiency are presented in Figure 4.14. Conventional rotor, stage, and overall hydraulic efficiency curves are shown in Figure 4.14(a), (b), and (c), respectively. These data, like the rotor performance data, are included primarily for completeness and possible future reference. A few points on the overall efficiency data (Figure 4.14(c)) are worth mentioning:

- The overall compressor efficiency at the off-design flow is higher than that at design flow over most of the blade span.
- The spanwise trends in overall compressor efficiency differ for the two flow rates.
- The spanwise trends in overall compressor efficiency are similar to the spanwise trends in overall head-rise (Figure 4.4(c)).

4.3.1.6. Mass-Averaged Performance

Radially mass-averaged data for the baseline 1 compressor build at the two different flow rates are presented in Table 4.8. The following comparisons are significant:

- The mass-average stator loss is greater at the off-design flow than at design flow for both stages.
- The mass-average stage efficiency is higher at the off-design flow than at design flow for both stages.
- The mass-average overall compressor efficiency is higher at the off-design flow than at design flow.

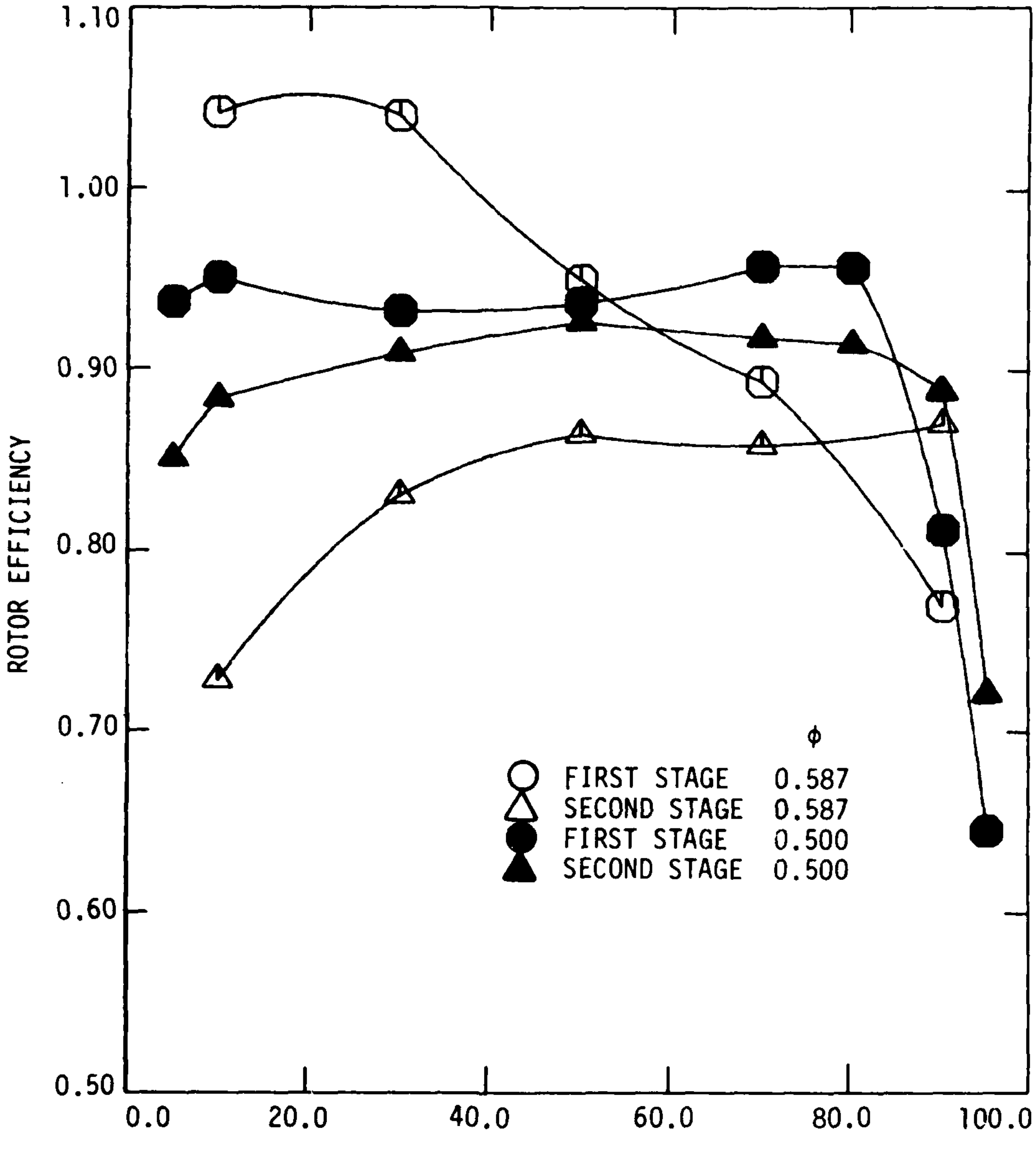


(a) ROTOR

Figure 4.14 Spanwise distribution of circumferential-mean hydraulic efficiences for the baseline 1 compressor build at the design ($\phi$ = 0.587 ) and the off-design ($\phi$ = 0.500) operating points.

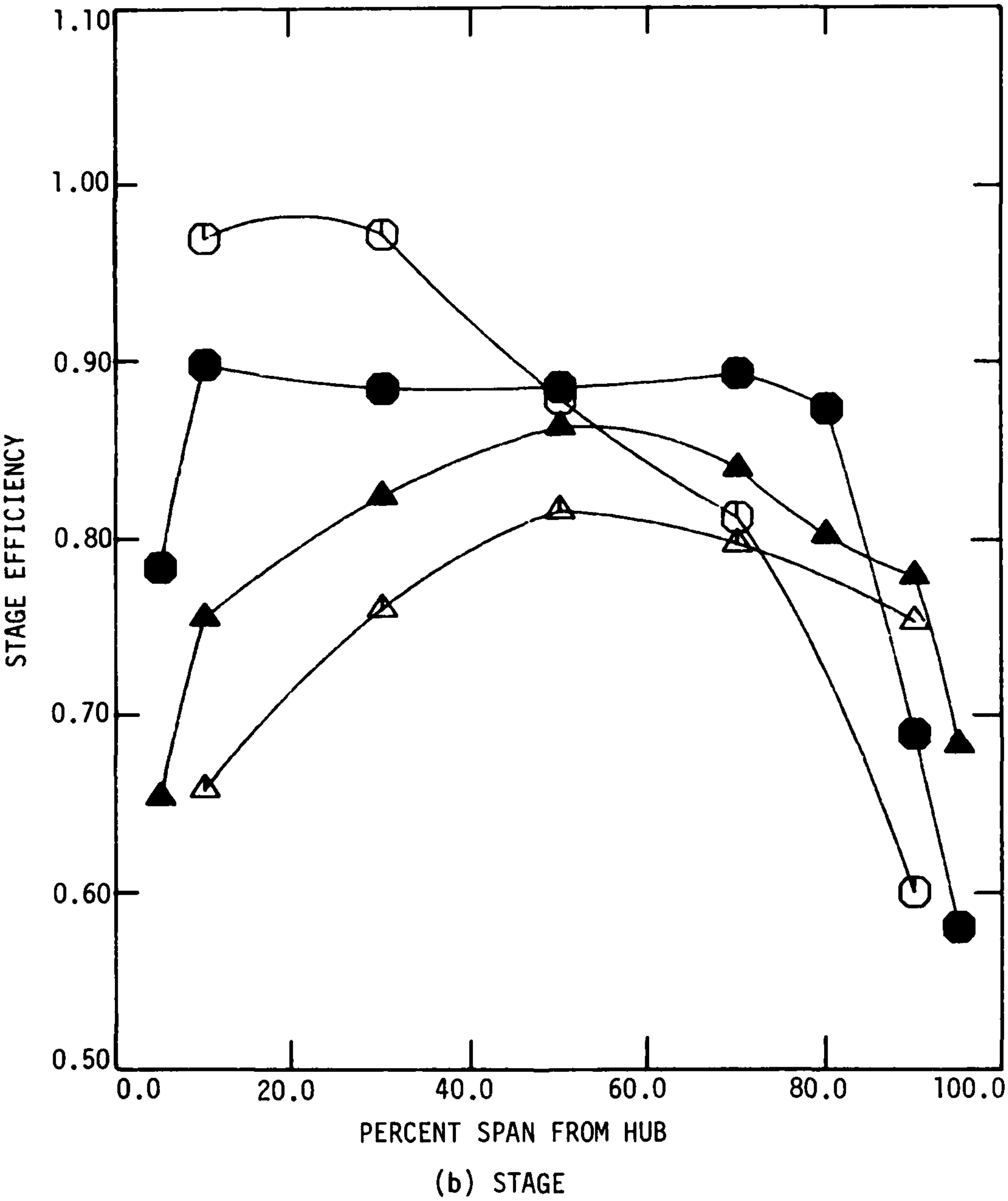


Figure 4.14 continued.

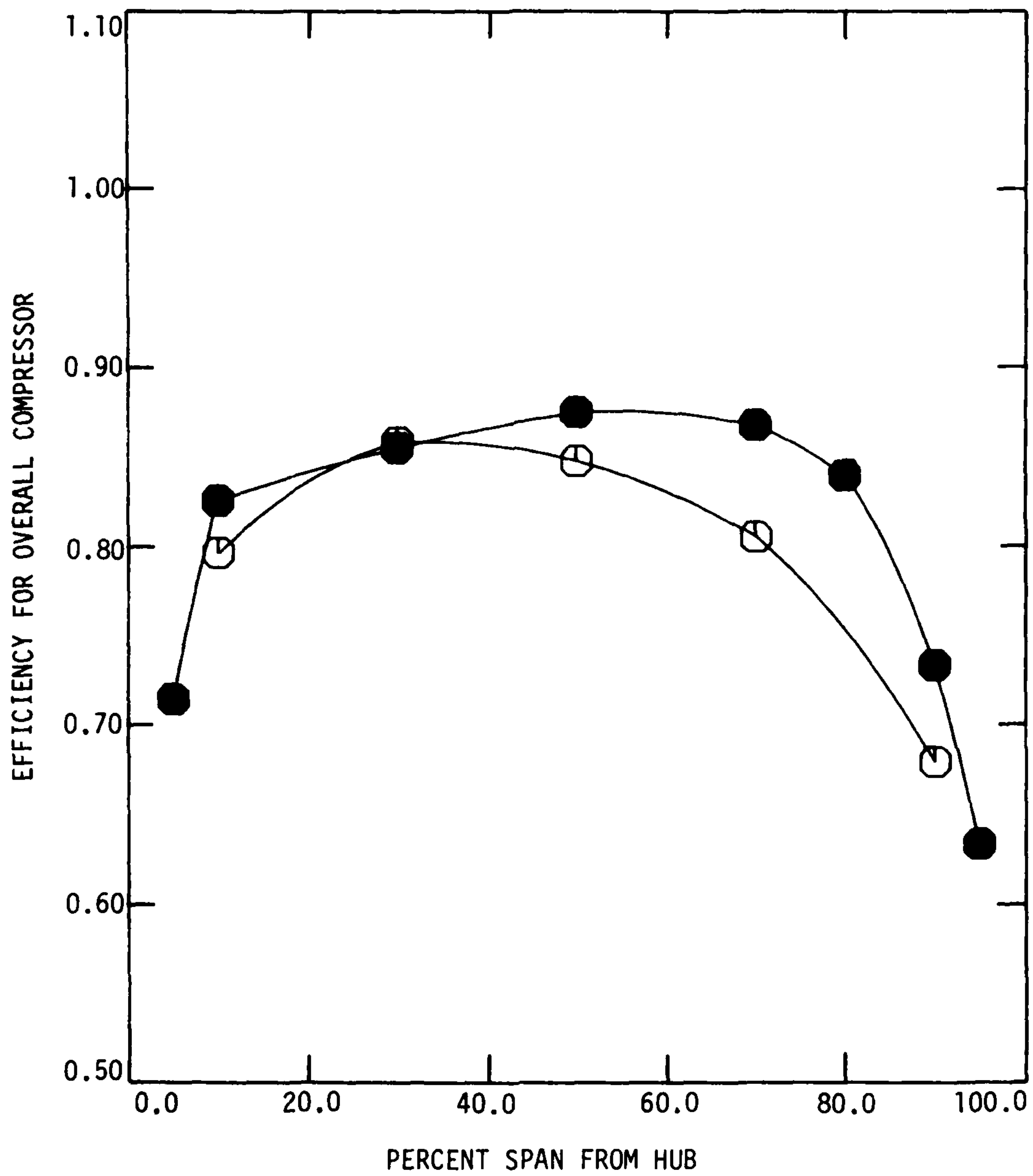


(c) OVERALL

Figure 4.14 concluded.

Table 4.8. Comparison of radially mass-averaged performance parameters for the baseline 1 compressor build at the design ($\phi$ = 0.587) and the off-design ($\phi$ = 0.500) operating points.

| Flow Coefficient | Head Rise Coefficient | | Loss Coefficient | | Efficiency | |
|---|---|---|---|---|---|---|
| | Rotor | Stage | Rotor | Stator | Rotor | Stage |
| **First Stage** | | | | | | |
| 0.500 | 0.236 | 0.217 | 0.045 | 0.100 | 0.913 | 0.840 |
| 0.587 | 0.178 | 0.160 | 0.025 | 0.083 | 0.926 | 0.833 |
| **Second Stage** | | | | | | |
| 0.500 | 0.226 | 0.204 | 0.051 | 0.116 | 0.899 | 0.813 |
| 0.587 | 0.175 | 0.159 | 0.063 | 0.071 | 0.833 | 0.760 |

Overall

| Flow Coefficient | Head Rise Coefficient | Efficiency |
|---|---|---|
| 0.500 | 0.421 | 0.827 |
| 0.587 | 0.319 | 0.795 |

The results listed in Table 4.8 reveal a peculiarity in the relationship between loss and efficiency. For example, at the off-design flow the first stage rotor and stator losses exceed those at design flow, yet the first stage efficiency is higher at the off-design flow. This apparent discrepancy is resolved by recognizing that efficiency depends on the losses as they relate to head-rise. The higher first stage rotor and stator row losses at the off-design flow are accompanied by a greater gain in stage head-rise over that at design flow.

### 4.3.2. First Stator Wake Tracking Through the Second Rotor

Contour maps of second rotor exit total-head for the baseline 1 compressor build at two flow coefficients (0.587 in Figure 4.6 and 0.500 in Figure 4.7) were presented in the preceding section. As was pointed out, the map for design flow (Figure 4.6) shows an interesting feature, namely, over most of the span and within one stator pitch there are two regions of lower total-head. In contrast, for the off-design flow (Figure 4.7) only one of these lower total-head regions exists.

When considering the first stator wake/second rotor blade row interaction, it seems reasonable to expect only one lower total-head region per stator pitch. Each first stator blade produces a continuous stream of low total-head wake fluid which enters the rotor row and is "chopped" into segments (see Smith [10] for a clear explanation of this concept of wake "chopping"). These "wake segments" are rotated within the rotor and are thus not reunited at the rotor exit. Upon exiting from the rotor row, these segments move downstream sequentially within a stationary "wake avenue," with one avenue for each upstream stator. When time-averaged total-pressure is measured at the rotor exit, this "wake avenue" is expected to appear as a region of lower total-pressure relative to the no-stator-wake portion of the rotor exit flow. Therefore, only one lower total-head region per stator pitch is anticipated. More detailed discussion concerning this type of stator wake/rotor blade interaction is given by Smith [10], Wagner et al. [11], and Zierke and Okiishi [12].

Several experiments were carried out on the research compressor to better understand the unusual "two lower total-head region" pattern observed at design flow. Although most of the data obtained in this effort were acquired with the modified 1 compressor build, the general behavior observed applies to both the baseiine and modified configurations.

The initial experiment consisted of making qualitative total-head surveys at mid-span of the second rotor exit within one stator pitch, over the entire range of compressor flow rates at design shaft speed. The results are presented in Figure 4.15.

Figure 4.15 demonstrates that the two-dip (two lower total-head region) pattern begins to appear at a flow coefficient of about 0.525, and remains for all higher flow rates. In general, both dips have similar magnitudes and move gradually to the right (rotor blades move left) as the flow coefficient increases. The single dip observed at lower flow coefficients also moves to the right as the flow coefficient increases.

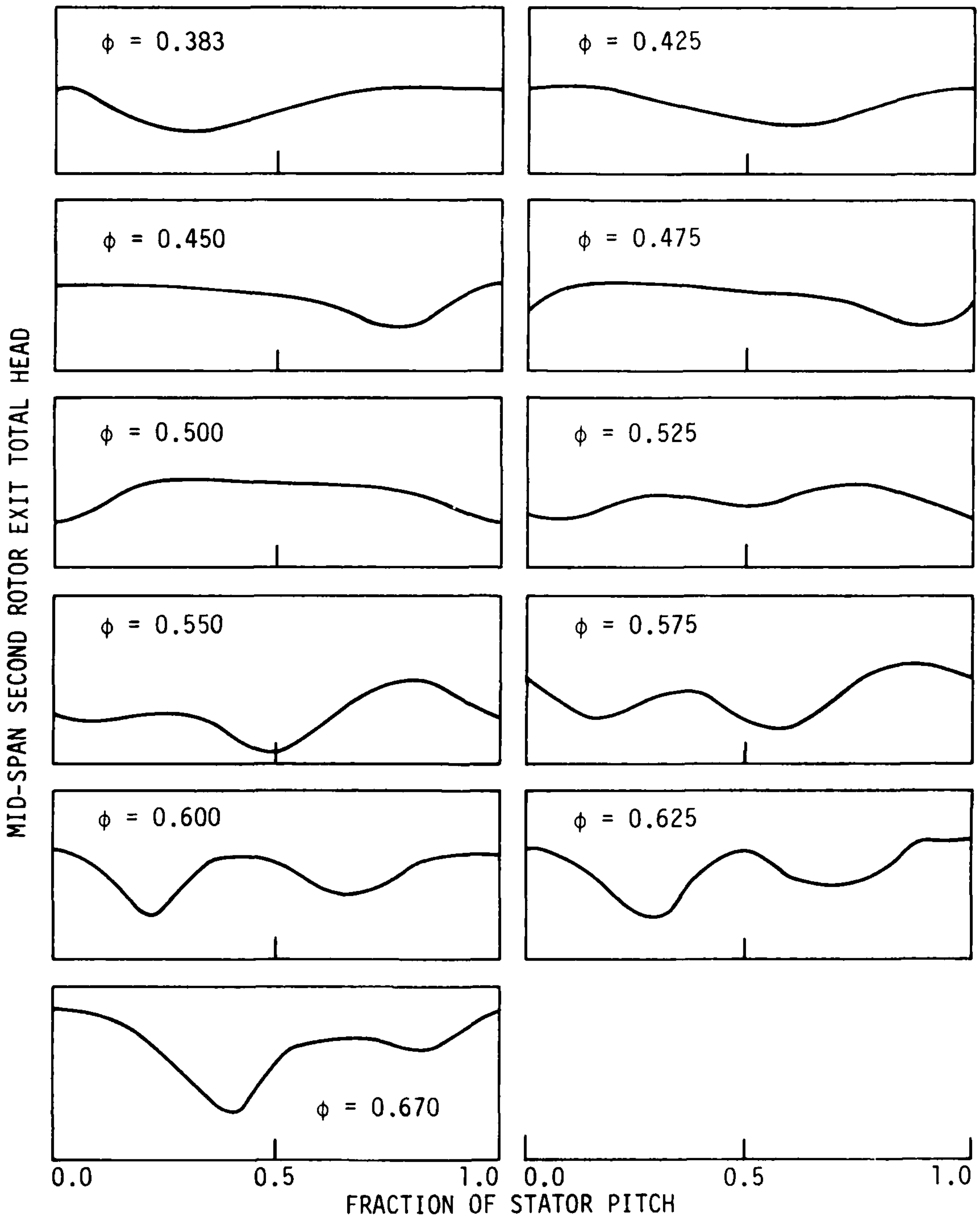


Figure 4.15 Qualitative variation of total head with circumferential extent at second rotor exit mid-span.

More qualitative data were obtained next. A specially constructed stator blade involving a wound heating element was used to produce a "warm" stator wake that could be tracked through the second stage rotor with a temperature survey at the second rotor exit. Details about the procedure and apparatus for obtaining these data were discussed earlier in the section on experimental procedure.

The variation of second rotor exit relative temperatures with circumferential extent at mid-span are presented in Figure 4.16. "Positions I and II" refer to the "warm" blade placement as illustrated in Figure 3.3. Figure 4.16(a) and (b) are for flow coefficients of 0.575 and 0.500, respectively, while in Figure 4.16(c) the results of three flow coefficients (0.575, 0.500, and 0.425) are compared. Included in Figure 4.16(a) and (b) are also total-head data which provide a means for comparing "normal wake" (no heating coil) data with "distorted wake" (cold heating coil) data, in order to ascertain the extent of wake distortion resulting from the heating coil. A relative temperature distribution is shown in Figure 4.16(b) for position II data taken with the heating coil turned off. These data illustrate that any significant increases in relative temperature are due solely to the fluid being heated by the coil.

At a flow coefficient of 0.575, the wake avenue (region of higher relative temperatures) extends over most, but not all, of the stator pitch. By comparing the circumferential wake distortion with the relative temperature distribution, a "corrected" wake avenue extent can be estimated. This corrected avenue extends

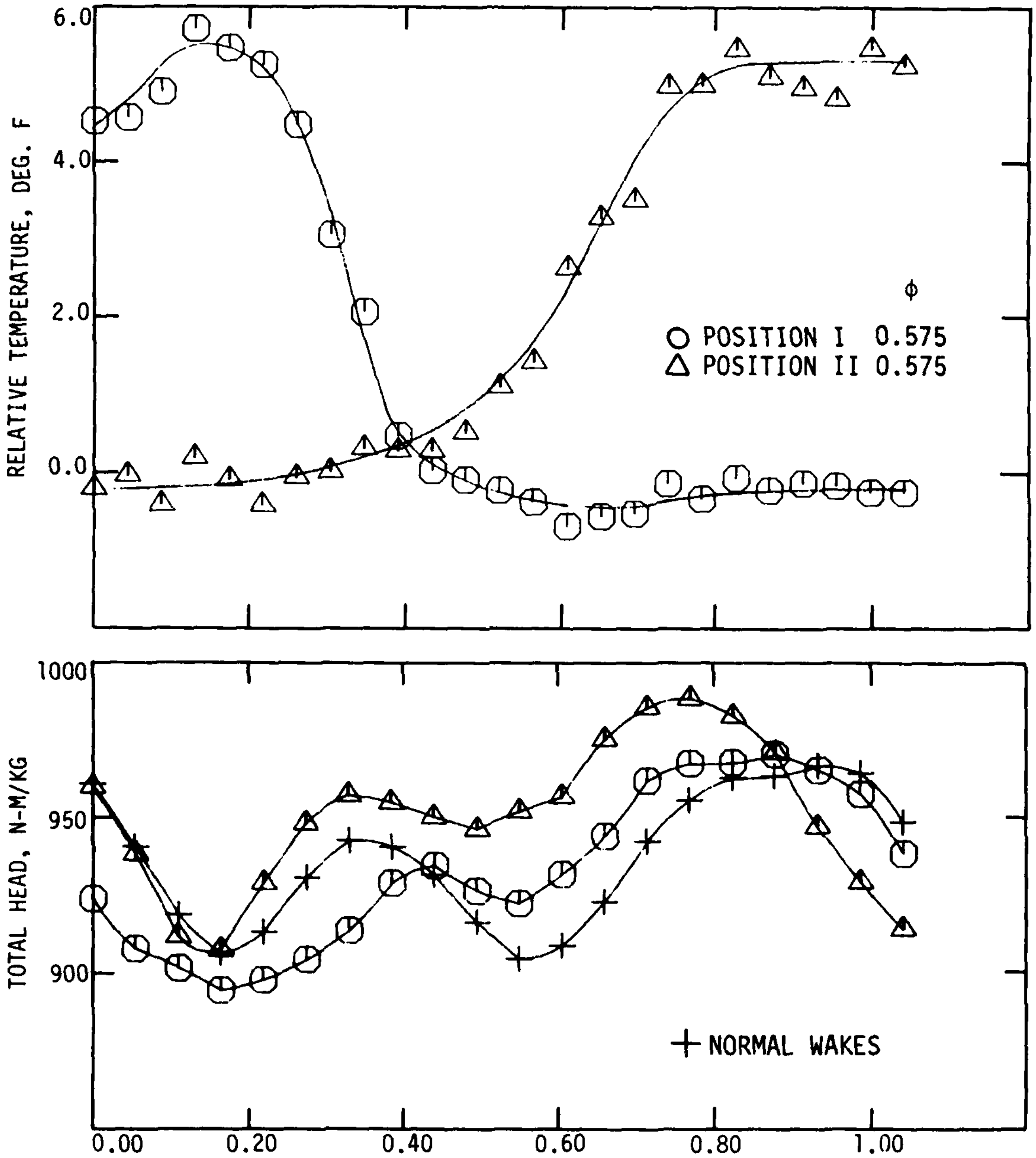


(a) $\phi$ = 0.575 (50 PERCENT SPAN)

**Figure 4.16** First stator wake tracking data measured at the second rotor exit (50 percent span from hub).

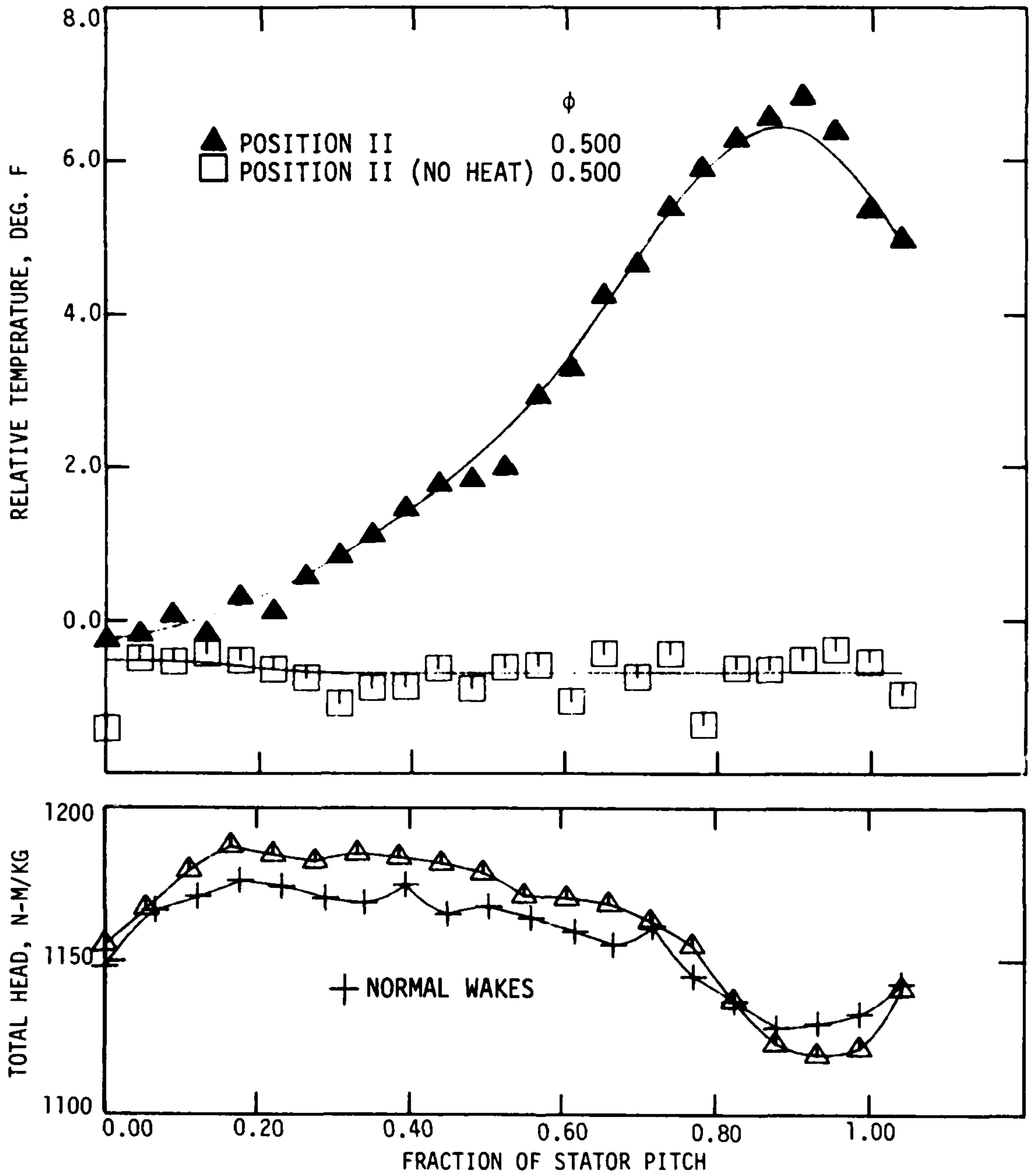


(b) $\phi$ = 0.500 (50 PERCENT SPAN)

Figure 4.16 continued.

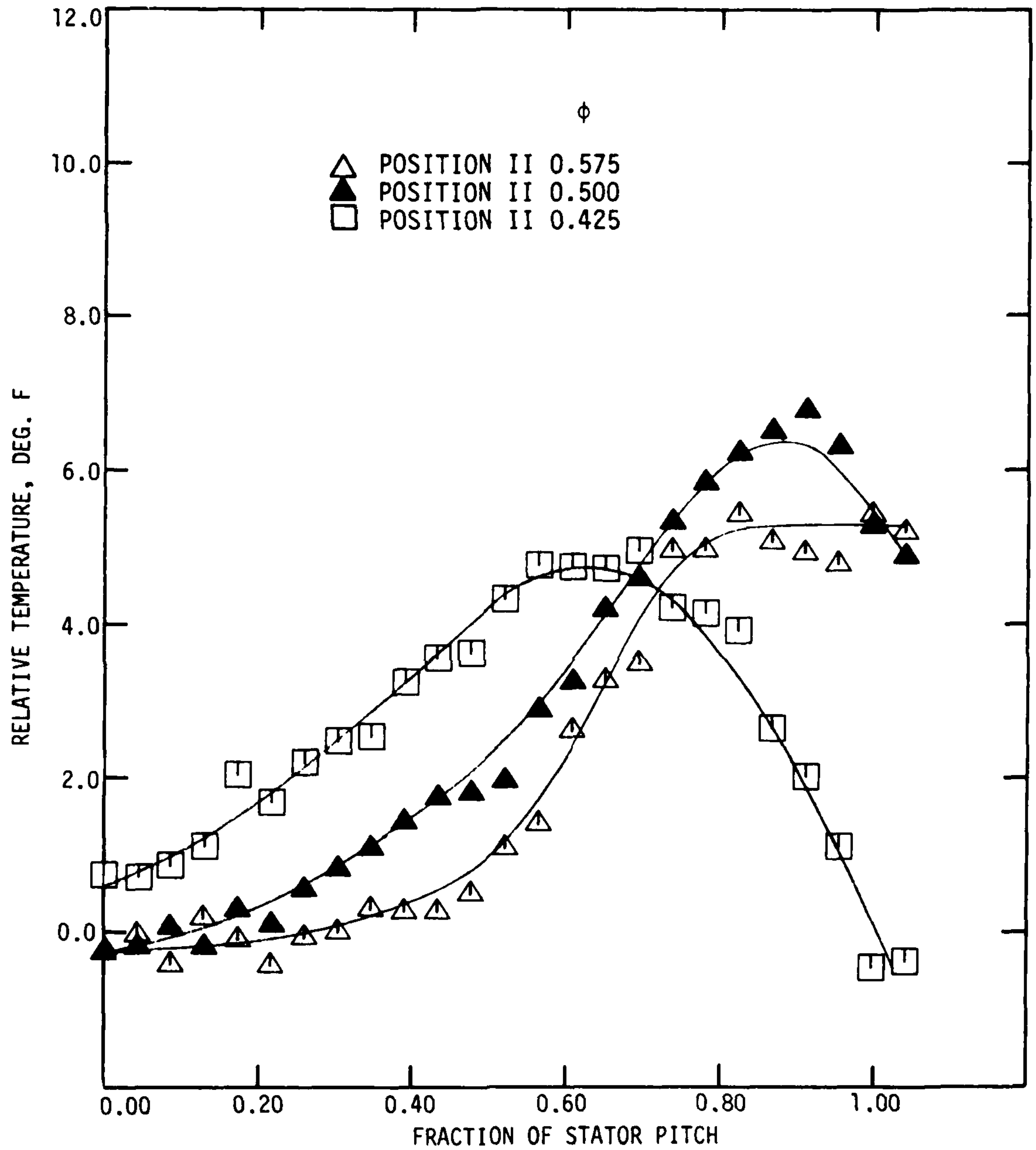


(c) FLOW COEFFICIENT COMPARISON (50 PERCENT SPAN)

**Figure 4.16 concluded.**

approximately from 0% to 35% and 55% to 100% of the stator pitch. Consequently, the region between wake avenues extends approximately from 35% to 55% of the stator pitch at this flow coefficient.

The wake avenue extent at flow coefficients of 0.500 or less can also be estimated by a similar analysis of data. From the data of Figure 4.15 and Figures 4.16(b) and (c), it is evident that for flow coefficients less than 0.5, the stator wake avenues overlap, and thus a region between wake avenues does not exist. At a flow coefficient of 0.500, one stator wake avenue extends from approximately 0% to 120% of the stator pitch. An overlap region between adjacent wake avenues extends from approximately 0% to 20% of the stator pitch.

Some general conclusions about changes in wake avenue extent and circumferential position with the flow rate variation are apparent from Figure 4.16(c):

- The "right-side" (as seen in Figure 4.16(c)) boundary of the wake avenue clearly shifts to the right (rotor blades move left) as the flow rate increases.
- The "left-side" boundary of the wake avenue shifts to the right as the flow rate increases, but in a much less definitive manner than the "right-side" boundary.
- At lower flow rates, the "left-side" boundary is spread out considerably (to the left) in circumferential extent.
- The "left-side" boundary becomes less spread out (more definite) as the flow rate increases.
- The "right-side" boundary maintains a somewhat definite form over the range of flow rates.

Figure 4.17(a) and (b) depict an interpretation--based on previously discussed data--of first stator wake/second rotor blade row interaction at mid-span for the two flow coefficients of 0.575 and 0.500, respectively. These drawings are similar to sketches presented by Smith [10], and, being approximately scaled, show the location of the circumferential measurement window with respect to the wake avenues.

The relationship between second rotor exit total-head variation and the blade-to-blade and wake-avenue widths is illustrated in Figure 4.18. This relationship at the flow coefficient of 0.575 is shown in Figure 4.18(a), while 4.18(b) shows it at the flow coefficient of 0.500. These drawings tend to illustrate clearly the previous results and conclusions.

For futher clarification of the observations made at mid-span, temperature data taken over the blade span were examined. Figures 4.19(a) and (b) represent second rotor exit relative temperature contour maps for the flow coefficients of 0.575 and 0.500, respectively. These two maps should be considered as they relate to the second rotor exit total-head contour maps (Figures 4.6 and 4.7) discussed earlier. The flow coefficient of 0.575 is not equal to the design value of 0.587 (for the total-head contour map). However, the temperature contours at a flow coefficient of 0.587 are not expected to be significantly different from those at the flow coefficient of 0.575. Also, as shown, some of the temperature contours for the flow coefficient of 0.500 are estimated, based on (1) the measured contours, (2) earlier conclusions on the extent of this wake

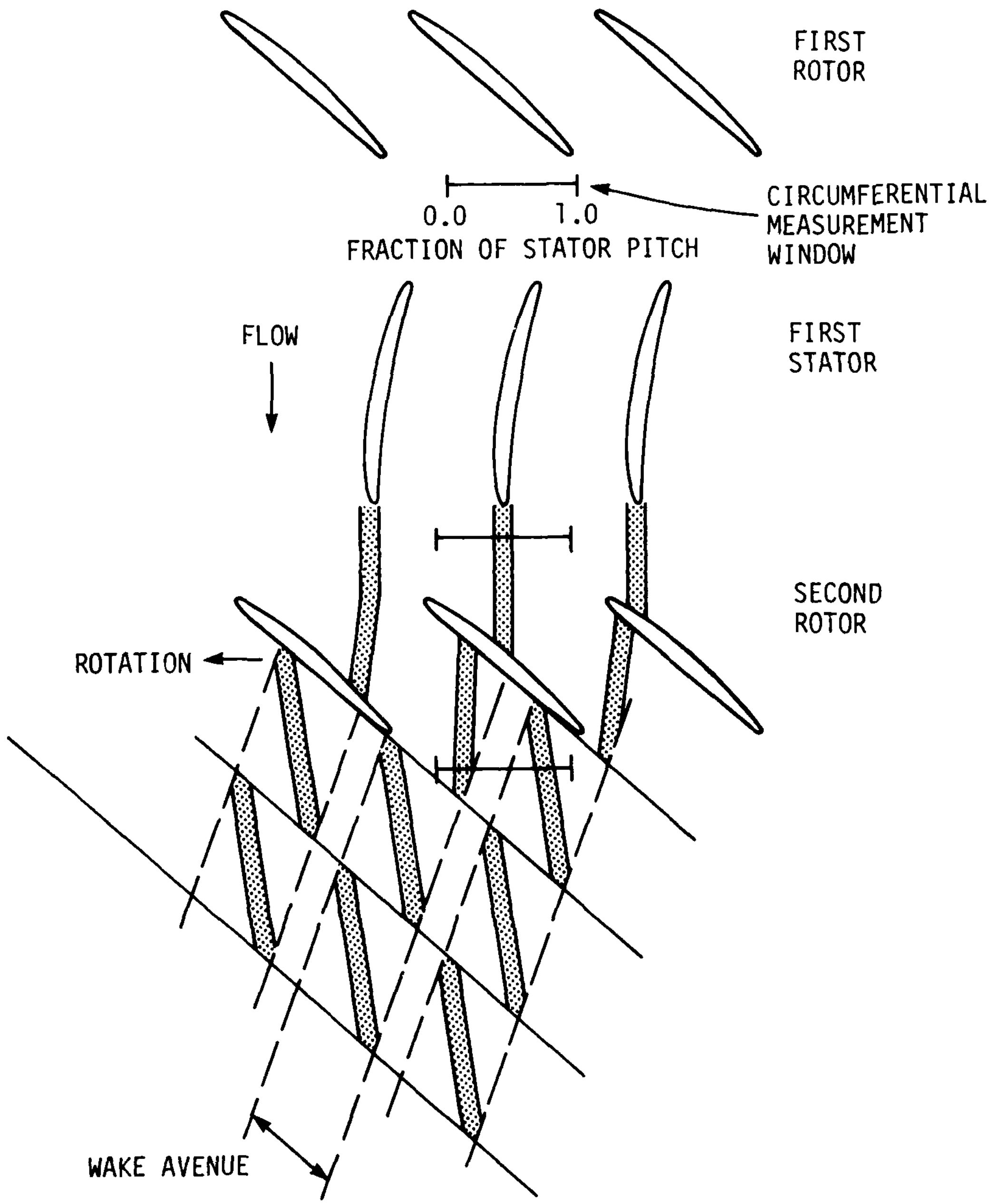


(a) $\phi$ = 0.575

Figure 4.17 First stator wake/second rotor blade interaction at two operating points ($\phi$ = 0.575 and $\phi$ = 0.500).

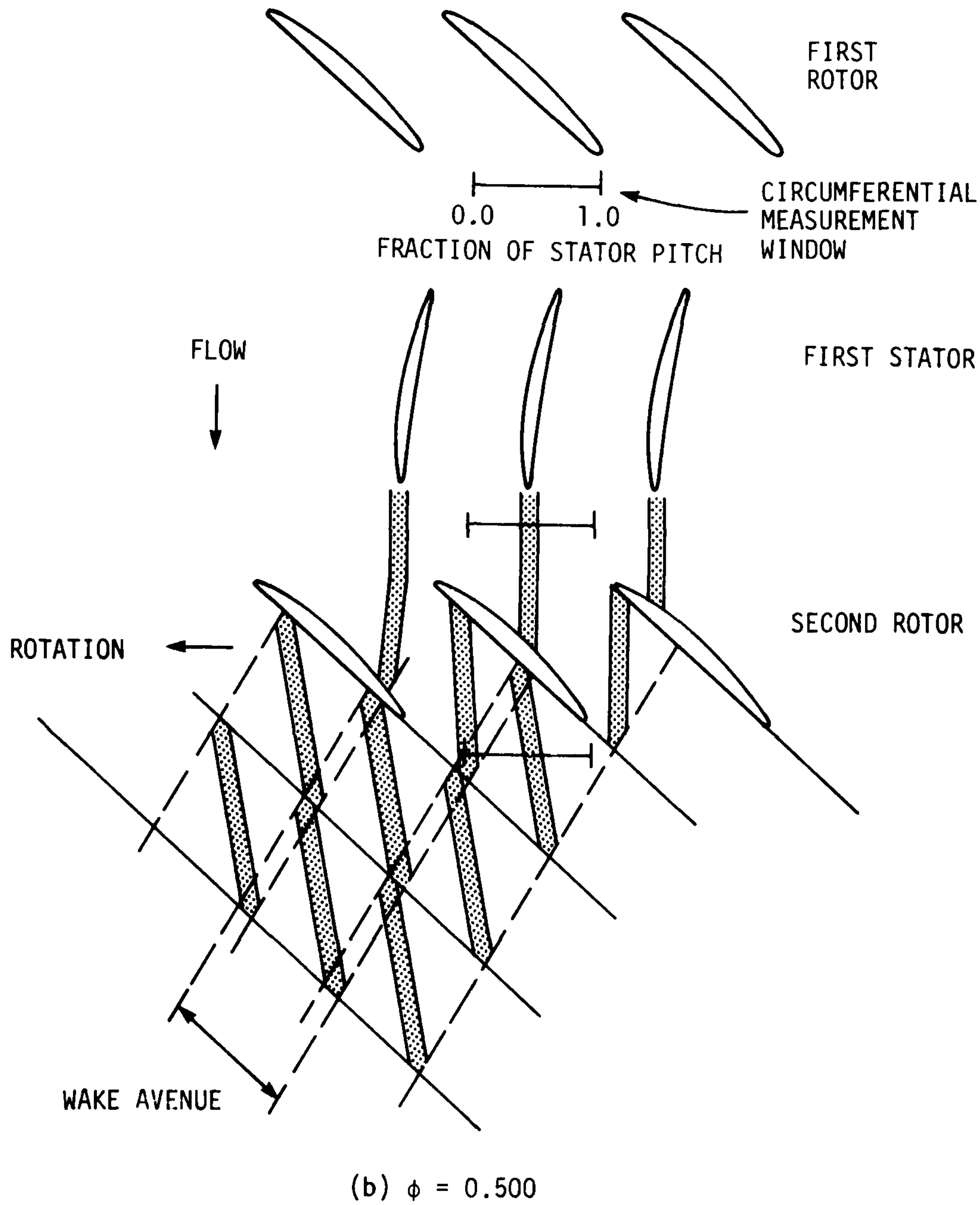


(b) $\phi = 0.500$

**Figure** 4.17 concluded.

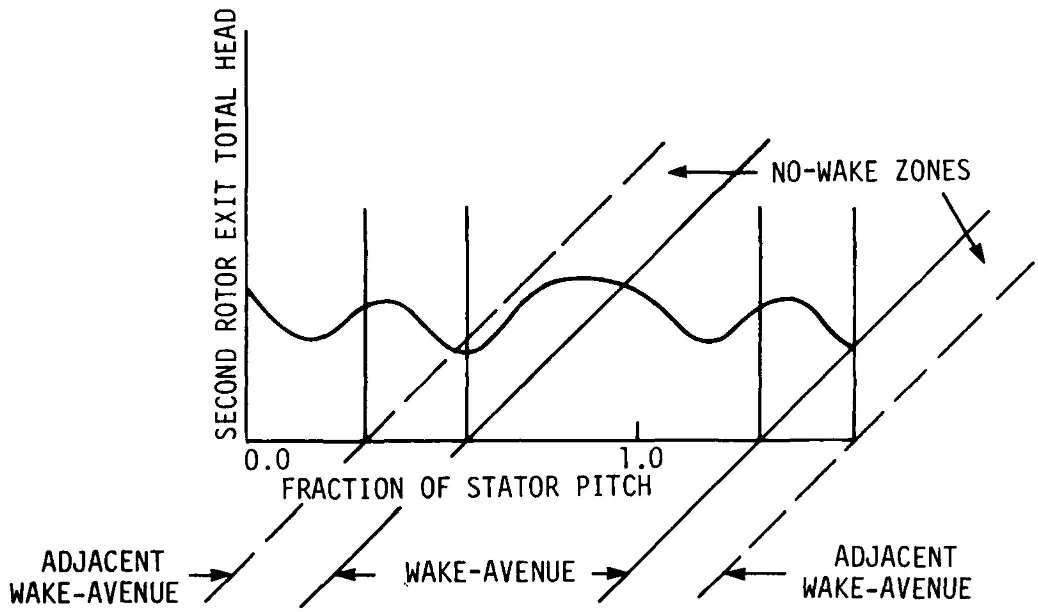


(a) $\phi$ = 0.575

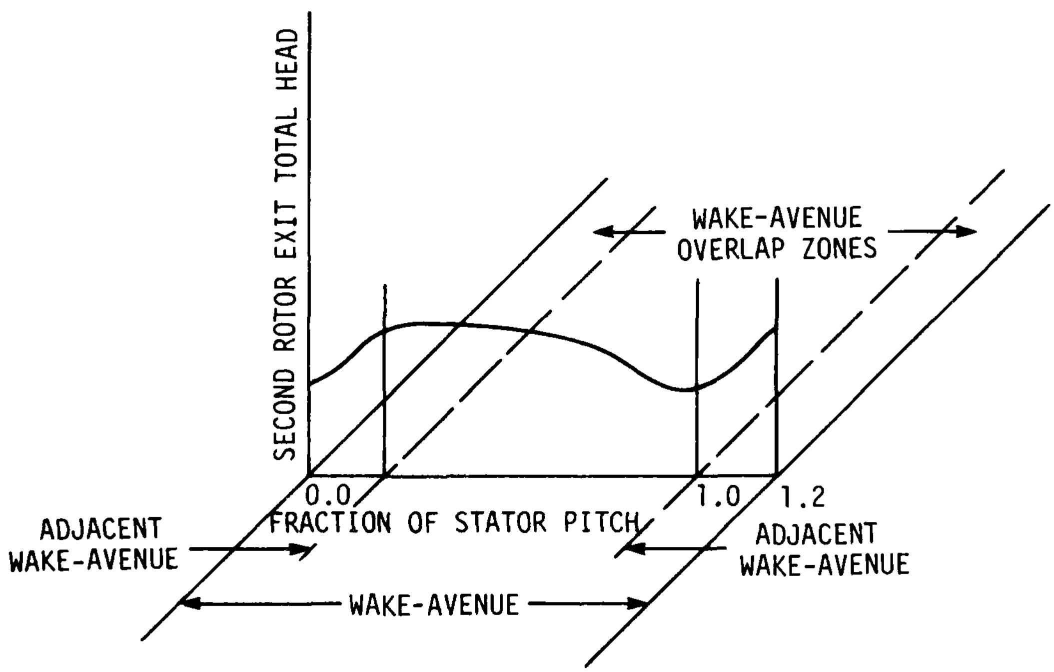


(b) $\phi$ = 0.500

Figure 4.18 Relationship between second rotor exit total-head variation and the blade-to-blade and wake-avenue widths.

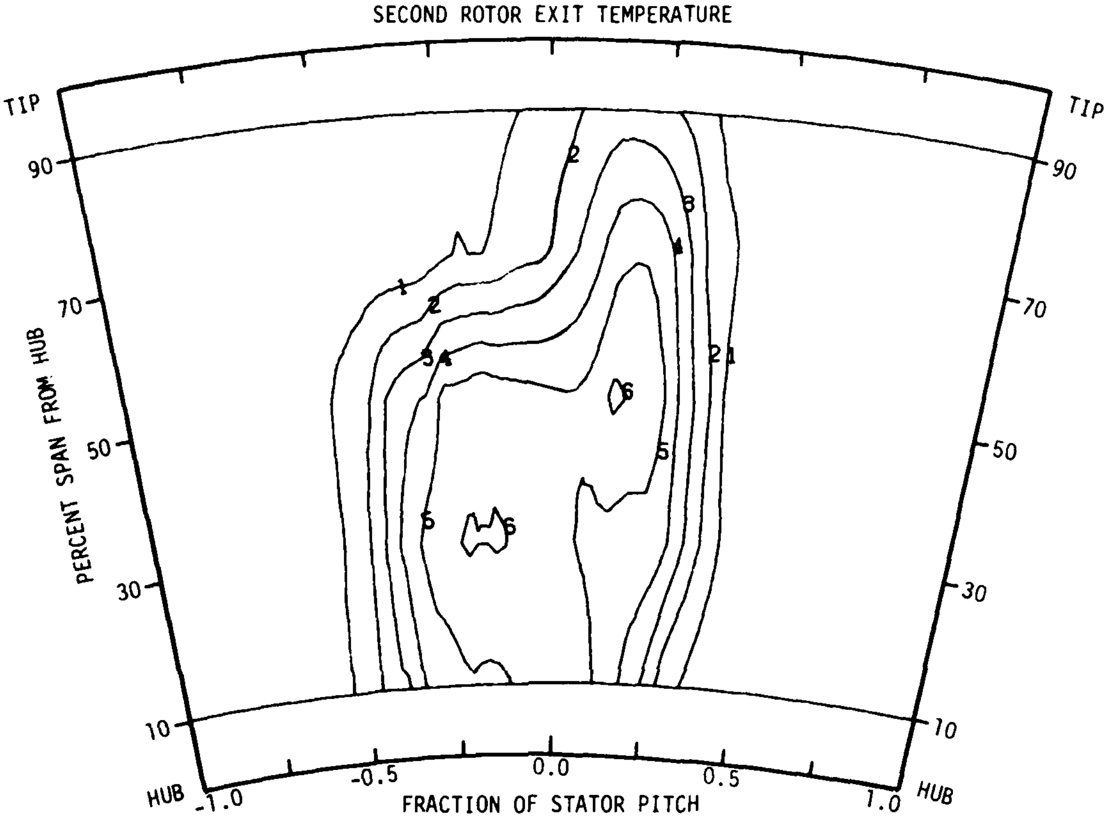


(a) $\phi$ = 0.575

| CURVE LABEL | CURVE VALUE (DEG. F) |
|---|---|
| 1 | 0.5 |
| 2 | 1.5 |
| 3 | 2.5 |
| 4 | 3.5 |
| 5 | 4.5 |
| 6 | 5.5 |

Figure 4.19 Contour maps of stator wake tracking temperatures measured at the second rotor exit.

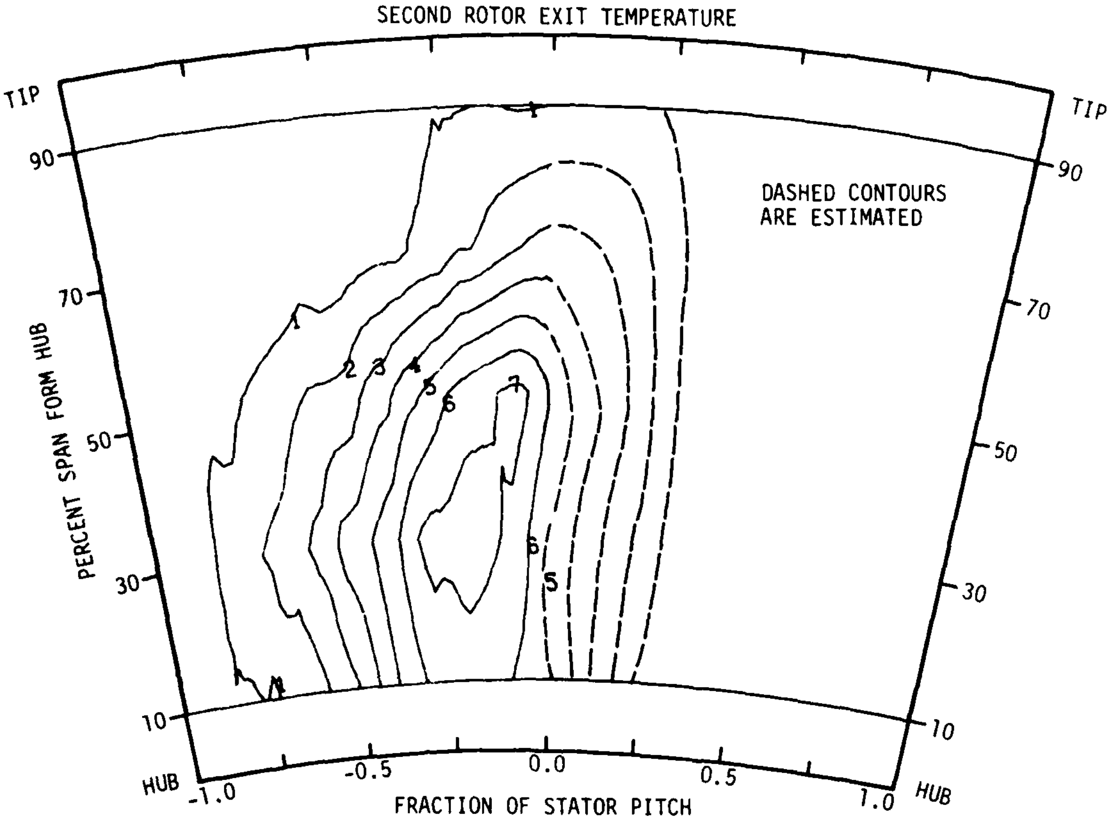


(b) $\phi$ = 0.500

| CURVE LABEL | CURVE VALUE (DEG. F) |
|---|---|
| 1 | 0.5 |
| 2 | 1.5 |
| 3 | 2.5 |
| 4 | 3.5 |
| 5 | 4.5 |
| 6 | 5.5 |
| 7 | 6.5 |

Figure 4.19 concluded.

avenue at mid-span, and (3) the spanwise behavior of corresponding contours for the flow coefficient of 0.575.

The following observations are based on the second rotor exit temperature and total-head contour maps:

- For each flow the wake avenue can be divided into two regions: (1) a "lower total-head sub-region" on the "right-side" portion of the wake avenue and (2) a "higher total-head sub-region" on the "left-side" portion of the wake avenue.
- At a flow coefficient of 0.500, adjacent wake avenues partially overlap from the hub to approximately 70% span from the hub. The single hub-to-tip valley in total head corresponds to the "lower total-head sub-region." The region of peak total head at 80% span is between wake avenues.
- At a flow coefficient of 0.587, adjacent wake avenues do not overlap at all over the entire span. The hub-to-tip valley in total head near 20% of the stator pitch corresponds to the "lower total-head sub-region" of a stator wake avenue. The second hub-to-tip valley crossing 50% of the stator pitch corresponds to the region between wake avenues. The region of peak total head from 30% to 50% span corresponds to the "higher total-head sub-region" of a stator wake avenue.
- At flow coefficients of 0.500 and less, adjacent wake avenues partially overlap over most of the span, and a single hub-to-tip valley in total head exists which corresponds to the "lower total-head sub-region" of a stator wake avenue.

- At flow coefficients of 0.525 and greater, adjacent wake avenues have a region between them which results in the formation of a second hub-to-tip valley in total head in one stator pitch.

An explanation of the variation in time-average total-head values within the wake avenues, and within the spaces between wake avenues, is beyond the scope of this study. Unsteady flow data would possibly clarify the physics involved. As pointed out by Zierke and Okiishi [12], the various kinds of fluid particles involved in chopped wake flow through a rotor (for example, freestream, stator wake, noninteracted rotor wake, interacted rotor wake) have different amounts of energy. The time-average total head at a point in space within the measurement window is a measure of the energy of the different kinds of particles that have passed through that measurement point.

## 4.4. Comparison of Compressor Builds

The detailed aerodynamic performance results obtained for the four different compressor builds at one operating point (venturi flow coefficient = 0.500 and shaft speed = 2400 rpm) are presented, compared, and analyzed in this section. Those data which most clearly show effects of stator geometry modification on the flow are emphasized. Two major subsections contained herein are:

1. Presentation and discussion of results
2. Analysis of stator geometry modification effects

The first major subsection proceeds in the following sequence:

- first stage performance
- second stage and overall performance
- first/second stage performance comparison
- mass-averaged performance

## 4.4.1. Presentation and Discussion of Results

### 4.4.1.1. First Stage Performance

Spanwise distributions of some first stage circumferential-mean performance parameters are presented in Figure 4.20. Conventional rotor and stage head-rise curves are shown in Figure 4.20(a) and (b), respectively. Figure 4.20(c) illustrates first stator loss variations, and Figure 4.20(d) involves first stator incidence and deviation angle data. First rotor head-rise performance is essentially unaffected by stator geometry modification. The differences between rotor head-rise curves in Figure 4.20(a) are not considered significant. This result is not surprising, since the upstream effect of the stator modification on rotor exit total head is expected to be small for the axial spacings involved. First rotor exit total-head contour maps for the baseline 1 and modified 1 builds are presented in Figure 4.21(a) and (b), respectively, and they demonstrate that first rotor exit total-head does not vary significantly with circumferential extent, thus substantiating the conclusion that stator blade influence on first rotor performance is nil. This constancy of first rotor head-rise performance between builds leads to the impression that the observed differences in first stage head-rise performance, indicated in

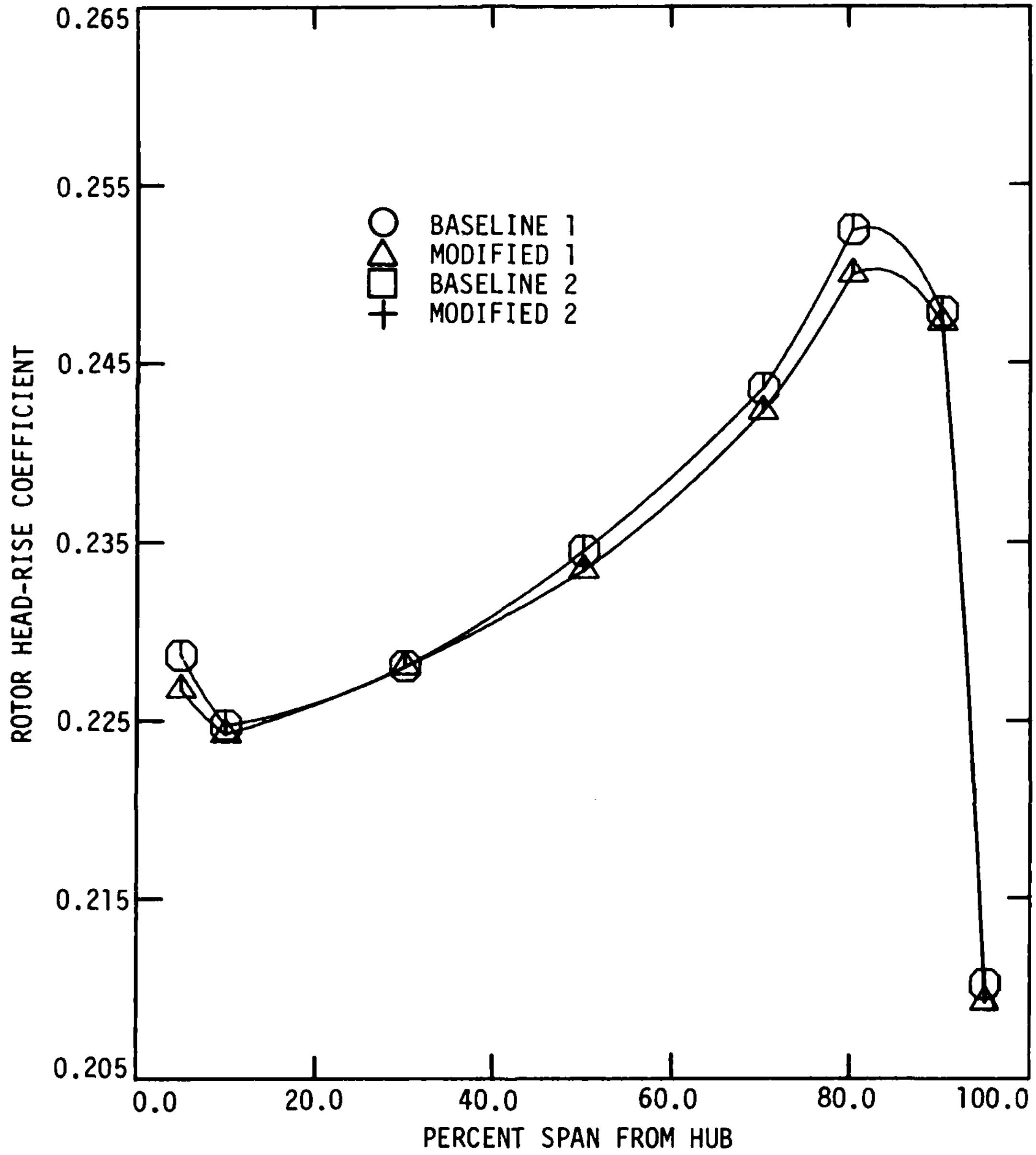


(a) ROTOR HEAD-RISE

Figure 4.20 Spanwise distribution of first stage circumferential-mean performance parameters for the different compressor builds ($\phi$ = 0.500).

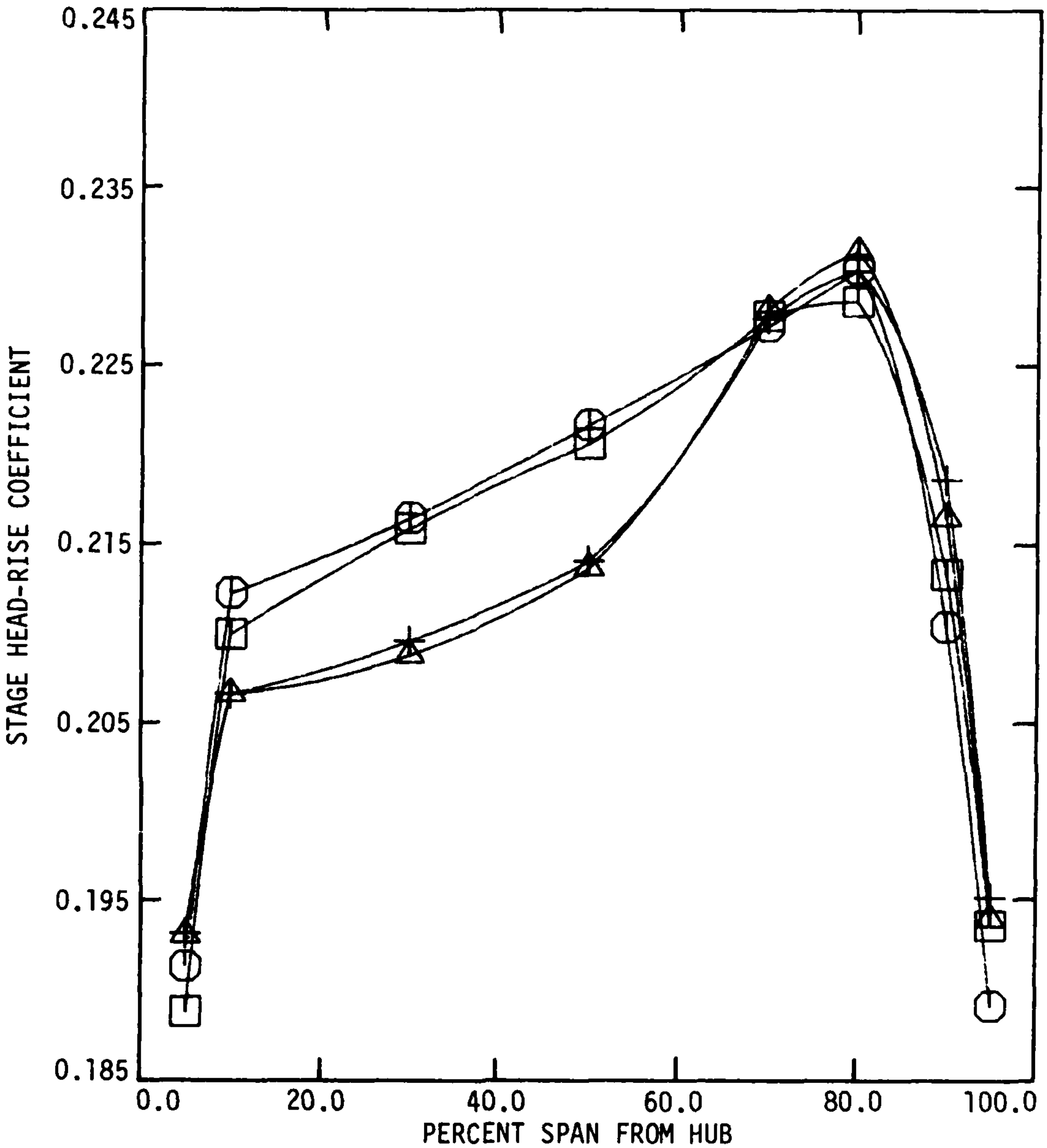


(b) STAGE HEAD-RISE

Figure 4.20 continued.

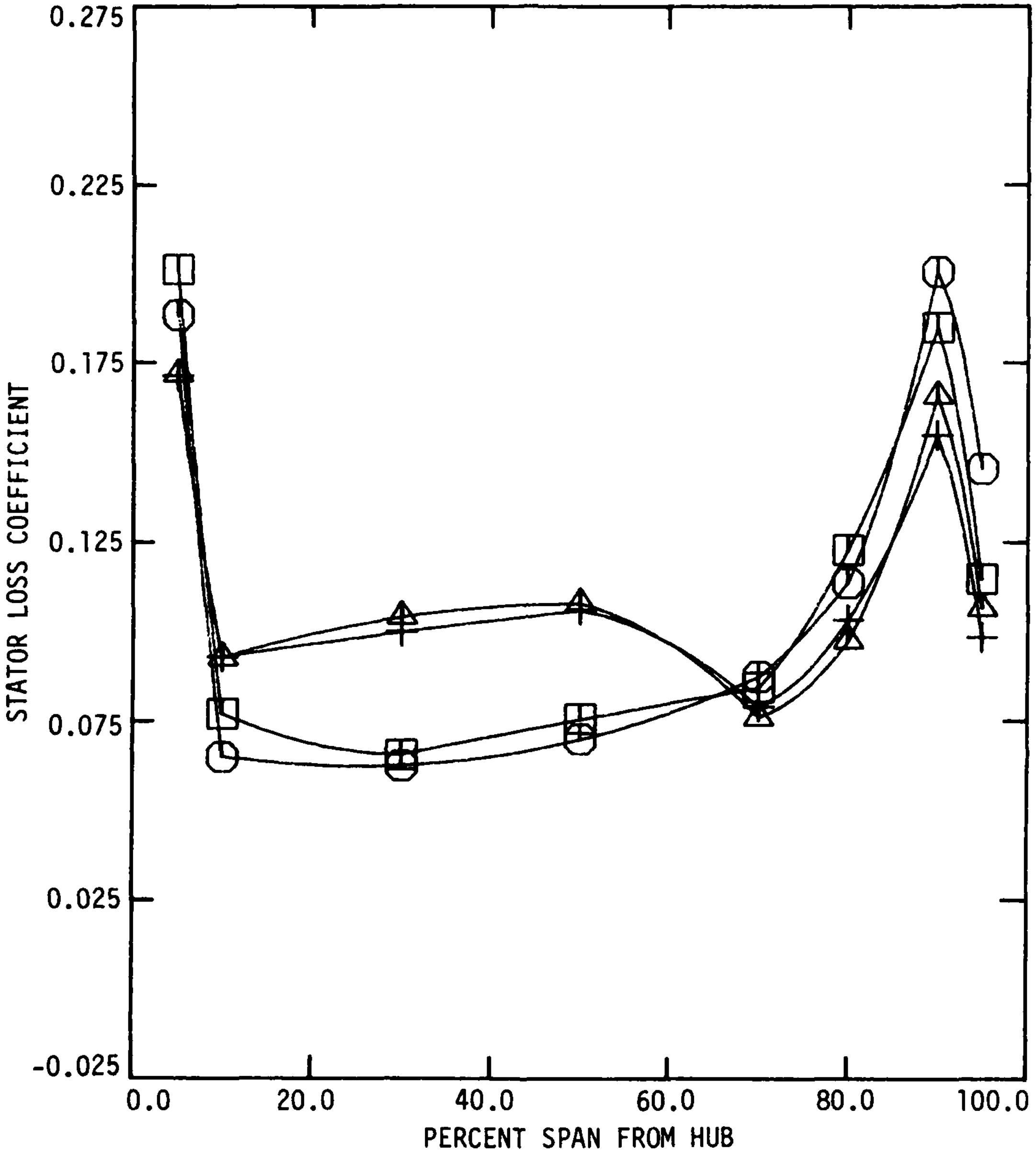

(c) STATOR LOSS

Figure 4.20 continued.

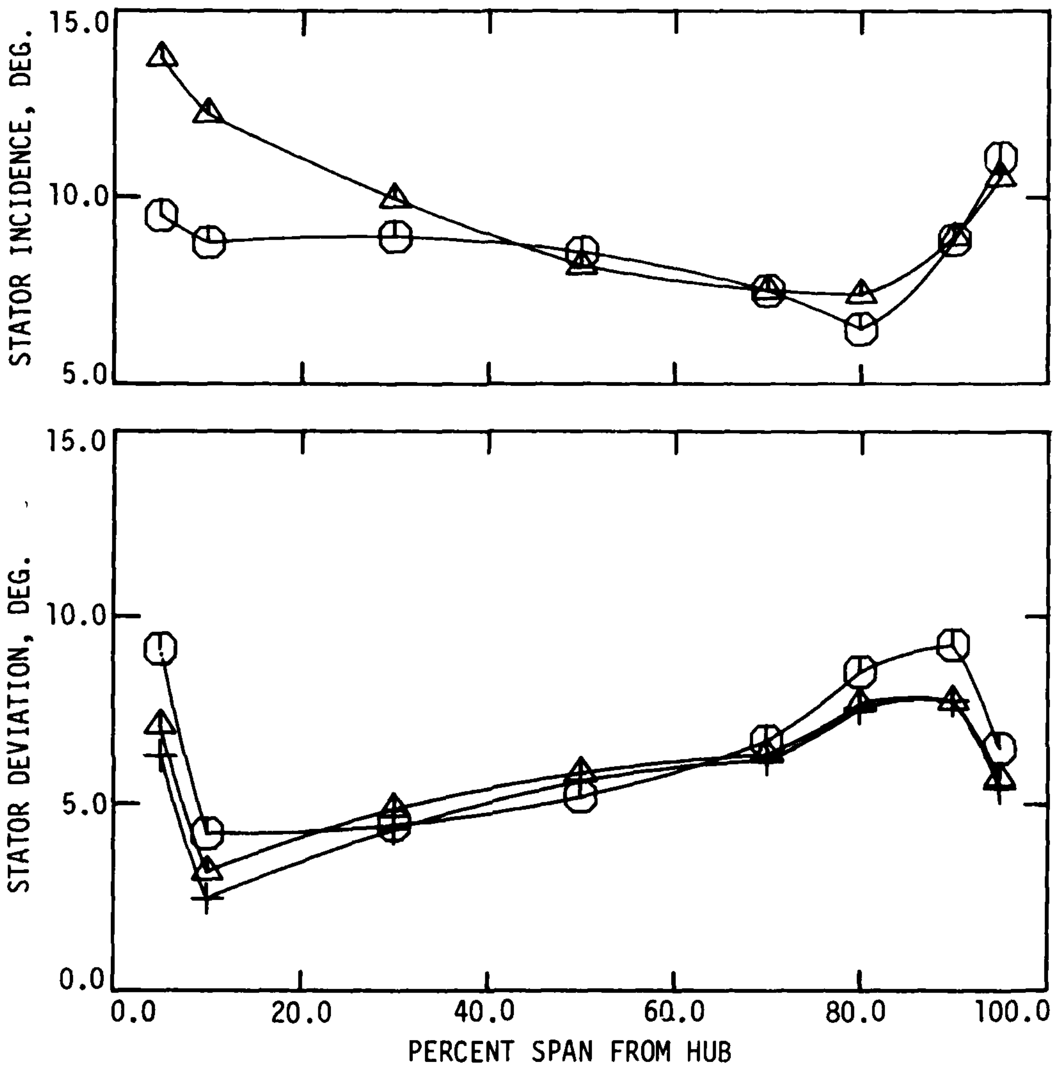


(d) STATOR INCIDENCE AND DEVIATION

Figure 4.20 concluded.

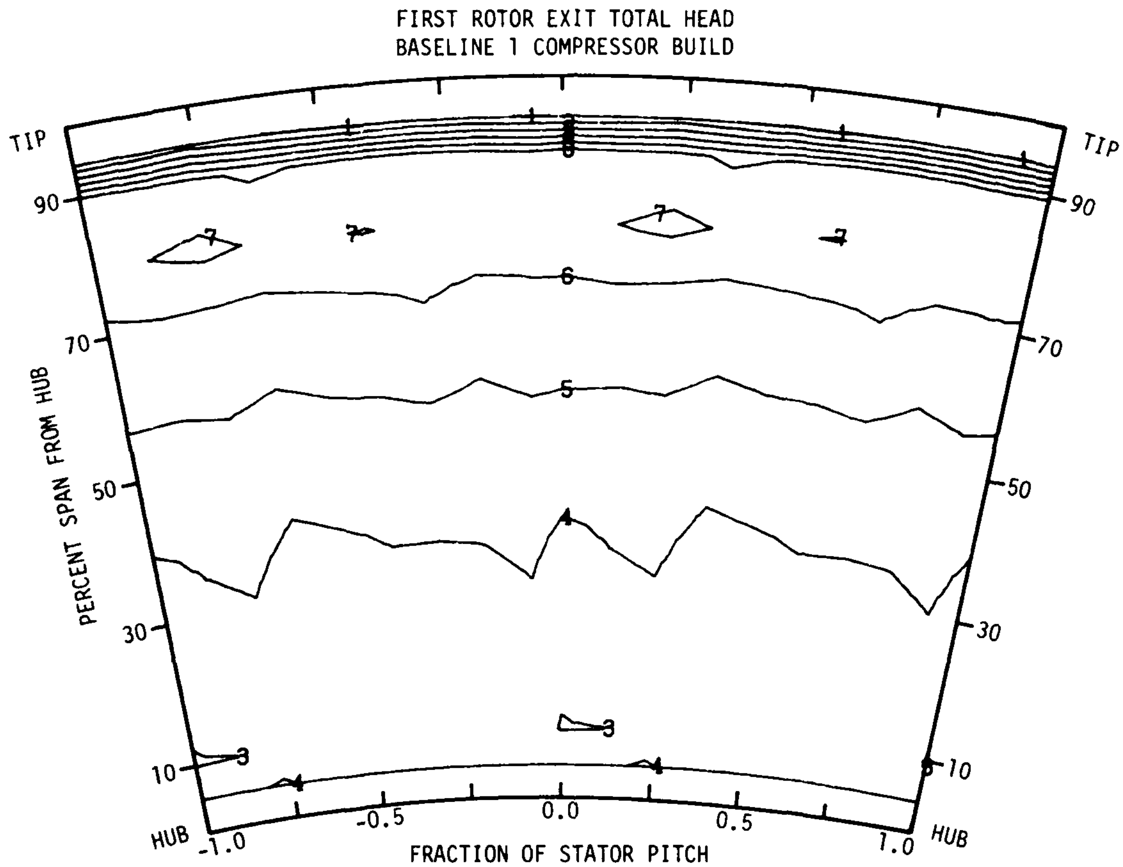


| CURVE LABEL | CURVE VALUE (N-M/KG) |
|---|---|
| 1 | 540 |
| 2 | 560 |
| 3 | 580 |
| 4 | 600 |
| 5 | 620 |
| 6 | 640 |
| 7 | 660 |

**Figure 4.21** First rotor exit total-head contour maps for the baseline 1 and modified 1 compressor builds ($\phi$ = 0.500).

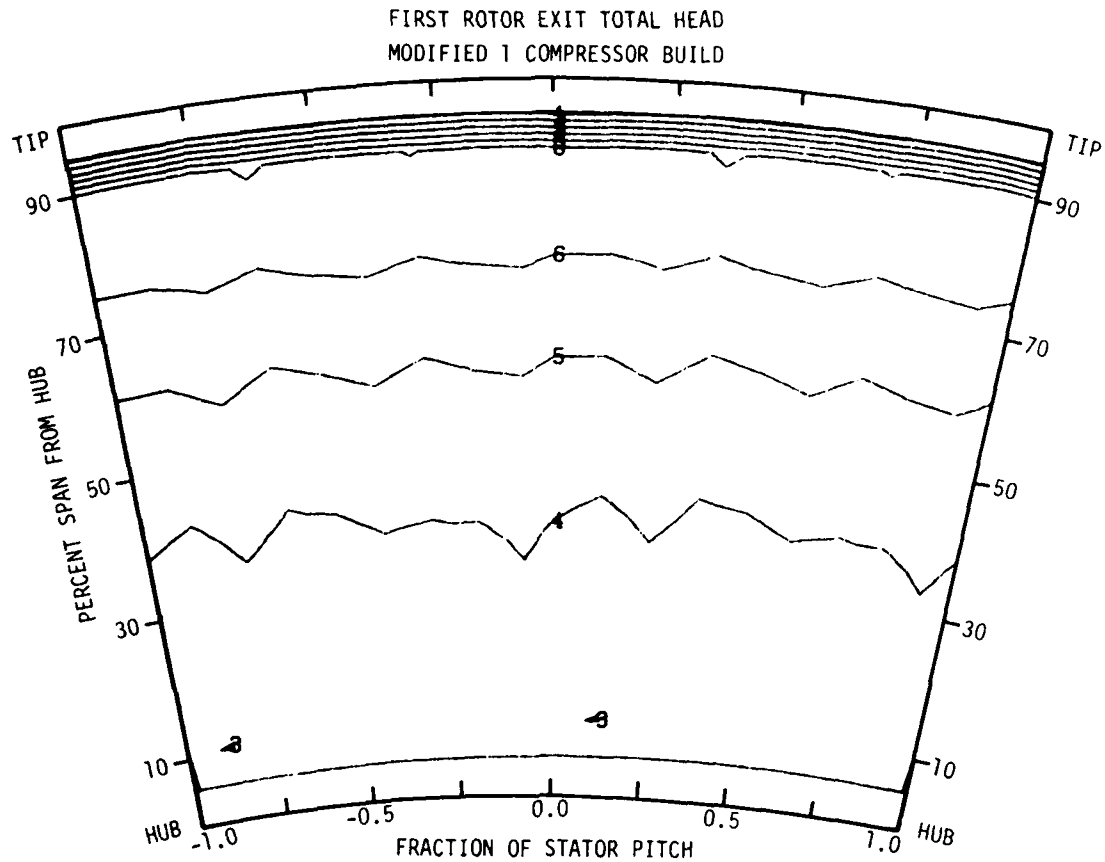


| CURVE LABEL | CURVE VALUE (N-M/KG) |
|---|---|
| 1 | 540 |
| 2 | 560 |
| 3 | 580 |
| 4 | 600 |
| 5 | 620 |
| 6 | 640 |

**Figure 4.21 concluded.**

Figure 4.20(b), can be directly attributed to the first stator loss performance shown in Figure 4.20(c).

The stator loss curves in Figure 4.20(c) suggest a significant difference in first stator loss performance by the baseline and modified stator blades. It should be noted (see Table 2.3 and Figure 2.5) that the two baseline builds, and similarly the two modified builds, are each pair identical in the first stage. Therefore, no difference in stator loss performance is expected between the builds based on a common stator. The data verify this, with the differences between baseline 1 and 2, and between modified 1 and 2 first stator data in Figure 4.20(c) being insignificant.

The difference in spanwise distribution of first stator loss between each pair of builds can be readily described:

- The baseline stator loss is substantially less than the modified stator loss from 10% to 50% span from the hub.
- The modified stator loss is somewhat (significantly) less than the baseline stator loss from 70% to 95% span from the hub, and also at 5% span from the hub.

The first stator exit total-head contour maps for the different builds are presented in Figure 4.22. These maps allow one to relate the above observed stator loss behavior for the different build pairs to the wake behavior of each kind of stator blade geometry. Only a baseline/modified comparison is made for the first stator; however, maps for all four builds are included for completeness, and also to confirm data repeatability.

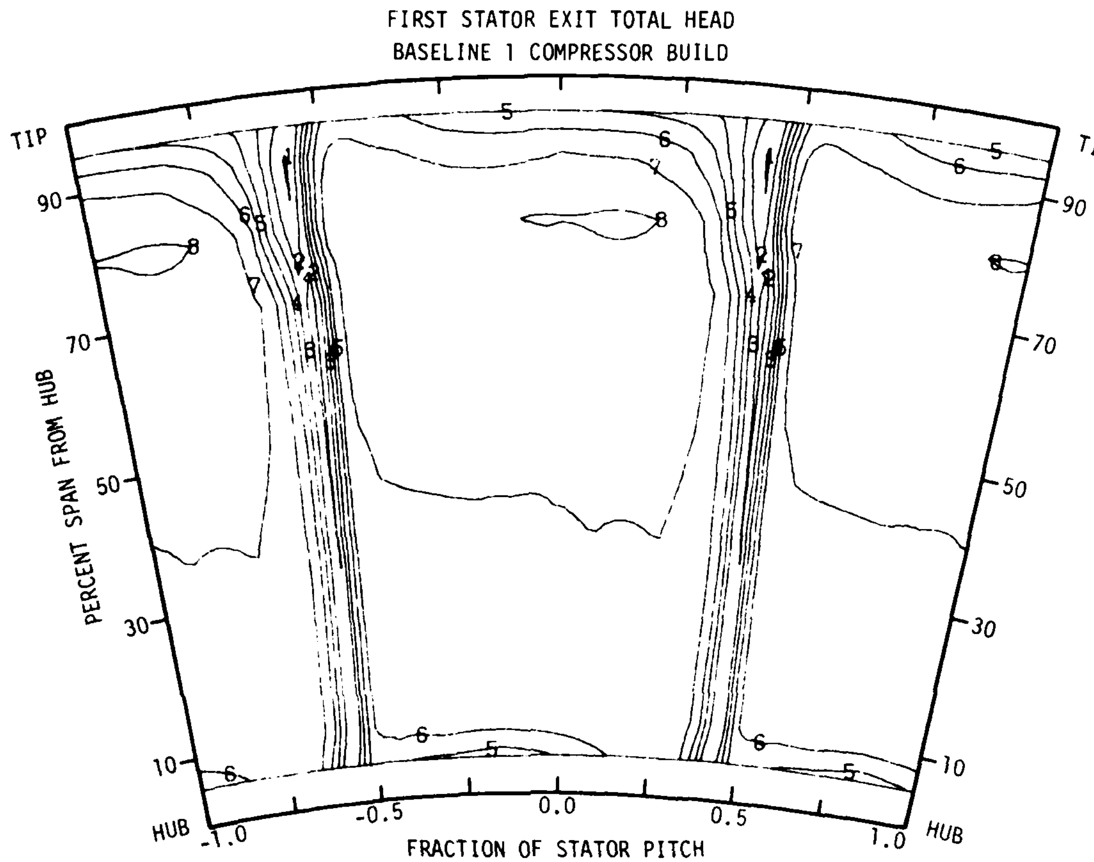


| CURVE LABEL | CURVE VALUE (N-M/KG) |
|---|---|
| 1 | 290 |
| 2 | 340 |
| 3 | 390 |
| 4 | 440 |
| 5 | 490 |
| 6 | 540 |
| 7 | 590 |
| 8 | 640 |

**Figure 4.22 First stator exit total-head contour maps for each compressor build ($\phi = 0.500$).**

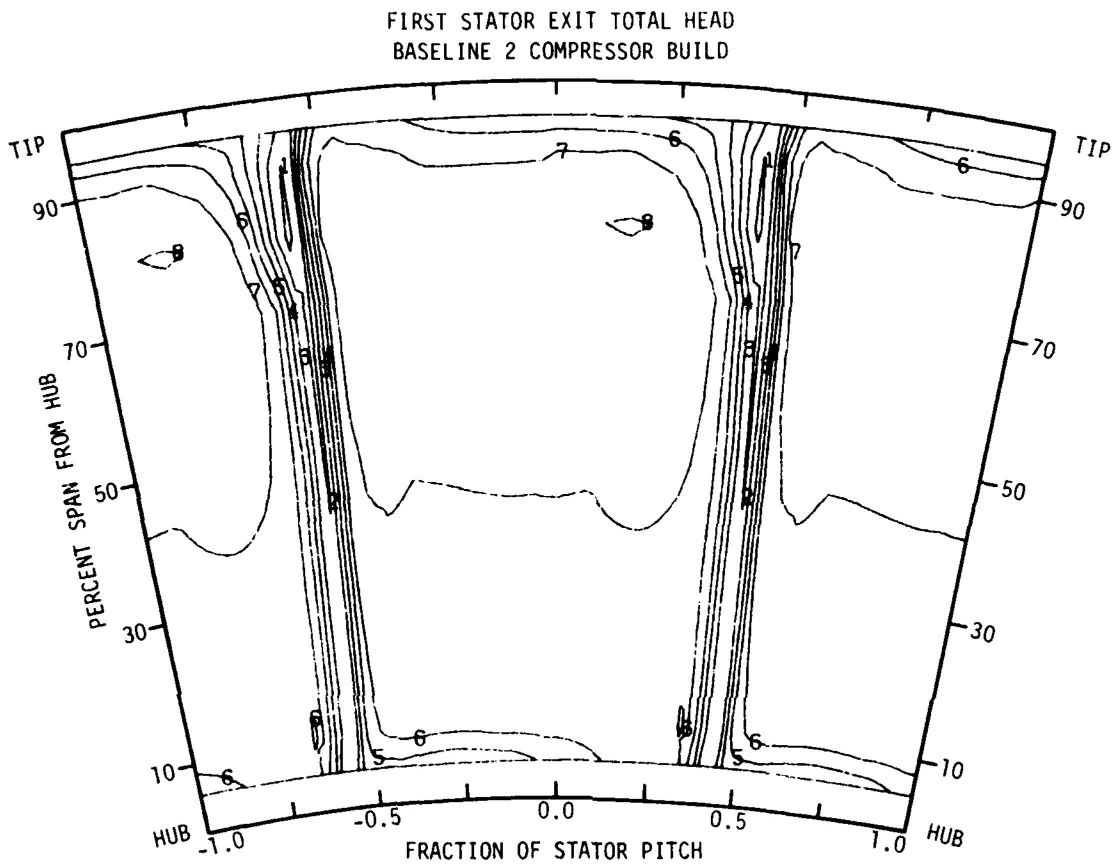


| CURVE LABEL | CURVE VALUE (N-M/KG) |
|---|---|
| 1 | 290 |
| 2 | 340 |
| 3 | 390 |
| 4 | 440 |
| 5 | 490 |
| 6 | 540 |
| 7 | 590 |
| 8 | 640 |

Figure 4.22 continued.

FIRST STATOR EXIT TOTAL HEAD
MODIFIED 1 COMPRESSOR BUILD

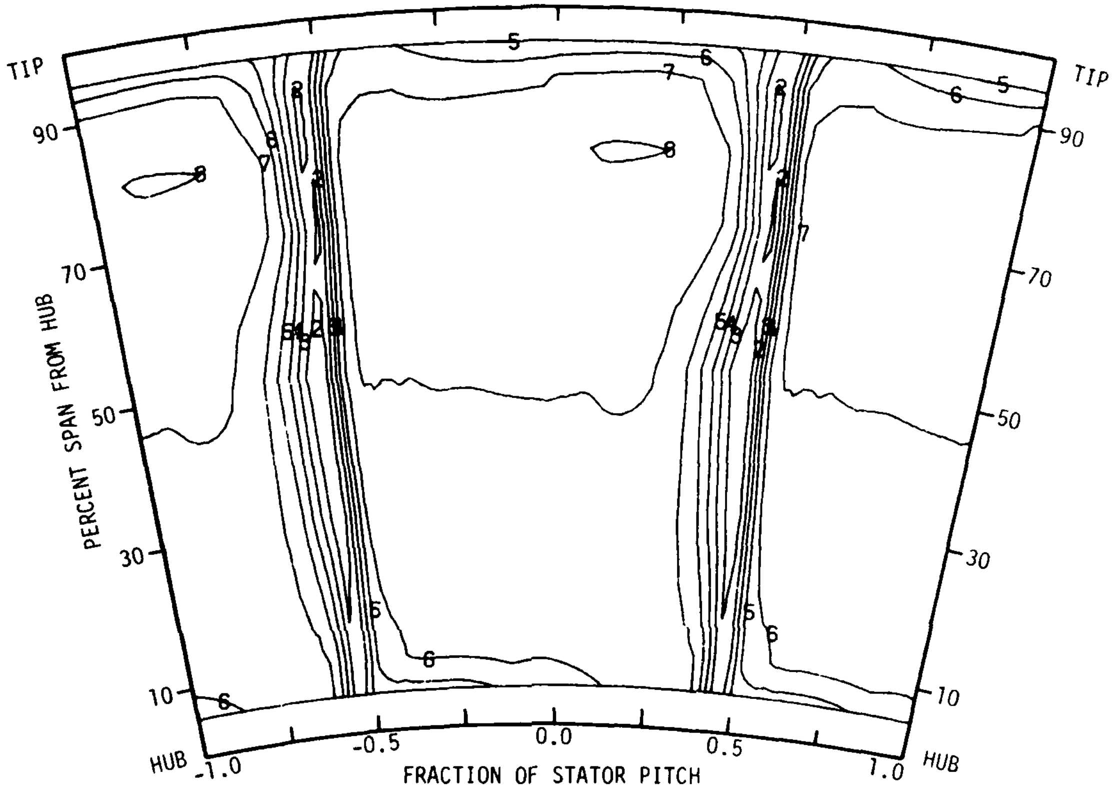


| CURVE LABEL | CURVE VALUE (N-M/KG) |
|---|---|
| 2 | 340 |
| 3 | 390 |
| 4 | 440 |
| 5 | 490 |
| 6 | 540 |
| 7 | 590 |
| 8 | 640 |

Figure 4.22 continued.

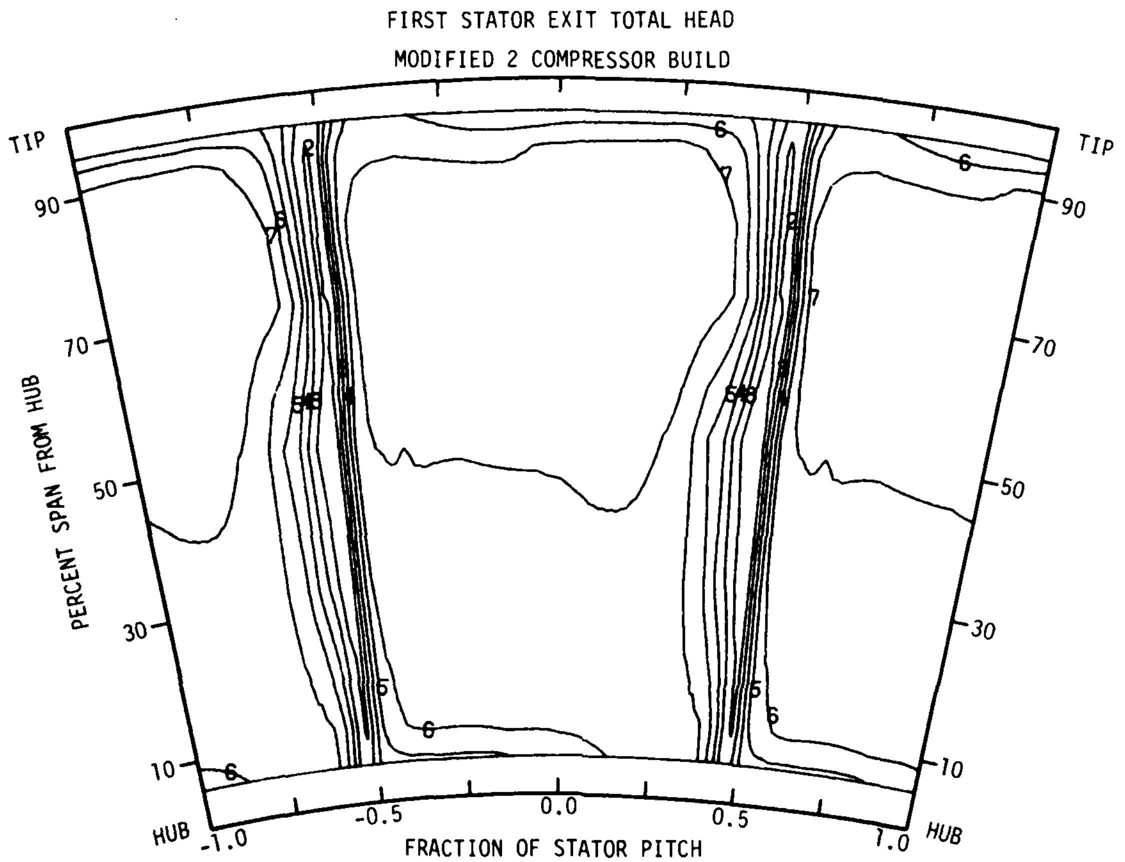


| CURVE LABEL | CURVE VALUE (N-M/KG) |
|---|---|
| 2 | 340 |
| 3 | 390 |
| 4 | 440 |
| 5 | 490 |
| 6 | 540 |
| 7 | 590 |

**Figure 4.22 concluded.**

The stator exit total-head contour maps display in some detail the stator exit wake and end-wall flows. On these maps, gradients in total head are easily discerned from the contours. From these gradients, the extent of the wake and end-wall flows can be inferred. Because stator row losses are generated mainly within these two flows, there exists a good correlation between the observed wake/end-wall region depth and extent and the corresponding circumferential-mean stator loss.

The following observations are based on the baseline first stator exit total-head contour map(s) (Figure 4.22) and the baseline first stator loss curve(s) (Figure 4.20(c)):

- The first stator wake is uniform in width and gradually increases in depth from 10% to 70% span from the hub. Correspondingly, the first stator loss gradually increases from 10% to 70% span from the hub.
- The first stator wake flairs out, mostly on the suction side, into an end-wall flow from 70% span to the tip. There is a corresponding increase in the first stator loss from 70% to 90% span from the hub. A probable reason for the drop in stator loss near the tip was previously discussed in section 4.3.1.
- Near the hub there is a "piling-up" of lower-momentum fluid on the pressure side of the stator blade. This is accompanied by a corresponding abrupt increase in stator loss near the hub. More detailed discussion concerning this was presented previously in section 4.3.1.

A comparison between the baseline and modified first stator exit total-head contour maps is shown in Figure 4.23. The following flow-field differences can be noted from this comparison, and related to corresponding first stator loss curves:

- The modified stator wake is substantially wider on the suction side, and somewhat deeper, than the baseline stator wake from 10% to 70% span from the hub. This is consistent with the first stator loss curves.
- The modified stator wake is similar in width and depth to the baseline stator wake at 70% span from the hub. Correspondingly, the first stator loss is almost the same for both geometries there.
- The modified stator wake "end-wall flair" on the suction side from 70% span to the tip, is substantially less than that for the baseline stator. The modified stator wake "end-wall flair" on the pressure side at both the hub and tip, is somewhat greater than that for the baseline stator. However, the net effect is seen as lower loss in the end-wall regions for the modified blade than for the baseline blade.

The first stator incidence and deviation angle results (Figure 4.20(d)) are discussed next. Only a few points seem salient:

- There is no recognizable relationship between the spanwise trends in first stator incidence angle and those in first stator loss.
- There is an approximate correlation between the spanwise trends in first stator deviation angle and those in first

FIRST STATOR EXIT TOTAL HEAD

BLACK BASELINE 1 BUILD
RED MODIFIED 1 BUILD

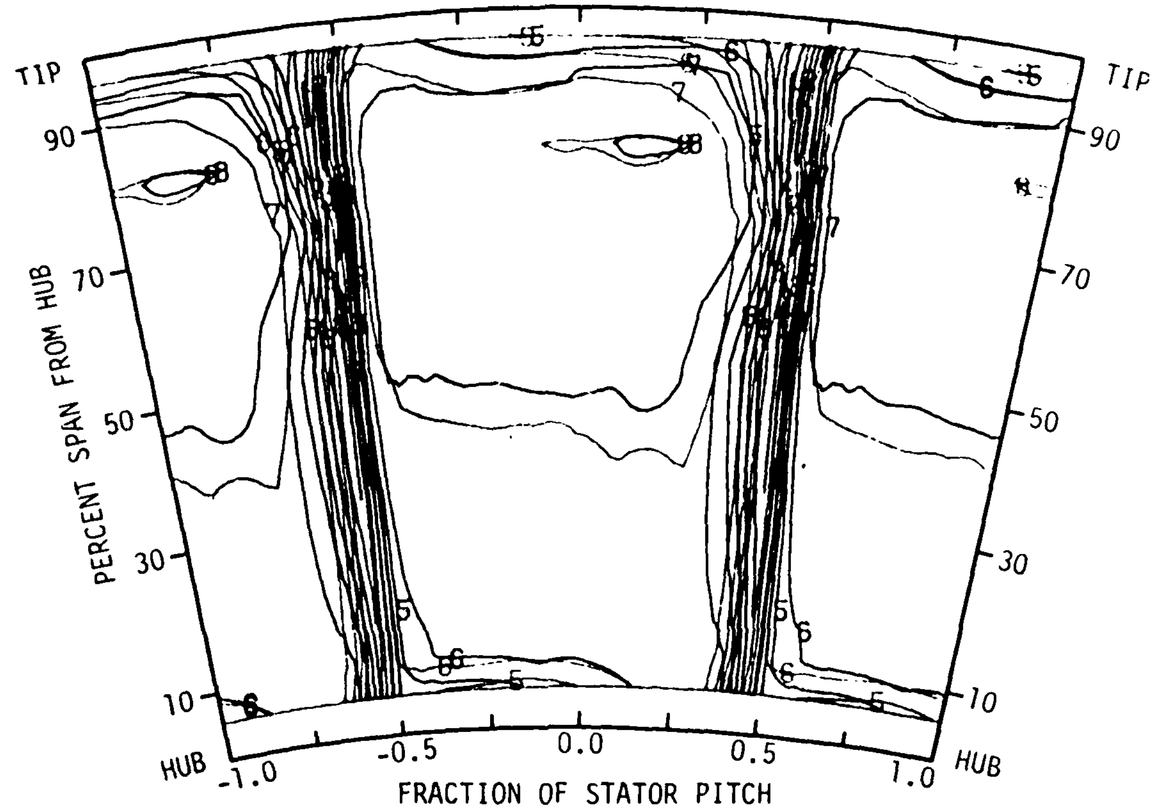


| CURVE LABEL | CURVE VALUE (N-M/KG) |
|---|---|
| 1 | 290 |
| 2 | 340 |
| 3 | 390 |
| 4 | 440 |
| 5 | 490 |
| 6 | 540 |
| 7 | 590 |
| 8 | 640 |

Figure 4.23 Map comparing the total-head contours at the first stator exit for the baseline 1 and modified 1 compressor builds ($\phi$ = 0.500).

stator loss. The modified stator tends to involve less deviation angle than the baseline stator in the end-wall regions.

- The difference between the baseline and modified first stator incidence angles near the hub indicates some upstream effect of the stator modification on first rotor exit absolute flow angle, but only near the hub.

### 4.4.1.2. Second Stage and Overall Performance

Spanwise distributions of second stage circumferential-mean performance parameters are presented in Figure 4.24. Conventional rotor and stage head-rise curves are included in Figure 4.24(a) and (b), respectively. In Figure 4.24(c) are found compressor-inlet to second-rotor-exit head-rise curves. Because the compressor-inlet total-head distribution is approximately uniform, Figure 4.24(c) actually provides an effective comparison of normalized second rotor exit total-head curves for the different builds. Figure 4.24(d) involves second stator loss data, and Figure 4.24(e) illustrates second stator incidence and deviation angle variations.

Results which show how first and second rotor head-rise values are related were discussed earlier (see section 4.3.1). First and second rotor exit total-head distributions over the blade span were shown to be similar, even though the head-rise distributions were not. Thus, it was concluded that the trends in the spanwise distribution of second rotor conventional head-rise coefficients were approximately similar to those of first stator loss. A comparison of the first stator loss curves in Figure 4.20(c) with the second

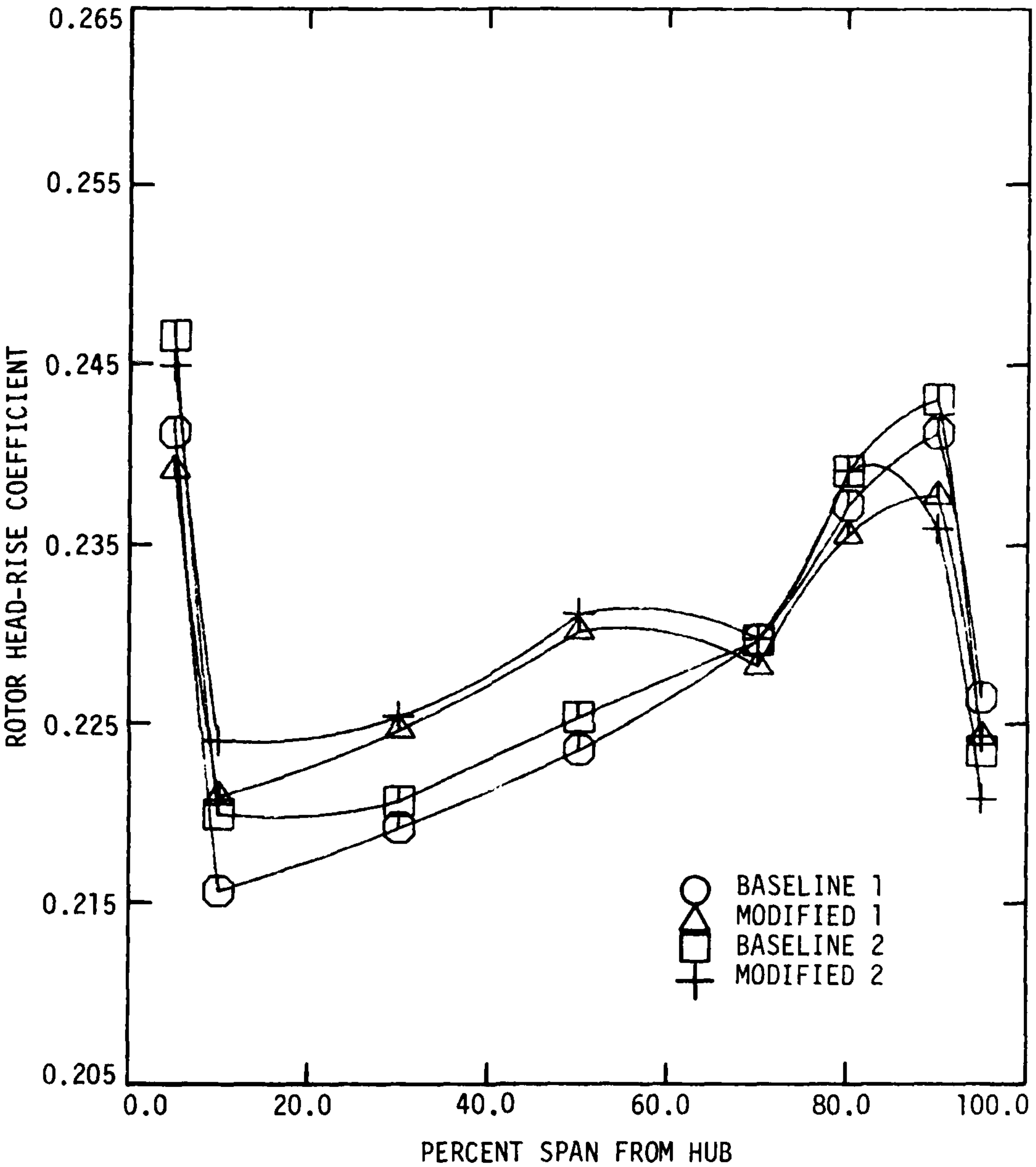


(a) ROTOR HEAD-RISE

Figure 4.24 Spanwise distribution of second stage circumferential-mean performance parameters for the different compressor builds ($\phi$ = 0.500).

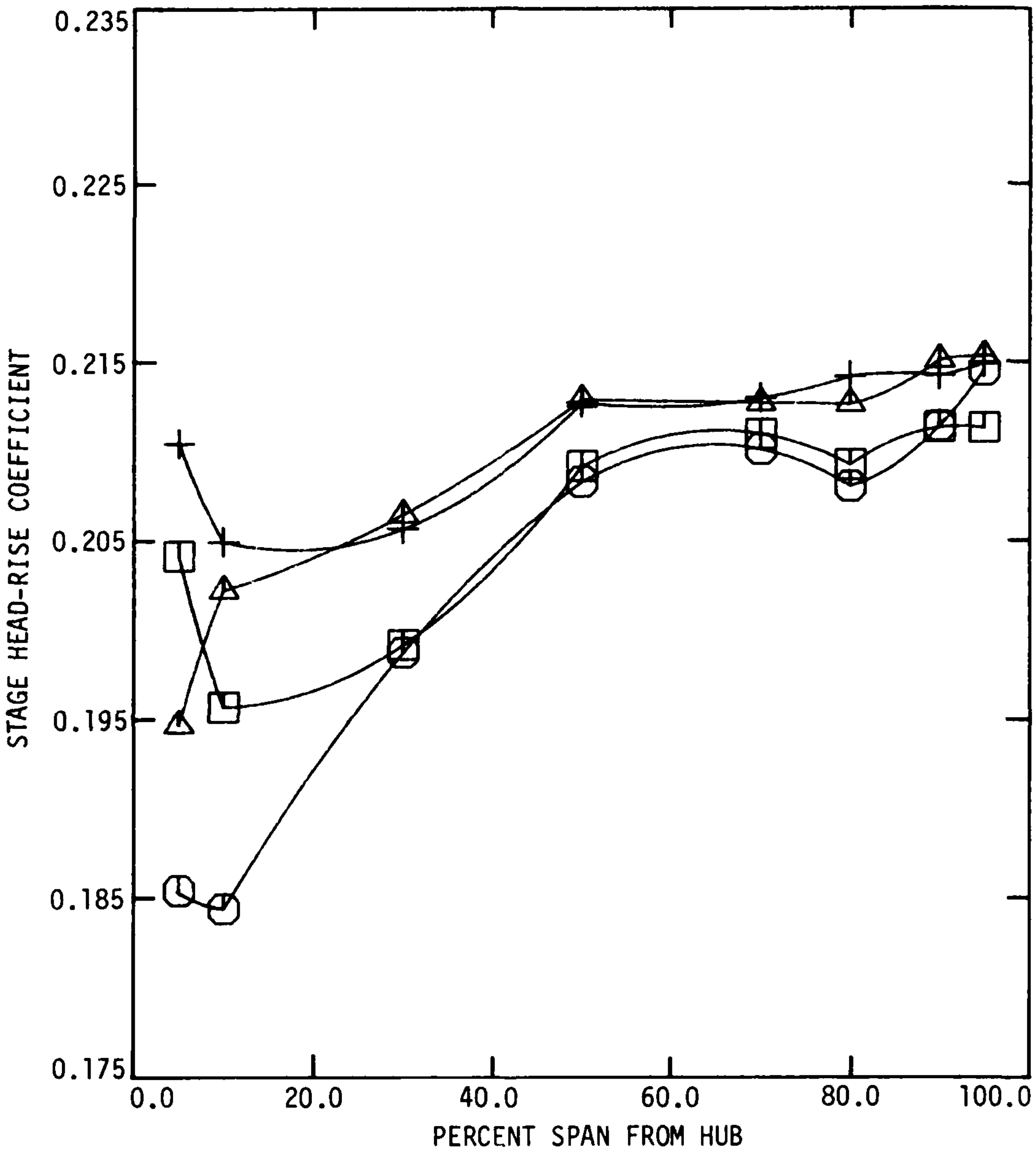


(b) STAGE HEAD-RISE

Figure 4.24 continued.

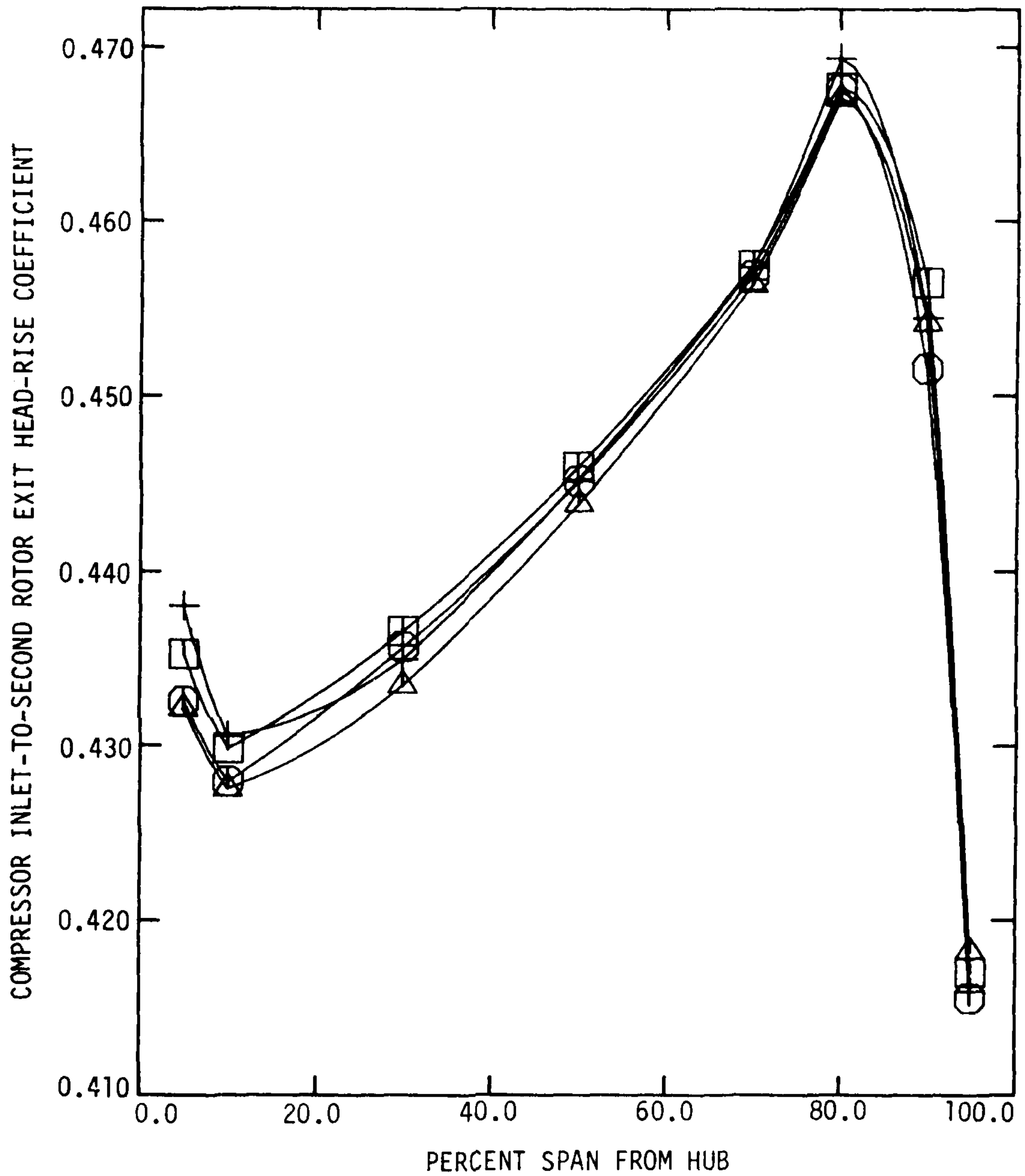


(c) COMPRESSOR INLET-TO-SECOND ROTOR EXIT HEAD-RISE

Figure 4.24 continued.

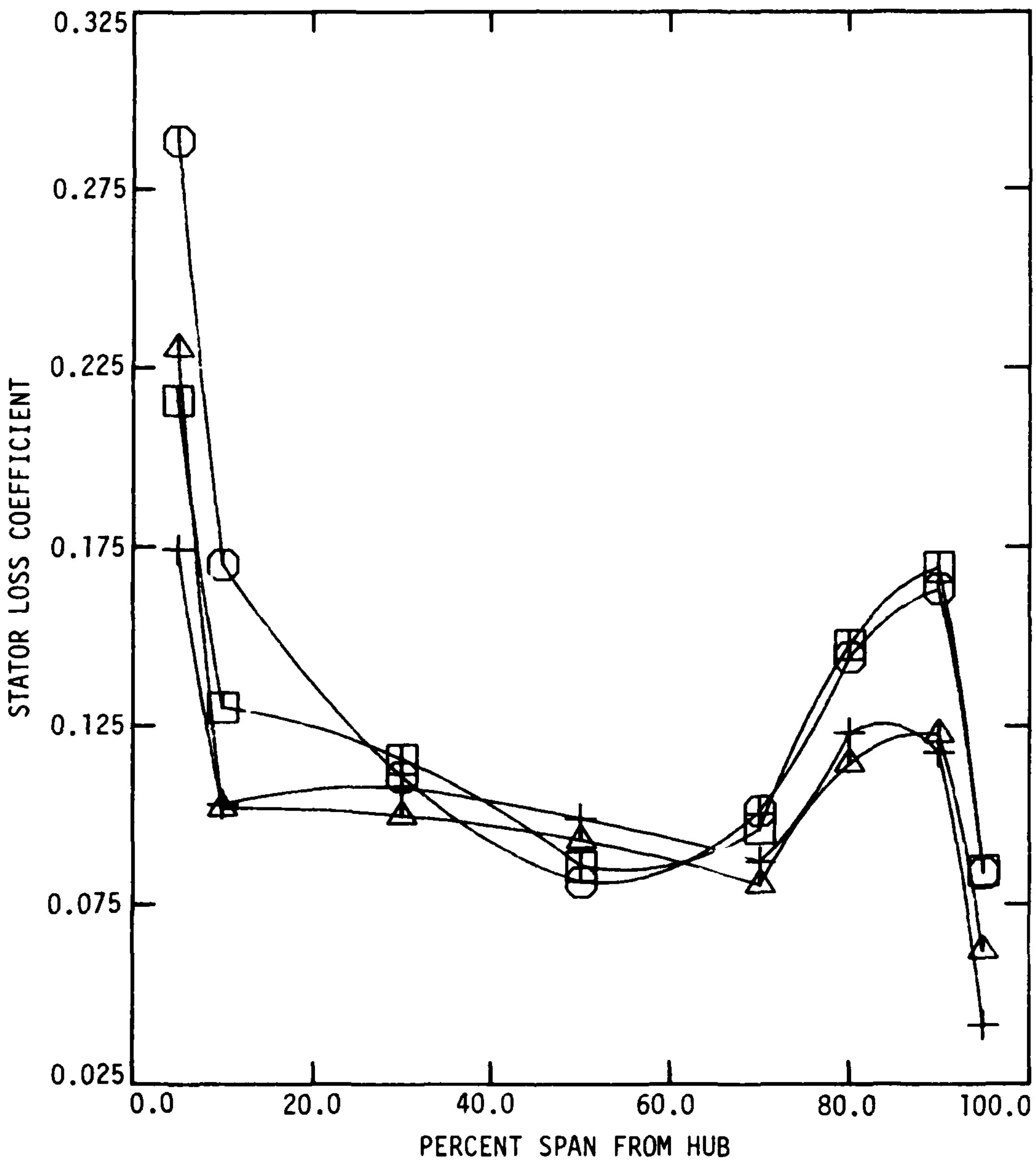


(d) STATOR LOSS

Figure 4.24 continued.

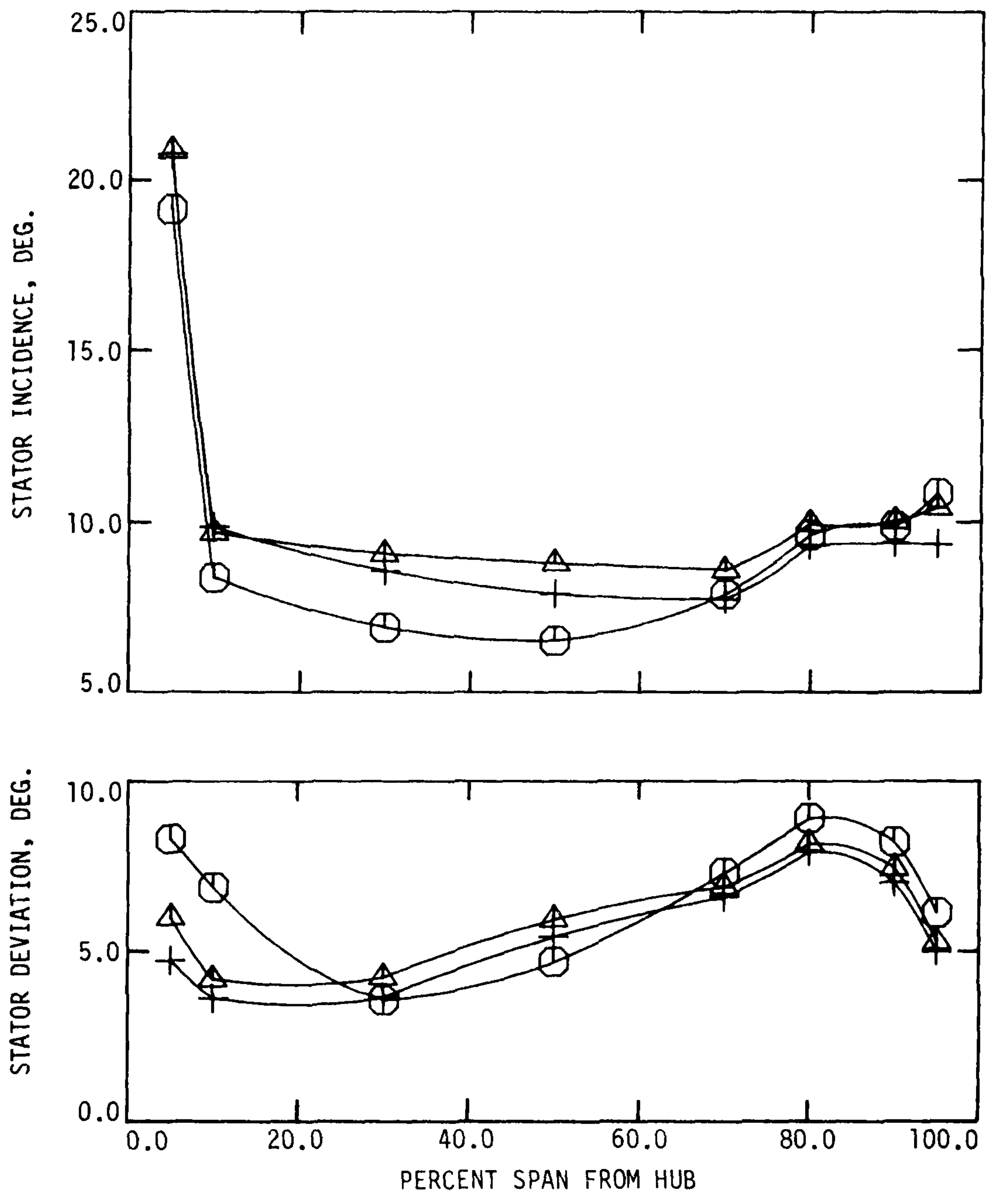

(e) STATOR INCIDENCE AND DEVIATION

Figure 4.24 concluded.

rotor head-rise curves in Figure 4.24(a) clearly verifies this relationship. Figure 4.24(c) can also be compared with Figure 4.20(a) to show the similarity in the first and second rotor exit total-head spanwise distributions, while also demonstrating the tendency of the second rotor row to compensate for variations in the spanwise distribution of total head at its inlet.

Second rotor exit total-head contour maps are presented in Figure 4.25. These maps demonstrate the general similarity of flow at the second rotor exit for the different builds, and confirm the trend indicated in Figure 4.24(c).

The second stage head-rise curves shown in Figure 4.24(b) contain a combination of second rotor and second stator performance information, and for that reason are difficult to analyze. Fortunately, it is not necessary to analyze these stage curves since enough useful information is obtained from an analysis of the second rotor and second stator flows. However, the stage curves do provide a comparison of the second stage head-rise performance. As is apparent by inspection of Figure 4.24(b), the two modified builds perform better in second stage head-rise than the two baseline builds over almost the entire span. The large differences between all four builds near the hub indicate that the second stator hub modifications decrease the near-hub losses considerably. This is clarified in some detail with the second stator loss curves (Figure 4.24(d)).

Curves showing the overall head-rise of the compressor for the different builds are presented in Figure 4.26. These curves are also closely related to the second stator loss curves. This follows

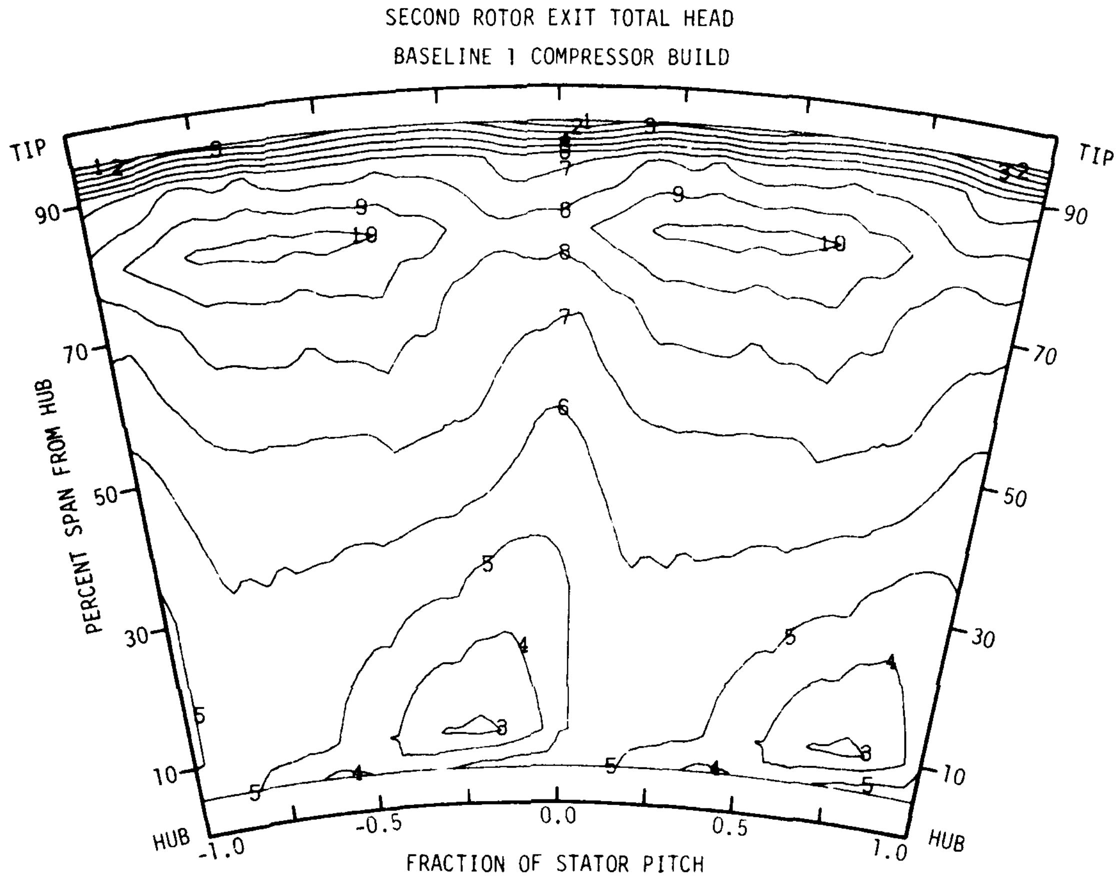


| CURVE LABEL | CURVE VALUE (N-M/KG) |
|---|---|
| 1 | 1050 |
| 2 | 1070 |
| 3 | 1090 |
| 4 | 1110 |
| 5 | 1130 |
| 6 | 1150 |
| 7 | 1170 |
| 8 | 1190 |
| 9 | 1210 |
| 10 | 1230 |

**Figure 4.25** Second rotor exit total-head contour maps for each compressor build ($\phi$ = 0.500).

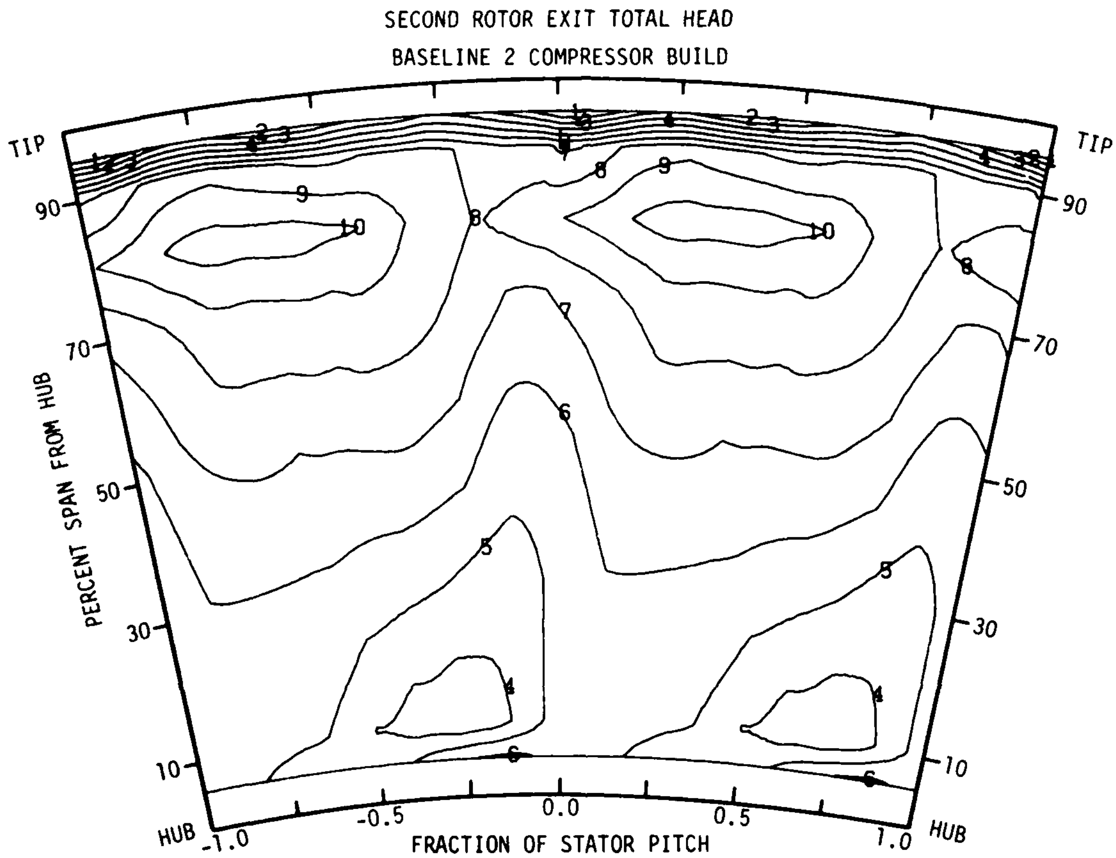


| CURVE LABEL | CURVE VALUE (N-M/KG) |
|---|---|
| 1 | 1050 |
| 2 | 1070 |
| 3 | 1090 |
| 4 | 1110 |
| 5 | 1130 |
| 6 | 1150 |
| 7 | 1170 |
| 8 | 1190 |
| 9 | 1200 |
| 10 | 1230 |

Figure 4.25 continued.

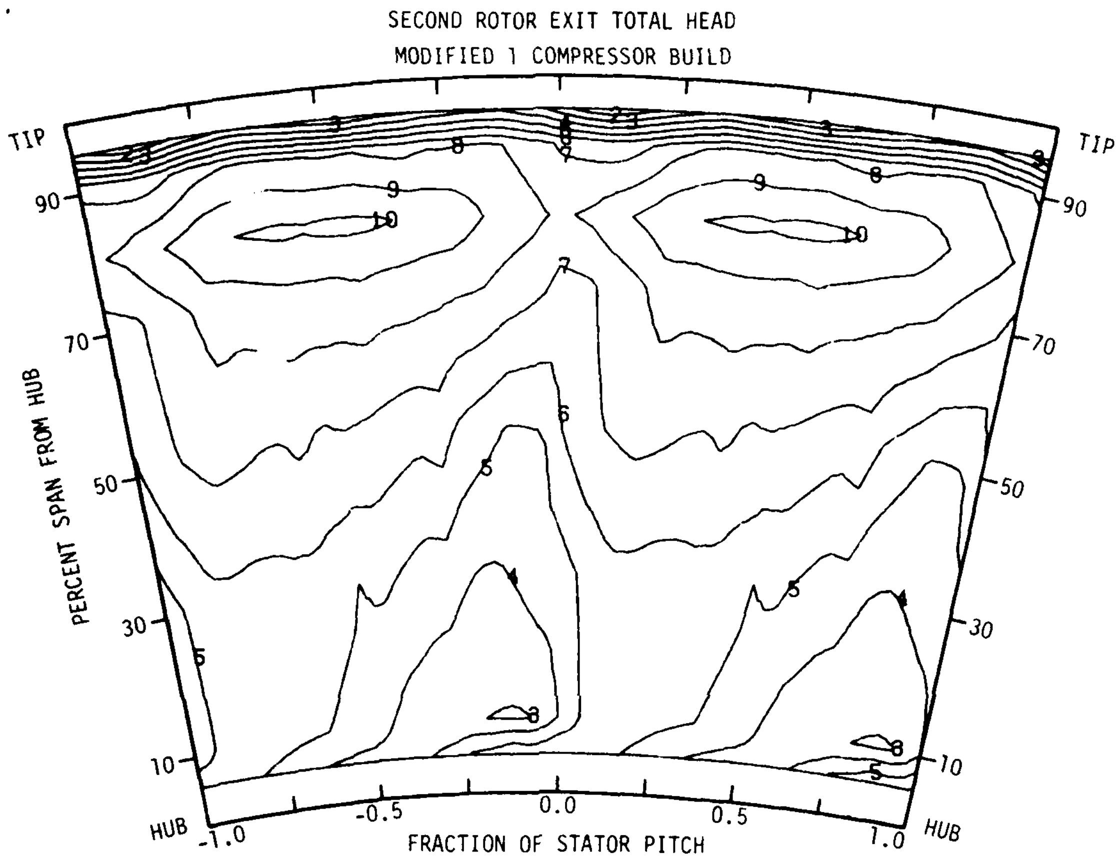


| CURVE LABEL | CURVE VALUE (N-M/KG) |
|---|---|
| 2 | 1070 |
| 3 | 1090 |
| 4 | 1110 |
| 5 | 1130 |
| 6 | 1150 |
| 7 | 1170 |
| 8 | 1190 |
| 9 | 1210 |
| 10 | 1230 |

Figure 4.25 continued.

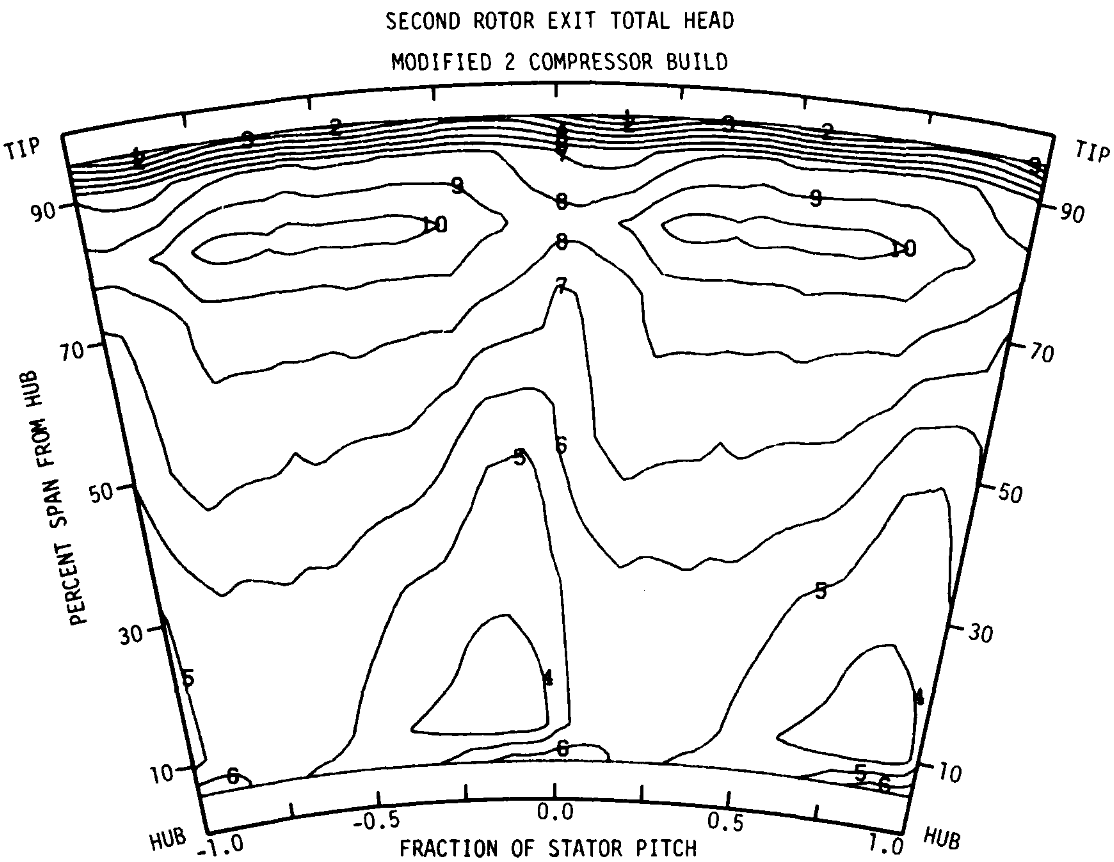


| CURVE LABEL | CURVE VALUE (N-M/KG) |
|---|---|
| 1 | 1050 |
| 2 | 1070 |
| 3 | 1090 |
| 4 | 1110 |
| 5 | 1130 |
| 6 | 1150 |
| 7 | 1170 |
| 8 | 1190 |
| 9 | 1210 |
| 10 | 1230 |

**Figure 4.25 concluded.**

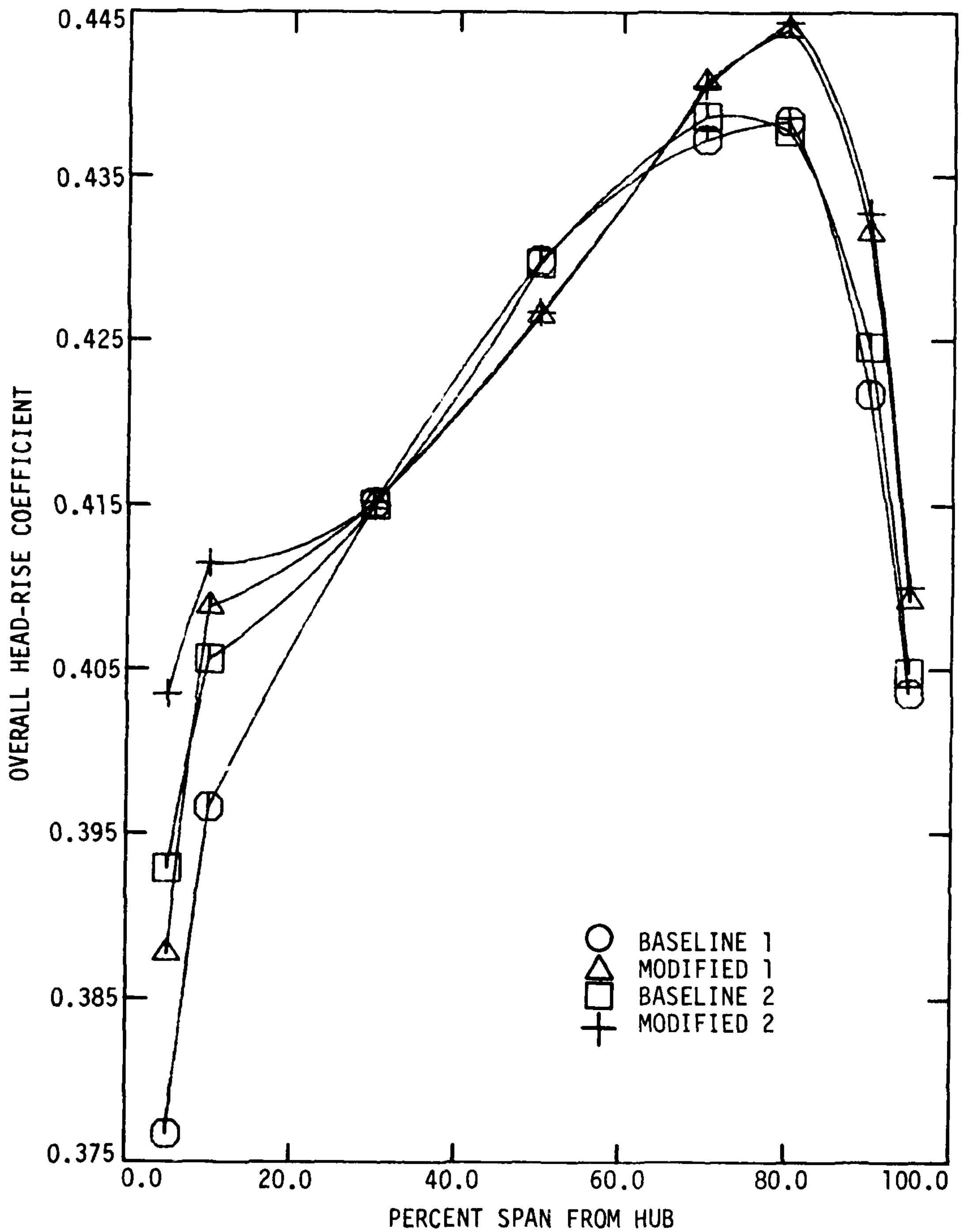


Figure 4.26 Spanwise distribution of circumferential-mean overall head-rise coefficients for the different compressor builds ($\phi = 0.500$).

from the similarity of all build spanwise distributions of second rotor exit total-head as shown in Figure 4.24(c).

The second stator loss curves in Figure 4.24(d) show significant differences in end-wall region loss performance between the different builds. Baseline 1 and 2 and modified 1 and 2 stator data differences from 30% to 90% span from the hub are not considered significant. The significant differences can be summarized as follows:

- The modified stator loss is substantially less than the baseline stator loss from 80% to 95% span from the hub, and also at 10% span from the hub.
- The modified stator loss is somewhat less than the baseline stator loss at 30% and 70% span from the hub, and somewhat greater at 50% span from the hub.
- The modified 2 build stator loss is substantially less than the modified 1 build stator loss at 5% and 95% span from the hub.
- The baseline 2 build stator loss is substantially less than the baseline 1 build stator loss at 5% and 10% span from the hub.

The second stator exit total-head contour maps for the different builds are presented separately in Figure 4.27. In Figure 4.28, second stator exit total-head contour maps are overlayed for more effective comparison of flow-field differences for the different builds. Specifically, Figure 4.28(a) compares the baseline 1 and modified 1 builds, Figure 4.28(b) compares the baseline 1 and 2 builds, and Figure 4.28(c) compares the modified 1 and 2 builds.

SECOND STATOR EXIT TOTAL HEAD
BASELINE 1 COMPRESSOR BUILD

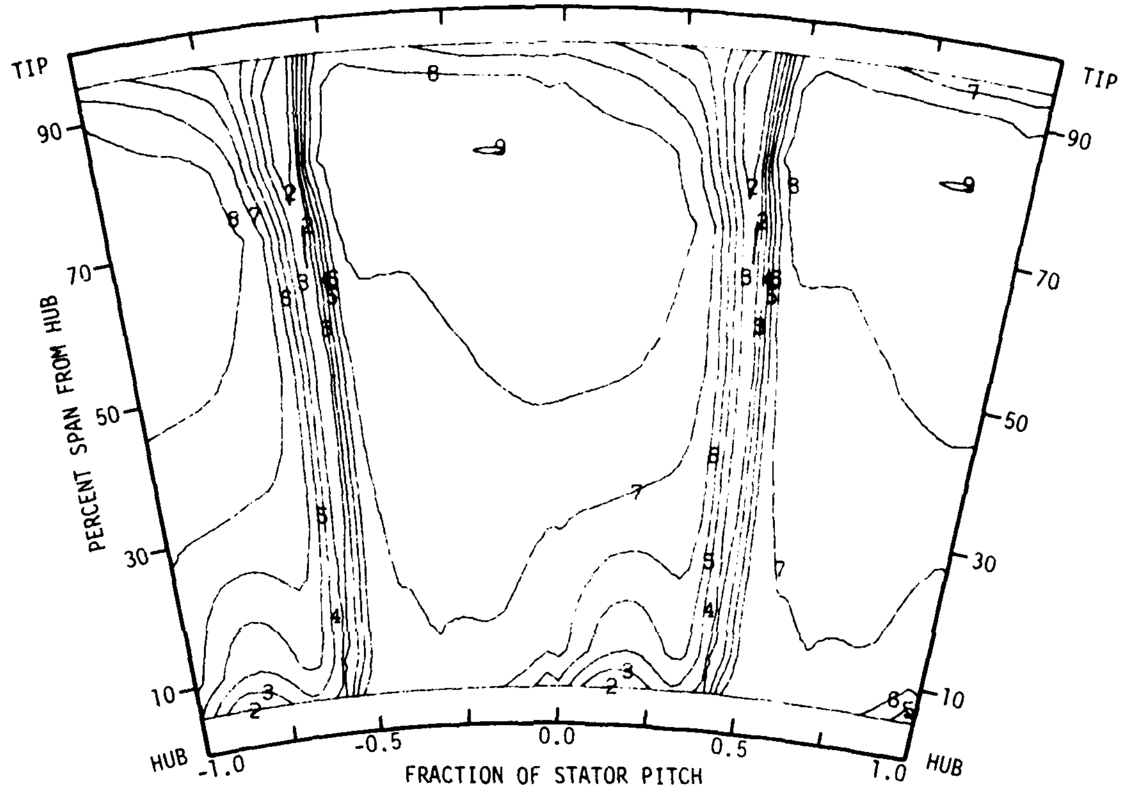


| CURVE LABEL | CURVE VALUE (N-M/KG) |
|---|---|
| 2 | 850 |
| 3 | 900 |
| 4 | 950 |
| 5 | 1000 |
| 6 | 1050 |
| 7 | 1100 |
| 8 | 1150 |
| 9 | 1200 |

**Figure 4.27** Second stator exit total-head contour maps for each compressor build ($\phi = 0.500$).

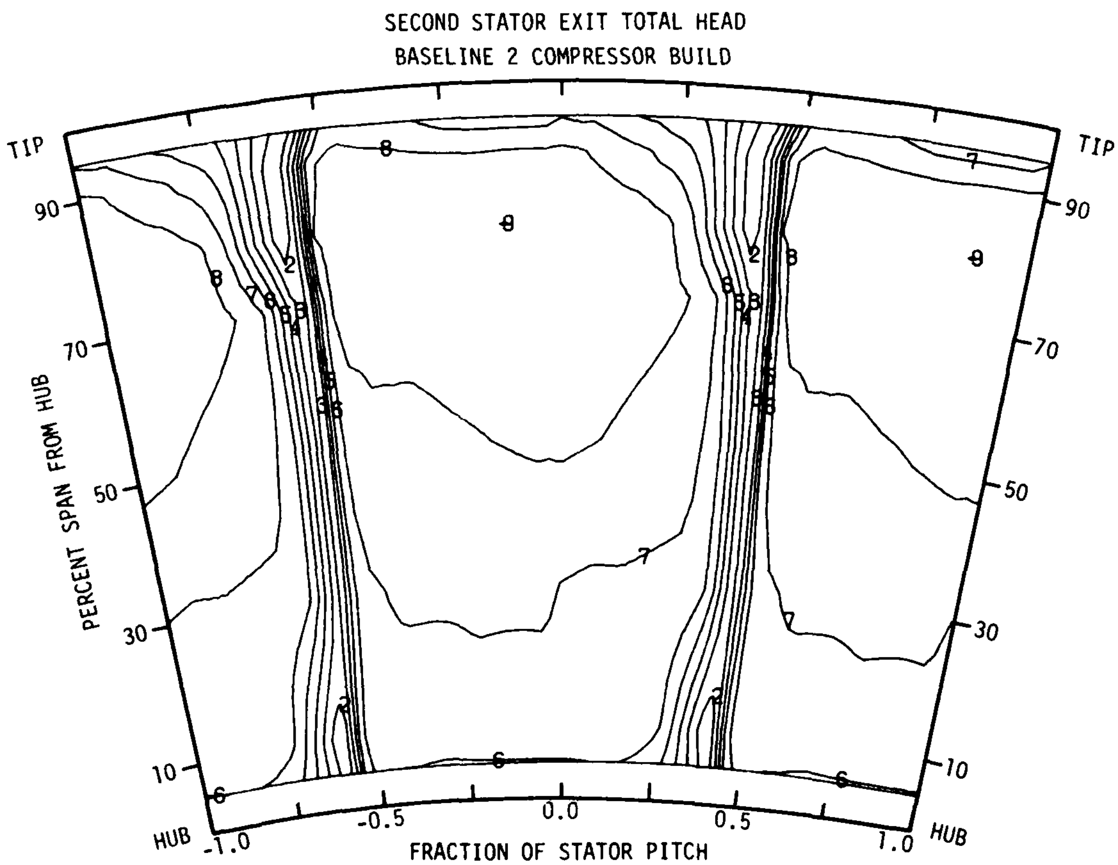


| CURVE LABEL | CURVE VALUE (N-M/KG) |
|---|---|
| 2 | 850 |
| 3 | 900 |
| 4 | 950 |
| 5 | 1000 |
| 6 | 1050 |
| 7 | 1100 |
| 8 | 1150 |
| 9 | 1200 |

Figure 4.27 continued.

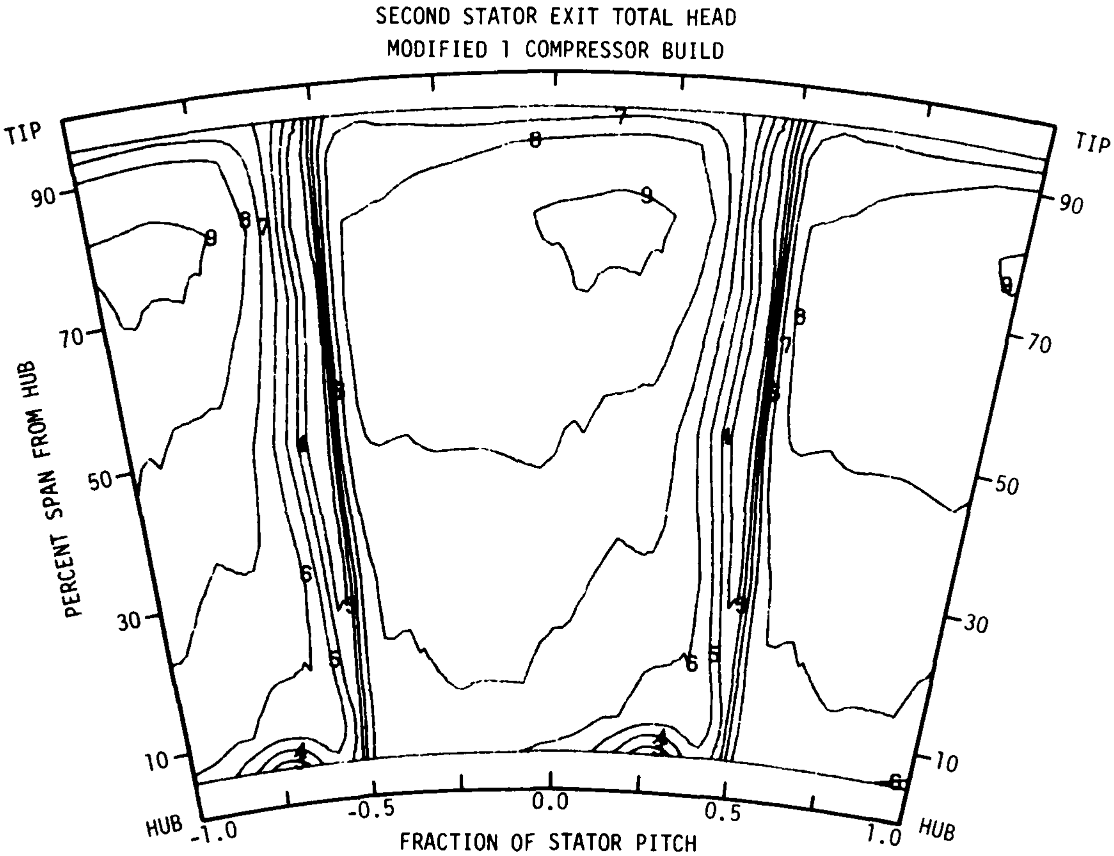


| CURVE LABEL | CURVE VALUE (N-M/KG) |
|---|---|
| 3 | 900 |
| 4 | 950 |
| 5 | 1000 |
| 6 | 1050 |
| 7 | 1100 |
| 8 | 1150 |
| 9 | 1200 |

**Figure 4.27 continued.**

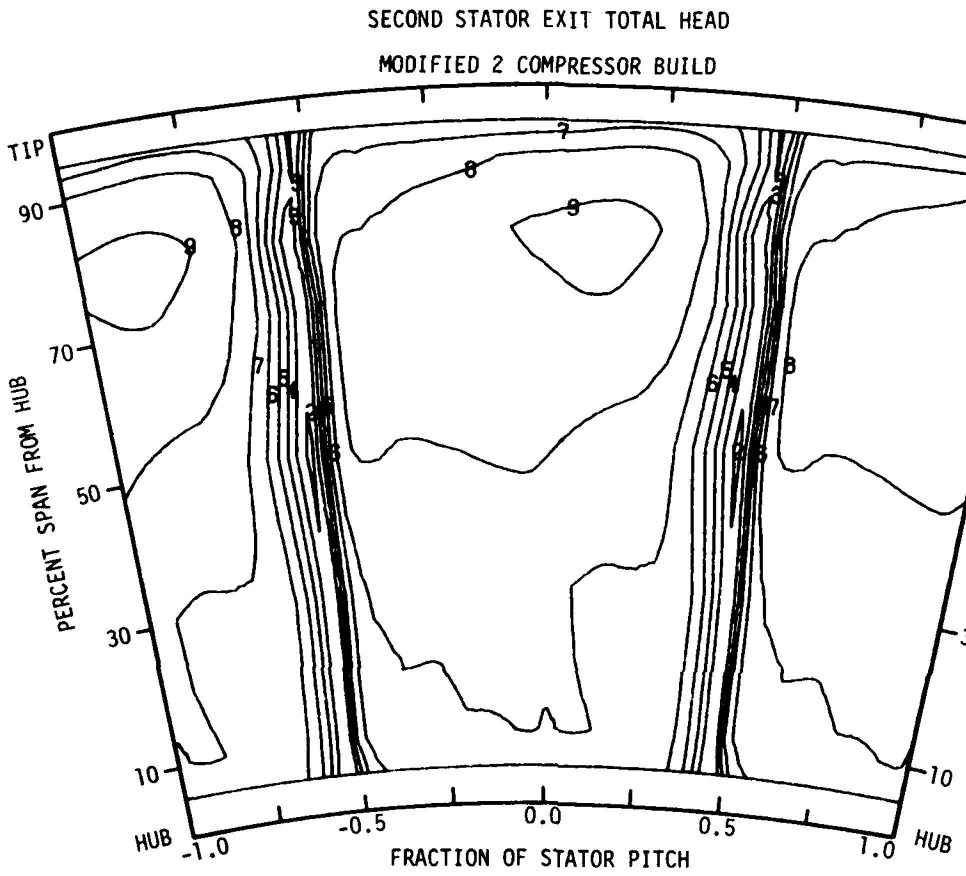


| CURVE LABEL | CURVE VALUE (N-M/KG) |
|---|---|
| 2 | 850 |
| 3 | 900 |
| 4 | 950 |
| 5 | 1000 |
| 6 | 1050 |
| 7 | 1100 |
| 8 | 1150 |
| 9 | 1200 |

Figure 4.27 concluded.

SECOND STATOR EXIT TOTAL HEAD

BLACK BASELINE 1 BUILD
RED MODIFIED 1 BUILD

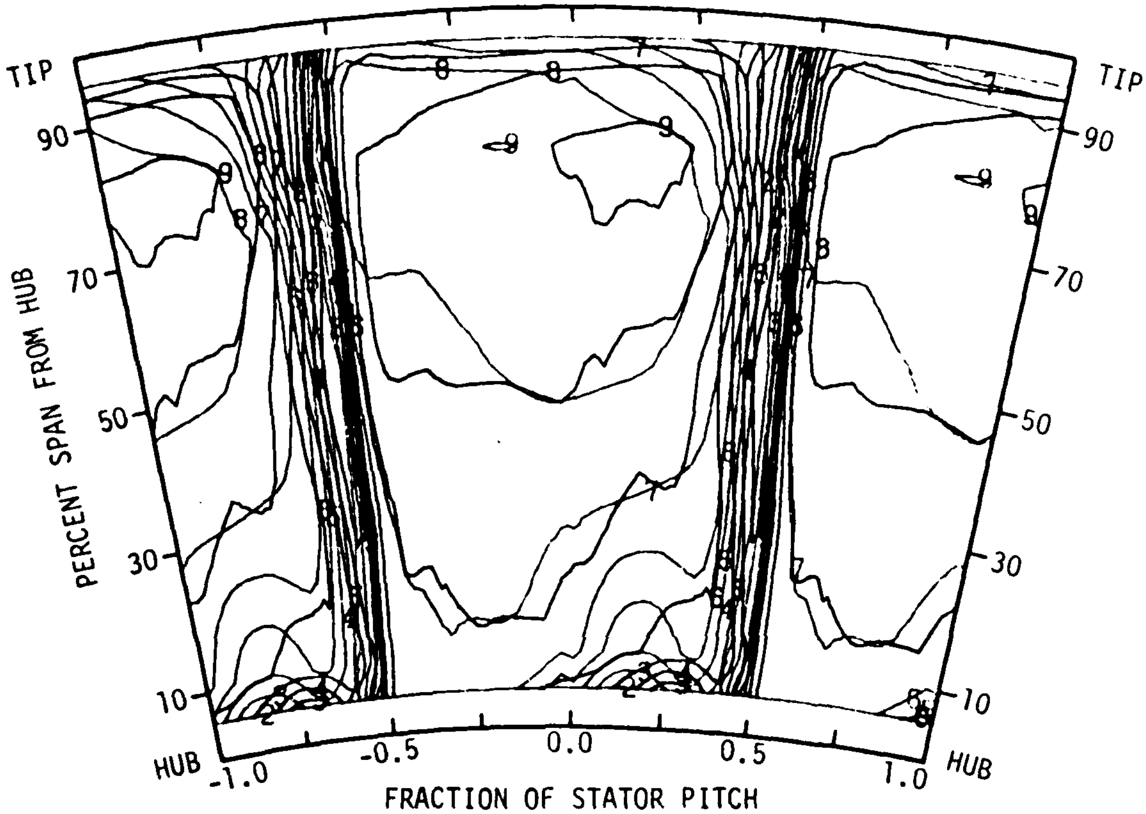


(a) BASELINE 1 AND MODIFIED 1 BUILDS

| CURVE LABEL | CURVE VALUE (N-M/KG) |
| --- | --- |
| 2 | 850 |
| 3 | 900 |
| 4 | 950 |
| 5 | 1000 |
| 6 | 1050 |
| 7 | 1100 |
| 8 | 1150 |
| 9 | 1200 |

Figure 4.28 Maps comparing the total-head contours at the second stator exit for the different compressor builds ($\phi$ = 0.500).

SECOND STATOR EXIT TOTAL HEAD

BLACK BASELINE 1 BUILD
RED BASELINE 2 BUILD

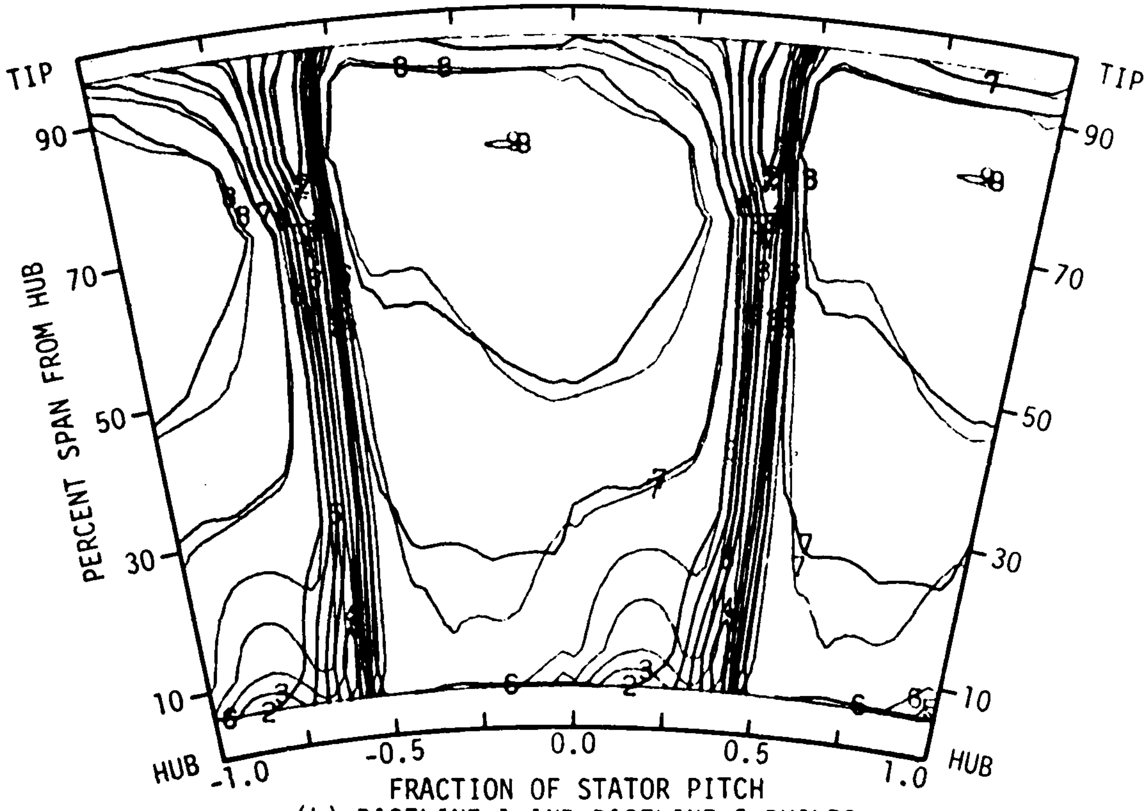


(b) BASELINE 1 AND BASELINE 2 BUILDS

| CURVE LABEL | CURVE VALUE (N-M/KG) |
|---|---|
| 2 | 850 |
| 3 | 900 |
| 4 | 950 |
| 5 | 1000 |
| 6 | 1050 |
| 7 | 1100 |
| 8 | 1150 |
| 9 | 1200 |

Figure 4.28 continued.

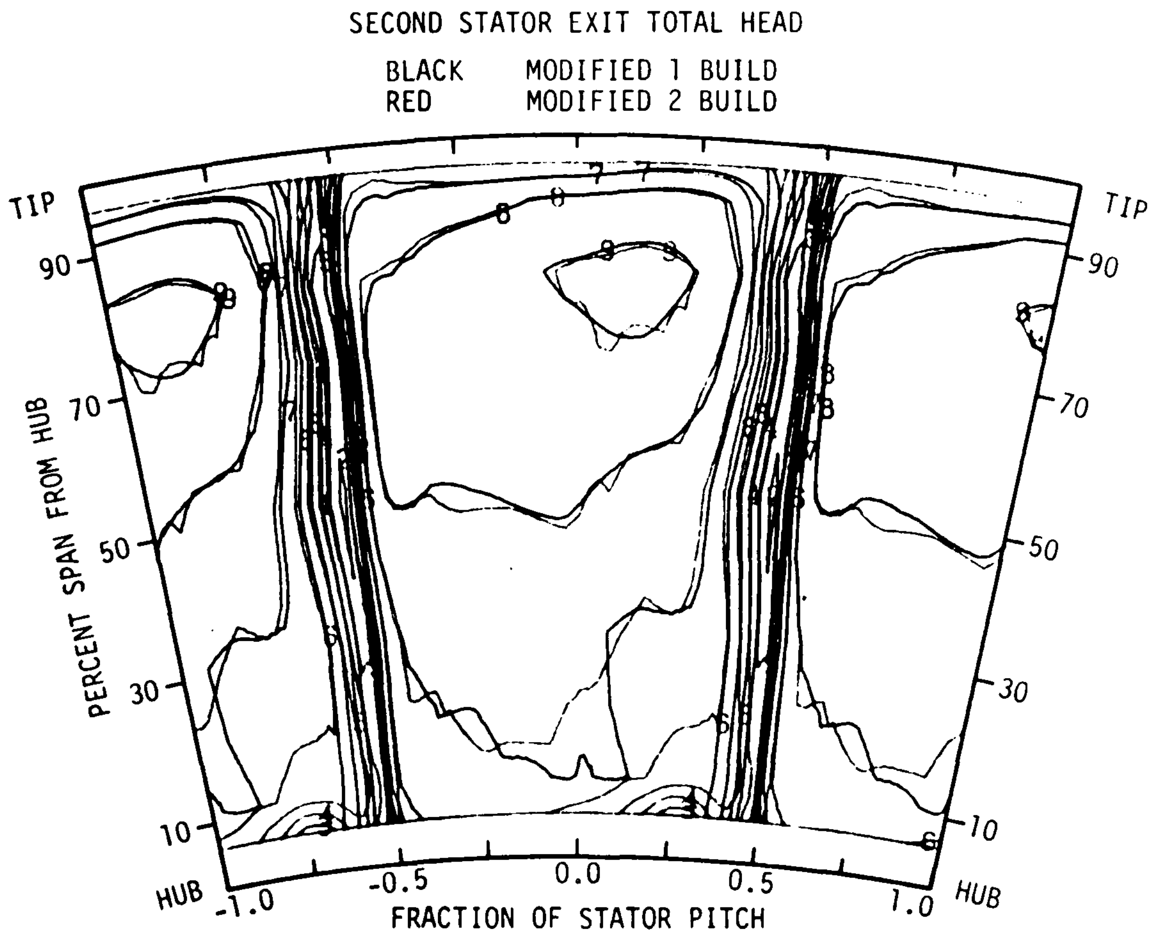


(c) MODIFIED 1 AND MODIFIED 2 BUILDS

| CURVE LABEL | CURVE VALUE (N-M/KG) |
|---|---|
| 2 | 850 |
| 3 | 900 |
| 4 | 950 |
| 5 | 1000 |
| 6 | 1050 |
| 7 | 1100 |
| 8 | 1150 |
| 9 | 1200 |

**Figure 4.28 concluded.**

In comparing the second stator exit flow fields for the different builds, it is convenient to divide the field into an outer (mid-span to tip) and an inner (mid-span to hub) flow portion. This is done mainly because the second stator exit outer portion flow field is similar to the first stator exit outer portion flow field for each build pair with a common stator geometry. Most of the baseline/modified differences observed for the first stator outer portion flow field also apply for the second stator, although only qualitatively.

The following characteristics about the second stator exit outer portion flow field and the corresponding second stator loss distributions can be noted:

- The second stator exit baseline/modified stator data differences (Figure 4.28(a)) are significantly larger than those for the first stator exit (Figure 4.23). Correspondingly, the baseline/modified second stator loss differences are larger (Figure 4.24(d)) than those for the first stator (Figure 4.20(c)) from 70% to 95% span.
- The baseline 1 and 2 builds have similar second stator exit outer portion flow fields (Figure 4.28(b)). The corresponding second stator loss distributions are similar (Figure 4.24(d)) from 30% to 95% span.
- The modified 1 and 2 builds have similar second stator exit outer portion flow fields (Figure 4.28(c)). The corresponding second stator loss distributions are similar (Figure 4.24(d)) from 10% to 90% span.

The second stator exit inner portion flow field (mid-span to hub) for the different builds (Figure 4.27) varies considerably. This corresponds to the noticeable variation in near-hub losses observed for the different builds (Figure 4.24(d)). Also, unlike the outer portion flow field, the second stator exit inner portion flow field is very different from that of the first stator. This difference is due to the second stator hub being stationary, while the first stator hub is moving.

The baseline 1 and modified 1 builds both indicate a substantial region of lower-momentum fluid adjacent to the second stator suction surface near the hub. This region was discussed earlier in some detail in section 4.3.1, where it was considered to be a "leakage vortex."

The following conclusions about the second stator exit inner portion flow field and the corresponding second stator loss distributions can be noted:

- The baseline 1 build leakage vortex is substantially larger than that of the modified 1 build (Figure 4.28(a)). Correspondingly, the baseline 1 build second stator loss is substantially greater than that of the modified 1 build at 5% and 10% span from the hub (Figure 4.24(d)).
- The baseline 2 and modified 2 builds eliminate the leakage vortex (Figure 4.28(b) and (c)). Correspondingly, the baseline 2 build second stator loss is substantially less than that of the baseline 1 build at 5% and 10% span from the hub. Similar loss behavior is seen for the modified 2

and modified 1 builds, but only at 5% span from the hub (Figure 4.24(d)).

- The baseline 2 and modified 2 build second stator wakes are approximately symmetrical about the mid-span. The baseline 2 build second stator wake is narrow over the mid-span and flairs out on its suction side near the hub and tip. Conversely, the modified 2 build second stator wake is relatively wide on its suction side over the mid-span and becomes narrower near the hub and tip (Figure 4.27). Correspondingly, the baseline 2 build second stator loss is less than that for the modified 2 build at mid-span, and is greater than that for the modified 2 build near the hub and tip (Figure 4.24(d)).

The second stator incidence and deviation results (Figure 4.24(e)) are similar to those for the first stator. Thus, most first stator comments made earlier apply again.

4.4.1.3. First/Second Stage Performance Comparison

Graphs useful for comparison of first and second stage performance data are provided in this subsection. The graphs are arranged into three groups:

1. Conventional head-rise and stator-related performance data in Figure 4.29
2. Ideal head-rise and rotor-related performance data in Figure 4.30
3. Hydraulic efficiency data in Figure 4.31

Most of these figures are not discussed, but are included for completeness and possible future reference.

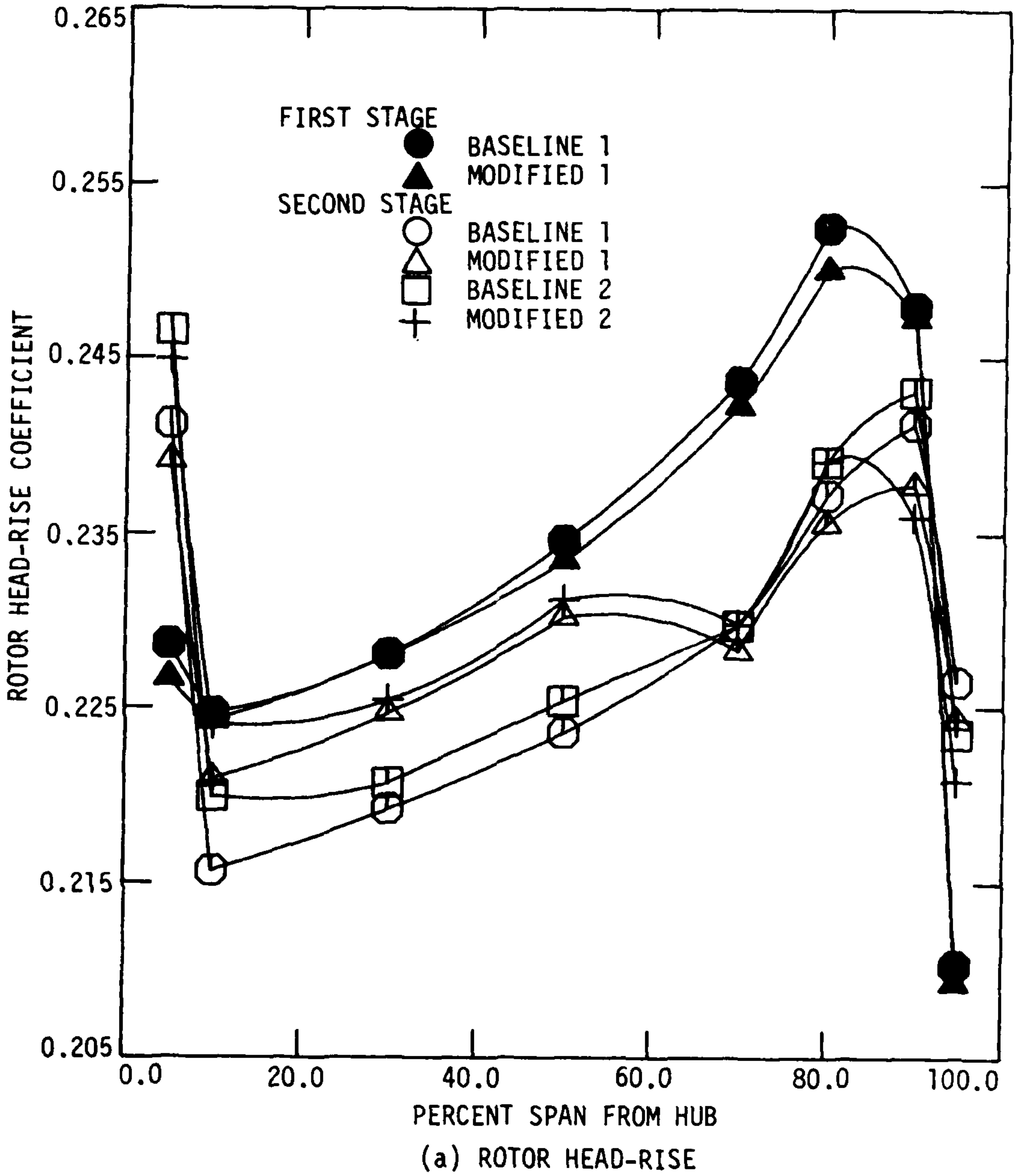


(a) ROTOR HEAD-RISE

Figure 4.29 Spanwise comparison between first and second stage circumferential-mean performance parameters for the different compressor builds ($\phi$ = 0.500).

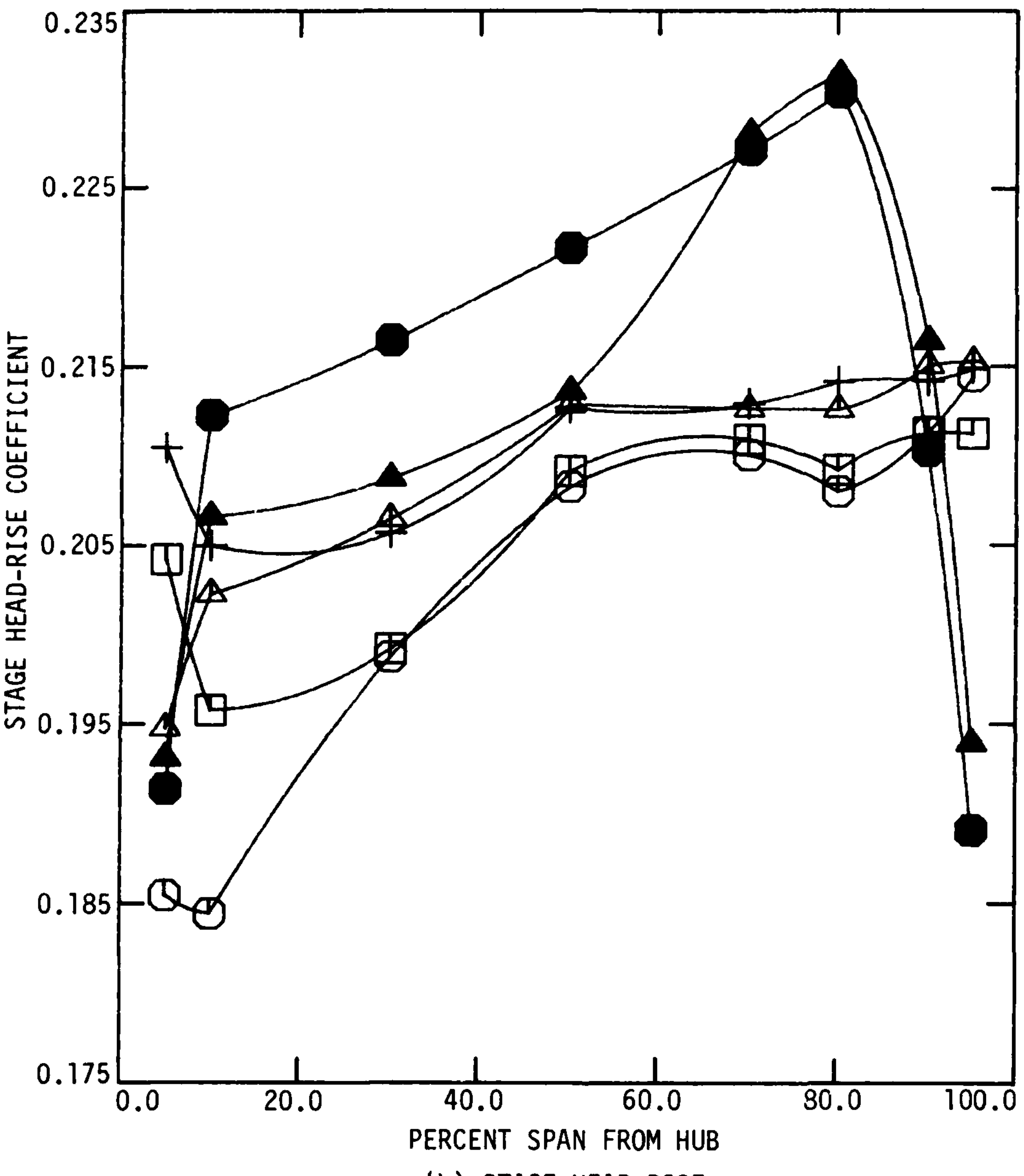

(b) STAGE HEAD-RISE

Figure 4.29 continued.

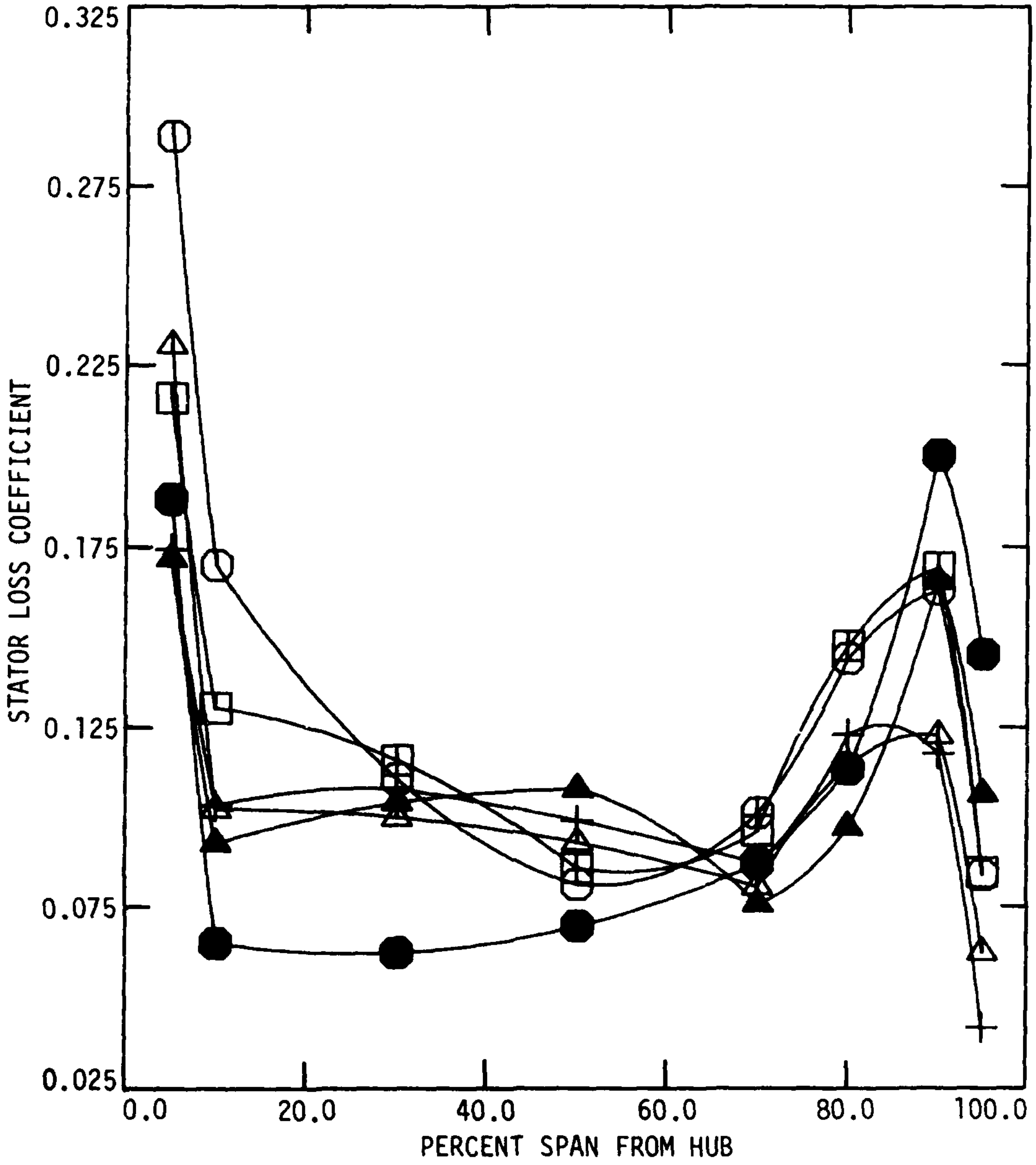


(c) STATOR LOSS

Figure 4.29 continued.

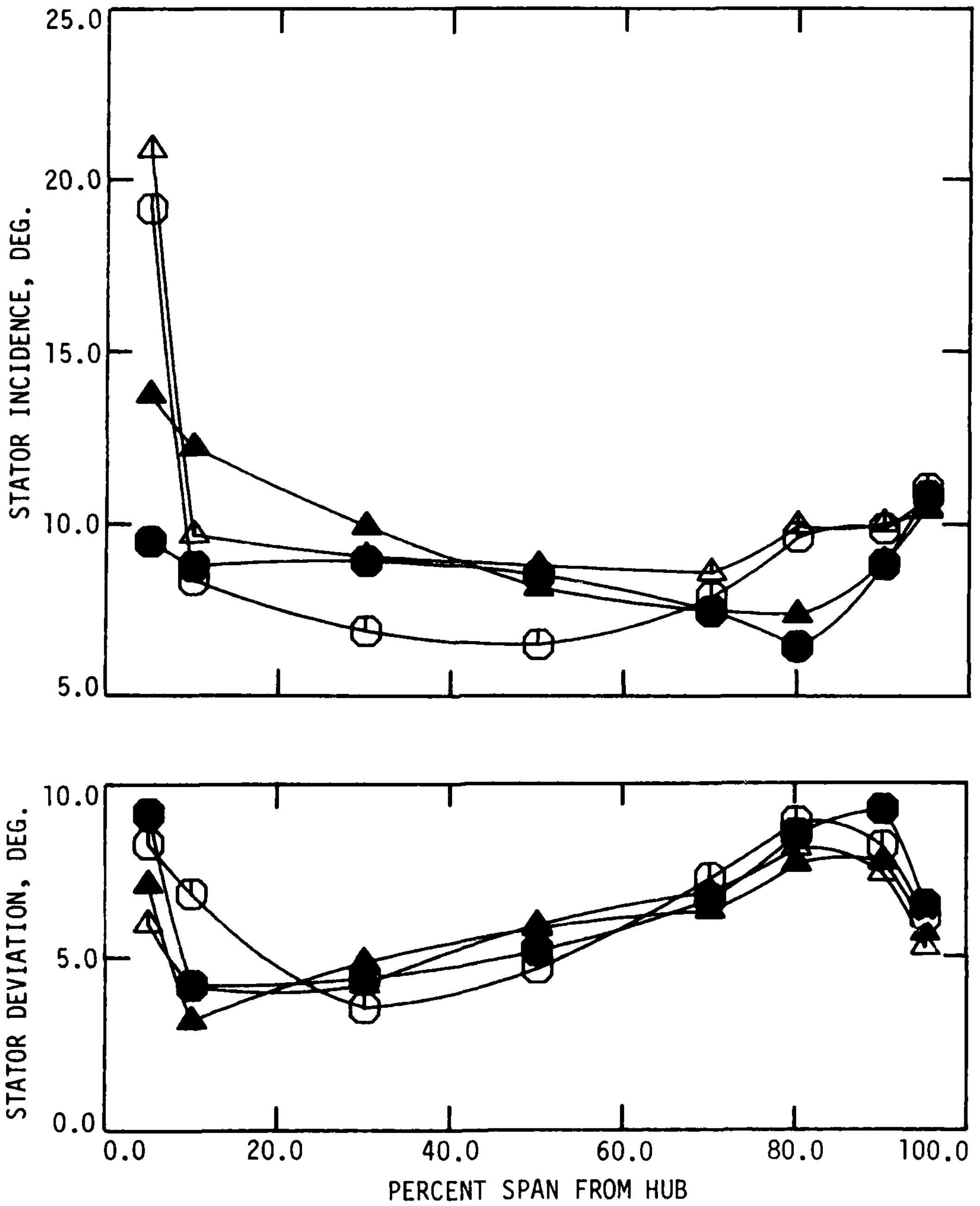


(d) STATOR INCIDENCE AND DEVIATION

Figure 4.29 continued.

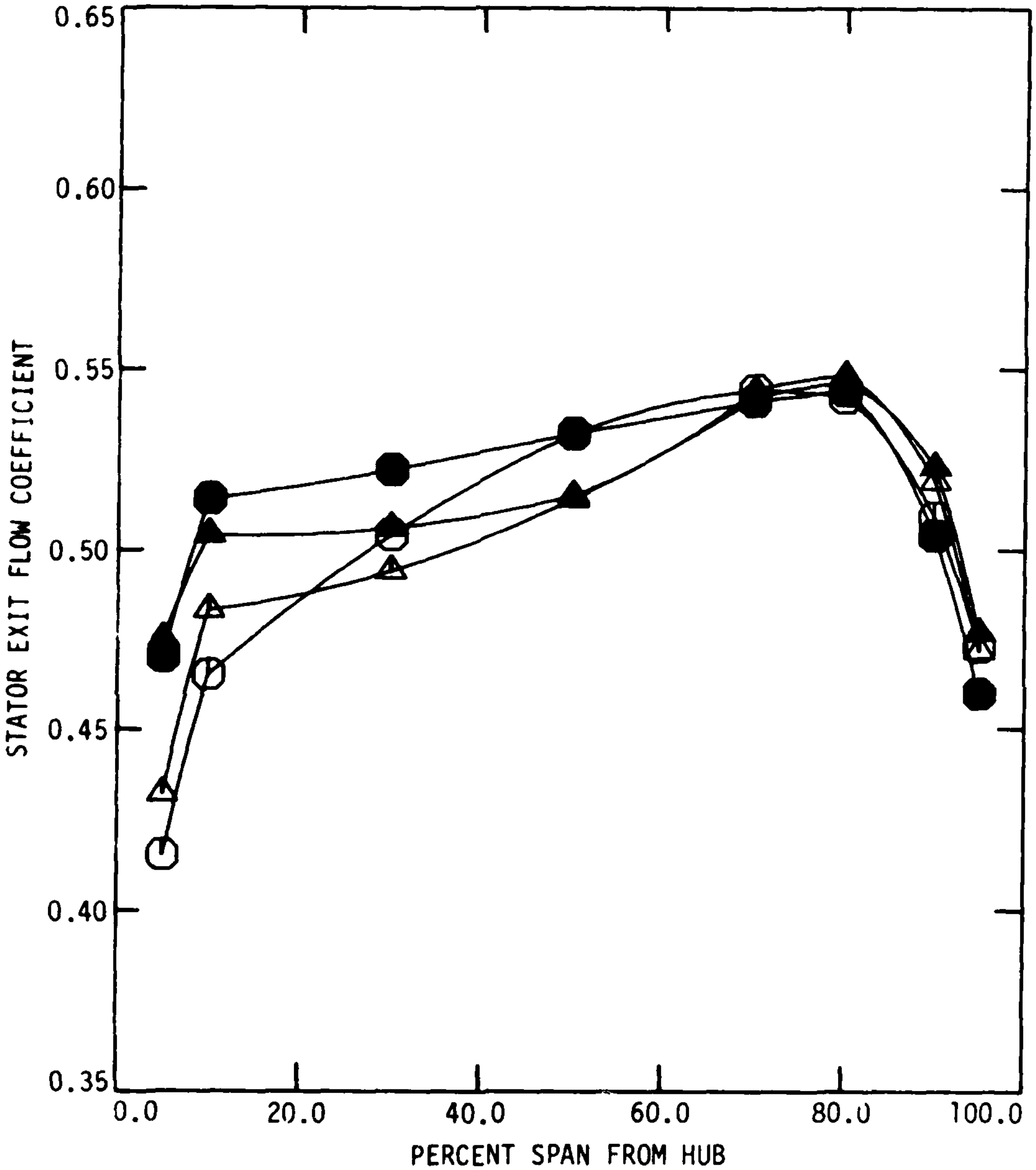


(e) STATOR EXIT FLOW COEFFICIENT

Figure 4.29 concluded.

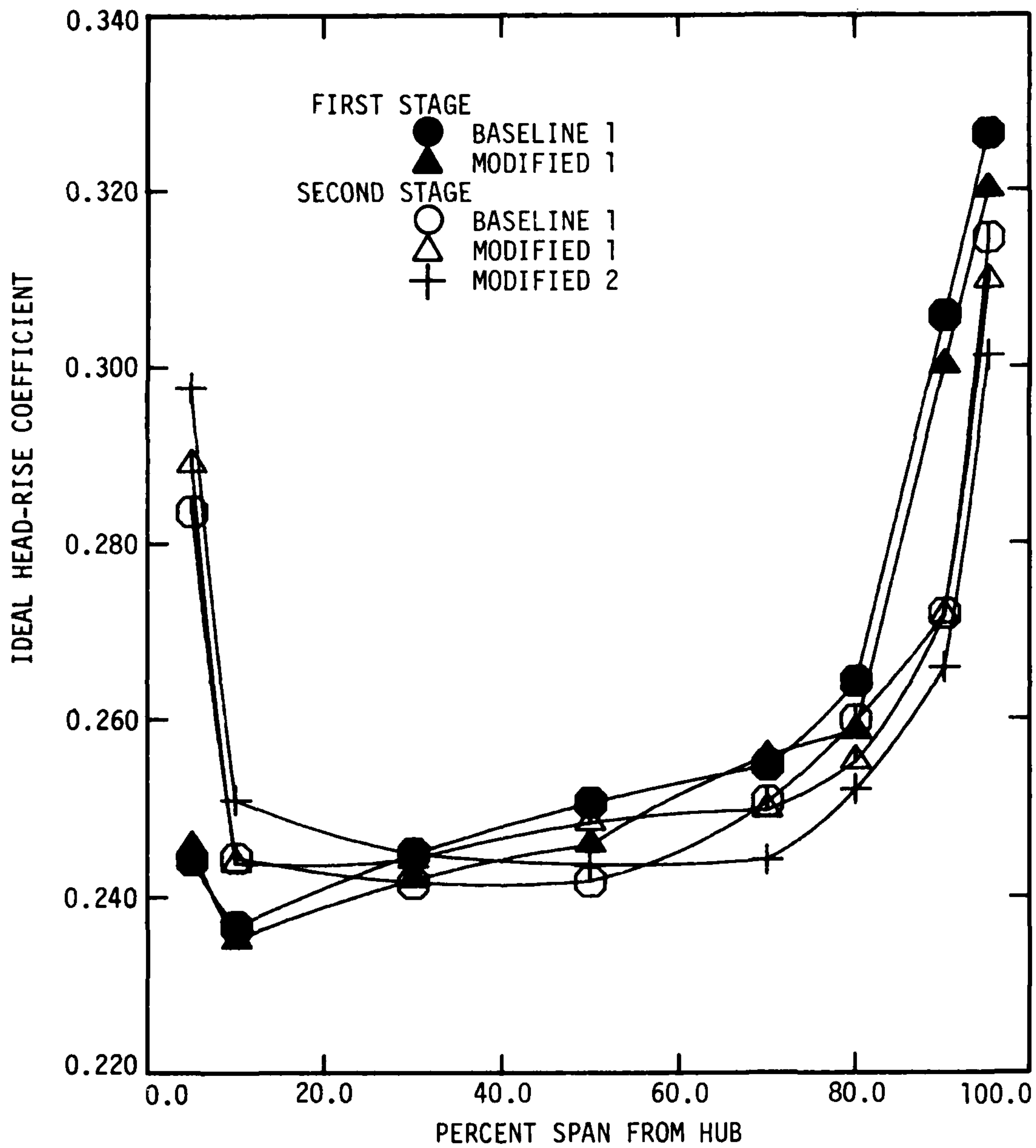


(a) IDEAL HEAD-RISE

**Figure 4.30** Spanwise distribution of circumferential-mean rotor performance parameters for the different compressor builds ($\phi = 0.500$).

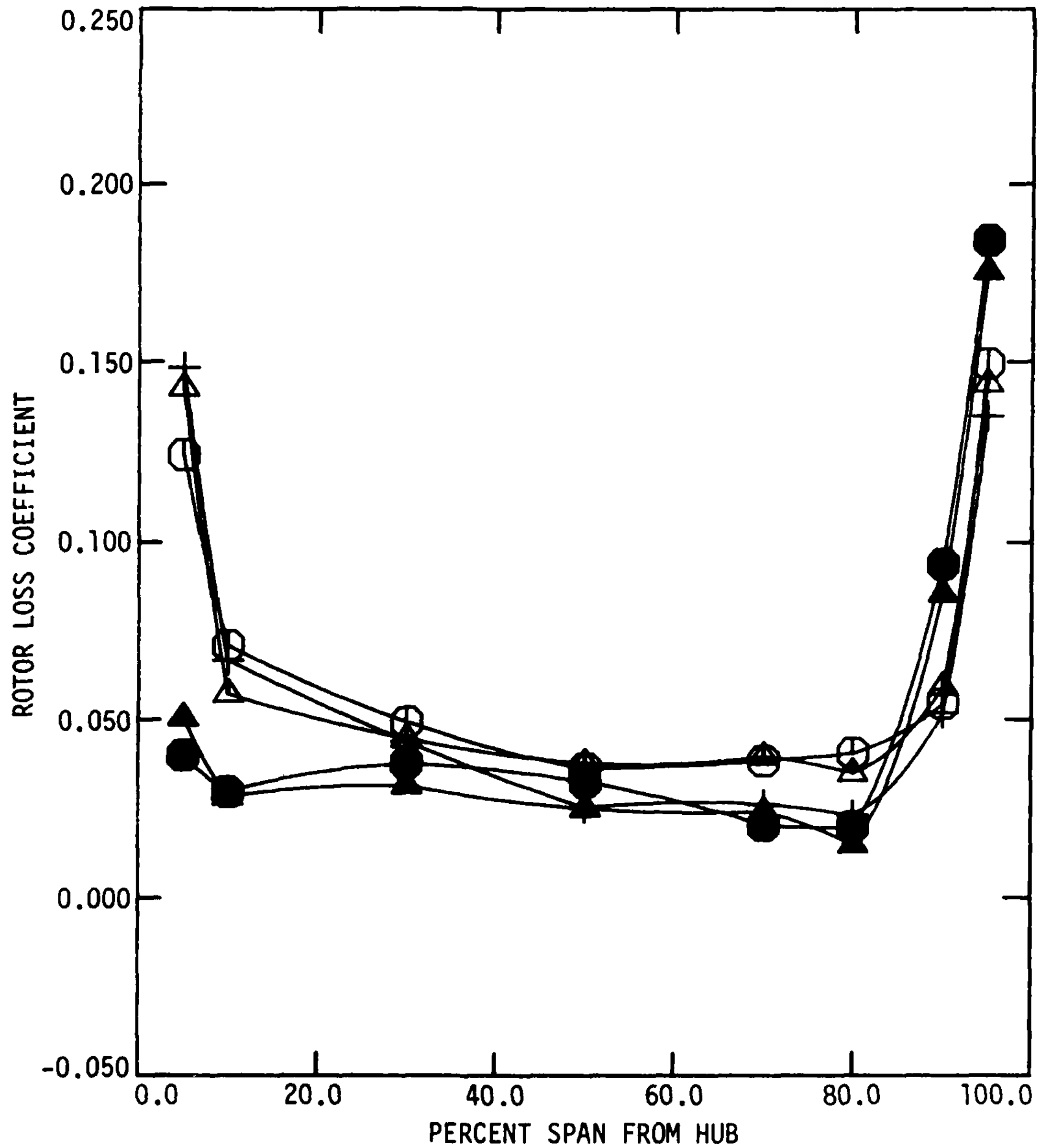


(b) ROTOR LOSS

**Figure 4.30 continued.**

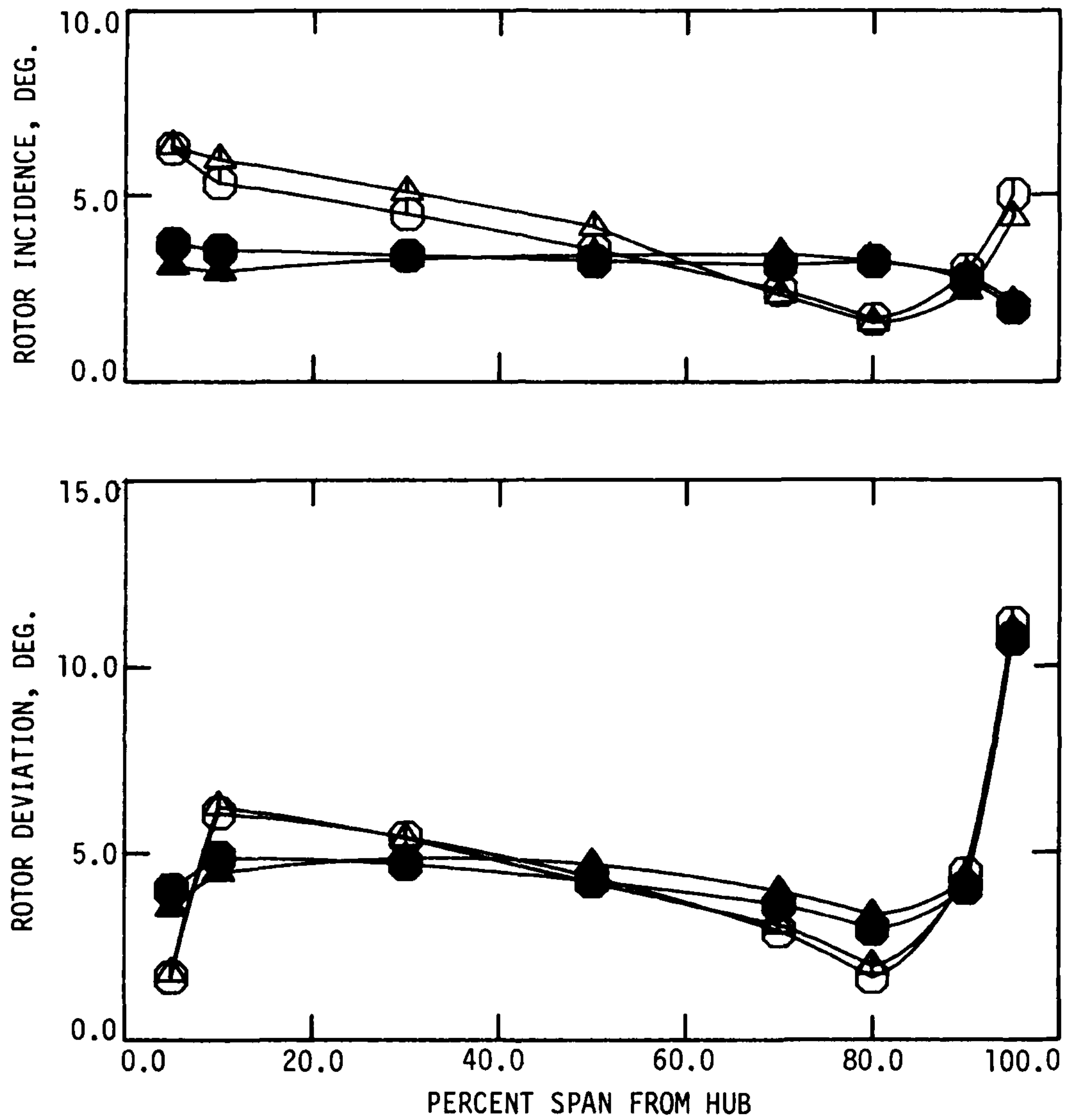


(c) ROTOR INCIDENCE AND DEVIATION

Figure 4.30 continued.

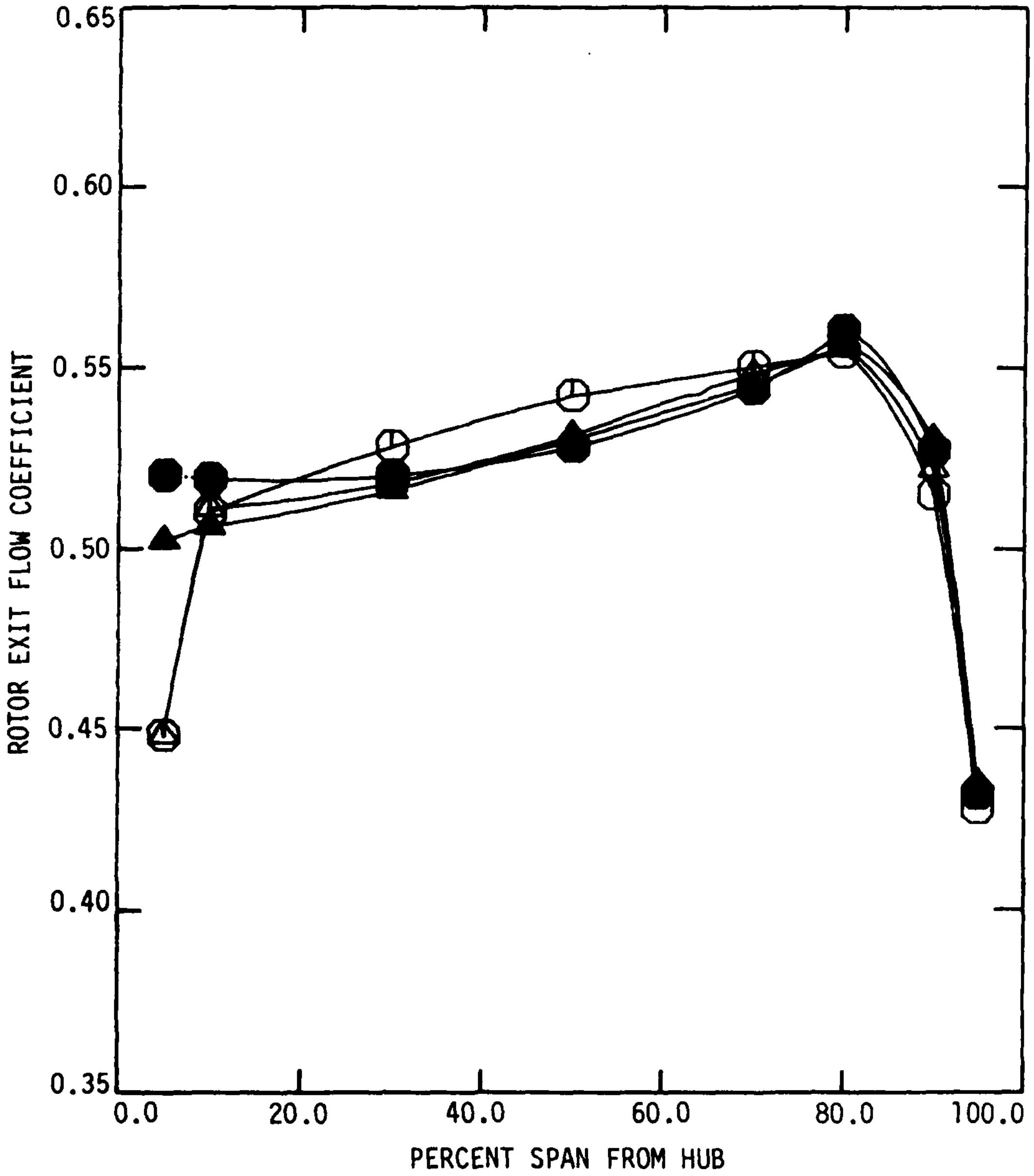


(d) ROTOR EXIT FLOW COEFFICIENT

Figure 4.30 concluded.

Some trends in conventional head-rise and stator loss are worth mentioning:

- For all builds, the first rotor and stage head-rise values are higher than those of the second stage over most of the span, the exceptions, occurring near the hub and tip (Figure 4.29(a) and (b)).
- The modified builds are somewhat close in head-rise performance between stages from 10% to 50% span from the hub. The baseline builds, conversely, are quite different in head-rise performance between stages over the entire span (Figure 4.29(b)).
- For all builds, the first stator loss is less than the second stator loss near the hub, whereas the opposite is observed near the tip (Figure 4.29(c)).
- The stator loss values are generally similar between stages for the modified builds, whereas they differ considerably between stages for the baseline builds (Figure 4.29(c)).

Ideal head-rise (Figure 4.30(a)), rotor loss (Figure 4.30(b)), and hydraulic efficiency (Figure 4.31) are affected considerably (see Figure 4.1) by the uncertainty in absolute flow angle measurement. Therefore, care should be exercised when drawing conclusions from these figures. Several general conclusions follow:

- Rotor loss is nearly constant over most of the blade span (Figure 4.30(b)).
- The rotor deviation angles (Figure 4.30(c)), like rotor loss data, are nearly constant over most of the blade span.

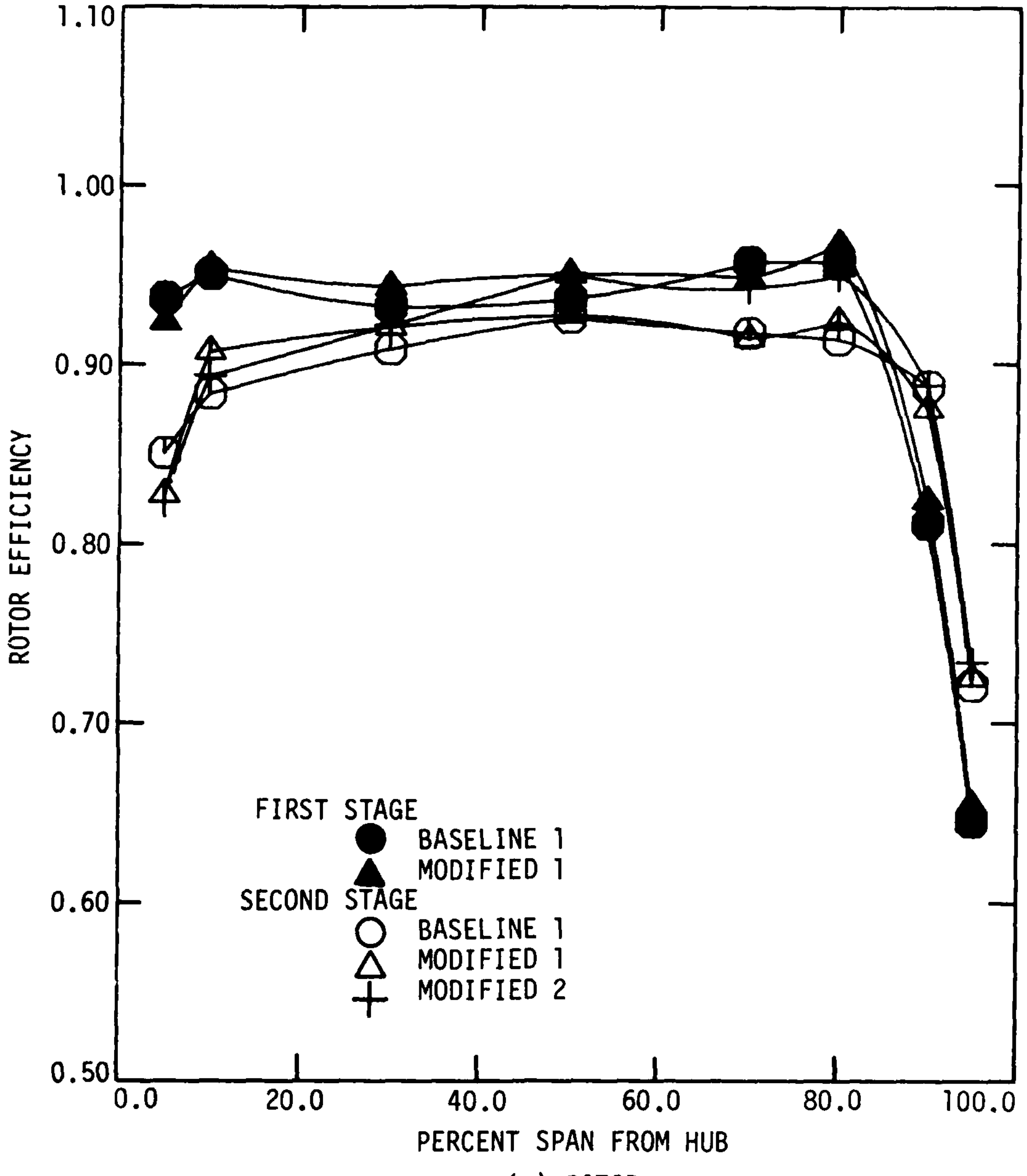


(a) ROTOR

Figure 4.31 Spanwise distribution of circumferential-mean hydraulic efficiencies for the different compressor builds ($\phi$ = 0.500).

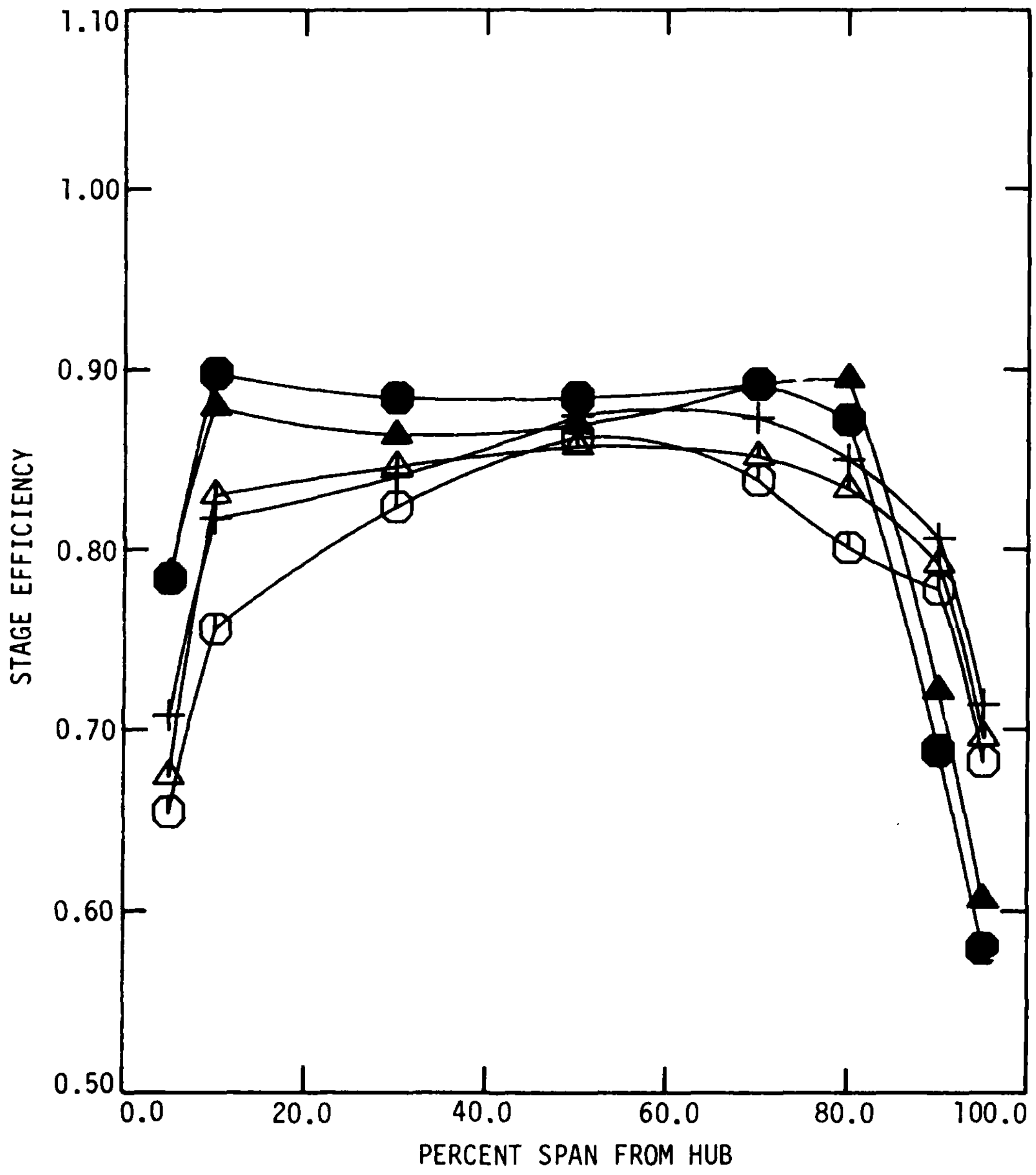

(b) STAGE

Figure 4.31 continued.

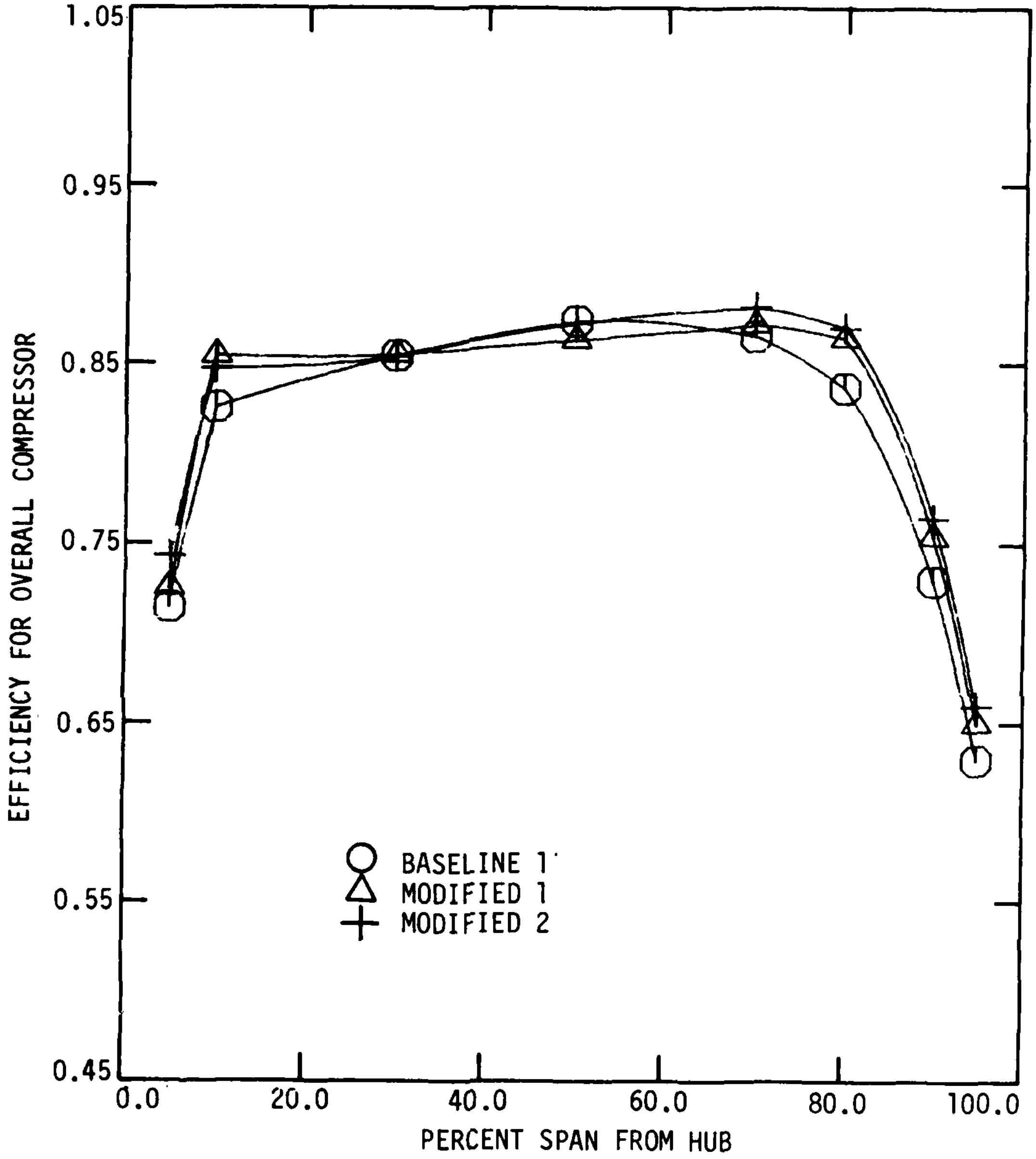


(c) OVERALL

Figure 4.31 concluded.

- The values of rotor loss (Figure 4.30(b)) are substantially less than those of stator loss (Figure 4.29(c)) over most of the blade span.
- The rotor efficiency curves (Figure 4.31(a)) reflect trends in the rotor loss curves (Figure 4.30(b)).
- The overall efficiency (Figure 4.31(c)) is nearly constant over most of the blade span for all builds. The modified 1 and 2 builds have higher overall efficiencies than does the baseline 1 build near the hub and tip.

#### 4.4.1.4. Mass-Averaged Performance

Radially mass-averaged data for the different compressor builds are presented in Table 4.9. Of particular interest are the stator loss and overall efficiency data. Clearly, the modified stator overall efficiency is higher than the baseline stator value. The first stator loss values indicate a higher loss for the modified stator than for the baseline stator. The second stator loss values, however, reveal a higher loss for the baseline stator than for the modified stator. These results are consistent with the spanwise stator loss data presented earlier.

### 4.4.2. Analysis of Stator Geometry Modification Effects

The aerodynamic effects of three basic stator geometry modifications are analyzed in this section:

- symmetrical leading-edge sweep
- sealing of the clearance gap at a stationary end wall
- large corner fillets

Table 4.9. Comparison of radially mass-averaged performance parameters for the different compressor builds ($\phi = 0.500$).

| Build | Head Rise Coefficient | | (Shroud Static) Head Rise Coefficient | | Loss Coefficient | | Efficiency | |
|---|---|---|---|---|---|---|---|---|
| | Rotor | Stage | Rotor | Stage | Rotor | Stator | Rotor | Stage |
| **First Stage** | | | | | | | | |
| Baseline 1 | 0.2357 | 0.2188 | 0.2066 | 0.2217 | 0.0447 | 0.0905 | 0.9125 | 0.8470 |
| Baseline 2 | -- | 0.2185 | -- | 0.2242 | -- | 0.0920 | -- | -- |
| Modified 1 | 0.2349 | 0.2158 | 0.2063 | 0.2206 | 0.0403 | 0.1031 | 0.9202 | 0.8455 |
| Modified 2 | -- | 0.2161 | -- | 0.2229 | -- | 0.1016 | -- | 0.8466 |
| **Second Stage** | | | | | | | | |
| Baseline 1 | 0.2258 | 0.2041 | 0.1932 | 0.2077 | 0.0505 | 0.1157 | 0.8998 | 0.8134 |
| Baseline 2 | 0.2273 | 0.2060 | 0.1913 | 0.2052 | -- | 0.1132 | -- | -- |
| Modified 1 | 0.2282 | 0.2106 | 0.1942 | 0.2129 | 0.0480 | 0.0949 | 0.9058 | 0.8356 |
| Modified 2 | 0.2294 | 0.2107 | 0.1946 | 0.2149 | 0.0408 | 0.1000 | 0.9188 | 0.8439 |

Overall

| Build | Head Rise Coefficient | (Shroud Static) Head Rise Coefficient | Efficiency |
|---|---|---|---|
| Baseline 1 | 0.4229 | 0.4294 | 0.8304 |
| Baseline 2 | 0.4245 | 0.4294 | -- |
| Modified 1 | 0.4264 | 0.4335 | 0.8406 |
| Modified 2 | 0.4268 | 0.4378 | 0.8452 |

Expected effects of these types of stator geometry modifications are compared with the experimental results.

Symmetrical sweeping of the stator leading edges was done in this research project primarily to reduce stator blade suction-surface/end-wall corner losses by drawing higher-momentum fluid into those corner regions. The well-known beneficial effect of leading-edge sweep in reducing the Mach number component normal to the leading edge is not realized in low-speed flow research, and so was not considered in this project. The basic aerodynamics involved can be briefly described in the following way. Consider the static pressure distribution generated on and near the blade surfaces, particularly on the suction surface near the blade/end-wall corners. By extending the blade chord near the end walls, a lower-pressure region is generated on the suction surface of the extended section, which tends to draw the main flow toward the blade suction-surface/end-wall corner [13]. Normally, the pressure decrease on the extended suction surface is greater than the pressure rise on the pressure surface so the net effect is beneficial. The flow of higher-momentum fluid into the corner region reduces the thickness of the corner boundary layer, and thus the corner loss.

Reduction of blade/end-wall corner losses was also the objective in using large corner fillets; the function being to lessen interference drag and corner boundary layer growth. This idea stems from aircraft design experience with the fillet geometry at a wing/fuselage juncture [14,15]. The expected results of this modification in the present study, however, were uncertain since only low-speed flow was involved. As Debruge [15] notes, it is possible for the large corner fillets to produce more loss than the small ones, particularly when a constant fillet radius is used around the entire airfoil circumference.

The sealing of the second stator/hub clearance gap was actually a modification resulting from the addition of large corner fillets at the hub for the modified stator blade geometry. However, after comparing results for the modified 1 and 2 builds, it was decided that additional useful data might be obtained by testing the baseline stator configuration with the second stator/hub clearance gap sealed. Thus, the effect of sealing a stationary blade/stationary end-wall clearance gap is apparent from the experimental results. Without sealing there is evidence of a substantial leakage vortex at the second stator exit hub (baseline 1 and modified 1 builds, Figure 4.28(a)), whereas with sealing, this leakage vortex is no longer present (baseline 2 and modified 2 builds, Figure 4.28(b) and (c)).

The experimental results show that symmetrically sweeping the stator blade leading edges affects the flow as anticipated. The previously discussed stator exit contour maps (Figures 4.23 and 4.28) indicate that the modified stator produces a flow field with substantially more higher-momentum fluid in the stator suction-surface/end-wall corners. This is accompanied by a small, but significant, reduction in higher-momentum fluid in the stator pressure-surface/end-wall corners. The increased flow into the suction-surface/end-wall corners, however, is associated with a noticeable mid-span thickening of the stator wake on the suction side. This would seem to indicate a radial migration of lower-momentum boundary layer fluid from the stator suction-surface/end-wall corners toward mid-span, since the baseline and modified stators should have similar mid-span profile losses (equal chord lengths and similar blade profiles at mid-span). The data further indicate that at a stationary blade/stationary end-wall clearance gap the stator leading-edge sweep is beneficial in reducing the strength of the leakage vortex (Figure 4.28(a)). This seems reasonable in view of the foregoing discussion. The stator blade/end-wall corner flows produced by the symmetrically swept stator leading edge oppose the leakage-vortex flow.

Several factors should be considered when analyzing the stator loss performance of the baseline and modified builds:

- The modified stator has a longer blade chord, and thus higher solidity, than does the baseline stator except at mid-span where they are equal. Thus, higher profile losses are expected for the modified builds, especially near the hub and tip.
- If the modified builds are to have less "total" stator loss than the baseline builds, then the potentially higher modified stator profile losses must be compensated for by substantially lower end-wall losses.
- The experimental results obtained are for relatively low Reynolds number and Mach number levels.

AD-A141 793 STATOR BLADE ROW GEOMETRY MODIFICATION INFLUENCE ON TWO-STAGE AXIAL-FLOW..(U) IOWA STATE UNIV AMES ENGINEERING RESEARCH INST D L TWEEDT ET AL. DEC 83 3/3

UNCLASSIFIED ISU-ERI-AMES-84179 AFOSR-TR-84-0418 F/G 21/5 NL

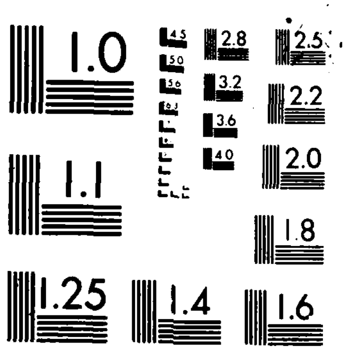


MICROCOPY RESOLUTION TEST CHART
NATIONAL BUREAU OF STANDARDS 1963 A

- The proportion of profile losses to end-wall losses may be considerably different at higher Reynolds number and Mach number levels.

As Table 4.9 indicates, the modified stator performed with higher mass-averaged (total) loss in the first stage and lower mass-averaged (total) loss in the second stage than did the baseline stator. However, the modified first stator might also have performed better than the baseline first stator if the expected profile losses were similar, instead of the mid-span chords. The better loss performance of the modified stator in the second stage is a strong indication that symmetrical leading-edge sweep is beneficial to stator loss performance. Also, the improvements in loss performance realized by symmetrically sweeping the stator leading edges may be greater where higher Reynolds number and Mach number levels are involved.

The experimental results do not show significant effects from using large corner fillets. The substantial improvement in second stator suction-surface/hub corner flow (Figure 4.28(c)) is considered to be primarily an effect of sealing the clearance gap. There is some evidence of a loss decrease near the casing end wall due to large corner fillets (Figure 4.24(d)), but the results are not conclusive. This general result, however, like the results concerning symmetrical leading-edge sweep, should be considered with Reynolds number and Mach number effects in mind.

# 5. CONCLUSIONS

Aerodynamic performance testing of four different builds of a two-stage axial-flow research compressor was accomplished in an effort to determine the effects of stator geometry modifications--symmetrical leading-edge sweep, large corner fillets, and hub clearance sealing--on flow management. An off-design operating point was selected for this comparative testing. Thus, a comparison of the baseline 1 compressor build performance at design and off-design operating points was also completed.

Substantial stator exit flow-field changes attributable to symmetrical sweeping of each stator leading edge were observed. These stator exit flow-field changes could be correlated with changes in the spanwise distributions of stator loss. The data clearly indicate that stator leading-edge sweep produced an increased flow of higher-momentum fluid into the stator blade suction-surface/end-wall corners with a resulting decrease in loss near the end walls. The increased flow into the stator suction-surface/end-wall corners, however, was accompanied by a substantial thickening of the stator wake (mainly on the suction side) over the mid-span portion of the blade with a resulting increase in loss there. Considering the above two changes together, it appears that symmetrically sweeping the stator leading edges induces an increased flow of higher-momentum fluid into the stator suction-surface/end-wall corners with an accompanying radial migration of stator suction-surface boundary layer fluid away from the end walls toward mid-span. The net effect of this secondary flow seems to be a reduction in stator blade loss, especially so in the case where the stator hub is shrouded. For the case of a rotating stator hub, the hub-region flow behavior is less certain, but the data show a substantial deterioration of stator loss performance from mid-span to near-hub in going from the baseline to the modified stator.

No definite conclusions could be drawn from the data concerning large corner fillets. However, the data do indicate a slight decrease in stator loss near to the casing end wall. It is important to realize that the effects of stator fillet geometry and symmetrical leading-edge sweep may be largely affected by the levels of Reynolds number and Mach number involved. Qualitatively, these stator geometry modifications could be expected to improve stator loss performance more for higher Reynolds number and Mach number flows.

A curious result (peculiar total-head variations)--realized when comparing the performance of the compressor at different flow rates--led to the study of first stator wake movement and dispersion through the second rotor blade row. For compressor operation at lower flow rates, first stator wake avenues observed at the second rotor exit extended circumferentially over more than one stator pitch, resulting in adjacent avenues partially overlapping with each other. At higher flow rates these wake avenues did not overlap, but instead were with a narrow (no stator wake) region between. It was also observed that these wake avenues changed in circumferential extent with spanwise location, particularly near the tip where they became narrower. These basic differences in rotor exit wake avenue interaction provided a reasonable explanation of the unusual second rotor exit total-head variations noted.

Some recommendations for further related research are in order. In the immediate future, it is recommended that time-average performance testing involving the different compressor builds continue at the maximum efficiency flow rate and at the design flow rate. Utilization of surface and through-flow flow visualization techniques could prove useful. These techniques may allow changes in the stator flow field produced by the geometry modifications--particularly symmetrical leading-edge sweep and clearance sealing--to be more clearly understood.

A final recommendation concerns stator solidity. For the present program, the mid-span stator solidity was kept constant between the baseline and modified stators, resulting in higher hub and tip solidities for the modified stators. However, if an "average" solidity was maintained constant between the baseline and modifed stators instead, a truer stator loss comparison could result since expected profile losses would be similar. That is, the relative effects of symmetrical leading-edge sweep on stator loss over the blade span could be more directly compared.

# 6. REFERENCES

1. Hathaway, M. D., and Okiishi, T. H. "Aerodynamic Design and Performance of a Two-Stage, Axial-Flow Compressor (Baseline)." ISU-ERI-Ames-84178, TCRL-24, December 1983.

2. Morgan, B. D. "A Water Column Balance Pressure Reference System." Unpublished Report. Department of Mechanical Engineering, Iowa State University, Ames, Iowa. 1979.

3. Greville, T. N. E. Theory and Applications of Spline Functions. New York: Academic Press, 1967.

4. Wylie, C. R. Advanced Engineering Mathematics. New York: McGraw-Hill Book Company, Inc., 1975.

5. Kline, S. J., and McClintock, F. A. "Describing Uncertainties in Single Sample Experiments." Mechanical Engineering, 75 (1953):3-8.

6. Moffat, R. J. "Contributions to the Theory of Single-Sample Uncertainty Analysis." Transactions of the ASME, Journal of Fluids Engineering, 104 (June 1982):250-260.

7. Smith, L. H., Jr. "Casing Boundary Layers in Multistage Axial-Flow Compressors," in Flow Research on Blading, L. S. Dzung, ed. New York: Elsevier Publishing Company, 1970.

8. Leboeuf, F., Bario, F., Boris, G., and Papailiou, K. D. "Experimental Study and Theoretical Prediction of Secondary Flows in a Transonic Axial Flow Compressor." ASME Paper No. 82-GT-14, 1982.

9. Johnsen, I. A., and Bullock, R. O., eds. "Aerodynamic Design of Axial-Flow Compressors." U.S. NASA SP-36, 1965.

10. Smith, L. H., Jr. "Wake Dispersion in Turbomachines." Transactions of the ASME, Journal of Basic Engineering, 88D (September 1966):688-690.

11. Wagner, J. H., Okiishi, T. H., and Holbrook, G. J. "Periodically Unsteady Flow in an Imbedded Stage of a Multistage, Axial-Flow Turbomachine." Transactions of the ASME, Journal of Engineering for Power, 101 (January 1979):42-51.

12. Zierke, W. C., and Okiishi, T. H. "Measurement and Analysis of Total-Pressure Unsteadiness Data from an Axial-Flow Compressor Stage." Transactions of the ASME, Journal of Engineering for Power, 104 (April 1982):479-488.

13. Senoo, Y., Taylor, E. S., Batra, S. K., and Hinck, E. "Control of Wall Boundary Layer in an Axial Compressor." Gas Turbine Laboratory Report No. 59. Massachusetts Institute of Technology. June 1960.

14. Wennerstrom, A. J. "Experimental Study of a High-Through-Flow Transonic Axial Compressor Stage." Paper scheduled for presentation at the 6th International Symposium on Air Breathing Engines, 6-10 June 1983, Paris, France.

15. Debruge, L. L. "The Aerodynamic Significane of Fillet Geometry in Turbocompressor Blade Rows." Transactions of the ASME, Journal of Engineering for Power, 102 (October 1980):984-993.

## 7. ACKNOWLEDGMENTS

The authors are grateful to their colleagues of the Iowa State University Engineering Research Institute/Mechanical Engineering Department Turbomachinery Components Research Laboratory for their helpful comments and assistance throughout. In particular, Mr. Jeffrey L. Hansen is appreciated for his help in obtaining some of the data. We remain indebted to Mr. Michael D. Hathaway for his fine related work. Mr. Leon Gerard and his associates are remembered for their dispatch of machining duties. To the staff of the Iowa State University Engineering Research Institute Office of Editorial Services and especially the technical editor and illustrators we offer thanks for patience and expertise. Finally, we sincerely acknowledge the support of the Air Force Office of Scientific Research (James D. Wilson--Contract Monitor) and the encouragement of George K. Serovy of Iowa State University and Arthur J. Wennerstrum of the Air Force Aero Propulsion Laboratory.

# 8. APPENDIX A: USER DEFINED CORRELATONS FOR NASA DESIGN CODE

Advanced compressor design codes frequently require the user to input various empirical correlations such as blade losses, incidence and deviation angle correlations, and annulus-wall blockage factors. The various user-defined correlations required as input to the NASA design code are presented in this section. The actual tabular input to the design code is given in Appendix B. The variables used in the correlation parameters are defined in the symbols and notation section.

## 8.1. Blade Loss

The blade loss correlations used are illustrated in Figure 8.1. The loss curves are typical of annular cascade tests of double-circular-arc blades. The correlating parameters are:

- Loss parameter $\equiv \dfrac{\bar{\omega}\cos\beta'_{y,2}}{2\sigma}$ $\equiv$ approximate measure of blade wake momentum thickness to chord ratio.

  where $\sigma = c/S$

- D-factor $\equiv 1 - \dfrac{V'_2}{V'_1} + \dfrac{(rV_y)_2 - (rV_y)_1}{\sigma(r_1 + r_2)V'_1}$

- Percent span from hub

The trends shown are similar to those indicated in Figure 203 of Reference 9.

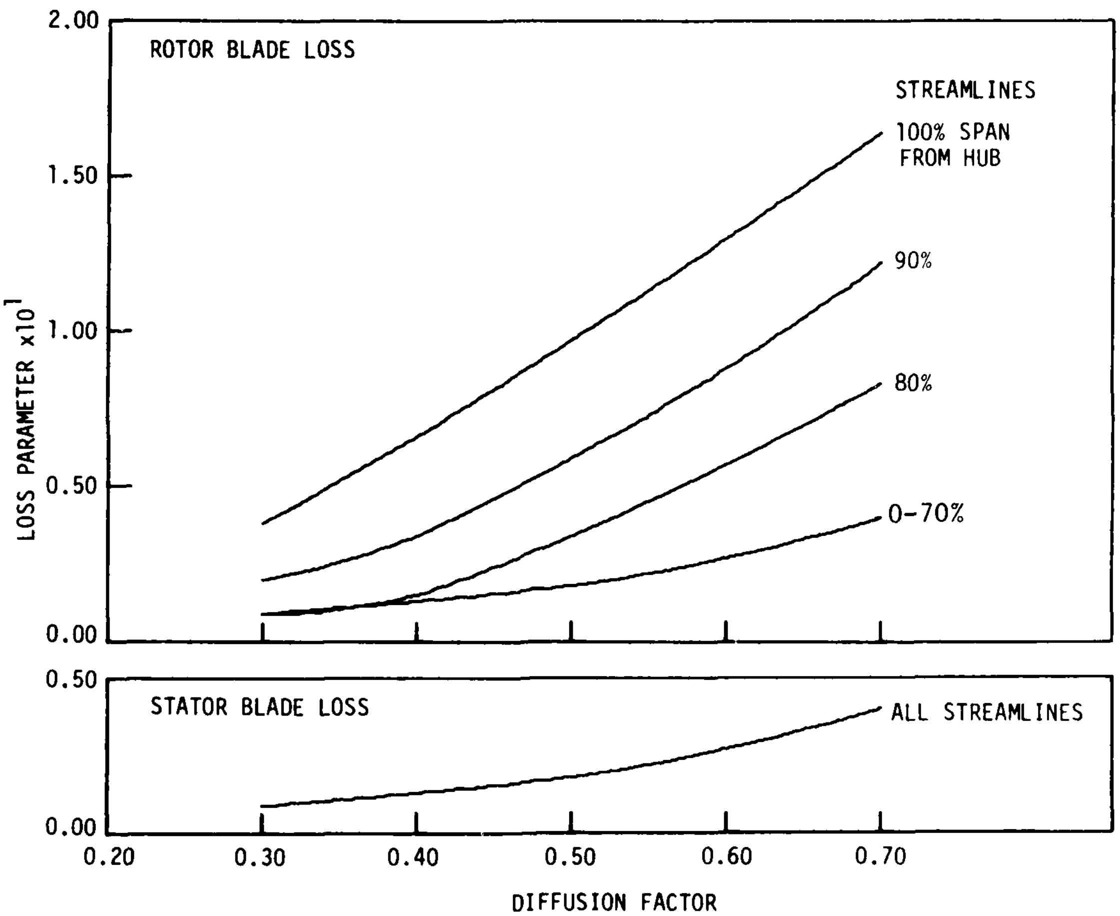


Figure 8.1 Blade loss correlation curves used in NASA design code.

## 8.2. Incidence and Deviation Angle

The design code provided several options for the incidence and deviation angle correlations. A two-dimensional incidence angle correlation was considered suitable for the baseline compressor design. Carter's rule was selected for the deviation angle correlation. Both correlations are described below.

The incidence angle correlation is described in Chapter VI of Reference 9 in the form of:

$$i = i_o + n\theta$$

where n is obtained from Figure 138 of Reference 9 as a function of

$\sigma$ and $\kappa_1$

$\theta$ = blade camber angle

$i_o = (K_i)_{sh}\ (K_i)_t\ (i_o)_{10}$ = incidence angle for zero camber

where

$(i_o)_{10}$ is obtained from Figure 137 of Reference 9

$(K_i)_{sh}$ = 0.7 for double circular arc blades

$(K_i)_t$ is obtained from Figure 142 of Reference 9 as a function of $t_{max}/c$

The deviation angle correlation (Carter's rule) described in Chapter VII of Reference 9 is

$$\delta = \frac{m_c \theta}{\sqrt{\sigma}}$$

where $m_c$ is obtained from Figure 160 of Reference 9 for circular arc blades.

# 9. APPENDIX B: NASA DESIGN CODE RESULTS

The output from the NASA design code is presented in the following tables. Table 9.1 lists in tabular form all input parameters and user defined correlations required for the design code analysis. Table 9.2 lists the aerodynamic output (e.g., velocity triangle information, blade element performance, etc.) for 11 streamlines at each axial computation station. The NASA design code gives the streamline radial positions as a percentage of the blade span measured from the shroud end-wall, whereas, the convention used for all data figures in this report is percent span measured from the hub end-wall. Table 9.3 lists the stage and overall mass-averaged aerodynamic performance parameters. Table 9.4 lists the manufacturing coordinates at 17 spanwise locations for the modified stator blade. Only the first stage stator blade manufacturing coordinates generated from the NASA design code are given as they were used for both stages of the modified compressor. Figure 9.1 shows a representative stator blade section and associated manufacturing coordinate nomenclature.

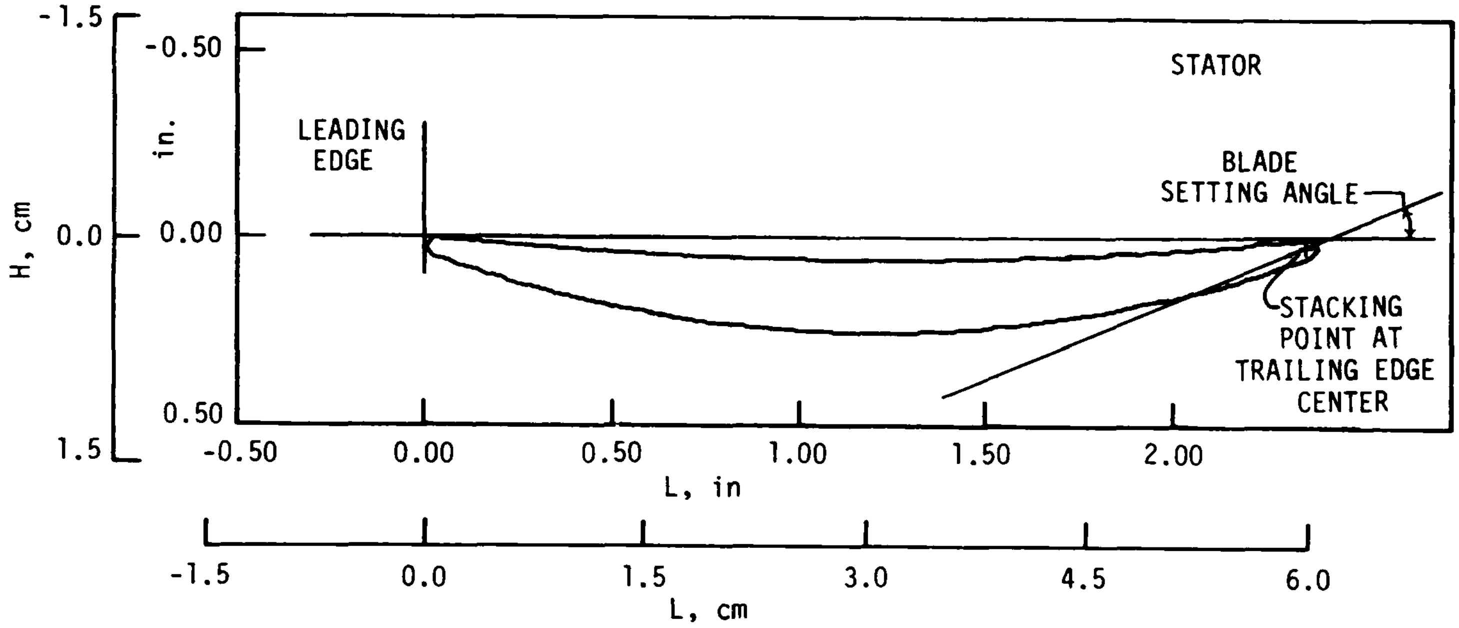


Figure 9.1. Typical modified stator blade section using manufacturing coordinates.

Table 9.1. Design code input parameters.

*** INPUT DATA FOR COMPRESSOR DESIGN PROGRAM ***

AFOSR/ISU TASK 4 2-STAGE HTF W/SP36 P248 LOSS 2400RPM 18MAR81

THE COMPRESSOR ROTATIONAL SPEED IS 2400.0 RPM.

THE DESIRED COMPRESSOR PRESSURE RATIO IS 1.019 .

CALCULATIONS WILL BE PERFORMED ON 11 STREAMLINES.

THE INLET FLOW RATE IS 5.250 (LB/SEC).

THE MOLECULAR WEIGHT IS 28.97 .

THE COMPRESSOR HAS 4 BLADE ROWS.

CALCULATIONS WILL BE MADE AT THE BLADE EDGES AND AT 7 ANNULAR STATIONS.

THE SPECIFIC HEAT POLYNOMIAL IS IN THE FOLLOWING FORM

CP = 0.23970D 00 + 0.0 *T + 0.0 *T**2 + 0.0 *T**3 + 0.0 *T**4 + 0.0 *T**5

INPUT DISTRIBUTIONS BY STREAMLINE OR STREAMTUBE

| STREAMLINE NO. | INLET TOTAL TEMPERATURE (DEG. R.) | INLET TOTAL PRESSURE (PSIA) | INLET WHIRL VELOCITY (FT/SEC) | STREAMTUBE NO. | STREAMTUBE FLOW FRACTION |
|---|---|---|---|---|---|
| 1 | 518.600 | 14.696 | 0.0 | 1 | 0.1000 |
| 2 | 518.600 | 14.696 | 0.0 | 2 | 0.2000 |
| 3 | 518.600 | 14.696 | 0.0 | 3 | 0.3000 |
| 4 | 518.600 | 14.696 | 0.0 | 4 | 0.4000 |
| 5 | 518.600 | 14.696 | 0.0 | 5 | 0.5000 |
| 6 | 518.600 | 14.696 | 0.0 | 6 | 0.6000 |
| 7 | 518.600 | 14.696 | 0.0 | 7 | 0.7000 |
| 8 | 518.600 | 14.696 | 0.0 | 8 | 0.8000 |
| 9 | 518.600 | 14.696 | 0.0 | 9 | 0.9000 |
| 10 | 518.600 | 14.696 | 0.0 | 10 | 1.0000 |
| 11 | 518.600 | 14.696 | 0.0 | | |

Table 9.1. Continued.

INPUT DATA POINTS FOR TIP AND HUB CONTOURS.

| TIP AXIAL COORDINATE (INCHES) | TIP RADIUS (INCHES) | HUB AXIAL COORDINATE (INCHES) | HUB RADIUS (INCHES) |
|---|---|---|---|
| -6.000 | 10.500 | -11.530 | 8.150 |
| -4.100 | 9.030 | -9.100 | 6.050 |
| -1.750 | 8.180 | -6.100 | 5.600 |
| 0.0 | 8.000 | -5.000 | 5.600 |
| 1.000 | 8.000 | -3.400 | 5.600 |
| 2.500 | 8.000 | 0.0 | 5.600 |
| 4.000 | 8.000 | 8.000 | 5.600 |
| 7.500 | 8.000 | 17.000 | 5.600 |
| 10.500 | 8.000 | | |
| 17.000 | 8.000 | | |

Table 9.1. Continued.

THE INPUT PROFILE LOSS TABLES - OMEGA(BAR)*COS(BETA)/(2.0*SIGMA)

** PROFILE LOSS TABLE NO. 1 **

| STREAMLINE | D-FACTOR | LOSS PARAM. | D-FACTOR | LOSS PARAM. | D-FACTOR | LOSS PARAM. | D-FACTOR | LOSS PARAM. | D-FACTOR | LOSS PARAM. |
|---|---|---|---|---|---|---|---|---|---|---|
| 1 | 0.3000 | 0.0380 | 0.4000 | 0.0660 | 0.5000 | 0.0970 | 0.6000 | 0.1300 | 0.7000 | 0.1640 |
| 2 | 0.3000 | 0.0200 | 0.4000 | 0.0340 | 0.5000 | 0.0590 | 0.6000 | 0.0880 | 0.7000 | 0.1220 |
| 3 | 0.3000 | 0.0090 | 0.4000 | 0.0150 | 0.5000 | 0.0340 | 0.6000 | 0.0570 | 0.7000 | 0.0830 |
| 4 | 0.3000 | 0.0090 | 0.4000 | 0.0130 | 0.5000 | 0.0180 | 0.6000 | 0.0270 | 0.7000 | 0.0400 |
| 5 | 0.3000 | 0.0090 | 0.4000 | 0.0130 | 0.5000 | 0.0180 | 0.6000 | 0.0270 | 0.7000 | 0.0400 |
| 6 | 0.3000 | 0.0090 | 0.4000 | 0.0130 | 0.5000 | 0.0180 | 0.6000 | 0.0270 | 0.7000 | 0.0400 |
| 7 | 0.3000 | 0.0090 | 0.4000 | 0.0130 | 0.5000 | 0.0180 | 0.6000 | 0.0270 | 0.7000 | 0.0400 |
| 8 | 0.3000 | 0.0090 | 0.4000 | 0.0130 | 0.5000 | 0.0180 | 0.6000 | 0.0270 | 0.7000 | 0.0400 |
| 9 | 0.3000 | 0.0090 | 0.4000 | 0.0130 | 0.5000 | 0.0180 | 0.6000 | 0.0270 | 0.7000 | 0.0400 |
| 10 | 0.3000 | 0.0090 | 0.4000 | 0.0130 | 0.5000 | 0.0180 | 0.6000 | 0.0270 | 0.7000 | 0.0400 |
| 11 | 0.3000 | 0.0090 | 0.4000 | 0.0130 | 0.5000 | 0.0180 | 0.6000 | 0.0270 | 0.7000 | 0.0400 |

** PROFILE LOSS TABLE NO. 2 **

| STREAMLINE | D-FACTOR | LOSS PARAM. | D-FACTOR | LOSS PARAM. | D-FACTOR | LOSS PARAM. | D-FACTOR | LOSS PARAM. | D-FACTOR | LOSS PARAM. |
|---|---|---|---|---|---|---|---|---|---|---|
| 1 | 0.3000 | 0.0090 | 0.4000 | 0.0130 | 0.5000 | 0.0180 | 0.6000 | 0.0270 | 0.7000 | 0.0400 |
| 2 | 0.3000 | 0.0090 | 0.4000 | 0.0130 | 0.5000 | 0.0180 | 0.6000 | 0.0270 | 0.7000 | 0.0400 |
| 3 | 0.3000 | 0.0090 | 0.4000 | 0.0130 | 0.5000 | 0.0180 | 0.6000 | 0.0270 | 0.7000 | 0.0400 |
| 4 | 0.3000 | 0.0090 | 0.4000 | 0.0130 | 0.5000 | 0.0180 | 0.6000 | 0.0270 | 0.7000 | 0.0400 |
| 5 | 0.3000 | 0.0090 | 0.4000 | 0.0130 | 0.5000 | 0.0180 | 0.6000 | 0.0270 | 0.7000 | 0.0400 |
| 6 | 0.3000 | 0.0090 | 0.4000 | 0.0130 | 0.5000 | 0.0180 | 0.6000 | 0.0270 | 0.7000 | 0.0400 |
| 7 | 0.3000 | 0.0090 | 0.4000 | 0.0130 | 0.5000 | 0.0180 | 0.6000 | 0.0270 | 0.7000 | 0.0400 |
| 8 | 0.3000 | 0.0090 | 0.4000 | 0.0130 | 0.5000 | 0.0180 | 0.6000 | 0.0270 | 0.7000 | 0.0400 |
| 9 | 0.3000 | 0.0090 | 0.4000 | 0.0130 | 0.5000 | 0.0180 | 0.6000 | 0.0270 | 0.7000 | 0.0400 |
| 10 | 0.3000 | 0.0090 | 0.4000 | 0.0130 | 0.5000 | 0.0180 | 0.6000 | 0.0270 | 0.7000 | 0.0400 |
| 11 | 0.3000 | 0.0090 | 0.4000 | 0.0130 | 0.5000 | 0.0180 | 0.6000 | 0.0270 | 0.7000 | 0.0400 |

Table 9.1. Continued.

*** PRINTOUT OF INPUT STATION DATA ***

** INPUT SET NO. 1 IS AN ANNULAR STATION **

| TIP AXIAL LOCATION (INCHES) | HUB AXIAL LOCATION (INCHES) | TIP BLOCKAGE FACTOR | HUB BLOCKAGE FACTOR | MASS BLEED FRACTION |
|---|---|---|---|---|
| -5.9500 | -11.4000 | 0.0 | 0.0 | 0.0 |

** INPUT SET NO. 2 IS AN ANNULAR STATION **

| TIP AXIAL LOCATION (INCHES) | HUB AXIAL LOCATION (INCHES) | TIP BLOCKAGE FACTOR | HUB BLOCKAGE FACTOR | MASS BLEED FRACTION |
|---|---|---|---|---|
| -4.7500 | -8.3500 | 0.0030 | 0.0030 | 0.0 |

** INPUT SET NO. 3 IS AN ANNULAR STATION **

| TIP AXIAL LOCATION (INCHES) | HUB AXIAL LOCATION (INCHES) | TIP BLOCKAGE FACTOR | HUB BLOCKAGE FACTOR | MASS BLEED FRACTION |
|---|---|---|---|---|
| -3.5800 | -4.9500 | 0.0060 | 0.0060 | 0.0 |

** INPUT SET NO. 4 IS AN ANNULAR STATION **

| TIP AXIAL LOCATION (INCHES) | HUB AXIAL LOCATION (INCHES) | TIP BLOCKAGE FACTOR | HUB BLOCKAGE FACTOR | MASS BLEED FRACTION |
|---|---|---|---|---|
| -1.4500 | -1.6000 | 0.0080 | 0.0080 | 0.0 |

Table 9.1. Continued.

*** PRINTOUT OF INPUT STATION DATA ***

** INPUT SET NO. 5 IS ROTOR NO. 1 **

* ALL PROGRAM OPTIONS EXCEPT OFF - DESIGN PUNCH ARE DESIRED FOR THIS BLADE *

| TIP C.G. AXIAL LOCATION (INCHES) | HUB C.G. AXIAL LOCATION (INCHES) | INLET TIP BLOCKAGE | INLET HUB BLOCKAGE | INLET MASS BLEED |
|---|---|---|---|---|
| 1.8300 | 1.8300 | 0.0090 | 0.0090 | 0.0 |
| LOSS SET USED | BLADE TILT ANGLE (DEGREES) | OUTLET TIP BLOCKAGE | OUTLET HUB BLOCKAGE | OUTLET MASS BLEED |
| 1 | C.0 | 0.0180 | 0.0090 | 0.0 |
| TIP D FACTOR LIMIT | HUB FLOW ANGLE LIMIT (DEGREES) | TIP SOLIDITY | NUMBER OF BLADES | CUM ENERGY ADD FRACT |
| 0.4000 | 0.0 | 1.0027 | 21 | 0.5000 |

* POLYNOMIAL CONSTANTS FOR THE FOLLOWING *

| TERM | ROTOR OUTLET PRESSURE | L.E. RADIUS/CHORD | T.E. RADIUS/CHORD | MAX. THICKNESS/CHORD | CHORD/TIP CHORD |
|---|---|---|---|---|---|
| CONSTANT | | 0.0100 | 0.0100 | 0.0600 | |
| LINEAR | 0.0 | 0.0 | 0.0 | 0.0400 | 0.0 |
| QUADRATIC | 0.0 | 0.0 | 0.0 | 0.0 | 0.0 |
| CUBIC | 0.0 | 0.0 | 0.0 | 0.0 | 0.0 |
| QUARTIC | 0.0 | | | | |
| QUINTIC | 0.0 | | | | |

* INPUT BLADE ELEMENT DEFINITION OPTIONS *

| INCIDENCE ANGLE | DEVIATION ANGLE | TURNING RATE RATIO | TRANSITION POINT | MAX. THICKNESS POINT | CHOKE MARGIN | BLADE MATERIAL DENSITY LB/(IN)**3 |
|---|---|---|---|---|---|---|
| 2-D | CARTERS RULE | CIRCULAR ARC | CIRCULAR ARC | TRANS. PT. | NONE | 0.10000 |

Table 9.1. Continued.

*** PRINTOUT OF INPUT STATION DATA ***

** INPUT SET NO. 6 IS A GUIDE VANE OR STATOR **

* ALL PROGRAM OPTIONS EXCEPT OFF - DESIGN PUNCH ARE DESIRED FOR THIS BLADE *

| TIP C.G. AXIAL LOCATION (INCHES) | HUB C.G. AXIAL LOCATION (INCHES) | INLET TIP BLOCKAGE | INLET HUB BLOCKAGE | INLET MASS BLEED |
|---|---|---|---|---|
| 6.4600 | 6.4600 | 0.0180 | 0.0090 | 0.0 |
| **LOSS SET USED** | **BLADE TILT ANGLE (DEGREES)** | **OUTLET TIP BLOCKAGE** | **OUTLET HUB BLOCKAGE** | **OUTLET MASS BLEED** |
| 2 | 0.0 | 0.0180 | 0.0180 | 0.0 |
| **HUB D FACTOR LIMIT** | **INLET HUB MACH LIMIT** | **TIP SOLIDITY** | **NUMBER OF BLADES** | **NTESTK NCVSTK** |
| 0.5000 | 0.5000 | 1.8200 | 30 | 1 0 |

* POLYNOMIAL CONSTANTS FOR THE FOLLOWING *

| TERM | STATOR OUTLET V(θ) | L.E. RADIUS/CHORD | T.E. RADIUS/CHORD | MAX. THICKNESS/CHORD | CHORD/TIP CHORD |
|---|---|---|---|---|---|
| INV.SQ. | 0.0 | | | | |
| INVERSE | 0.0 | | | | |
| CONSTANT | 0.0 | 0.0100 | 0.0100 | 0.1000 | |
| LINEAR | 0.0 | 0.0 | 0.0 | -0.0400 | -0.8721 |
| QUADRATIC | 0.0 | 0.0 | 0.0 | 0.0 | 0.8721 |
| CUBIC | | 0.0 | 0.0 | 0.0 | 0.0 |

* INPUT BLADE ELEMENT DEFINITION OPTIONS *

| INCIDENCE ANGLE | DEVIATION ANGLE | TURNING RATE RATIO | TRANSITION POINT | MAX. THICKNESS POINT | CHOKE MARGIN |
|---|---|---|---|---|---|
| 2-D | CARTERS RULE | CIRCULAR ARC | CIRCULAR ARC | TRANS. PT. | NONE |

Table 9.1. Continued.

*** PRINTOLT OF INPUT STATION DATA ***

** INPUT SET NO. 7 IS ROTOR NO. 2 **

* ALL PROGRAM OPTIONS EXCEPT OFF - DESIGN PUNCH ARE DESIRED FOR THIS BLADE *

| TIP C.G. AXIAL LOCATION (INCHES) | HUB C.G. AXIAL LOCATION (INCHES) | INLET TIP BLOCKAGE | INLET HUB BLOCKAGE | INLET MASS BLEED |
|---|---|---|---|---|
| 8.2700 | 8.2700 | 0.0180 | 0.0180 | 0.0 |
| **LOSS SET USED** | **BLADE TILT ANGLE (DEGREES)** | **OUTLET TIP BLOCKAGE** | **OUTLET HUB BLOCKAGE** | **OUTLET MASS BLEED** |
| 1 | 0.0 | 0.0270 | 0.0180 | 0.0 |
| **TIP D FACTOR LIMIT** | **HUB FLOW ANGLE LIMIT (DEGREES)** | **TIP SOLIDITY** | **NUMBER OF BLADES** | **CUM ENERGY ADD FRACT** |
| 0.4000 | 0.0 | 1.0027 | 21 | 1.0000 |

* POLYNOMIAL CONSTANTS FOR THE FOLLOWING *

| TERM | ROTOR OUTLET PRESSURE | L.E. RADIUS/CHORD | T.E. RADIUS/CHORD | MAX. THICKNESS/CHORD | CHORD/TIP CHORD |
|---|---|---|---|---|---|
| CONSTANT | | 0.0100 | 0.0100 | 0.0600 | |
| LINEAR | 0.0 | 0.0 | 0.0 | 0.0400 | 0.0 |
| QUADRATIC | 0.0 | 0.0 | 0.0 | 0.0 | 0.0 |
| CUBIC | 0.0 | 0.0 | 0.0 | 0.0 | 0.0 |
| QUARTIC | 0.0 | | | | |
| QUINTIC | 0.0 | | | | |

* INPUT BLADE ELEMENT DEFINITION OPTIONS *

| INCIDENCE ANGLE | DEVIATION ANGLE | TURNING RATE RATIO | TRANSITION POINT | MAX. THICKNESS POINT | CHOKE MARGIN | BLADE MATERIAL DENSITY LB/(IN)**3 |
|---|---|---|---|---|---|---|
| 2-D | CARTERS RULE | CIRCULAR ARC | CIRCULAR ARC | TRANS. PT. | NONE | 0.10000 |

Table 9.1. Continued.

*** PRINTOUT OF INPUT STATION DATA ***

** INPUT SET NO. 8 IS A GUIDE VANE OR STATOR **

* ALL PROGRAM OPTIONS EXCEPT OFF - DESIGN PUNCH ARE DESIRED FOR THIS BLADE *

| TIP C.G. AXIAL LOCATION (INCHES) | HUB C.G. AXIAL LOCATION (INCHES) | INLET TIP BLOCKAGE | INLET HUB BLOCKAGE | INLET MASS BLEED |
|---|---|---|---|---|
| 12.9000 | 12.9000 | 0.0270 | 0.0180 | 0.0 |
| **LOSS SET USED** | **BLADE TILT ANGLE (DEGREES)** | **OUTLET TIP BLOCKAGE** | **OUTLET HUB BLOCKAGE** | **OUTLET MASS BLEED** |
| 2 | 0.0 | 0.0270 | 0.0270 | 0.0 |
| **HUB D FACTOR LIMIT** | **INLET HUB MACH LIMIT** | **TIP SOLIDITY** | **NUMBER OF BLADES** | **NTESTK NCVSTK** |
| 0.5000 | 0.5000 | 1.8200 | 30 | 1 0 |

* POLYNOMIAL CONSTANTS FOR THE FOLLOWING *

| TERM | STATOR OUTLET V(0) | L.E. RADIUS/CHORD | T.E. RADIUS/CHORD | MAX. THICKNESS/CHORD | CHORD/TIP CHORD |
|---|---|---|---|---|---|
| INV.SQ. | 0.0 | | | | |
| INVERSE | 0.0 | | | | |
| CONSTANT | 0.0 | 0.0100 | 0.0100 | 0.1000 | |
| LINEAR | 0.0 | 0.0 | 0.0 | -0.0400 | -0.8721 |
| QUADRATIC | 0.0 | 0.0 | 0.0 | 0.0 | 0.8721 |
| CUBIC | | 0.0 | 0.0 | 0.0 | 0.0 |

* INPUT BLADE ELEMENT DEFINITION OPTIONS *

| INCIDENCE ANGLE | DEVIATION ANGLE | TURNING RATE RATIO | TRANSITION POINT | MAX. THICKNESS POINT | CHOKE MARGIN |
|---|---|---|---|---|---|
| 2-D | CARTERS RULE | CIRCULAR ARC | CIRCULAR ARC | TRANS. PT. | NONE |

Table 9.1. Concluded.

*** PRINTOUT OF INPUT STATION DATA ***

** INPUT SET NO. 9 IS AN ANNULAR STATION **

| TIP AXIAL LOCATION (INCHES) | HUB AXIAL LOCATION (INCHES) | TIP BLOCKAGE FACTOR | HUB BLOCKAGE FACTOR | MASS BLEED FRACTION |
|---|---|---|---|---|
| 14.5000 | 14.5000 | 0.0270 | 0.0270 | 0.0 |

** INPUT SET NO. 10 IS AN ANNULAR STATION **

| TIP AXIAL LOCATION (INCHES) | HUB AXIAL LOCATION (INCHES) | TIP BLOCKAGE FACTOR | HUB BLOCKAGE FACTOR | MASS BLEED FRACTION |
|---|---|---|---|---|
| 15.5000 | 15.5000 | 0.0270 | 0.0270 | 0.0 |

** INPUT SET NO. 11 IS AN ANNULAR STATION **

| TIP AXIAL LOCATION (INCHES) | HUB AXIAL LOCATION (INCHES) | TIP BLOCKAGE FACTOR | HUB BLOCKAGE FACTOR | MASS BLEED FRACTION |
|---|---|---|---|---|
| 16.5000 | 16.5000 | 0.0270 | 0.0270 | 0.0 |

| I | IFT | Z(IFT,JM) | AR | I | Z(I,J) | AR |
|---|---|---|---|---|---|---|
| 1 | 1 | -8.4947 | 0.0 | 1 | -8.4947 | 0.0 |
| 2 | 2 | -6.3346 | 1.6969 | 2 | -6.3345 | 1.6969 |
| 3 | 3 | -4.1903 | 1.4520 | 3 | -4.1903 | 1.4520 |
| 4 | 4 | -1.5182 | 0.9303 | 4 | -1.5182 | 0.9303 |
| 5 | 5 | 1.0003 | 0.9356 | 5 | 1.0003 | 0.9356 |
| 6 | 6 | 2.7808 | 1.3125 | 6 | 2.7808 | 1.3125 |
| 7 | 7 | 3.8350 | 2.2171 | 7 | 3.8350 | 2.2171 |
| 8 | 8 | 6.4600 | 0.8805 | 8 | 6.4600 | 0.8805 |
| 9 | 9 | 7.4405 | 2.3566 | 9 | 7.4405 | 2.3566 |
| 10 | 10 | 9.2206 | 1.2875 | 10 | 9.2206 | 1.2875 |
| 11 | 11 | 10.2750 | 2.1739 | 11 | 10.2750 | 2.1739 |
| 12 | 12 | 12.9000 | 0.8634 | 12 | 12.9000 | 0.8634 |
| 13 | 13 | 14.5000 | 1.4166 | 13 | 14.5000 | 1.4166 |
| 14 | 14 | 15.5000 | 2.2666 | 14 | 15.5000 | 2.2666 |
| 15 | 15 | 16.5000 | 2.2666 | 15 | 16.5000 | 2.2666 |

FACT1 = 1.2548 FACT2 = 1.0193

Table 9.2. Design code predictions of aerodynamic parameters.

** VALUES OF PARAMETERS ON STREAMLINES AT STATION, 1, WHICH IS AN ANNULUS **

| STREAMLINE NO. | RADIUS (IN.) | AXIAL COORD. (IN.) | AXIAL VEL. (FT/SEC) | MERD. VEL. (FT/SEC) | TANG. VEL. (FT/SEC) | ABS. VEL. (FT/SEC) | ABS. MACH NO. | ABS.FLOW ANGLE (DEG) | STREAM. SLOPE (DEG) | STREAM. CURV. (1./IN.) | TOTAL PRESS. (PSIA) | TOTAL TEMP. (DEG.R.) | STATIC PRESS. (PSIA) | STATIC TEMP. (DEG.R.) |
|---|---|---|---|---|---|---|---|---|---|---|---|---|---|---|
| TIP | 10.454 | -5.950 | | | | | | | | | | | | |
| 1 | 10.454 | -5.950 | 30.91 | 42.24 | 0.0 | 42.24 | 0.0378 | 0.0 | -42.97 | 0.044 | 14.696 | 518.60 | 14.681 | 518.45 |
| 2 | 10.289 | -6.317 | 30.58 | 40.32 | 0.0 | 40.32 | 0.0361 | 0.0 | -40.68 | 0.040 | 14.696 | 518.60 | 14.683 | 518.46 |
| 3 | 10.110 | -6.715 | 30.02 | 38.40 | 0.0 | 38.40 | 0.0344 | 0.0 | -38.58 | 0.037 | 14.696 | 518.60 | 14.684 | 518.48 |
| 4 | 9.914 | -7.150 | 29.27 | 36.51 | 0.0 | 36.51 | 0.0327 | 0.0 | -36.70 | 0.035 | 14.696 | 518.60 | 14.685 | 518.49 |
| 5 | 9.700 | -7.624 | 28.35 | 34.64 | 0.0 | 34.64 | 0.0310 | 0.0 | -35.07 | 0.034 | 14.696 | 518.60 | 14.686 | 518.50 |
| 6 | 9.466 | -8.144 | 27.29 | 32.84 | 0.0 | 32.84 | 0.0294 | 0.0 | -33.80 | 0.034 | 14.696 | 518.60 | 14.687 | 518.51 |
| 7 | 9.210 | -8.714 | 26.10 | 31.14 | 0.0 | 31.14 | 0.0279 | 0.0 | -33.06 | 0.035 | 14.696 | 518.60 | 14.688 | 518.52 |
| 8 | 8.931 | -9.333 | 24.79 | 29.62 | 0.0 | 29.62 | 0.0265 | 0.0 | -33.18 | 0.038 | 14.696 | 518.60 | 14.689 | 518.53 |
| 9 | 8.632 | -9.999 | 23.34 | 28.38 | 0.0 | 28.38 | 0.0254 | 0.0 | -34.65 | 0.042 | 14.696 | 518.60 | 14.689 | 518.53 |
| 10 | 8.319 | -10.695 | 21.63 | 27.58 | 0.0 | 27.58 | 0.0247 | 0.0 | -38.35 | 0.048 | 14.696 | 518.60 | 14.690 | 518.54 |
| 11 | 8.001 | -11.400 | 19.00 | 27.20 | 0.0 | 27.20 | 0.0244 | 0.0 | -45.69 | 0.050 | 14.696 | 518.60 | 14.690 | 518.54 |
| HUB | 8.001 | -11.400 | | | | | | | | | | | | |

** VALUES OF PARAMETERS ON STREAMLINES AT STATION, 2, WHICH IS AN ANNULUS **

| STREAMLINE NO. | RADIUS (IN.) | AXIAL COORD. (IN.) | AXIAL VEL. (FT/SEC) | MERD. VEL. (FT/SEC) | TANG. VEL. (FT/SEC) | ABS. VEL. (FT/SEC) | ABS. MACH NO. | ABS.FLOW ANGLE (DEG) | STREAM. SLOPE (DEG) | STREAM. CURV. (1./IN.) | TOTAL PRESS. (PSIA) | TOTAL TEMP. (DEG.R.) | STATIC PRESS. (PSIA) | STATIC TEMP. (DEG.R.) |
|---|---|---|---|---|---|---|---|---|---|---|---|---|---|---|
| TIP | 9.459 | -4.750 | | | | | | | | | | | | |
| 1 | 9.450 | -4.759 | 47.63 | 59.06 | 0.0 | 59.06 | 0.0529 | 0.0 | -36.24 | 0.117 | 14.696 | 518.60 | 14.667 | 518.31 |
| 2 | 9.238 | -4.965 | 46.94 | 56.62 | 0.0 | 56.62 | 0.0507 | 0.0 | -33.99 | 0.104 | 14.696 | 518.60 | 14.670 | 518.33 |
| 3 | 9.011 | -5.187 | 46.05 | 54.20 | 0.0 | 54.20 | 0.0486 | 0.0 | -31.82 | 0.095 | 14.696 | 518.60 | 14.672 | 518.36 |
| 4 | 8.764 | -5.427 | 44.96 | 51.76 | 0.0 | 51.76 | 0.0464 | 0.0 | -29.70 | 0.089 | 14.696 | 518.60 | 14.674 | 518.38 |
| 5 | 8.496 | -5.689 | 43.64 | 49.25 | 0.0 | 49.25 | 0.0441 | 0.0 | -27.62 | 0.086 | 14.696 | 518.60 | 14.676 | 518.40 |
| 6 | 8.200 | -5.978 | 42.03 | 46.59 | 0.0 | 46.59 | 0.0417 | 0.0 | -25.56 | 0.086 | 14.696 | 518.60 | 14.678 | 518.42 |
| 7 | 7.870 | -6.300 | 40.05 | 43.68 | 0.0 | 43.68 | 0.0391 | 0.0 | -23.53 | 0.092 | 14.696 | 518.60 | 14.680 | 518.44 |
| 8 | 7.494 | -6.666 | 37.55 | 40.37 | 0.0 | 40.37 | 0.0362 | 0.0 | -21.55 | 0.104 | 14.696 | 518.60 | 14.683 | 518.46 |
| 9 | 7.054 | -7.096 | 34.27 | 36.40 | 0.0 | 36.40 | 0.0326 | 0.0 | -19.74 | 0.127 | 14.696 | 518.60 | 14.685 | 518.49 |
| 10 | 6.513 | -7.623 | 29.74 | 31.35 | 0.0 | 31.35 | 0.0281 | 0.0 | -18.46 | 0.169 | 14.696 | 518.60 | 14.688 | 518.52 |
| 11 | 5.784 | -8.334 | 22.97 | 24.31 | 0.0 | 24.31 | 0.0218 | 0.0 | -19.13 | 0.248 | 14.696 | 518.60 | 14.691 | 518.55 |
| HUB | 5.768 | -8.350 | | | | | | | | | | | | |

Table 9.2. Continued.

** VALUES OF PARAMETERS ON STREAMLINES AT STATION, 3, WHICH IS AN ANNULUS **

| STREAMLINE NO. | RADIUS (IN.) | AXIAL COORD. (IN.) | AXIAL VEL. (FT/SEC) | MERD. VEL. (FT/SEC) | TANG. VEL. (FT/SEC) | ABS. VEL. (FT/SEC) | ABS. MACH NO. | ABS.FLOW ANGLE (DEG) | STREAM. SLOPE (DEG) | STREAM. CURV. (1./IN.) | TOTAL PRESS. (PSIA) | TOTAL TEMP. (DEG.R.) | STATIC PRESS. (PSIA) | STATIC TEMP. (DEG.R.) |
|---|---|---|---|---|---|---|---|---|---|---|---|---|---|---|
| TIP | 8.755 | -3.580 | | | | | | | | | | | | |
| 1 | 8.740 | -3.587 | 70.43 | 78.16 | 0.0 | 78.16 | 0.0700 | 0.0 | -25.70 | 0.152 | 14.696 | 518.60 | 14.646 | 518.09 |
| 2 | 8.522 | -3.681 | 69.13 | 75.61 | 0.0 | 75.61 | 0.0678 | 0.0 | -23.91 | 0.135 | 14.696 | 518.60 | 14.649 | 518.12 |
| 3 | 8.290 | -3.782 | 67.82 | 73.18 | 0.0 | 73.18 | 0.0656 | 0.0 | -22.07 | 0.121 | 14.696 | 518.60 | 14.652 | 518.15 |
| 4 | 8.044 | -3.889 | 66.51 | 70.86 | 0.0 | 70.86 | 0.0635 | 0.0 | -20.16 | 0.106 | 14.696 | 518.60 | 14.655 | 518.18 |
| 5 | 7.782 | -4.003 | 65.19 | 68.61 | 0.0 | 68.61 | 0.0615 | 0.0 | -18.16 | 0.093 | 14.696 | 518.60 | 14.657 | 518.21 |
| 6 | 7.500 | -4.125 | 63.87 | 66.44 | 0.0 | 66.44 | 0.0595 | 0.0 | -16.00 | 0.079 | 14.696 | 518.60 | 14.660 | 518.23 |
| 7 | 7.195 | -4.257 | 62.53 | 64.33 | 0.0 | 64.33 | 0.0576 | 0.0 | -13.61 | 0.064 | 14.696 | 518.60 | 14.662 | 518.26 |
| 8 | 6.864 | -4.401 | 61.17 | 62.28 | 0.0 | 62.28 | 0.0558 | 0.0 | -10.84 | 0.047 | 14.696 | 518.60 | 14.664 | 518.28 |
| 9 | 6.500 | -4.559 | 59.79 | 60.30 | 0.0 | 60.30 | 0.0540 | 0.0 | -7.50 | 0.026 | 14.696 | 518.60 | 14.666 | 518.30 |
| 10 | 6.093 | -4.735 | 58.31 | 58.40 | 0.0 | 58.40 | 0.0523 | 0.0 | -3.17 | -0.006 | 14.696 | 518.60 | 14.668 | 518.32 |
| 11 | 5.626 | -4.939 | 56.62 | 56.70 | 0.0 | 56.70 | 0.0508 | 0.0 | 3.10 | -0.058 | 14.696 | 518.60 | 14.669 | 518.33 |
| HUB | 5.600 | -4.950 | | | | | | | | | | | | |

** VALUES OF PARAMETERS ON STREAMLINES AT STATION, 4, WHICH IS AN ANNULUS **

| STREAMLINE NO. | RADIUS (IN.) | AXIAL COORD. (IN.) | AXIAL VEL. (FT/SEC) | MERD. VEL. (FT/SEC) | TANG. VEL. (FT/SEC) | ABS. VEL. (FT/SEC) | ABS. MACH NO. | ABS.FLOW ANGLE (DEG) | STREAM. SLOPE (DEG) | STREAM. CURV. (1./IN.) | TOTAL PRESS. (PSIA) | TOTAL TEMP. (DEG.R.) | STATIC PRESS. (PSIA) | STATIC TEMP. (DEG.R.) |
|---|---|---|---|---|---|---|---|---|---|---|---|---|---|---|
| TIP | 8.128 | -1.450 | | | | | | | | | | | | |
| 1 | 8.111 | -1.451 | 99.08 | 100.07 | 0.0 | 100.07 | 0.0897 | 0.0 | -8.06 | 0.108 | 14.696 | 518.60 | 14.613 | 517.77 |
| 2 | 7.912 | -1.463 | 97.24 | 98.11 | 0.0 | 98.11 | 0.0879 | 0.0 | -7.66 | 0.098 | 14.696 | 518.60 | 14.617 | 517.80 |
| 3 | 7.704 | -1.475 | 95.53 | 96.30 | 0.0 | 96.30 | 0.0863 | 0.0 | -7.24 | 0.088 | 14.696 | 518.60 | 14.620 | 517.83 |
| 4 | 7.486 | -1.488 | 94.00 | 94.66 | 0.0 | 94.66 | 0.0848 | 0.0 | -6.73 | 0.077 | 14.696 | 518.60 | 14.622 | 517.85 |
| 5 | 7.258 | -1.502 | 92.64 | 93.18 | 0.0 | 93.18 | 0.0835 | 0.0 | -6.12 | 0.067 | 14.696 | 518.60 | 14.624 | 517.88 |
| 6 | 7.019 | -1.516 | 91.45 | 91.86 | 0.0 | 91.86 | 0.0823 | 0.0 | -5.42 | 0.057 | 14.696 | 518.60 | 14.626 | 517.90 |
| 7 | 6.769 | -1.531 | 90.41 | 90.70 | 0.0 | 90.70 | 0.0813 | 0.0 | -4.63 | 0.048 | 14.696 | 518.60 | 14.628 | 517.91 |
| 8 | 6.505 | -1.546 | 89.52 | 89.71 | 0.0 | 89.71 | 0.0804 | 0.0 | -3.73 | 0.038 | 14.696 | 518.60 | 14.630 | 517.93 |
| 9 | 6.228 | -1.563 | 88.77 | 88.87 | 0.0 | 88.87 | 0.0796 | 0.0 | -2.76 | 0.029 | 14.696 | 518.60 | 14.631 | 517.94 |
| 10 | 5.936 | -1.580 | 88.13 | 88.17 | 0.0 | 88.17 | 0.0790 | 0.0 | -1.71 | 0.022 | 14.696 | 518.60 | 14.632 | 517.95 |
| 11 | 5.625 | -1.599 | 87.54 | 87.54 | 0.0 | 87.54 | 0.0785 | 0.0 | -0.66 | 0.019 | 14.696 | 518.60 | 14.633 | 517.96 |
| HUB | 5.600 | -1.600 | | | | | | | | | | | | |

Table 9.2. Continued.

** VALUES OF PARAMETERS ON STREAMLINES AT STATION. 5. WHICH IS THE INLET OF ROTOR NUMBER. 1 **

| STREAMLINE NO. | RADIUS (IN.) | AXIAL COORD. (IN.) | AXIAL VEL. (FT/SEC) | MERD. VEL. (FT/SEC) | TANG. VEL. (FT/SEC) | ABS. VEL. (FT/SEC) | ABS. MACH NO. | ABS.FLOW ANGLE (DEG) | STREAM. SLOPE (DEG) | STREAM. CURV. (1./IN.) | TOTAL PRESS. (PSIA) | TOTAL TEMP. (DEG.R.) | STATIC PRESS. (PSIA) | STATIC TEMP. (DEG.R.) |
|---|---|---|---|---|---|---|---|---|---|---|---|---|---|---|
| TIP | 8.001 | 1.145 | | | | | | | | | | | | |
| 1 | 7.982 | 1.144 | 98.25 | 98.26 | 0.0 | 98.26 | 0.0881 | 0.0 | -0.52 | -0.009 | 14.696 | 518.60 | 14.616 | 517.80 |
| 2 | 7.779 | 1.129 | 98.45 | 98.47 | 0.0 | 98.47 | 0.0883 | 0.0 | -0.90 | -0.009 | 14.696 | 518.60 | 14.616 | 517.79 |
| 3 | 7.570 | 1.114 | 98.59 | 98.60 | 0.0 | 98.60 | 0.0884 | 0.0 | -0.96 | -0.004 | 14.696 | 518.60 | 14.616 | 517.79 |
| 4 | 7.356 | 1.098 | 98.63 | 98.64 | 0.0 | 98.64 | 0.0884 | 0.0 | -0.94 | 0.000 | 14.696 | 518.60 | 14.616 | 517.79 |
| 5 | 7.135 | 1.081 | 98.59 | 98.60 | 0.0 | 98.60 | 0.0884 | 0.0 | -0.90 | 0.003 | 14.696 | 518.60 | 14.616 | 517.79 |
| 6 | 6.907 | 1.062 | 98.50 | 98.51 | 0.0 | 98.51 | 0.0883 | 0.0 | -0.84 | 0.004 | 14.696 | 518.60 | 14.616 | 517.79 |
| 7 | 6.671 | 1.043 | 98.38 | 98.39 | 0.0 | 98.39 | 0.0882 | 0.0 | -0.74 | 0.005 | 14.696 | 518.60 | 14.616 | 517.79 |
| 8 | 6.426 | 1.022 | 98.25 | 98.25 | 0.0 | 98.25 | 0.0881 | 0.0 | -0.61 | 0.004 | 14.696 | 518.60 | 14.616 | 517.80 |
| 9 | 6.171 | 0.998 | 98.14 | 98.15 | 0.0 | 98.15 | 0.0880 | 0.0 | -0.45 | 0.002 | 14.696 | 518.60 | 14.617 | 517.80 |
| 10 | 5.905 | 0.972 | 98.11 | 98.11 | 0.0 | 98.11 | 0.0879 | 0.0 | -0.25 | -0.002 | 14.696 | 518.60 | 14.617 | 517.80 |
| 11 | 5.625 | 0.944 | 98.25 | 98.25 | 0.0 | 98.25 | 0.0881 | 0.0 | -0.03 | -0.011 | 14.696 | 518.60 | 14.616 | 517.80 |
| HUB | 5.600 | 0.941 | | | | | | | | | | | | |

| STREAMLINE NO. | R/RTIP | REL.FLOW ANGLE (DEG) | REL. TANG.VEL. (FT/SEC) | REL. VEL. (FT/SEC) | REL.MACH NUMBER | WHEEL SPEED (FT/SEC) | FLOW COEF. | L.E.RAD. /CHORD | MAX.TH. /CHORD | MAX.TH. PT.LOC. /CHORD | TRAN.PT. LOCATION /CHORD | SEGMENT IN/OUT TURN.RATE | LAYOUT CONE ANG. (DEG) |
|---|---|---|---|---|---|---|---|---|---|---|---|---|---|
| TIP | 1.0000 | | | | | 167.57 | | | | | | | |
| 1 | 0.9977 | 59.56 | 167.19 | 193.92 | 0.1738 | 167.19 | 0.5863 | 0.0100 | 0.0600 | 0.5000 | 0.5000 | 1.0000 | -0.77 |
| 2 | 0.9723 | 58.85 | 162.92 | 190.37 | 0.1706 | 162.92 | 0.5875 | 0.0100 | 0.0635 | 0.5000 | 0.5000 | 1.0000 | -1.05 |
| 3 | 0.9462 | 58.12 | 158.55 | 186.71 | 0.1674 | 158.55 | 0.5883 | 0.0100 | 0.0670 | 0.5000 | 0.5000 | 1.0000 | -0.96 |
| 4 | 0.9194 | 57.37 | 154.07 | 182.94 | 0.1640 | 154.07 | 0.5886 | 0.0100 | 0.0706 | 0.5000 | 0.5000 | 1.0000 | -0.83 |
| 5 | 0.8918 | 56.58 | 149.44 | 179.04 | 0.1605 | 149.44 | 0.5884 | 0.0100 | 0.0744 | 0.5000 | 0.5000 | 1.0000 | -0.70 |
| 6 | 0.8633 | 55.75 | 144.67 | 175.02 | 0.1569 | 144.67 | 0.5878 | 0.0100 | 0.0782 | 0.5000 | 0.5000 | 1.0000 | -0.59 |
| 7 | 0.8338 | 54.85 | 139.73 | 170.89 | 0.1532 | 139.73 | 0.5871 | 0.0100 | 0.0823 | 0.5000 | 0.5000 | 1.0000 | -0.47 |
| 8 | 0.8032 | 53.87 | 134.60 | 166.64 | 0.1494 | 134.60 | 0.5863 | 0.0100 | 0.0864 | 0.5000 | 0.5000 | 1.0000 | -0.34 |
| 9 | 0.7713 | 52.79 | 129.25 | 162.29 | 0.1455 | 129.25 | 0.5857 | 0.0100 | 0.0907 | 0.5000 | 0.5000 | 1.0000 | -0.22 |
| 10 | 0.7380 | 51.57 | 123.67 | 157.87 | 0.1415 | 123.67 | 0.5855 | 0.0100 | 0.0953 | 0.5000 | 0.5000 | 1.0000 | -0.10 |
| 11 | 0.7032 | 50.18 | 117.83 | 153.42 | 0.1375 | 117.83 | 0.5863 | 0.0100 | 0.1000 | 0.5000 | 0.5000 | 1.0000 | -0.00 |
| HUB | 0.6999 | | | | | | | | | | | | |

| | --- INLET STREAMLINE --- | | ++++++++++++++++++++++++++++++++++ | | | | | LAYOUT CONE | ++++++++++++++++++++++++++++++++++++ | | | | |
|---|---|---|---|---|---|---|---|---|---|---|---|---|---|
| STREAMLINE NO. | PCT. SPAN | INC. ANGLE (DEG) | S.S.INC. ANGLE (DEG) | IN.BLADE ANGLE (DEG) | IN.BLADE ANGLE (DEG) | TRAN.PT. BL.ANGLE (DEG) | BLD.SET ANGLE (DEG) | 1ST SEG. S.S.CAM. (DEG) | MACH NO. AT SHOCK LOCATION | SH.LOC. AS FRACT OF S.S. | COV.CHAN. AS FRACT OF S.S. | MIN.CHK. AREA MARGIN | MIN.CHK. PT.LOC.IN COV.CHAN. | L.E.EDGE CIR.CENT. R*DB/DR |
| 1 | 0.77 | -1.94 | -6.58 | 61.50 | 61.50 | 53.07 | 53.06 | 13.07 | 0.2739 | 0.7925 | 0.2075 | 2.6806 | 0.0 | -0.0646 |
| 2 | 9.24 | 0.22 | -4.95 | 58.64 | 58.64 | 53.15 | 53.15 | 10.55 | 0.2526 | 0.7668 | 0.2332 | 2.6555 | 0.0 | -0.0459 |
| 3 | 17.93 | 0.72 | -4.76 | 57.40 | 57.40 | 52.32 | 52.32 | 10.56 | 0.2447 | 0.7366 | 0.2634 | 2.6635 | 0.0 | -0.0407 |
| 4 | 26.85 | 0.84 | -5.06 | 56.53 | 56.53 | 51.21 | 51.21 | 11.22 | 0.2396 | 0.7052 | 0.2948 | 2.7131 | 0.0 | -0.0419 |
| 5 | 36.05 | 0.94 | -5.39 | 55.65 | 55.65 | 49.99 | 49.99 | 11.98 | 0.2343 | 0.6730 | 0.3270 | 2.7712 | 0.0 | -0.0434 |
| 6 | 45.54 | 1.04 | -5.72 | 54.70 | 54.70 | 48.66 | 48.66 | 12.81 | 0.2287 | 0.6402 | 0.3598 | 2.8321 | 0.0 | -0.0460 |
| 7 | 55.37 | 1.16 | -6.07 | 53.69 | 53.69 | 47.20 | 47.20 | 13.71 | 0.2228 | 0.6066 | 0.3934 | 2.8969 | 0.0 | -0.0505 |
| 8 | 65.57 | 1.28 | -6.42 | 52.59 | 52.59 | 45.58 | 45.58 | 14.71 | 0.2164 | 0.5720 | 0.4280 | 2.9662 | 0.0 | -0.0567 |
| 9 | 76.19 | 1.41 | -6.78 | 51.38 | 51.37 | 43.75 | 43.75 | 15.81 | 0.2097 | 0.5363 | 0.4637 | 3.0404 | 0.0 | -0.0650 |
| 10 | 87.29 | 1.56 | -7.13 | 50.02 | 50.01 | 41.67 | 41.67 | 17.03 | 0.2025 | 0.4993 | 0.5007 | 3.1186 | 0.0474 | -0.0762 |
| 11 | 98.90 | 1.74 | -7.48 | 48.44 | 48.44 | 39.28 | 39.28 | 18.38 | 0.1947 | 0.4606 | 0.5394 | 3.1933 | 0.0960 | -0.0884 |

Table 9.2. Continued.

** VALUES OF PARAMETERS ON STREAMLINES AT STATION, 6, WHICH IS THE OUTLET OF ROTOR NUMBER, 1 **

| STREAMLINE NO. | RADIUS (IN.) | AXIAL COORD. (IN.) | AXIAL VEL. (FT/SEC) | MERD. VEL. (FT/SEC) | TANG. VEL. (FT/SEC) | ABS. VEL. (FT/SEC) | ABS. MACH NO. | ABS.FLOW ANGLE (DEG) | STREAM. SLOPE (DEG) | STREAM. CURV. (1./IN.) | TOTAL PRESS. (PSIA) | TOTAL TEMP. (DEG.R.) | STATIC PRESS. (PSIA) | STATIC TEMP. (DEG.R.) |
|---|---|---|---|---|---|---|---|---|---|---|---|---|---|---|
| TIP | 8.000 | 2.603 | | | | | | | | | | | | |
| 1 | 7.963 | 2.600 | 90.29 | 90.30 | 54.52 | 105.48 | 0.0944 | 31.12 | -0.91 | -0.001 | 14.786 | 520.12 | 14.694 | 519.19 |
| 2 | 7.752 | 2.582 | 98.38 | 98.39 | 39.45 | 106.00 | 0.0949 | 21.85 | -0.93 | 0.007 | 14.786 | 519.67 | 14.693 | 518.73 |
| 3 | 7.546 | 2.594 | 100.14 | 100.14 | 36.95 | 106.75 | 0.0956 | 20.25 | -0.77 | 0.008 | 14.786 | 519.57 | 14.692 | 518.62 |
| 4 | 7.334 | 2.614 | 100.08 | 100.08 | 37.89 | 107.02 | 0.0958 | 20.74 | -0.59 | 0.007 | 14.786 | 519.57 | 14.691 | 518.62 |
| 5 | 7.116 | 2.635 | 99.93 | 99.93 | 39.16 | 107.33 | 0.0961 | 21.40 | -0.44 | 0.007 | 14.786 | 519.57 | 14.691 | 518.61 |
| 6 | 6.891 | 2.658 | 99.79 | 99.79 | 40.44 | 107.67 | 0.0964 | 22.06 | -0.31 | 0.007 | 14.786 | 519.57 | 14.690 | 518.61 |
| 7 | 6.659 | 2.683 | 99.65 | 99.65 | 41.86 | 108.09 | 0.0968 | 22.79 | -0.17 | 0.007 | 14.786 | 519.57 | 14.689 | 518.60 |
| 8 | 6.416 | 2.710 | 99.51 | 99.51 | 43.44 | 108.58 | 0.0972 | 23.59 | -0.04 | 0.007 | 14.786 | 519.57 | 14.688 | 518.59 |
| 9 | 6.165 | 2.739 | 99.33 | 99.33 | 45.22 | 109.13 | 0.0977 | 24.48 | 0.12 | 0.009 | 14.786 | 519.57 | 14.687 | 518.58 |
| 10 | 5.902 | 2.771 | 99.07 | 99.07 | 47.24 | 109.76 | 0.0983 | 25.49 | 0.30 | 0.013 | 14.786 | 519.57 | 14.686 | 518.57 |
| 11 | 5.626 | 2.806 | 98.62 | 98.63 | 49.59 | 110.39 | 0.0989 | 26.69 | 0.60 | 0.022 | 14.786 | 519.57 | 14.685 | 518.56 |
| HUB | 5.600 | 2.809 | | | | | | | | | | | | |

| STREAMLINE NO. | R/RTIP | REL.FLOW ANGLE (DEG) | REL. TANG.VEL. (FT/SEC) | REL. VEL. (FT/SEC) | REL.MACH NUMBER | WHEEL SPEED (FT/SEC) | FLOW COEF. | HEAD COEF. | IDEAL HEAD COEF. | ADIAB. EFF. | DIFFUSION FACTOR | LOSS COEF. | SHOCK LOSS COEF. | ELEMENT SOLIDITY |
|---|---|---|---|---|---|---|---|---|---|---|---|---|---|---|
| TIP | 1.0000 | | | | | | | | | | | | | |
| 1 | 0.9954 | 51.19 | 112.26 | 144.07 | 0.1290 | 166.77 | 0.5388 | 0.1933 | 0.3238 | 0.5969 | 0.3971 | 0.1964 | 0.0 | 1.0027 |
| 2 | 0.9691 | 51.32 | 122.92 | 157.44 | 0.1410 | 162.36 | 0.5871 | 0.1933 | 0.2281 | 0.8474 | 0.2734 | 0.0544 | 0.0 | 1.0295 |
| 3 | 0.9432 | 50.41 | 121.08 | 157.13 | 0.1407 | 158.03 | 0.5976 | 0.1933 | 0.2080 | 0.9293 | 0.2519 | 0.0239 | 0.0 | 1.0577 |
| 4 | 0.9168 | 49.14 | 115.71 | 152.99 | 0.1370 | 153.61 | 0.5972 | 0.1933 | 0.2073 | 0.9324 | 0.2587 | 0.0237 | 0.0 | 1.0884 |
| 5 | 0.8896 | 47.72 | 109.89 | 148.53 | 0.1330 | 149.04 | 0.5963 | 0.1933 | 0.2078 | 0.9299 | 0.2678 | 0.0257 | 0.0 | 1.1219 |
| 6 | 0.8614 | 46.15 | 103.88 | 144.05 | 0.1290 | 144.33 | 0.5955 | 0.1933 | 0.2079 | 0.9297 | 0.2766 | 0.0270 | 0.0 | 1.1587 |
| 7 | 0.8323 | 44.40 | 97.58 | 139.48 | 0.1249 | 139.45 | 0.5947 | 0.1933 | 0.2079 | 0.9296 | 0.2858 | 0.0283 | 0.0 | 1.1995 |
| 8 | 0.8021 | 42.42 | 90.94 | 134.80 | 0.1207 | 134.38 | 0.5938 | 0.1933 | 0.2079 | 0.9296 | 0.2957 | 0.0298 | 0.0 | 1.2449 |
| 9 | 0.7706 | 40.19 | 83.90 | 130.02 | 0.1164 | 129.11 | 0.5927 | 0.1933 | 0.2079 | 0.9296 | 0.3063 | 0.0314 | 0.0 | 1.2960 |
| 10 | 0.7378 | 37.63 | 76.37 | 125.09 | 0.1120 | 123.61 | 0.5912 | 0.1933 | 0.2079 | 0.9294 | 0.3181 | 0.0333 | 0.0 | 1.3541 |
| 11 | 0.7033 | 34.68 | 68.24 | 119.93 | 0.1074 | 117.83 | 0.5885 | 0.1933 | 0.2081 | 0.9288 | 0.3320 | 0.0355 | 0.0 | 1.4209 |
| HUB | 0.7000 | | | | | | | | | | | | | |

| STREAMLINE NO. | PCT. SPAN | PRESS. RATIO | TEMP. RATIO | AERO. CHORD (IN.) | MEAN SPACING (IN.) | LOCAL BLADE FORCES RADIUS (IN.) | LOCAL BLADE FORCES FOR.AXIAL (LBS/IN) | LOCAL BLADE FORCES TANG. (LBS/IN) | --- OUTLET STREAMLINE --- T.E.RAD. /CHORD | DEV. ANGLE (DEG) | OUT.BLADE ANGLE (DEG) | ++ LAYOUT CONE +++ OUT.BLADE ANGLE (DEG) | MAX.CAMB. PT.LOC. /CHORD | T.E.EDGE CIR.CENT R*DØ/DR |
|---|---|---|---|---|---|---|---|---|---|---|---|---|---|---|
| 1 | 1.54 | 1.0061 | 1.0029 | 2.3919 | 2.3854 | 7.973 | 0.1549 | -0.2046 | 0.0100 | 6.53 | 44.66 | 44.63 | 0.5000 | -0.3871 |
| 2 | 10.31 | 1.0061 | 1.0021 | 2.3919 | 2.3235 | 7.766 | 0.1783 | -0.1478 | 0.0100 | 3.66 | 47.66 | 47.67 | 0.5000 | -0.1348 |
| 3 | 18.92 | 1.0061 | 1.0019 | 2.3919 | 2.2613 | 7.558 | 0.1769 | -0.1366 | 0.0100 | 3.17 | 47.24 | 47.24 | 0.5000 | 0.0262 |
| 4 | 27.73 | 1.0061 | 1.0019 | 2.3919 | 2.1977 | 7.345 | 0.1706 | -0.1363 | 0.0100 | 3.24 | 45.90 | 45.89 | 0.5000 | 0.0618 |
| 5 | 36.81 | 1.0061 | 1.0019 | 2.3919 | 2.1320 | 7.126 | 0.1638 | -0.1365 | 0.0100 | 3.38 | 44.34 | 44.33 | 0.5000 | 0.0675 |
| 6 | 46.19 | 1.0061 | 1.0019 | 2.3918 | 2.0643 | 6.899 | 0.1568 | -0.1364 | 0.0100 | 3.51 | 42.64 | 42.63 | 0.5000 | 0.0725 |
| 7 | 55.90 | 1.0061 | 1.0019 | 2.3918 | 1.9941 | 6.665 | 0.1496 | -0.1362 | 0.0100 | 3.66 | 40.73 | 40.72 | 0.5000 | 0.0799 |
| 8 | 65.97 | 1.0061 | 1.0019 | 2.3918 | 1.9213 | 6.421 | 0.1420 | -0.1360 | 0.0100 | 3.84 | 38.59 | 38.57 | 0.5000 | 0.0888 |
| 9 | 76.46 | 1.0061 | 1.0019 | 2.3918 | 1.8455 | 6.168 | 0.1340 | -0.1357 | 0.0100 | 4.04 | 36.15 | 36.13 | 0.5000 | 0.0996 |
| 10 | 87.41 | 1.0061 | 1.0019 | 2.3918 | 1.7663 | 5.903 | 0.1255 | -0.1355 | 0.0100 | 4.26 | 33.37 | 33.34 | 0.5000 | 0.1129 |
| 11 | 98.90 | 1.0061 | 1.0019 | 2.3918 | 1.6833 | 5.626 | 0.1164 | -0.1389 | 0.0100 | 4.51 | 30.17 | 30.12 | 0.5000 | 0.1265 |

Table 9.2. Continued.

** VALUES OF PARAMETERS ON STREAMLINES AT STATION. 7. WHICH IS THE INLET OF STATOR NUMBER. 1. OF STAGE NUMBER. 1 **

| STREAMLINE NO. | RADIUS (IN.) | AXIAL COORD. (IN.) | AXIAL VEL. (FT/SEC) | MERD. VEL. (FT/SEC) | TANG. VEL. (FT/SEC) | ABS. VEL. (FT/SEC) | ABS. MACH NO. | ABS.FLOW ANGLE (DEG) | STREAM. SLOPE (DEG) | STREAM. CURV. (1./IN.) | TOTAL PRESS. (PSIA) | TOTAL TEMP. (DEG.R.) | STATIC PRESS. (PSIA) | STATIC TEMP. (DEG.R.) |
|---|---|---|---|---|---|---|---|---|---|---|---|---|---|---|
| TIP | 8.000 | 3.470 | | | | | | | | | | | | |
| 1 | 7.951 | 3.512 | 91.79 | 91.79 | 54.60 | 106.80 | 0.0956 | 30.75 | -0.48 | 0.017 | 14.786 | 520.12 | 14.692 | 519.16 |
| 2 | 7.742 | 3.695 | 99.75 | 99.75 | 39.50 | 107.29 | 0.0961 | 21.60 | -0.15 | 0.016 | 14.786 | 519.67 | 14.691 | 518.71 |
| 3 | 7.537 | 3.861 | 101.33 | 101.33 | 37.00 | 107.88 | 0.0966 | 20.06 | 0.01 | 0.013 | 14.786 | 519.57 | 14.690 | 518.60 |
| 4 | 7.329 | 3.993 | 101.16 | 101.16 | 37.92 | 108.04 | 0.0968 | 20.55 | 0.11 | 0.010 | 14.786 | 519.57 | 14.689 | 518.60 |
| 5 | 7.113 | 4.085 | 100.96 | 100.96 | 39.18 | 108.29 | 0.0970 | 21.21 | 0.17 | 0.007 | 14.786 | 519.57 | 14.689 | 518.60 |
| 6 | 6.890 | 4.131 | 100.82 | 100.82 | 40.45 | 108.63 | 0.0973 | 21.86 | 0.21 | 0.005 | 14.786 | 519.57 | 14.688 | 518.59 |
| 7 | 6.660 | 4.128 | 100.72 | 100.72 | 41.85 | 109.07 | 0.0977 | 22.57 | 0.26 | 0.003 | 14.786 | 519.57 | 14.687 | 518.58 |
| 8 | 6.421 | 4.071 | 100.63 | 100.63 | 43.41 | 109.60 | 0.0982 | 23.34 | 0.31 | 0.001 | 14.786 | 519.57 | 14.686 | 518.57 |
| 9 | 6.171 | 3.953 | 100.56 | 100.57 | 45.17 | 110.24 | 0.0987 | 24.19 | 0.40 | -0.001 | 14.786 | 519.57 | 14.685 | 518.56 |
| 10 | 5.911 | 3.766 | 100.48 | 100.49 | 47.17 | 111.01 | 0.0994 | 25.15 | 0.55 | -0.004 | 14.786 | 519.57 | 14.684 | 518.55 |
| 11 | 5.635 | 3.499 | 100.41 | 100.42 | 49.50 | 111.96 | 0.1003 | 26.24 | 0.84 | -0.010 | 14.786 | 519.57 | 14.682 | 518.53 |
| HUB | 5.600 | 3.464 | | | | | | | | | | | | |

| STREAMLINE NO. | R/RTIP | FLOW COEF. | REL.FLOW ANGLE (DEG) | L.E.RAD. /CHORD | MAX.TH. /CHORD | MAX.TH. PT.LOC. /CHORD | TRAN.PT. LOCATION /CHORD | SEGMENT IN/OUT TURN.RATE | LAYOUT CONE ANG. (DEG) |
|---|---|---|---|---|---|---|---|---|---|
| TIP | 1.0000 | | | | | | | | |
| 1 | 0.9939 | 0.5478 | 50.64 | 0.0100 | 0.1000 | 0.5000 | 0.5000 | 1.0000 | 0.25 |
| 2 | 0.9678 | 0.5953 | 50.98 | 0.0100 | 0.0964 | 0.5000 | 0.5000 | 1.0000 | 0.41 |
| 3 | 0.9422 | 0.6047 | 50.02 | 0.0100 | 0.0929 | 0.5000 | 0.5000 | 1.0000 | 0.40 |
| 4 | 0.9161 | 0.6037 | 48.80 | 0.0100 | 0.0892 | 0.5000 | 0.5000 | 1.0000 | 0.36 |
| 5 | 0.8892 | 0.6025 | 47.40 | 0.0100 | 0.0855 | 0.5000 | 0.5000 | 1.0000 | 0.33 |
| 6 | 0.8614 | 0.6016 | 45.85 | 0.0100 | 0.0817 | 0.5000 | 0.5000 | 1.0000 | 0.30 |
| 7 | 0.8325 | 0.6010 | 44.11 | 0.0100 | 0.0777 | 0.5000 | 0.5000 | 1.0000 | 0.28 |
| 8 | 0.8026 | 0.6005 | 42.14 | 0.0100 | 0.0736 | 0.5000 | 0.5000 | 1.0000 | 0.27 |
| 9 | 0.7715 | 0.6001 | 39.90 | 0.0100 | 0.0693 | 0.5000 | 0.5000 | 1.0000 | 0.27 |
| 10 | 0.7389 | 0.5996 | 37.33 | 0.0100 | 0.0647 | 0.5000 | 0.5000 | 1.0000 | 0.28 |
| 11 | 0.7045 | 0.5992 | 34.31 | 0.0100 | 0.0600 | 0.5000 | 0.5000 | 1.0000 | 0.31 |
| HUB | 0.7000 | | | | | | | | |

| | | --- INLET STREAMLINE --- | | | ++++++++++ LAYOUT CONE ++++++++++ | | | | | | | | |
|---|---|---|---|---|---|---|---|---|---|---|---|---|---|
| STREAMLINE NO. | PCT. SPAN | INC. ANGLE (DEG) | S.S.INC. ANGLE (DEG) | IN.BLADE ANGLE (DEG) | IN.BLADE ANGLE (DEG) | TRAN.PT. BL.ANGLE (DEG) | BLD.SET ANGLE (DEG) | 1ST SEG. S.S.CAM. (DEG) | MACH NO. AT SHOCK LOCATION | SH.LOC. AS FRACT OF S.S. | COV.CHAN. AS FRACT OF S.S. | MIN.CHK. AREA MARGIN | MIN.CHK. PT.LOC.IN COV.CHAN. | L.E.EDGE CIR.CENT. R*DØ/DR |
| 1 | 2.04 | 2.07 | -6.95 | 28.68 | 28.05 | 11.04 | 11.05 | 26.02 | 0.1187 | 0.2099 | 0.7453 | 4.5402 | 0.3568 | -1.1351 |
| 2 | 10.74 | 1.47 | -7.27 | 20.14 | 19.97 | 7.88 | 7.89 | 20.82 | 0.0961 | 0.1648 | 0.8005 | 4.3192 | 0.4151 | -0.3404 |
| 3 | 19.26 | 1.21 | -7.14 | 18.85 | 18.90 | 7.44 | 7.45 | 19.80 | 0.0966 | 0.1625 | 0.8031 | 4.3750 | 0.3927 | 0.1472 |
| 4 | 27.96 | 1.09 | -6.84 | 19.46 | 19.50 | 7.65 | 7.65 | 19.79 | 0.0968 | 0.1708 | 0.7923 | 4.4434 | 0.3758 | 0.2085 |
| 5 | 36.94 | 1.04 | -6.46 | 20.17 | 20.19 | 7.90 | 7.91 | 19.79 | 0.1022 | 0.1776 | 0.7837 | 4.4887 | 0.3616 | 0.1689 |
| 6 | 46.21 | 1.07 | -5.99 | 20.79 | 20.80 | 8.15 | 8.16 | 19.71 | 0.1060 | 0.1810 | 0.7797 | 4.5146 | 0.3485 | 0.1199 |
| 7 | 55.82 | 1.20 | -5.41 | 21.37 | 21.37 | 8.42 | 8.42 | 19.55 | 0.1090 | 0.1805 | 0.7810 | 4.5209 | 0.3376 | 0.0723 |
| 8 | 65.79 | 1.45 | -4.68 | 21.88 | 21.88 | 8.70 | 8.71 | 19.31 | 0.1117 | 0.1757 | 0.7881 | 4.5079 | 0.3305 | 0.0309 |
| 9 | 76.18 | 1.85 | -3.79 | 22.34 | 22.33 | 9.00 | 9.00 | 18.98 | 0.1142 | 0.1665 | 0.8008 | 4.4749 | 0.3288 | 0.0042 |
| 10 | 87.04 | 2.41 | -2.72 | 22.74 | 22.74 | 9.30 | 9.30 | 18.56 | 0.1170 | 0.1536 | 0.8181 | 4.4217 | 0.3331 | 0.0025 |
| 11 | 98.48 | 3.12 | -1.47 | 23.12 | 23.11 | 9.62 | 9.62 | 18.08 | 0.1202 | 0.1379 | 0.8386 | 4.3501 | 0.3386 | 0.0256 |

Table 9.2. Continued.

** VALUES OF PARAMETERS ON STREAMLINES AT STATION. 8. WHICH IS THE OUTLET OF STATOR NUMBER. 1. OF STAGE NUMBER. 1 **

| STREAMLINE NO. | RADIUS (IN.) | AXIAL COORD. (IN.) | AXIAL VEL. (FT/SEC) | MERD. VEL. (FT/SEC) | TANG. VEL. (FT/SEC) | ABS. VEL. (FT/SEC) | ABS. MACH NO. | ABS.FLOW ANGLE (DEG) | STREAM. SLOPE (DEG) | STREAM. CURV. (1./IN.) | TOTAL PRESS. (PSIA) | TOTAL TEMP. (DEG.R.) | STATIC PRESS. (PSIA) | STATIC TEMP. (DEG.R.) |
|---|---|---|---|---|---|---|---|---|---|---|---|---|---|---|
| TIP | 8.000 | 6.491 | | | | | | | | | | | | |
| 1 | 7.963 | 6.490 | 99.05 | 99.05 | 0.0 | 99.05 | 0.0887 | 0.0 | 0.24 | -0.009 | 14.784 | 520.12 | 14.703 | 519.30 |
| 2 | 7.762 | 6.488 | 99.50 | 99.50 | 0.0 | 99.50 | 0.0891 | 0.0 | 0.31 | -0.010 | 14.784 | 519.67 | 14.703 | 518.84 |
| 3 | 7.556 | 6.486 | 99.74 | 99.75 | 0.0 | 99.75 | 0.0893 | 0.0 | 0.27 | -0.009 | 14.784 | 519.57 | 14.702 | 518.74 |
| 4 | 7.344 | 6.485 | 99.90 | 99.90 | 0.0 | 99.90 | 0.0895 | 0.0 | 0.22 | -0.008 | 14.784 | 519.57 | 14.702 | 518.74 |
| 5 | 7.127 | 6.484 | 100.02 | 100.02 | 0.0 | 100.02 | 0.0896 | 0.0 | 0.18 | -0.007 | 14.784 | 519.57 | 14.702 | 518.74 |
| 6 | 6.903 | 6.484 | 100.12 | 100.12 | 0.0 | 100.12 | 0.0897 | 0.0 | 0.15 | -0.006 | 14.784 | 519.57 | 14.701 | 518.74 |
| 7 | 6.671 | 6.484 | 100.19 | 100.19 | 0.0 | 100.19 | 0.0897 | 0.0 | 0.12 | -0.005 | 14.784 | 519.57 | 14.701 | 518.74 |
| 8 | 6.432 | 6.484 | 100.23 | 100.23 | 0.0 | 100.23 | 0.0898 | 0.0 | 0.10 | -0.004 | 14.784 | 519.57 | 14.701 | 518.74 |
| 9 | 6.183 | 6.486 | 100.22 | 100.22 | 0.0 | 100.22 | 0.0897 | 0.0 | 0.08 | -0.003 | 14.784 | 519.57 | 14.701 | 518.74 |
| 10 | 5.924 | 6.488 | 100.13 | 100.13 | 0.0 | 100.13 | 0.0897 | 0.0 | 0.07 | -0.002 | 14.784 | 519.57 | 14.701 | 518.74 |
| 11 | 5.652 | 6.490 | 99.91 | 99.91 | 0.0 | 99.91 | 0.0899 | 0.0 | 0.13 | 0.002 | 14.783 | 519.57 | 14.701 | 518.74 |
| HUB | 5.600 | 6.491 | | | | | | | | | | | | |

| STREAMLINE NO. | R/RTIP | FLOW COEF. | HEAD COEF. | IDEAL HEAD COEF. | STATOR PO.RATIO | STAGE PO.RATIO | STAGE AD.EFF. | DIFFUSION FACTOR | STATOR LOSS COEF. | SHOCK LOSS COEF. | ELEMENT SOLIDITY | AERO. CHORD (IN.) | MEAN SPACING (IN.) |
|---|---|---|---|---|---|---|---|---|---|---|---|---|---|
| TIP | 1.0000 | | | | | | | | | | | | |
| 1 | 0.9954 | 0.5911 | 0.1892 | 0.3238 | 0.9999 | 1.0060 | 0.5843 | 0.2129 | 0.0201 | 0.0 | 1.8200 | 3.0331 | 1.6665 |
| 2 | 0.9702 | 0.5938 | 0.1903 | 0.2281 | 0.9999 | 1.0060 | 0.8345 | 0.1785 | 0.0144 | 0.0 | 1.7365 | 2.8192 | 1.6235 |
| 3 | 0.9444 | 0.5952 | 0.1904 | 0.2080 | 0.9999 | 1.0060 | 0.9156 | 0.1776 | 0.0138 | 0.0 | 1.6747 | 2.6470 | 1.5805 |
| 4 | 0.9180 | 0.5961 | 0.1903 | 0.2073 | 0.9999 | 1.0060 | 0.9183 | 0.1825 | 0.0141 | 0.0 | 1.6360 | 2.5138 | 1.5365 |
| 5 | 0.8908 | 0.5969 | 0.1902 | 0.2078 | 0.9999 | 1.0060 | 0.9152 | 0.1876 | 0.0146 | 0.0 | 1.6244 | 2.4222 | 1.4912 |
| 6 | 0.8628 | 0.5975 | 0.1901 | 0.2079 | 0.9999 | 1.0060 | 0.9143 | 0.1914 | 0.0153 | 0.0 | 1.6452 | 2.3764 | 1.4444 |
| 7 | 0.8339 | 0.5979 | 0.1898 | 0.2079 | 0.9999 | 1.0060 | 0.9132 | 0.1938 | 0.0162 | 0.0 | 1.7054 | 2.3808 | 1.3961 |
| 8 | 0.8040 | 0.5981 | 0.1896 | 0.2079 | 0.9999 | 1.0060 | 0.9118 | 0.1946 | 0.0173 | 0.0 | 1.8137 | 2.4411 | 1.3459 |
| 9 | 0.7729 | 0.5981 | 0.1892 | 0.2079 | 0.9999 | 1.0060 | 0.9100 | 0.1942 | 0.0189 | 0.0 | 1.9818 | 2.5639 | 1.2937 |
| 10 | 0.7404 | 0.5975 | 0.1887 | 0.2079 | 0.9999 | 1.0060 | 0.9073 | 0.1933 | 0.0210 | 0.0 | 2.2252 | 2.7576 | 1.2393 |
| 11 | 0.7065 | 0.5962 | 0.1878 | 0.2081 | 0.9998 | 1.0059 | 0.9028 | 0.1937 | 0.0243 | 0.0 | 2.5659 | 3.0331 | 1.1821 |
| HUB | 0.7000 | | | | | | | | | | | | |

| STREAMLINE NO. | PCT. SPAN | LOCAL BLADE FORCES RADIUS (IN.) | FOR.AXIAL (LBS/IN) | TANG. (LBS/IN) | --- OUTLET STREAMLINE --- T.E.RAD. /CHORD | DEV. ANGLE (DEG) | OUT.BLADE ANGLE (DEG) | ++ LAYOUT CONE +++ OUT.BLADE ANGLE (DEG) | MAX.CAMB. PT.LOC. /CHORD | T.E.EDGE CIR.CENT R*DO/DR |
|---|---|---|---|---|---|---|---|---|---|---|
| 1 | 1.53 | 7.957 | 0.0380 | 0.1447 | 0.0100 | 5.96 | -5.96 | -5.96 | 0.5000 | 0.0 |
| 2 | 9.93 | 7.752 | 0.0186 | 0.1047 | 0.0100 | 4.21 | -4.21 | -4.21 | 0.5000 | 0.0 |
| 3 | 18.52 | 7.547 | 0.0157 | 0.0969 | 0.0100 | 4.01 | -4.01 | -4.01 | 0.5000 | 0.0 |
| 4 | 27.33 | 7.336 | 0.0161 | 0.0967 | 0.0100 | 4.21 | -4.21 | -4.21 | 0.5000 | 0.0 |
| 5 | 36.39 | 7.120 | 0.0167 | 0.0969 | 0.0100 | 4.39 | -4.39 | -4.39 | 0.5000 | 0.0 |
| 6 | 45.72 | 6.897 | 0.0173 | 0.0969 | 0.0100 | 4.50 | -4.50 | -4.50 | 0.5000 | 0.0 |
| 7 | 55.36 | 6.666 | 0.0179 | 0.0968 | 0.0100 | 4.53 | -4.53 | -4.53 | 0.5000 | 0.0 |
| 8 | 65.34 | 6.426 | 0.0186 | 0.0967 | 0.0100 | 4.48 | -4.48 | -4.48 | 0.5000 | 0.0 |
| 9 | 75.70 | 6.177 | 0.0193 | 0.0966 | 0.0100 | 4.34 | -4.34 | -4.34 | 0.5000 | 0.0 |
| 10 | 86.51 | 5.917 | 0.0201 | 0.0963 | 0.0100 | 4.14 | -4.14 | -4.14 | 0.5000 | 0.0 |
| 11 | 97.82 | 5.644 | 0.0209 | 0.0986 | 0.0100 | 3.88 | -3.88 | -3.88 | 0.5000 | 0.0 |

Table 9.2. Continued.

** VALUES OF PARAMETERS ON STREAMLINES AT STATION. 9. WHICH IS THE INLET OF ROTOR NUMBER. 2 **

| STREAMLINE NO. | RADIUS (IN.) | AXIAL COORD. (IN.) | AXIAL VEL. (FT/SEC) | MERD. VEL. (FT/SEC) | TANG. VEL. (FT/SEC) | ABS. VEL. (FT/SEC) | ABS. MACH NO. | ABS.FLOW ANGLE (DEG) | STREAM. SLOPE (DEG) | STREAM. CURV. (1./IN.) | TOTAL PRESS. (PSIA) | TOTAL TEMP. (DEG.R.) | STATIC PRESS. (PSIA) | STATIC TEMP. (DEG.R.) |
|---|---|---|---|---|---|---|---|---|---|---|---|---|---|---|
| TIP | 8.000 | 7.581 | | | | | | | | | | | | |
| 1 | 7.963 | 7.578 | 98.90 | 98.91 | 0.0 | 98.91 | 0.0885 | 0.0 | -0.27 | -0.008 | 14.784 | 520.12 | 14.703 | 519.30 |
| 2 | 7.761 | 7.563 | 99.38 | 99.38 | 0.0 | 99.38 | 0.0890 | 0.0 | -0.39 | -0.012 | 14.784 | 519.67 | 14.703 | 518.84 |
| 3 | 7.555 | 7.547 | 99.67 | 99.67 | 0.0 | 99.67 | 0.0893 | 0.0 | -0.36 | -0.011 | 14.784 | 519.57 | 14.702 | 518.75 |
| 4 | 7.344 | 7.530 | 99.86 | 99.86 | 0.0 | 99.86 | 0.0894 | 0.0 | -0.31 | -0.010 | 14.784 | 519.57 | 14.702 | 518.74 |
| 5 | 7.126 | 7.513 | 100.02 | 100.02 | 0.0 | 100.02 | 0.0896 | 0.0 | -0.25 | -0.008 | 14.784 | 519.57 | 14.702 | 518.74 |
| 6 | 6.902 | 7.494 | 100.12 | 100.13 | 0.0 | 100.13 | 0.0897 | 0.0 | -0.21 | -0.006 | 14.784 | 519.57 | 14.701 | 518.74 |
| 7 | 6.671 | 7.474 | 100.19 | 100.19 | 0.0 | 100.19 | 0.0897 | 0.0 | -0.17 | -0.005 | 14.784 | 519.57 | 14.701 | 518.74 |
| 8 | 6.431 | 7.453 | 100.22 | 100.22 | 0.0 | 100.22 | 0.0897 | 0.0 | -0.15 | -0.004 | 14.784 | 519.57 | 14.701 | 518.74 |
| 9 | 6.183 | 7.430 | 100.23 | 100.23 | 0.0 | 100.23 | 0.0898 | 0.0 | -0.14 | -0.005 | 14.784 | 519.57 | 14.701 | 518.74 |
| 10 | 5.923 | 7.404 | 100.23 | 100.23 | 0.0 | 100.23 | 0.0898 | 0.0 | -0.16 | -0.007 | 14.784 | 519.57 | 14.701 | 518.74 |
| 11 | 5.652 | 7.376 | 100.33 | 100.33 | 0.0 | 100.33 | 0.0898 | 0.0 | -0.23 | -0.016 | 14.783 | 519.57 | 14.700 | 518.73 |
| HUB | 5.600 | 7.371 | | | | | | | | | | | | |

| STREAMLINE NO. | R/RTIP | REL.FLOW ANGLE (DEG) | REL. TANG.VEL. (FT/SEC) | REL. VEL. (FT/SEC) | REL.MACH NUMBER | WHEEL SPEED (FT/SEC) | FLOW COEF. | L.E.RAD. /CHORD | MAX.TH. /CHORD | MAX.TH. PT.LOC. /CHORD | TRAN.PT. LOCATION /CHORD | SEGMENT IN/OUT TURN.RATE | LAYOUT CONE ANG. (DEG) |
|---|---|---|---|---|---|---|---|---|---|---|---|---|---|
| TIP | 1.0000 | | | | | 167.55 | | | | | | | |
| 1 | 0.9954 | 59.33 | 166.78 | 193.90 | 0.1735 | 166.78 | 0.5903 | 0.0100 | 0.0600 | 0.5000 | 0.5000 | 1.0000 | -0.72 |
| 2 | 0.9702 | 58.56 | 162.55 | 190.53 | 0.1706 | 162.55 | 0.5931 | 0.0100 | 0.0635 | 0.5000 | 0.5000 | 1.0000 | -0.94 |
| 3 | 0.9444 | 57.79 | 158.23 | 187.01 | 0.1675 | 158.23 | 0.5949 | 0.0100 | 0.0671 | 0.5000 | 0.5000 | 1.0000 | -0.83 |
| 4 | 0.9180 | 57.00 | 153.80 | 183.38 | 0.1642 | 153.80 | 0.5960 | 0.0100 | 0.0707 | 0.5000 | 0.5000 | 1.0000 | -0.68 |
| 5 | 0.8908 | 56.17 | 149.25 | 179.66 | 0.1609 | 149.25 | 0.5969 | 0.0100 | 0.0745 | 0.5000 | 0.5000 | 1.0000 | -0.53 |
| 6 | 0.8628 | 55.29 | 144.56 | 175.85 | 0.1575 | 144.56 | 0.5976 | 0.0100 | 0.0784 | 0.5000 | 0.5000 | 1.0000 | -0.40 |
| 7 | 0.8339 | 54.35 | 139.71 | 171.93 | 0.1540 | 139.71 | 0.5980 | 0.0100 | 0.0824 | 0.5000 | 0.5000 | 1.0000 | -0.28 |
| 8 | 0.8039 | 53.35 | 134.70 | 167.89 | 0.1503 | 134.70 | 0.5982 | 0.0100 | 0.0865 | 0.5000 | 0.5000 | 1.0000 | -0.17 |
| 9 | 0.7725 | 52.26 | 129.49 | 163.74 | 0.1466 | 129.49 | 0.5982 | 0.0100 | 0.0908 | 0.5000 | 0.5000 | 1.0000 | -0.07 |
| 10 | 0.7404 | 51.06 | 124.06 | 159.49 | 0.1428 | 124.06 | 0.5982 | 0.0100 | 0.0953 | 0.5000 | 0.5000 | 1.0000 | -0.00 |
| 11 | 0.7066 | 49.72 | 118.38 | 155.18 | 0.1390 | 118.38 | 0.5988 | 0.0100 | 0.1000 | 0.5000 | 0.5000 | 1.0000 | 0.01 |
| HUB | 0.7000 | | | | | | | | | | | | |

--- INLET STREAMLINE --- ++++++++++++++++++++++++++++++++++++ LAYOUT CONE ++++++++++++++++++++++++++++++++++++++++

| STREAMLINE NO. | PCT. SPAN | INC. ANGLE (DEG) | S.S.INC. ANGLE (DEG) | IN.BLADE ANGLE (DEG) | IN.BLADE ANGLE (DEG) | TRAN.PT. BL.ANGLE (DEG) | BLD.SET ANGLE (DEG) | 1ST SEG. S.S.CAM. (DEG) | MACH NO. AT SHOCK LOCATION | SH.LOC. AS FRACT OF S.S. | COV.CHAN. AS FRACT OF S.S. | MIN.CHK. AREA MARGIN | MIN.CHK. PT.LOC.IN COV.CHAN. | L.E.EDGE CIR.CENT. R*DB/DR |
|---|---|---|---|---|---|---|---|---|---|---|---|---|---|---|
| 1 | 1.54 | -1.91 | -6.55 | 61.24 | 61.24 | 52.60 | 52.60 | 13.28 | 0.2749 | 0.7883 | 0.2117 | 2.6871 | 0.0 | -0.0386 |
| 2 | 9.94 | -0.02 | -5.08 | 58.58 | 58.58 | 52.53 | 52.52 | 11.12 | 0.2556 | 0.7619 | 0.2381 | 2.6616 | 0.0 | -0.0409 |
| 3 | 18.54 | 0.51 | -4.97 | 57.28 | 57.29 | 51.68 | 51.66 | 11.08 | 0.2474 | 0.7318 | 0.2682 | 2.6672 | 0.0 | -0.0480 |
| 4 | 27.35 | 0.63 | -5.27 | 56.38 | 56.38 | 50.51 | 50.50 | 11.78 | 0.2425 | 0.7002 | 0.2998 | 2.7131 | 0.0 | -0.0518 |
| 5 | 36.41 | 0.73 | -5.61 | 55.45 | 55.45 | 49.24 | 49.23 | 12.55 | 0.2372 | 0.6681 | 0.3319 | 2.7662 | 0.0 | -0.0525 |
| 6 | 45.74 | 0.83 | -5.94 | 54.46 | 54.46 | 47.86 | 47.86 | 13.38 | 0.2316 | 0.6354 | 0.3646 | 2.8223 | 0.0 | -0.0547 |
| 7 | 55.38 | 0.94 | -6.29 | 53.41 | 53.42 | 46.36 | 46.36 | 14.28 | 0.2257 | 0.6019 | 0.3981 | 2.8820 | 0.0 | -0.0581 |
| 8 | 65.36 | 1.06 | -6.64 | 52.29 | 52.29 | 44.70 | 44.70 | 15.29 | 0.2195 | 0.5677 | 0.4323 | 2.9464 | 0.0 | -0.0629 |
| 9 | 75.72 | 1.18 | -7.00 | 51.08 | 51.08 | 42.86 | 42.86 | 16.40 | 0.2128 | 0.5326 | 0.4674 | 3.0163 | 0.0 | -0.0697 |
| 10 | 86.52 | 1.32 | -7.36 | 49.74 | 49.74 | 40.77 | 40.77 | 17.65 | 0.2058 | 0.4963 | 0.5037 | 3.0933 | 0.0052 | -0.0799 |
| 11 | 97.81 | 1.48 | -7.72 | 48.24 | 48.23 | 38.37 | 38.37 | 19.06 | 0.1984 | 0.4586 | 0.5414 | 3.1695 | 0.0557 | -0.0917 |

Table 9.2. Continued.

** VALUES OF PARAMETERS ON STREAMLINES AT STATION, 10, WHICH IS THE OUTLET OF ROTOR NUMBER. 2 **

| STREAMLINE NO. | RADIUS (IN.) | AXIAL COORD. (IN.) | AXIAL VEL. (FT/SEC) | MERD. VEL. (FT/SEC) | TANG. VEL. (FT/SEC) | ABS. VEL. (FT/SEC) | ABS. MACH NO. | ABS.FLOW ANGLE (DEG) | STREAM. SLOPE (DEG) | STREAM. CURV. (1./IN.) | TOTAL PRESS. (PSIA) | TOTAL TEMP. (DEG.R.) | STATIC PRESS. (PSIA) | STATIC TEMP. (DEG.R.) |
|---|---|---|---|---|---|---|---|---|---|---|---|---|---|---|
| TIP | 8.000 | 9.050 | | | | | | | | | | | | |
| 1 | 7.945 | 9.046 | 92.20 | 92.22 | 54.42 | 107.08 | 0.0957 | 30.54 | -1.30 | -0.017 | 14.879 | 521.62 | 14.784 | 520.67 |
| 2 | 7.737 | 9.033 | 99.45 | 99.47 | 41.45 | 107.76 | 0.0964 | 22.62 | -1.14 | -0.006 | 14.879 | 520.79 | 14.783 | 519.82 |
| 3 | 7.533 | 9.045 | 101.44 | 101.45 | 38.80 | 108.62 | 0.0972 | 20.93 | -0.90 | -0.001 | 14.879 | 520.59 | 14.781 | 519.61 |
| 4 | 7.325 | 9.065 | 101.60 | 101.60 | 39.84 | 109.13 | 0.0976 | 21.41 | -0.66 | 0.001 | 14.879 | 520.59 | 14.780 | 519.60 |
| 5 | 7.112 | 9.087 | 101.55 | 101.55 | 41.13 | 109.56 | 0.0980 | 22.05 | -0.46 | 0.003 | 14.879 | 520.59 | 14.779 | 519.59 |
| 6 | 6.891 | 9.111 | 101.48 | 101.48 | 42.49 | 110.02 | 0.0984 | 22.72 | -0.26 | 0.005 | 14.879 | 520.59 | 14.779 | 519.59 |
| 7 | 6.663 | 9.136 | 101.36 | 101.36 | 44.00 | 110.50 | 0.0989 | 23.47 | -0.08 | 0.007 | 14.879 | 520.60 | 14.778 | 519.58 |
| 8 | 6.426 | 9.163 | 101.16 | 101.16 | 45.70 | 111.01 | 0.0993 | 24.31 | 0.13 | 0.010 | 14.879 | 520.60 | 14.777 | 519.57 |
| 9 | 6.180 | 9.192 | 100.86 | 100.86 | 47.62 | 111.54 | 0.0998 | 25.27 | 0.37 | 0.015 | 14.879 | 520.60 | 14.776 | 519.56 |
| 10 | 5.923 | 9.223 | 100.34 | 100.35 | 49.85 | 112.05 | 0.1003 | 26.42 | 0.72 | 0.024 | 14.879 | 520.60 | 14.775 | 519.56 |
| 11 | 5.653 | 9.258 | 99.35 | 99.37 | 52.52 | 112.40 | 0.1006 | 27.86 | 1.34 | 0.045 | 14.879 | 520.61 | 14.774 | 519.56 |
| HUB | 5.600 | 9.264 | | | | | | | | | | | | |

| STREAMLINE NO. | R/RTIP | REL.FLOW ANGLE (DEG) | REL. TANG.VEL. (FT/SEC) | REL. VEL. (FT/SEC) | REL.MACH NUMBER | WHEEL SPEED (FT/SEC) | FLOW COEF. | HEAD COEF. | IDEAL HEAD COEF. | ADIAB. EFF. | DIFFUSION FACTOR | LOSS COEF. | SHOCK LOSS COEF. | ELEMENT SOLIDITY |
|---|---|---|---|---|---|---|---|---|---|---|---|---|---|---|
| TIP | 1.0000 | | | | | | | | | | | | | |
| 1 | 0.9931 | 50.53 | 111.97 | 145.06 | 0.1297 | 166.39 | 0.5503 | 0.2043 | 0.3225 | 0.6335 | 0.3917 | 0.1779 | 0.0 | 1.0027 |
| 2 | 0.9672 | 50.43 | 120.59 | 156.32 | 0.1398 | 162.05 | 0.5935 | 0.2030 | 0.2393 | 0.8484 | 0.2851 | 0.0566 | 0.0 | 1.0292 |
| 3 | 0.9417 | 49.55 | 118.98 | 156.36 | 0.1399 | 157.78 | 0.6054 | 0.2029 | 0.2181 | 0.9303 | 0.2619 | 0.0246 | 0.0 | 1.0572 |
| 4 | 0.9157 | 48.19 | 113.59 | 152.40 | 0.1364 | 153.42 | 0.6064 | 0.2030 | 0.2177 | 0.9322 | 0.2687 | 0.0248 | 0.0 | 1.0874 |
| 5 | 0.8890 | 46.71 | 107.81 | 148.11 | 0.1325 | 148.94 | 0.6061 | 0.2031 | 0.2182 | 0.9306 | 0.2777 | 0.0265 | 0.0 | 1.1203 |
| 6 | 0.8614 | 45.10 | 101.83 | 143.76 | 0.1286 | 144.32 | 0.6057 | 0.2033 | 0.2185 | 0.9304 | 0.2869 | 0.0278 | 0.0 | 1.1564 |
| 7 | 0.8329 | 43.31 | 95.54 | 139.29 | 0.1246 | 139.55 | 0.6049 | 0.2035 | 0.2187 | 0.9302 | 0.2968 | 0.0292 | 0.0 | 1.1962 |
| 8 | 0.8033 | 41.31 | 88.90 | 134.67 | 0.1205 | 134.59 | 0.6038 | 0.2037 | 0.2191 | 0.9300 | 0.3075 | 0.0308 | 0.0 | 1.2405 |
| 9 | 0.7725 | 39.05 | 81.82 | 129.87 | 0.1162 | 129.44 | 0.6020 | 0.2041 | 0.2196 | 0.9296 | 0.3195 | 0.0325 | 0.0 | 1.2902 |
| 10 | 0.7404 | 36.48 | 74.21 | 124.81 | 0.1117 | 124.06 | 0.5989 | 0.2047 | 0.2203 | 0.9291 | 0.3335 | 0.0347 | 0.0 | 1.3464 |
| 11 | 0.7066 | 33.54 | 65.87 | 119.22 | 0.1067 | 118.39 | 0.5929 | 0.2055 | 0.2215 | 0.9277 | 0.3516 | 0.0375 | 0.0 | 1.4109 |
| HUB | 0.7000 | | | | | | | | | | | | | |

| STREAMLINE NO. | PCT. SPAN | PRESS. RATIO | TEMP. RATIO | AERO. CHORD (IN.) | MEAN SPACING (IN.) | LOCAL BLADE FORCES RADIUS (IN.) | LOCAL BLADE FORCES FOR.AXIAL (LBS/IN) | LOCAL BLADE FORCES TANG. (LBS/IN) | --- OUTLET STREAMLINE --- T.E.RAD. /CHORD | DEV. ANGLE (DEG) | OUT.BLADE ANGLE (DEG) | ++ LAYOUT CONE +++ OUT.BLADE ANGLE (DEG) | MAX.CAMB. PT.LOC. /CHORD | T.E.EDGE CIR.CENT R*D0/DR |
|---|---|---|---|---|---|---|---|---|---|---|---|---|---|---|
| 1 | 2.31 | 1.0064 | 1.0029 | 2.3862 | 2.3798 | 7.954 | 0.1674 | -0.2067 | 0.0100 | 6.48 | 44.04 | 43.96 | 0.5000 | -0.2969 |
| 2 | 10.95 | 1.0064 | 1.0022 | 2.3862 | 2.3186 | 7.749 | 0.1859 | -0.1573 | 0.0100 | 4.00 | 46.48 | 46.47 | 0.5000 | -0.1022 |
| 3 | 19.44 | 1.0064 | 1.0020 | 2.3862 | 2.2572 | 7.544 | 0.1848 | -0.1454 | 0.0100 | 3.47 | 46.08 | 46.08 | 0.5000 | 0.0335 |
| 4 | 28.11 | 1.0064 | 1.0020 | 2.3862 | 2.1945 | 7.335 | 0.1782 | -0.1456 | 0.0100 | 3.56 | 44.63 | 44.63 | 0.5000 | 0.0718 |
| 5 | 37.02 | 1.0064 | 1.0020 | 2.3862 | 2.1300 | 7.119 | 0.1712 | -0.1460 | 0.0100 | 3.69 | 43.03 | 43.02 | 0.5000 | 0.0760 |
| 6 | 46.21 | 1.0064 | 1.0020 | 2.3862 | 2.0634 | 6.897 | 0.1640 | -0.1461 | 0.0100 | 3.83 | 41.27 | 41.26 | 0.5000 | 0.0810 |
| 7 | 55.72 | 1.0064 | 1.0020 | 2.3861 | 1.9947 | 6.667 | 0.1566 | -0.1463 | 0.0100 | 3.99 | 39.32 | 39.31 | 0.5000 | 0.0878 |
| 8 | 65.57 | 1.0064 | 1.0020 | 2.3861 | 1.9235 | 6.429 | 0.1488 | -0.1464 | 0.0100 | 4.17 | 37.13 | 37.12 | 0.5000 | 0.0962 |
| 9 | 75.82 | 1.0064 | 1.0020 | 2.3861 | 1.8495 | 6.181 | 0.1407 | -0.1465 | 0.0100 | 4.36 | 34.67 | 34.64 | 0.5000 | 0.1069 |
| 10 | 86.54 | 1.0065 | 1.0020 | 2.3861 | 1.7722 | 5.923 | 0.1320 | -0.1466 | 0.0100 | 4.62 | 31.86 | 31.80 | 0.5000 | 0.1209 |
| 11 | 97.81 | 1.0065 | 1.0020 | 2.3861 | 1.6912 | 5.653 | 0.1227 | -0.1507 | 0.0100 | 4.90 | 28.64 | 28.51 | 0.5000 | 0.1358 |

Table 9.2. Continued.

** VALUES OF PARAMETERS ON STREAMLINES AT STATION, 11, WHICH IS THE INLET OF STATOR NUMBER, 1, OF STAGE NUMBER, 2 **

| STREAMLINE NO. | RADIUS (IN.) | AXIAL COORD. (IN.) | AXIAL VEL. (FT/SEC) | MERD. VEL. (FT/SEC) | TANG. VEL. (FT/SEC) | ABS. VEL. (FT/SEC) | ABS. MACH NO. | ABS.FLOW ANGLE (DEG) | STREAM. SLOPE (DEG) | STREAM. CURV. (1./IN.) | TOTAL PRESS. (PSIA) | TOTAL TEMP. (DEG.R.) | STATIC PRESS. (PSIA) | STATIC TEMP. (DEG.R.) |
|---|---|---|---|---|---|---|---|---|---|---|---|---|---|---|
| TIP | 8.000 | 9.885 | | | | | | | | | | | | |
| 1 | 7.924 | 9.956 | 96.11 | 96.12 | 54.56 | 110.53 | 0.0988 | 29.58 | -0.92 | 0.031 | 14.879 | 521.62 | 14.778 | 520.61 |
| 2 | 7.721 | 10.145 | 102.55 | 102.55 | 41.54 | 110.64 | 0.0990 | 22.05 | -0.48 | 0.026 | 14.879 | 520.79 | 14.777 | 519.77 |
| 3 | 7.521 | 10.311 | 103.97 | 103.97 | 38.86 | 110.99 | 0.0993 | 20.49 | -0.21 | 0.020 | 14.879 | 520.59 | 14.777 | 519.57 |
| 4 | 7.317 | 10.442 | 103.75 | 103.75 | 39.87 | 111.15 | 0.0995 | 21.02 | -0.03 | 0.014 | 14.879 | 520.59 | 14.777 | 519.56 |
| 5 | 7.108 | 10.533 | 103.48 | 103.48 | 41.15 | 111.36 | 0.0996 | 21.68 | 0.08 | 0.010 | 14.879 | 520.59 | 14.776 | 519.56 |
| 6 | 6.891 | 10.579 | 103.32 | 103.32 | 42.48 | 111.72 | 0.1000 | 22.35 | 0.17 | 0.005 | 14.879 | 520.59 | 14.775 | 519.55 |
| 7 | 6.667 | 10.575 | 103.22 | 103.22 | 43.97 | 112.20 | 0.1004 | 23.07 | 0.25 | 0.001 | 14.879 | 520.60 | 14.775 | 519.55 |
| 8 | 6.435 | 10.519 | 103.17 | 103.17 | 45.63 | 112.81 | 0.1009 | 23.86 | 0.36 | -0.004 | 14.879 | 520.60 | 14.773 | 519.54 |
| 9 | 6.194 | 10.401 | 103.18 | 103.18 | 47.51 | 113.59 | 0.1016 | 24.73 | 0.55 | -0.010 | 14.879 | 520.60 | 14.772 | 519.52 |
| 10 | 5.941 | 10.215 | 103.18 | 103.19 | 49.70 | 114.54 | 0.1025 | 25.71 | 0.89 | -0.018 | 14.879 | 520.60 | 14.770 | 519.51 |
| 11 | 5.674 | 9.950 | 103.20 | 103.25 | 52.32 | 115.75 | 0.1036 | 26.88 | 1.61 | -0.032 | 14.879 | 520.61 | 14.768 | 519.49 |
| HUB | 5.600 | 9.877 | | | | | | | | | | | | |

| STREAMLINE NO. | R/RTIP | FLOW COEF. | REL.FLOW ANGLE (DEG) | L.E.RAD. /CHORD | MAX.TH. /CHORD | MAX.TH. PT.LOC. /CHORD | TRAN.PT. LOCATION /CHORD | SEGMENT IN/OUT TURN.RATE | LAYOUT CONE ANG. (DEG) |
|---|---|---|---|---|---|---|---|---|---|
| TIP | 1.0000 | | | | | | | | |
| 1 | 0.9905 | 0.5736 | 49.21 | 0.0100 | 0.1000 | 0.5000 | 0.5000 | 1.0000 | 0.41 |
| 2 | 0.9651 | 0.6120 | 49.52 | 0.0100 | 0.0964 | 0.5000 | 0.5000 | 1.0000 | 0.54 |
| 3 | 0.9401 | 0.6205 | 48.78 | 0.0100 | 0.0928 | 0.5000 | 0.5000 | 1.0000 | 0.51 |
| 4 | 0.9147 | 0.6192 | 47.54 | 0.0100 | 0.0892 | 0.5000 | 0.5000 | 1.0000 | 0.45 |
| 5 | 0.8885 | 0.6176 | 46.15 | 0.0100 | 0.0855 | 0.5000 | 0.5000 | 1.0000 | 0.39 |
| 6 | 0.8614 | 0.6167 | 44.59 | 0.0100 | 0.0816 | 0.5000 | 0.5000 | 1.0000 | 0.32 |
| 7 | 0.8334 | 0.6161 | 42.83 | 0.0100 | 0.0777 | 0.5000 | 0.5000 | 1.0000 | 0.26 |
| 8 | 0.8044 | 0.6158 | 40.83 | 0.0100 | 0.0735 | 0.5000 | 0.5000 | 1.0000 | 0.19 |
| 9 | 0.7742 | 0.6158 | 38.54 | 0.0100 | 0.0692 | 0.5000 | 0.5000 | 1.0000 | 0.13 |
| 10 | 0.7426 | 0.6158 | 35.91 | 0.0100 | 0.0648 | 0.5000 | 0.5000 | 1.0000 | 0.09 |
| 11 | 0.7092 | 0.6160 | 32.79 | 0.0100 | 0.0600 | 0.5000 | 0.5000 | 1.0000 | 0.09 |
| HUB | 0.7000 | | | | | | | | |

| STREAMLINE NO. | PCT. SPAN | --- INLET STREAMLINE --- INC. ANGLE (DEG) | S.S.INC. ANGLE (DEG) | IN.BLADE ANGLE (DEG) | ++++ LAYOUT CONE ++++ IN.BLADE ANGLE (DEG) | TRAN.PT. BL.ANGLE (DEG) | BLD.SET ANGLE (DEG) | 1ST SEG. S.S.CAM. (DEG) | MACH NO. AT SHOCK LOCATION | SH.LOC. AS FRACT OF S.S. | COV.CHAN. AS FRACT OF S.S. | MIN.CHK. AREA MARGIN | MIN.CHK. PT.LOC.IN COV.CHAN. | L.E.EDGE CIR.CENT. R*DB/DR |
|---|---|---|---|---|---|---|---|---|---|---|---|---|---|---|
| 1 | 3.18 | 2.05 | -6.99 | 27.53 | 26.60 | 10.45 | 10.46 | 25.19 | 0.1202 | 0.2010 | 0.7558 | 4.3399 | 0.3662 | -0.8856 |
| 2 | 11.64 | 1.48 | -7.24 | 20.57 | 20.35 | 8.02 | 8.03 | 21.05 | 0.0990 | 0.1675 | 0.7971 | 4.1950 | 0.4044 | -0.2458 |
| 3 | 19.96 | 1.22 | -7.12 | 19.27 | 19.37 | 7.63 | 7.64 | 20.08 | 0.0993 | 0.1661 | 0.7986 | 4.2540 | 0.3821 | 0.1567 |
| 4 | 28.44 | 1.10 | -6.92 | 19.92 | 20.02 | 7.85 | 7.85 | 20.09 | 0.1013 | 0.1749 | 0.7873 | 4.3251 | 0.3618 | 0.2167 |
| 5 | 37.18 | 1.04 | -6.45 | 20.64 | 20.69 | 8.09 | 8.10 | 20.09 | 0.1067 | 0.1817 | 0.7786 | 4.3741 | 0.3445 | 0.1737 |
| 6 | 46.20 | 1.06 | -5.99 | 21.29 | 21.31 | 8.34 | 8.35 | 20.01 | 0.1103 | 0.1852 | 0.7745 | 4.4014 | 0.3283 | 0.1234 |
| 7 | 55.53 | 1.19 | -5.41 | 21.88 | 21.88 | 8.61 | 8.62 | 19.87 | 0.1134 | 0.1848 | 0.7756 | 4.4085 | 0.3143 | 0.0738 |
| 8 | 65.21 | 1.45 | -4.58 | 22.41 | 22.41 | 8.90 | 8.90 | 19.63 | 0.1161 | 0.1800 | 0.7827 | 4.3947 | 0.3050 | 0.0307 |
| 9 | 75.27 | 1.85 | -3.79 | 22.88 | 22.88 | 9.20 | 9.20 | 19.31 | 0.1188 | 0.1709 | 0.7954 | 4.3582 | 0.3031 | 0.0037 |
| 10 | 85.80 | 2.41 | -2.71 | 23.30 | 23.30 | 9.52 | 9.52 | 18.91 | 0.1217 | 0.1579 | 0.8128 | 4.2971 | 0.3115 | 0.0035 |
| 11 | 96.94 | 3.14 | -1.44 | 23.74 | 23.71 | 9.85 | 9.85 | 18.44 | 0.1254 | 0.1421 | 0.8335 | 4.2183 | 0.3205 | 0.0298 |

Table 9.2. Continued.

** VALUES OF PARAMETERS ON STREAMLINES AT STATION. 12. WHICH IS THE OUTLET OF STATOR NUMBER. 1. OF STAGE NUMBER. 2 **

| STREAMLINE NO. | RADIUS (IN.) | AXIAL COORD. (IN.) | AXIAL VEL. (FT/SEC) | MERD. VEL. (FT/SEC) | TANG. VEL. (FT/SEC) | ABS. VEL. (FT/SEC) | ABS. MACH NO. | ABS.FLOW ANGLE (DEG) | STREAM. SLOPE (DEG) | STREAM. CURV. (1./IN.) | TOTAL PRESS. (PSIA) | TOTAL TEMP. (DEG.R.) | STATIC PRESS. (PSIA) | STATIC TEMP. (DEG.R.) |
|---|---|---|---|---|---|---|---|---|---|---|---|---|---|---|
| TIP | 8.000 | 12.931 | | | | | | | | | | | | |
| 1 | 7.945 | 12.930 | 100.54 | 100.54 | 0.0 | 100.54 | 0.0899 | 0.0 | 0.40 | -0.016 | 14.877 | 521.62 | 14.793 | 520.76 |
| 2 | 7.747 | 12.928 | 101.06 | 101.07 | 0.0 | 101.07 | 0.0904 | 0.0 | 0.44 | -0.014 | 14.877 | 520.79 | 14.793 | 519.94 |
| 3 | 7.544 | 12.926 | 101.39 | 101.40 | 0.0 | 101.40 | 0.0907 | 0.0 | 0.41 | -0.012 | 14.878 | 520.59 | 14.792 | 519.74 |
| 4 | 7.337 | 12.925 | 101.59 | 101.59 | 0.0 | 101.59 | 0.0909 | 0.0 | 0.36 | -0.009 | 14.877 | 520.59 | 14.792 | 519.73 |
| 5 | 7.124 | 12.924 | 101.72 | 101.72 | 0.0 | 101.72 | 0.0910 | 0.0 | 0.30 | -0.006 | 14.877 | 520.59 | 14.791 | 519.73 |
| 6 | 6.904 | 12.924 | 101.79 | 101.79 | 0.0 | 101.79 | 0.0911 | 0.0 | 0.23 | -0.004 | 14.877 | 520.59 | 14.791 | 519.73 |
| 7 | 6.678 | 12.924 | 101.80 | 101.80 | 0.0 | 101.80 | 0.0911 | 0.0 | 0.16 | -0.002 | 14.877 | 520.60 | 14.791 | 519.73 |
| 8 | 6.443 | 12.924 | 101.73 | 101.73 | 0.0 | 101.73 | 0.0910 | 0.0 | 0.07 | -0.000 | 14.877 | 520.60 | 14.791 | 519.74 |
| 9 | 6.199 | 12.926 | 101.56 | 101.56 | 0.0 | 101.56 | 0.0909 | 0.0 | -0.02 | 0.002 | 14.877 | 520.60 | 14.791 | 519.74 |
| 10 | 5.945 | 12.927 | 101.25 | 101.25 | 0.0 | 101.25 | 0.0906 | 0.0 | -0.12 | 0.005 | 14.876 | 520.60 | 14.791 | 519.75 |
| 11 | 5.678 | 12.930 | 100.72 | 100.72 | 0.0 | 100.72 | 0.0901 | 0.0 | -0.25 | 0.010 | 14.876 | 520.61 | 14.792 | 519.76 |
| HUB | 5.600 | 12.931 | | | | | | | | | | | | |

| STREAMLINE NO. | R/RTIP | FLOW COEF. | HEAD COEF. | IDEAL HEAD COEF. | STATOR PO.RATIO | STAGE PO.RATIO | STAGE AD.EFF. | DIFFUSION FACTOR | STATOR LOSS COEF. | SHOCK LOSS COEF. | ELEMENT SOLIDITY | AERO. CHORD (IN.) | MEAN SPACING (IN.) |
|---|---|---|---|---|---|---|---|---|---|---|---|---|---|
| TIP | 1.0000 | | | | | | | | | | | | |
| 1 | 0.9931 | 0.6000 | 0.1996 | 0.3225 | 0.9999 | 1.0063 | 0.6187 | 0.2258 | 0.0220 | 0.0 | 1.8200 | 3.0244 | 1.6617 |
| 2 | 0.9683 | 0.6032 | 0.1994 | 0.2393 | 0.9999 | 1.0063 | 0.8332 | 0.1945 | 0.0166 | 0.0 | 1.7354 | 2.8109 | 1.6197 |
| 3 | 0.9430 | 0.6051 | 0.1995 | 0.2181 | 0.9999 | 1.0063 | 0.9147 | 0.1910 | 0.0155 | 0.0 | 1.6726 | 2.6387 | 1.5776 |
| 4 | 0.9171 | 0.6053 | 0.1995 | 0.2177 | 0.9999 | 1.0063 | 0.9163 | 0.1957 | 0.0158 | 0.0 | 1.6330 | 2.5059 | 1.5346 |
| 5 | 0.8905 | 0.6071 | 0.1995 | 0.2182 | 0.9999 | 1.0063 | 0.9142 | 0.2004 | 0.0163 | 0.0 | 1.6204 | 2.4149 | 1.4903 |
| 6 | 0.8630 | 0.6075 | 0.1995 | 0.2185 | 0.9999 | 1.0063 | 0.9132 | 0.2047 | 0.0170 | 0.0 | 1.6401 | 2.3694 | 1.4447 |
| 7 | 0.8347 | 0.6076 | 0.1994 | 0.2187 | 0.9999 | 1.0063 | 0.9117 | 0.2079 | 0.0181 | 0.0 | 1.6988 | 2.3740 | 1.3975 |
| 8 | 0.8054 | 0.6071 | 0.1993 | 0.2191 | 0.9999 | 1.0063 | 0.9098 | 0.2102 | 0.0195 | 0.0 | 1.8049 | 2.4342 | 1.3486 |
| 9 | 0.7749 | 0.6062 | 0.1992 | 0.2196 | 0.9998 | 1.0063 | 0.9071 | 0.2120 | 0.0216 | 0.0 | 1.9698 | 2.5565 | 1.2978 |
| 10 | 0.7431 | 0.6043 | 0.1989 | 0.2203 | 0.9998 | 1.0063 | 0.9031 | 0.2141 | 0.0246 | 0.0 | 2.2088 | 2.7493 | 1.2447 |
| 11 | 0.7098 | 0.6011 | 0.1985 | 0.2215 | 0.9998 | 1.0063 | 0.8964 | 0.2186 | 0.0292 | 0.0 | 2.5441 | 3.0243 | 1.1888 |
| HUB | 0.7000 | | | | | | | | | | | | |

| STREAMLINE NO. | PCT. SPAN | LOCAL BLADE FORCES RADIUS (IN.) | FOR.AXIAL (LBS/IN) | TANG. (LBS/IN) | --- OUTLET STREAMLINE --- T.E.RAD. /CHORD | DEV. ANGLE (DEG) | OUT.BLADE ANGLE (DEG) | ++ LAYOUT CONE +++ OUT.BLADE ANGLE (DEG) | MAX.CAMB. PT.LOC. /CHORD | T.E.EDGE CIR.CENT R*DO/DR |
|---|---|---|---|---|---|---|---|---|---|---|
| 1 | 2.30 | 7.934 | 0.0372 | 0.1479 | 0.0100 | 5.70 | -5.70 | -5.70 | 0.5000 | 0.0 |
| 2 | 10.56 | 7.734 | 0.0204 | 0.1125 | 0.0100 | 4.30 | -4.30 | -4.30 | 0.5000 | 0.0 |
| 3 | 18.99 | 7.533 | 0.0172 | 0.1040 | 0.0100 | 4.11 | -4.11 | -4.11 | 0.5000 | 0.0 |
| 4 | 27.64 | 7.327 | 0.0177 | 0.1041 | 0.0100 | 4.32 | -4.32 | -4.32 | 0.5000 | 0.0 |
| 5 | 36.51 | 7.116 | 0.0184 | 0.1043 | 0.0100 | 4.50 | -4.50 | -4.50 | 0.5000 | 0.0 |
| 6 | 45.66 | 6.898 | 0.0190 | 0.1043 | 0.0100 | 4.62 | -4.62 | -4.62 | 0.5000 | 0.0 |
| 7 | 55.10 | 6.673 | 0.0197 | 0.1043 | 0.0100 | 4.66 | -4.66 | -4.66 | 0.5000 | 0.0 |
| 8 | 64.87 | 6.439 | 0.0205 | 0.1043 | 0.0100 | 4.61 | -4.61 | -4.61 | 0.5000 | 0.0 |
| 9 | 75.03 | 6.197 | 0.0213 | 0.1042 | 0.0100 | 4.47 | -4.47 | -4.47 | 0.5000 | 0.0 |
| 10 | 85.63 | 5.943 | 0.0222 | 0.1039 | 0.0100 | 4.26 | -4.26 | -4.26 | 0.5000 | 0.0 |
| 11 | 96.74 | 5.676 | 0.0231 | 0.1066 | 0.0100 | 4.01 | -4.01 | -4.01 | 0.5000 | 0.0 |

Table 9.2. Continued.

** VALUES OF PARAMETERS ON STREAMLINES AT STATION, 13, WHICH IS AN ANNULUS **

| STREAMLINE NO. | RADIUS (IN.) | AXIAL COORD. (IN.) | AXIAL VEL. (FT/SEC) | MERD. VEL. (FT/SEC) | TANG. VEL. (FT/SEC) | ABS. VEL. (FT/SEC) | ABS. MACH NO. | ABS.FLOW ANGLE (DEG) | STREAM. SLOPE (DEG) | STREAM. CURV. (1./IN.) | TOTAL PRESS. (PSIA) | TOTAL TEMP. (DEG.R.) | STATIC PRESS. (PSIA) | STATIC TEMP. (DEG.R.) |
|---|---|---|---|---|---|---|---|---|---|---|---|---|---|---|
| TIP | 8.000 | 14.500 | | | | | | | | | | | | |
| 1 | 7.945 | 14.500 | 101.51 | 101.51 | 0.0 | 101.51 | 0.0907 | 0.0 | -0.09 | 0.005 | 14.877 | 521.62 | 14.791 | 520.77 |
| 2 | 7.748 | 14.500 | 101.6€ | 101.66 | 0.0 | 101.66 | 0.0909 | 0.0 | -0.06 | 0.003 | 14.877 | 520.79 | 14.792 | 519.93 |
| 3 | 7.547 | 14.500 | 101.67 | 101.67 | 0.0 | 101.67 | 0.0910 | 0.0 | -0.04 | 0.002 | 14.878 | 520.59 | 14.792 | 519.73 |
| 4 | 7.340 | 14.500 | 101.63 | 101.63 | 0.0 | 101.63 | 0.0909 | 0.0 | -0.01 | 0.000 | 14.877 | 520.59 | 14.792 | 519.73 |
| 5 | 7.127 | 14.500 | 101.60 | 101.60 | 0.0 | 101.60 | 0.0909 | 0.0 | 0.00 | -0.000 | 14.877 | 520.59 | 14.792 | 519.73 |
| 6 | 6.907 | 14.500 | 101.56 | 101.56 | 0.0 | 101.56 | 0.0909 | 0.0 | 0.01 | -0.001 | 14.877 | 520.59 | 14.792 | 519.74 |
| 7 | 6.680 | 14.500 | 101.50 | 101.50 | 0.0 | 101.50 | 0.0908 | 0.0 | 0.02 | -0.001 | 14.877 | 520.60 | 14.792 | 519.74 |
| 8 | 6.445 | 14.500 | 101.41 | 101.41 | 0.0 | 101.41 | 0.0907 | 0.0 | 0.02 | -0.001 | 14.877 | 520.60 | 14.792 | 519.74 |
| 9 | 6.200 | 14.500 | 101.28 | 101.28 | 0.0 | 101.28 | 0.0906 | 0.0 | 0.03 | -0.001 | 14.877 | 520.60 | 14.792 | 519.75 |
| 10 | 5.945 | 14.500 | 101.09 | 101.09 | 0.0 | 101.09 | 0.0904 | 0.0 | 0.03 | -0.001 | 14.876 | 520.60 | 14.792 | 519.75 |
| 11 | 5.678 | 14.500 | 100.82 | 100.82 | 0.0 | 100.82 | 0.0902 | 0.0 | 0.05 | -0.003 | 14.876 | 520.61 | 14.791 | 519.76 |
| HUB | 5.600 | 14.500 | | | | | | | | | | | | |

** VALUES OF PARAMETERS ON STREAMLINES AT STATION, 14, WHICH IS AN ANNULUS **

| STREAMLINE NO. | RADIUS (IN.) | AXIAL COORD. (IN.) | AXIAL VEL. (FT/SEC) | MERD. VEL. (FT/SEC) | TANG. VEL. (FT/SEC) | ABS. VEL. (FT/SEC) | ABS. MACH NO. | ABS.FLOW ANGLE (DEG) | STREAM. SLOPE (DEG) | STREAM. CURV. (1./IN.) | TOTAL PRESS. (PSIA) | TOTAL TEMP. (DEG.R.) | STATIC PRESS. (PSIA) | STATIC TEMP. (DEG.R.) |
|---|---|---|---|---|---|---|---|---|---|---|---|---|---|---|
| TIP | 8.000 | 15.500 | | | | | | | | | | | | |
| 1 | 7.945 | 15.500 | 101.39 | 101.39 | 0.0 | 101.39 | 0.0906 | 0.0 | 0.02 | -0.001 | 14.877 | 521.62 | 14.792 | 520.77 |
| 2 | 7.748 | 15.500 | 101.63 | 101.63 | 0.0 | 101.63 | 0.0909 | 0.0 | 0.01 | -0.001 | 14.877 | 520.79 | 14.792 | 519.93 |
| 3 | 7.547 | 15.500 | 101.69 | 101.69 | 0.0 | 101.69 | 0.0910 | 0.0 | 0.00 | -0.000 | 14.878 | 520.59 | 14.792 | 519.73 |
| 4 | 7.340 | 15.500 | 101.68 | 101.68 | 0.0 | 101.68 | 0.0910 | 0.0 | -0.00 | 0.000 | 14.877 | 520.59 | 14.792 | 519.73 |
| 5 | 7.127 | 15.500 | 101.64 | 101.64 | 0.0 | 101.64 | 0.0909 | 0.0 | -0.00 | 0.000 | 14.877 | 520.59 | 14.792 | 519.73 |
| 6 | 6.907 | 15.500 | 101.59 | 101.59 | 0.0 | 101.59 | 0.0909 | 0.0 | -0.00 | 0.000 | 14.877 | 520.59 | 14.792 | 519.73 |
| 7 | 6.680 | 15.500 | 101.52 | 101.52 | 0.0 | 101.52 | 0.0908 | 0.0 | -0.00 | -0.000 | 14.877 | 520.60 | 14.792 | 519.74 |
| 8 | 6.445 | 15.500 | 101.42 | 101.42 | 0.0 | 101.42 | 0.0907 | 0.0 | -0.00 | -0.000 | 14.877 | 520.60 | 14.792 | 519.74 |
| 9 | 6.200 | 15.500 | 101.27 | 101.27 | 0.0 | 101.27 | 0.0906 | 0.0 | -0.00 | -0.000 | 14.877 | 520.60 | 14.792 | 519.75 |
| 10 | 5.945 | 15.500 | 101.05 | 101.05 | 0.0 | 101.05 | 0.0904 | 0.0 | -0.01 | 0.000 | 14.876 | 520.60 | 14.792 | 519.75 |
| 11 | 5.678 | 15.500 | 100.71 | 100.71 | 0.0 | 100.71 | 0.0901 | 0.0 | -0.02 | 0.001 | 14.876 | 520.61 | 14.792 | 519.76 |
| HUB | 5.600 | 15.500 | | | | | | | | | | | | |

Table 9.2. Concluded.

** VALUES OF PARAMETERS ON STREAMLINES AT STATION, 15, WHICH IS AN ANNULUS **

| STREAMLINE NO. | RADIUS (IN.) | AXIAL COORD. (IN.) | AXIAL VEL. (FT/SEC) | MERD. VEL. (FT/SEC) | TANG. VEL. (FT/SEC) | ABS. VEL. (FT/SEC) | ABS. MACH NO. | ABS.FLOW ANGLE (DEG) | STREAM. SLOPE (DEG) | STREAM. CURV. (1./IN.) | TOTAL PRESS. (PSIA) | TOTAL TEMP. (DEG.R.) | STATIC PRESS. (PSIA) | STATIC TEMP. (DEG.R.) |
|---|---|---|---|---|---|---|---|---|---|---|---|---|---|---|
| TIP | 8.000 | 16.500 | | | | | | | | | | | | |
| 1 | 7.945 | 16.500 | 101.40 | 101.40 | 0.0 | 101.40 | 0.0906 | 0.0 | -0.02 | -0.001 | 14.877 | 521.62 | 14.792 | 520.77 |
| 2 | 7.748 | 16.500 | 101.63 | 101.63 | 0.0 | 101.63 | 0.0909 | 0.0 | -0.01 | -0.000 | 14.877 | 520.79 | 14.792 | 519.93 |
| 3 | 7.546 | 16.500 | 101.69 | 101.69 | 0.0 | 101.69 | 0.0910 | 0.0 | -0.01 | -0.000 | 14.878 | 520.59 | 14.792 | 519.73 |
| 4 | 7.340 | 16.500 | 101.68 | 101.68 | 0.0 | 101.68 | 0.0910 | 0.0 | -0.00 | 0.000 | 14.877 | 520.59 | 14.792 | 519.73 |
| 5 | 7.127 | 16.500 | 101.64 | 101.64 | 0.0 | 101.64 | 0.0909 | 0.0 | -0.00 | 0.000 | 14.877 | 520.59 | 14.792 | 519.73 |
| 6 | 6.907 | 16.500 | 101.59 | 101.59 | 0.0 | 101.59 | 0.0909 | 0.0 | -0.00 | 0.000 | 14.877 | 520.59 | 14.792 | 519.73 |
| 7 | 6.680 | 16.500 | 101.52 | 101.52 | 0.0 | 101.52 | 0.0908 | 0.0 | -0.00 | -0.000 | 14.877 | 520.60 | 14.792 | 519.74 |
| 8 | 6.445 | 16.500 | 101.41 | 101.41 | 0.0 | 101.41 | 0.0907 | 0.0 | -0.00 | -0.000 | 14.877 | 520.60 | 14.792 | 519.74 |
| 9 | 6.200 | 16.500 | 101.27 | 101.27 | 0.0 | 101.27 | 0.0906 | 0.0 | -0.00 | -0.000 | 14.877 | 520.60 | 14.792 | 519.75 |
| 10 | 5.945 | 16.500 | 101.05 | 101.05 | 0.0 | 101.05 | 0.0904 | 0.0 | -0.00 | 0.000 | 14.876 | 520.60 | 14.792 | 519.75 |
| 11 | 5.678 | 16.500 | 100.71 | 100.71 | 0.0 | 100.71 | 0.0901 | 0.0 | 0.01 | 0.000 | 14.876 | 520.61 | 14.792 | 519.76 |
| HUB | 5.600 | 16.500 | | | | | | | | | | | | |

Table 9.3. Design code stage and overall performance predictions.

*** COMPUTED COMPRESSOR DESIGN PARAMETERS FOR A ROTATIONAL SPEED OF, 2400.0, RPM ***

** THE CORRECTED WEIGHTFLOW PER UNIT OF CASING ANNULAR AREA AT THE INLET FACE OF THE FIRST BLADE ROW IS 7.37 LBS/SEC/FT SQ **

** MASS AVERAGED ROTOR AND STAGE AERODYNAMIC PARAMETERS **

| STAGE NO. | BLADE TYPE | FLOW COEF. | HEAD COEF. | ID. HEAD COEF. | PRESS. RATIO | TEMP. RATIO | ADIA. EFF. | POLY. EFF. | ASPECT RATIO | FOR. AX. THRUST (LBS) | GAS BENDING MOMENTS FOR. AX. (FT-LBS) | GAS BENDING MOMENTS TANG. (FT-LBS) | TORQUE (FT-LBS) | POWER (HP) |
|---|---|---|---|---|---|---|---|---|---|---|---|---|---|---|
| 1 | ROTOR | 0.5871 | 0.1933 | 0.2157 | 1.0061 | 1.0019 | 0.8962 | 0.8962 | 1.00 | 7.54 | 0.037 | -0.033 | | |
| 1 | STATOR | 0.5983 | 0.1897 | 0.2157 | 1.0060 | 1.0019 | 0.8797 | 0.8798 | 1.01 | -13.59 | 0.004 | 0.022 | 3.93 | 1.80 |
| 2 | ROTOR | 0.5966 | 0.2036 | 0.2261 | 1.0064 | 1.0020 | 0.9003 | 0.9004 | 1.01 | 7.51 | 0.038 | -0.034 | | |
| 2 | STATOR | 0.6144 | 0.1993 | 0.2261 | 1.0063 | 1.0020 | 0.8814 | 0.8815 | 1.01 | -13.46 | 0.004 | 0.022 | 4.12 | 1.88 |

** CUMULATIVE SUMS OF MASS AVERAGED ROTOR AND STAGE AERODYDAMIC PARAMETERS **

| STAGE NO. | BLADE TYPE | WEIGHT FLOW (LBS/SEC) | TOTAL PRESS. (PSIA) | TOTAL TEMP. (DEG. R.) | PRESS. RATIO | TEMP. RATIO | HEAD COEF. | IDEAL HEAD COEF. | ADIA. EFF. | POLY. EFF. | FOR. AX. THRUST (LBS) | TORQUE (FT-LBS) | POWER (HP) | FRACT ENERGY |
|---|---|---|---|---|---|---|---|---|---|---|---|---|---|---|
| 1 | INLET | 5.25 | 14.696 | 518.60 | | | | | | | | | | |
| 1 | ROTOR | 5.25 | 14.786 | 519.61 | 1.0061 | 1.0019 | 0.1933 | 0.2157 | 0.8962 | 0.8962 | 7.54 | | | |
| 1 | STATOR | 5.25 | 14.784 | 519.61 | 1.0060 | 1.0019 | 0.1897 | 0.2157 | 0.8797 | 0.8798 | -6.05 | 3.93 | 1.80 | 0.4882 |
| 2 | ROTOR | 5.25 | 14.879 | 520.67 | 1.0125 | 1.0040 | 0.3932 | 0.4418 | 0.8902 | 0.8903 | 1.27 | | | |
| 2 | STATOR | 5.25 | 14.877 | 520.67 | 1.0123 | 1.0040 | 0.3889 | 0.4418 | 0.8805 | 0.8807 | -12.20 | 8.05 | 3.68 | 1.0000 |

Table 9.4 Modified-stator blade manufacturing coordinates generated by NASA design code.

** BLADE SECTION PROPERTIES OF STATOR NO. 1 FOLLOWING ROTOR NO. 1 **

NUMBER OF BLADES = 30.0 AXIAL LOCATION OF STACKING LINE IN COMPRESSOR = 5.460 IN.

| BLADE SECTION NO. | RAD. LOC. (IN.) | STACKING POINT COORDINATES L (IN.) | STACKING POINT COORDINATES H (IN.) | SECTION SETTING ANGLE (DEG.) | BLADE SECTION C.G. COORDINATES L (IN.) | BLADE SECTION C.G. COORDINATES H (IN.) | SECTION AREA (IN.)**2 | MOMENTS OF INERTIA THROUGH C.G. IMIN (IN.)**4 | MOMENTS OF INERTIA THROUGH C.G. IMAX (IN.)**4 | IMAX SETTING ANGLE (DEG.) | SECTION TORSION CONSTANT (IN.)**4 | SECTION TWIST STIFFNESS (IN.)**6 |
|---|---|---|---|---|---|---|---|---|---|---|---|---|
| 1 | 8.020 | 3.1244 | 0.0310 | 13.813 | 1.5758 | 0.2547 | 0.73732 | 0.000000 | 0.01432 | 13.860 | 0.016801 | 0.137932 |
| 2 | 7.840 | 2.8999 | 0.0290 | 9.181 | 1.4640 | 0.1650 | 0.61107 | 0.000199 | -1.48665 | 0.910 | 0.011383 | 14.271236 |
| 3 | 7.660 | 2.7251 | 0.0273 | 7.496 | 1.3774 | 0.1302 | 0.52229 | 0.000065 | -1.07957 | 2.046 | 0.008090 | 8.936669 |
| 4 | 7.480 | 2.5947 | 0.0259 | 7.447 | 1.3066 | 0.1232 | 0.45653 | 0.000035 | -0.82823 | 3.048 | 0.005978 | 6.046024 |

| SECTION NO. 1 COORDINATES L (IN.) | HP (IN.) | HS (IN.) | SECTION NO. 2 COORDINATES L (IN.) | HP (IN.) | HS (IN.) | SECTION NO. 3 COORDINATES L (IN.) | HP (IN.) | HS (IN.) | SECTION NO. 4 COORDINATES L (IN.) | HP (IN.) | HS (IN.) |
|---|---|---|---|---|---|---|---|---|---|---|---|
| 0.0 | 0.0346 | 0.0346 | 0.0 | 0.0301 | 0.0301 | 0.0 | 0.0275 | 0.0275 | 0.0 | 0.0259 | 0.0259 |
| 0.0346 | 0.0000 | 0.0747 | 0.0301 | 0.0000 | 0.0629 | 0.0275 | 0.0000 | 0.0566 | 0.0259 | 0.0 | 0.0534 |
| 0.1000 | 0.0157 | 0.1132 | 0.1000 | 0.0070 | 0.0922 | 0.1000 | 0.0034 | 0.0817 | 0.1000 | 0.0038 | 0.0784 |
| 0.2000 | 0.0387 | 0.1672 | 0.2000 | 0.0163 | 0.1308 | 0.2000 | 0.0079 | 0.1139 | 0.2000 | 0.0086 | 0.1097 |
| 0.3000 | 0.0593 | 0.2157 | 0.3000 | 0.0247 | 0.1657 | 0.3000 | 0.0119 | 0.1433 | 0.3000 | 0.0130 | 0.1382 |
| 0.4000 | 0.0778 | 0.2591 | 0.4000 | 0.0321 | 0.1972 | 0.4000 | 0.0157 | 0.1699 | 0.4000 | 0.0171 | 0.1639 |
| 0.5000 | 0.0943 | 0.2979 | 0.5000 | 0.0387 | 0.2255 | 0.5000 | 0.0190 | 0.1939 | 0.5000 | 0.0207 | 0.1868 |
| 0.6000 | 0.1088 | 0.3324 | 0.6000 | 0.0445 | 0.2506 | 0.6000 | 0.0220 | 0.2152 | 0.6000 | 0.0239 | 0.2069 |
| 0.7000 | 0.1215 | 0.3628 | 0.7000 | 0.0494 | 0.2728 | 0.7000 | 0.0246 | 0.2338 | 0.7000 | 0.0267 | 0.2244 |
| 0.8000 | 0.1325 | 0.3895 | 0.8000 | 0.0537 | 0.2920 | 0.8000 | 0.0269 | 0.2498 | 0.8000 | 0.0291 | 0.2392 |
| 0.9000 | 0.1418 | 0.4125 | 0.9000 | 0.0572 | 0.3083 | 0.9000 | 0.0288 | 0.2633 | 0.9000 | 0.0311 | 0.2513 |
| 1.0000 | 0.1495 | 0.4320 | 1.0000 | 0.0600 | 0.3219 | 1.0000 | 0.0303 | 0.2742 | 1.0000 | 0.0326 | 0.2607 |
| 1.1000 | 0.1556 | 0.4481 | 1.1000 | 0.0622 | 0.3327 | 1.1000 | 0.0314 | 0.2825 | 1.1000 | 0.0338 | 0.2675 |
| 1.2000 | 0.1603 | 0.4610 | 1.2000 | 0.0637 | 0.3409 | 1.2000 | 0.0322 | 0.2883 | 1.2000 | 0.0345 | 0.2717 |
| 1.3000 | 0.1636 | 0.4706 | 1.3000 | 0.0646 | 0.3463 | 1.3000 | 0.0327 | 0.2916 | 1.3000 | 0.0347 | 0.2733 |
| 1.4000 | 0.1655 | 0.4770 | 1.4000 | 0.0648 | 0.3490 | 1.4000 | 0.0328 | 0.2924 | 1.4000 | 0.0346 | 0.2722 |
| 1.5000 | 0.1660 | 0.4802 | 1.5000 | 0.0644 | 0.3491 | 1.5000 | 0.0325 | 0.2906 | 1.5000 | 0.0340 | 0.2686 |
| 1.6000 | 0.1652 | 0.4803 | 1.6000 | 0.0635 | 0.3465 | 1.6000 | 0.0318 | 0.2862 | 1.6000 | 0.0330 | 0.2622 |
| 1.7000 | 0.1631 | 0.4773 | 1.7000 | 0.0619 | 0.3413 | 1.7000 | 0.0308 | 0.2794 | 1.7000 | 0.0316 | 0.2533 |
| 1.8000 | 0.1597 | 0.4711 | 1.8000 | 0.0598 | 0.3334 | 1.8000 | 0.0295 | 0.2700 | 1.8000 | 0.0297 | 0.2416 |
| 1.9000 | 0.1551 | 0.4617 | 1.9000 | 0.0571 | 0.3227 | 1.9000 | 0.0278 | 0.2580 | 1.9000 | 0.0275 | 0.2273 |
| 2.0000 | 0.1492 | 0.4491 | 2.0000 | 0.0538 | 0.3094 | 2.0000 | 0.0257 | 0.2434 | 2.0000 | 0.0247 | 0.2103 |
| 2.1000 | 0.1421 | 0.4333 | 2.1000 | 0.0500 | 0.2933 | 2.1000 | 0.0232 | 0.2262 | 2.1000 | 0.0216 | 0.1905 |
| 2.2000 | 0.1337 | 0.4142 | 2.2000 | 0.0456 | 0.2744 | 2.2000 | 0.0205 | 0.2063 | 2.2000 | 0.0179 | 0.1678 |
| 2.3000 | 0.1242 | 0.3918 | 2.3000 | 0.0407 | 0.2528 | 2.3000 | 0.0173 | 0.1837 | 2.3000 | 0.0139 | 0.1423 |
| 2.4000 | 0.1134 | 0.3659 | 2.4000 | 0.0353 | 0.2282 | 2.4000 | 0.0138 | 0.1584 | 2.4000 | 0.0094 | 0.1139 |
| 2.5000 | 0.1014 | 0.3366 | 2.5000 | 0.0292 | 0.2007 | 2.5000 | 0.0100 | 0.1302 | 2.5000 | 0.0045 | 0.0825 |
| 2.6000 | 0.0882 | 0.3036 | 2.6000 | 0.0227 | 0.1703 | 2.6000 | 0.0057 | 0.0992 | 2.5847 | 0.0000 | 0.0535 |
| 2.7000 | 0.0738 | 0.2669 | 2.7000 | 0.0156 | 0.1368 | 2.7000 | 0.0012 | 0.0653 | 2.6000 | 0.0050 | 0.0469 |
| 2.8000 | 0.0582 | 0.2264 | 2.8000 | 0.0080 | 0.1002 | 2.7251 | 0.0000 | 0.0563 | 2.6107 | 0.0259 | 0.0259 |
| 2.9000 | 0.0415 | 0.1820 | 2.8999 | 0.0000 | 0.0603 | 2.7523 | 0.0273 | 0.0273 | | | |
| 3.0000 | 0.0235 | 0.1333 | 2.9000 | 0.0000 | 0.0603 | | | | | | |
| 3.1000 | 0.0043 | 0.0803 | 2.9289 | 0.0290 | 0.0290 | | | | | | |
| 3.1244 | -0.0000 | 0.0667 | | | | | | | | | |
| 3.15 4 | 0.0310 | 0.0310 | | | | | | | | | |

Table 9.4. Continued.

** BLADE SECTION PROPERTIES OF STATOR NO. 1 FOLLOWING ROTOR NO. 1 **

NUMBER OF BLADES = 30.0    AXIAL LOCATION OF STACKING LINE IN COMPRESSOR = 6.460 IN.

| BLADE SECTION NO. | RAD. LOC. (IN.) | STACKING POINT COORDINATES L (IN.) | STACKING POINT COORDINATES H (IN.) | SECTION SETTING ANGLE (DEG.) | BLADE SECTION C.G. COORDINATES L (IN.) | BLADE SECTION C.G. COORDINATES H (IN.) | SECTION AREA (IN.)**2 | MOMENTS OF INERTIA THROUGH C.G. IMIN (IN.)**4 | MOMENTS OF INERTIA THROUGH C.G. IMAX (IN.)**4 | IMAX SETTING ANGLE (DEG.) | SECTION TORSION CONSTANT (IN.)**4 | SECTION TWIST STIFFNESS (IN.)**6 |
|---|---|---|---|---|---|---|---|---|---|---|---|---|
| 5 | 7.300 | 2.4774 | 0.0249 | 7.666 | 1.2521 | 0.1213 | 0.40737 | 0.000030 | -0.66451 | 3.283 | 0.004594 | 4.366084 |
| 6 | 7.120 | 2.4024 | 0.0242 | 7.877 | 1.2139 | 0.1204 | 0.37168 | 0.000028 | -0.55715 | 3.342 | 0.003686 | 3.365907 |
| 7 | 6.940 | 2.3594 | 0.0238 | 8.081 | 1.1919 | 0.1205 | 0.34744 | 0.000028 | -0.48988 | 3.412 | 0.003099 | 2.786083 |
| 8 | 6.760 | 2.3483 | 0.0237 | 8.285 | 1.1860 | 0.1218 | 0.33315 | 0.000029 | -0.45316 | 3.505 | 0.002738 | 2.488973 |

| SECTION NO. 5 COORDINATES L (IN.) | HP (IN.) | HS (IN.) | SECTION NO. 6 COORDINATES L (IN.) | HP (IN.) | HS (IN.) | SECTION NO. 7 COORDINATES L (IN.) | HP (IN.) | HS (IN.) | SECTION NO. 8 COORDINATES L (IN.) | HP (IN.) | HS (IN.) |
|---|---|---|---|---|---|---|---|---|---|---|---|
| 0.0 | 0.0249 | 0.0249 | 0.0 | 0.0241 | 0.0241 | 0.0 | 0.0237 | 0.0237 | 0.0 | 0.0237 | 0.0237 |
| 0.0249 | 0.0 | 0.0512 | 0.0241 | 0.0 | 0.0497 | 0.0237 | 0.0 | 0.0489 | 0.0237 | 0.0 | 0.0487 |
| 0.1000 | 0.0048 | 0.0767 | 0.1000 | 0.0058 | 0.0755 | 0.1000 | 0.0066 | 0.0749 | 0.1000 | 0.0074 | 0.0747 |
| 0.2000 | 0.0108 | 0.1080 | 0.2000 | 0.0129 | 0.1068 | 0.2000 | 0.0148 | 0.1060 | 0.2000 | 0.0166 | 0.1057 |
| 0.3000 | 0.0163 | 0.1363 | 0.3000 | 0.0194 | 0.1349 | 0.3000 | 0.0222 | 0.1340 | 0.3000 | 0.0249 | 0.1336 |
| 0.4000 | 0.0212 | 0.1616 | 0.4000 | 0.0252 | 0.1600 | 0.4000 | 0.0289 | 0.1588 | 0.4000 | 0.0323 | 0.1583 |
| 0.5000 | 0.0256 | 0.1841 | 0.5000 | 0.0304 | 0.1820 | 0.5000 | 0.0347 | 0.1806 | 0.5000 | 0.0388 | 0.1798 |
| 0.6000 | 0.0295 | 0.2036 | 0.6000 | 0.0349 | 0.2011 | 0.6000 | 0.0398 | 0.1993 | 0.6000 | 0.0445 | 0.1984 |
| 0.7000 | 0.0329 | 0.2204 | 0.7000 | 0.0387 | 0.2173 | 0.7000 | 0.0441 | 0.2151 | 0.7000 | 0.0493 | 0.2140 |
| 0.8000 | 0.0357 | 0.2343 | 0.8000 | 0.0419 | 0.2306 | 0.8000 | 0.0476 | 0.2279 | 0.8000 | 0.0531 | 0.2266 |
| 0.9000 | 0.0380 | 0.2455 | 0.9000 | 0.0444 | 0.2409 | 0.9000 | 0.0504 | 0.2378 | 0.9000 | 0.0562 | 0.2363 |
| 1.0000 | 0.0397 | 0.2538 | 1.0000 | 0.0462 | 0.2485 | 1.0000 | 0.0523 | 0.2448 | 1.0000 | 0.0583 | 0.2431 |
| 1.1000 | 0.0409 | 0.2595 | 1.1000 | 0.0474 | 0.2532 | 1.1000 | 0.0535 | 0.2489 | 1.1000 | 0.0595 | 0.2470 |
| 1.2000 | 0.0415 | 0.2623 | 1.2000 | 0.0479 | 0.2550 | 1.2000 | 0.0539 | 0.2502 | 1.2000 | 0.0599 | 0.2481 |
| 1.3000 | 0.0415 | 0.2625 | 1.3000 | 0.0477 | 0.2541 | 1.3000 | 0.0534 | 0.2485 | 1.3000 | 0.0594 | 0.2463 |
| 1.4000 | 0.0410 | 0.2599 | 1.4000 | 0.0468 | 0.2503 | 1.4000 | 0.0522 | 0.2440 | 1.4000 | 0.0579 | 0.2416 |
| 1.5000 | 0.0400 | 0.2545 | 1.5000 | 0.0452 | 0.2437 | 1.5000 | 0.0502 | 0.2366 | 1.5000 | 0.0556 | 0.2340 |
| 1.6000 | 0.0384 | 0.2464 | 1.6000 | 0.0430 | 0.2342 | 1.6000 | 0.0474 | 0.2263 | 1.6000 | 0.0524 | 0.2235 |
| 1.7000 | 0.0362 | 0.2355 | 1.7000 | 0.0400 | 0.2218 | 1.7000 | 0.0438 | 0.2131 | 1.7000 | 0.0483 | 0.2101 |
| 1.8000 | 0.0335 | 0.2218 | 1.8000 | 0.0364 | 0.2065 | 1.8000 | 0.0394 | 0.1969 | 1.8000 | 0.0433 | 0.1938 |
| 1.9000 | 0.0302 | 0.2052 | 1.9000 | 0.0321 | 0.1883 | 1.9000 | 0.0342 | 0.1777 | 1.9000 | 0.0374 | 0.1744 |
| 2.0000 | 0.0263 | 0.1857 | 2.0000 | 0.0271 | 0.1670 | 2.0000 | 0.0282 | 0.1554 | 2.0000 | 0.0306 | 0.1519 |
| 2.1000 | 0.0219 | 0.1634 | 2.1000 | 0.0214 | 0.1427 | 2.1000 | 0.0214 | 0.1301 | 2.1000 | 0.0229 | 0.1264 |
| 2.2000 | 0.0168 | 0.1380 | 2.2000 | 0.0150 | 0.1153 | 2.2000 | 0.0137 | 0.1015 | 2.2000 | 0.0143 | 0.0976 |
| 2.3000 | 0.0113 | 0.1096 | 2.3000 | 0.0079 | 0.0847 | 2.3000 | 0.0053 | 0.0696 | 2.3000 | 0.0048 | 0.0656 |
| 2.4000 | 0.0051 | 0.0780 | 2.4000 | 0.0001 | 0.0508 | 2.3594 | 0.0000 | 0.0491 | 2.3483 | 0.0000 | 0.0489 |
| 2.4774 | 0.0000 | 0.0514 | 2.4024 | 0.0000 | 0.0499 | 2.3833 | 0.0238 | 0.0238 | 2.3720 | 0.0237 | 0.0237 |
| 2.5000 | 0.0143 | 0.0355 | 2.4266 | 0.0242 | 0.0242 | | | | | | |
| 2.5024 | 0.0249 | 0.0249 | | | | | | | | | |

Table 9.4. Continued.

** BLADE SECTION PROPERTIES OF STATOR NO. 1 FOLLOWING ROTOR NO. 1 **

NUMBER OF BLADES = 30.0 AXIAL LOCATION OF STACKING LINE IN COMPRESSOR = 6.460 IN.

| BLADE SECTION NO. | RAD. LOC. (IN.) | STACKING POINT COORDINATES L (IN.) | STACKING POINT COORDINATES H (IN.) | SECTION SETTING ANGLE (DEG.) | BLADE SECTION C.G. COORDINATES L (IN.) | BLADE SECTION C.G. COORDINATES H (IN.) | SECTION AREA (IN.)**2 | MOMENTS OF INERTIA THROUGH C.G. IMIN (IN.)**4 | MOMENTS OF INERTIA THROUGH C.G. IMAX (IN.)**4 | IMAX SETTING ANGLE (DEG.) | SECTION TORSION CONSTANT (IN.)**4 | SECTION TWIST STIFFNESS (IN.)**6 |
|---|---|---|---|---|---|---|---|---|---|---|---|---|
| 9 | 6.580 | 2.3687 | 0.0240 | 8.493 | 1.1959 | 0.1243 | 0.32773 | 0.000032 | -0.44163 | 3.623 | 0.002542 | 2.406001 |
| 10 | 6.400 | 2.4204 | 0.0245 | 8.703 | 1.2216 | 0.1281 | 0.33046 | 0.000036 | -0.45310 | 3.760 | 0.002475 | 2.515519 |
| 11 | 6.240 | 2.4924 | 0.0253 | 8.888 | 1.2575 | 0.1327 | 0.33936 | 0.000042 | -0.48596 | 3.893 | 0.002509 | 2.821126 |
| 12 | 6.080 | 2.5886 | 0.0263 | 9.072 | 1.3056 | 0.1383 | 0.35418 | 0.000051 | -0.53786 | 4.043 | 0.002623 | 3.316427 |

SECTION NO. 9 COORDINATES

| L (IN.) | HP (IN.) | HS (IN.) |
|---|---|---|
| 0.0 | 0.0239 | 0.0239 |
| 0.0239 | 0.0 | 0.0492 |
| 0.1000 | 0.0082 | 0.0750 |
| 0.2000 | 0.0182 | 0.1060 |
| 0.3000 | 0.0274 | 0.1337 |
| 0.4000 | 0.0355 | 0.1583 |
| 0.5000 | 0.0427 | 0.1798 |
| 0.6000 | 0.0490 | 0.1984 |
| 0.7000 | 0.0543 | 0.2140 |
| 0.8000 | 0.0586 | 0.2257 |
| 0.9000 | 0.0620 | 0.2365 |
| 1.0000 | 0.0644 | 0.2435 |
| 1.1000 | 0.0658 | 0.2476 |
| 1.2000 | 0.0663 | 0.2489 |
| 1.3000 | 0.0658 | 0.2474 |
| 1.4000 | 0.0644 | 0.2430 |
| 1.5000 | 0.0619 | 0.2359 |
| 1.6000 | 0.0585 | 0.2258 |
| 1.7000 | 0.0542 | 0.2129 |
| 1.8000 | 0.0488 | 0.1971 |
| 1.9000 | 0.0425 | 0.1783 |
| 2.0000 | 0.0352 | 0.1566 |
| 2.1000 | 0.0269 | 0.1317 |
| 2.2000 | 0.0177 | 0.1038 |
| 2.3000 | 0.0075 | 0.0727 |
| 2.3687 | 0.0000 | 0.0494 |
| 2.3926 | 0.0240 | 0.0240 |

SECTION NO. 10 COORDINATES

| L (IN.) | HP (IN.) | HS (IN.) |
|---|---|---|
| 0.0 | 0.0245 | 0.0245 |
| 0.0245 | 0.0000 | 0.0504 |
| 0.1000 | 0.0088 | 0.0758 |
| 0.2000 | 0.0197 | 0.1067 |
| 0.3000 | 0.0297 | 0.1343 |
| 0.4000 | 0.0386 | 0.1590 |
| 0.5000 | 0.0465 | 0.1806 |
| 0.6000 | 0.0534 | 0.1993 |
| 0.7000 | 0.0592 | 0.2151 |
| C.8000 | 0.0641 | 0.2281 |
| 0.9000 | 0.0679 | 0.2383 |
| 1.0000 | 0.0707 | 0.2458 |
| 1.1000 | 0.0725 | 0.2505 |
| 1.2000 | 0.0733 | 0.2524 |
| 1.3000 | 0.0730 | 0.2516 |
| 1.4000 | 0.0717 | 0.2481 |
| 1.5000 | 0.0694 | 0.2418 |
| 1.6000 | 0.0661 | 0.2328 |
| 1.7000 | 0.0617 | 0.2210 |
| 1.8000 | 0.0563 | 0.2064 |
| 1.9000 | 0.0499 | 0.1890 |
| 2.0000 | 0.0425 | 0.1687 |
| 2.1000 | 0.0340 | 0.1454 |
| 2.2000 | 0.0245 | 0.1192 |
| 2.3000 | 0.0139 | 0.0899 |
| 2.4000 | 0.0023 | 0.0575 |
| 2.4204 | 0.0000 | 0.0505 |
| 2.4449 | 0.0245 | 0.0245 |

SECTION NO. 11 COORDINATES

| L (IN.) | HP (IN.) | HS (IN.) |
|---|---|---|
| 0.0 | 0.0253 | 0.0253 |
| 0.0253 | 0.0 | 0.0520 |
| 0.1000 | 0.0092 | 0.0770 |
| 0.2000 | 0.C210 | 0.1077 |
| 0.3000 | 0.0316 | 0.1354 |
| 0.4000 | 0.0412 | 0.1601 |
| 0.5000 | 0.0497 | 0.1819 |
| 0.6000 | 0.0572 | 0.2008 |
| 0.7000 | 0.0636 | 0.2170 |
| 0.8000 | 0.0690 | 0.2304 |
| 0.9000 | 0.0733 | 0.2412 |
| 1.0000 | 0.0766 | 0.2493 |
| 1.1000 | 0.0788 | 0.2547 |
| 1.2000 | 0.0799 | 0.2575 |
| 1.3000 | 0.0801 | 0.2576 |
| 1.4000 | 0.0791 | 0.2552 |
| 1.5000 | 0.0771 | 0.2501 |
| 1.6000 | 0.0740 | 0.2424 |
| 1.7000 | 0.0699 | 0.2320 |
| 1.8000 | 0.0648 | 0.2189 |
| 1.9000 | 0.0585 | 0.2032 |
| 2.0000 | 0.0512 | 0.1847 |
| 2.1000 | 0.0429 | 0.1634 |
| 2.2000 | 0.0335 | 0.1393 |
| 2.3000 | 0.0230 | 0.1123 |
| 2.4000 | 0.0114 | 0.0824 |
| 2.4924 | -0.0000 | 0.0521 |
| 2.5000 | 0.0012 | 0.0494 |
| 2.5177 | 0.0253 | 0.0253 |

SECTION NO. 12 COORDINATES

| L (IN.) | HP (IN.) | HS (IN.) |
|---|---|---|
| 0.0 | 0.0263 | 0.0263 |
| 0.0263 | 0.0000 | 0.0541 |
| 0.1000 | 0.0096 | 0.0786 |
| 0.2000 | 0.0221 | 0.1092 |
| 0.3000 | 0.0335 | 0.1369 |
| 0.4000 | 0.0437 | 0.1617 |
| 0.5000 | 0.0529 | 0.1837 |
| 0.6000 | 0.0610 | 0.2029 |
| 0.7000 | 0.0681 | 0.2196 |
| 0.8000 | 0.0740 | 0.2336 |
| 0.9000 | 0.0789 | 0.2450 |
| 1.0000 | 0.0827 | 0.2539 |
| 1.1000 | 0.0855 | 0.2602 |
| 1.2000 | 0.0872 | 0.2640 |
| 1.3000 | 0.0878 | 0.2654 |
| 1.4000 | 0.0873 | 0.2642 |
| 1.5000 | 0.0858 | 0.2606 |
| 1.6000 | 0.0832 | 0.2544 |
| 1.7000 | 0.0795 | 0.2457 |
| 1.8000 | 0.0748 | 0.2345 |
| 1.9000 | 0.0690 | 0.2208 |
| 2.0000 | 0.0621 | 0.2045 |
| 2.1000 | 0.0542 | 0.1855 |
| 2.2000 | 0.0451 | 0.1640 |
| 2.3000 | 0.0350 | 0.1397 |
| 2.4000 | 0.0238 | 0.1127 |
| 2.5000 | 0.0116 | 0.0829 |
| 2.5886 | -0.0000 | 0.0541 |
| 2.6000 | 0.0026 | 0.0501 |
| 2.6150 | 0.0263 | 0.0263 |

Table 9.4. Continued.

** BLADE SECTION PROPERTIES OF STATOR NO. 1 FOLLOWING ROTOR NO. 1 **

NUMBER OF BLADES = 30.0 AXIAL LOCATION OF STACKING LINE IN COMPRESSOR = 6.460 IN.

| BLADE SECTION NO. | RAD. LOC. (IN.) | STACKING POINT COORDINATES L (IN.) | STACKING POINT COORDINATES H (IN.) | SECTION SETTING ANGLE (DEG.) | BLADE SECTION C.G. COORDINATES L (IN.) | BLADE SECTION C.G. COORDINATES H (IN.) | SECTION AREA (IN.)**2 | MOMENTS OF INERTIA THROUGH C.G. IMIN (IN.)**4 | MOMENTS OF INERTIA THROUGH C.G. IMAX (IN.)**4 | IMAX SETTING ANGLE (DEG.) | SECTION TORSION CONSTANT (IN.)**4 | SECTION TWIST STIFFNESS (IN.)**6 |
|---|---|---|---|---|---|---|---|---|---|---|---|---|
| 13 | 5.920 | 2.7087 | 0.0276 | 9.254 | 1.3655 | 0.1450 | 0.37484 | 0.000062 | -0.61413 | 4.203 | 0.002815 | 4.092050 |
| 14 | 5.760 | 2.8522 | 0.0291 | 9.433 | 1.4370 | 0.1529 | 0.40131 | 0.000078 | -0.72005 | 4.370 | 0.003087 | 5.263619 |
| 15 | 5.600 | 3.0185 | 0.0309 | 9.610 | 1.5199 | 0.1619 | 0.43360 | 0.000099 | -0.86280 | 4.541 | 0.003442 | 7.007969 |
| 16 | 5.560 | 3.0536 | 0.0314 | 9.654 | 1.5423 | 0.1643 | 0.44258 | 0.000106 | -0.98861 | 4.592 | 0.003544 | 8.984628 |

SECTION NO. 13 COORDINATES

| L (IN.) | HP (IN.) | HS (IN.) |
|---|---|---|
| 0.0 | 0.0276 | 0.0276 |
| 0.0276 | 0.0 | 0.0567 |
| 0.1000 | 0.0100 | 0.0807 |
| 0.2000 | 0.0231 | 0.1112 |
| 0.3000 | 0.0352 | 0.1388 |
| 0.4000 | 0.0462 | 0.1638 |
| 0.5000 | 0.0560 | 0.1860 |
| 0.6000 | 0.0648 | 0.2057 |
| 0.7000 | 0.0725 | 0.2228 |
| 0.8000 | 0.0792 | 0.2374 |
| 0.9000 | 0.0847 | 0.2496 |
| 1.0000 | 0.0892 | 0.2594 |
| 1.1000 | 0.0925 | 0.2668 |
| 1.2000 | 0.0949 | 0.2718 |
| 1.3000 | 0.0961 | 0.2744 |
| 1.4000 | 0.0963 | 0.2747 |
| 1.5000 | 0.0954 | 0.2727 |
| 1.6000 | 0.0934 | 0.2682 |
| 1.7000 | 0.0904 | 0.2615 |
| 1.8000 | 0.0863 | 0.2523 |
| 1.9000 | 0.0811 | 0.2408 |
| 2.0000 | 0.0749 | 0.2269 |
| 2.1000 | 0.0676 | 0.2105 |
| 2.2000 | 0.0592 | 0.1917 |
| 2.3000 | 0.0497 | 0.1704 |
| 2.4000 | 0.0392 | 0.1466 |
| 2.5000 | 0.0275 | 0.1202 |
| 2.6000 | 0.0148 | 0.0913 |
| 2.7000 | 0.0010 | 0.0596 |
| 2.7087 | -0.0000 | 0.0567 |
| 2.7363 | 0.0276 | 0.0276 |

SECTION NO. 14 COORDINATES

| L (IN.) | HP (IN.) | HS (IN.) |
|---|---|---|
| 0.0 | 0.0292 | 0.0292 |
| 0.0292 | 0.0 | 0.0599 |
| 0.1000 | 0.0102 | 0.0832 |
| 0.2000 | 0.0241 | 0.1136 |
| 0.3000 | 0.0369 | 0.1413 |
| 0.4000 | 0.0486 | 0.1664 |
| 0.5000 | 0.0592 | 0.1889 |
| 0.6000 | 0.0687 | 0.2090 |
| 0.7000 | 0.0771 | 0.2266 |
| 0.8000 | 0.0844 | 0.2420 |
| 0.9000 | 0.0907 | 0.2550 |
| 1.0000 | 0.0959 | 0.2657 |
| 1.1000 | 0.1000 | 0.2741 |
| 1.2000 | 0.1030 | 0.2804 |
| 1.3000 | 0.1050 | 0.2844 |
| 1.4000 | 0.1059 | 0.2862 |
| 1.5000 | 0.1058 | 0.2858 |
| 1.6000 | 0.1046 | 0.2832 |
| 1.7000 | 0.1023 | 0.2785 |
| 1.8000 | 0.0990 | 0.2715 |
| 1.9000 | 0.0947 | 0.2623 |
| 2.0000 | 0.0892 | 0.2508 |
| 2.1000 | 0.0828 | 0.2372 |
| 2.2000 | 0.0752 | 0.2212 |
| 2.3000 | 0.0666 | 0.2030 |
| 2.4000 | 0.0569 | 0.1825 |
| 2.5000 | 0.0461 | 0.1596 |
| 2.6000 | 0.0343 | 0.1343 |
| 2.7000 | 0.0214 | 0.1067 |
| 2.8000 | 0.0074 | 0.0765 |
| 2.8522 | -0.0000 | 0.0598 |
| 2.8813 | 0.0291 | 0.0291 |

SECTION NO. 15 COORDINATES

| L (IN.) | HP (IN.) | HS (IN.) |
|---|---|---|
| 0.0 | 0.0310 | 0.0310 |
| 0.0310 | 0.0 | 0.0636 |
| 0.1000 | 0.0105 | 0.0861 |
| 0.2000 | 0.0251 | 0.1165 |
| 0.3000 | 0.0386 | 0.1443 |
| 0.4000 | 0.0510 | 0.1695 |
| 0.5000 | 0.0623 | 0.1923 |
| 0.6000 | 0.0726 | 0.2128 |
| 0.7000 | 0.0817 | 0.2311 |
| 0.8000 | 0.0898 | 0.2471 |
| 0.9000 | 0.0969 | 0.2609 |
| 1.0000 | 0.1028 | 0.2726 |
| 1.1000 | 0.1077 | 0.2821 |
| 1.2000 | 0.1116 | 0.2896 |
| 1.3000 | 0.1144 | 0.2950 |
| 1.4000 | 0.1162 | 0.2983 |
| 1.5000 | 0.1169 | 0.2996 |
| 1.6000 | 0.1166 | 0.2989 |
| 1.7000 | 0.1152 | 0.2961 |
| 1.8000 | 0.1128 | 0.2913 |
| 1.9000 | 0.1094 | 0.2844 |
| 2.0000 | 0.1049 | 0.2754 |
| 2.1000 | 0.0994 | 0.2644 |
| 2.2000 | 0.0928 | 0.2514 |
| 2.3000 | 0.0852 | 0.2362 |
| 2.4000 | 0.0765 | 0.2189 |
| 2.5000 | 0.0668 | 0.1995 |
| 2.6000 | 0.0561 | 0.1779 |
| 2.7000 | 0.0443 | 0.1541 |
| 2.8000 | 0.0314 | 0.1281 |
| 2.9000 | 0.0175 | 0.0999 |
| 3.0000 | 0.0025 | 0.0694 |
| 3.0185 | -0.0000 | 0.0634 |
| 3.0495 | 0.0309 | 0.0309 |

SECTION NO. 16 COORDINATES

| L (IN.) | HP (IN.) | HS (IN.) |
|---|---|---|
| 0.0 | 0.0315 | 0.0315 |
| 0.0315 | 0.0000 | 0.0646 |
| 0.1000 | 0.0105 | 0.0870 |
| 0.2000 | 0.0253 | 0.1173 |
| 0.3000 | 0.0390 | 0.1451 |
| 0.4000 | 0.0516 | 0.1704 |
| 0.5000 | 0.0631 | 0.1933 |
| 0.6000 | 0.0736 | 0.2139 |
| 0.7000 | 0.0829 | 0.2323 |
| 0.8000 | 0.0912 | 0.2484 |
| 0.9000 | 0.0985 | 0.2625 |
| 1.0000 | 0.1046 | 0.2744 |
| 1.1000 | 0.1097 | 0.2842 |
| 1.2000 | 0.1138 | 0.2920 |
| 1.3000 | 0.1168 | 0.2977 |
| 1.4000 | 0.1188 | 0.3015 |
| 1.5000 | 0.1198 | 0.3032 |
| 1.6000 | 0.1197 | 0.3029 |
| 1.7000 | 0.1186 | 0.3006 |
| 1.8000 | 0.1164 | 0.2963 |
| 1.9000 | 0.1132 | 0.2900 |
| 2.0000 | 0.1090 | 0.2816 |
| 2.1000 | 0.1037 | 0.2713 |
| 2.2000 | 0.0974 | 0.2589 |
| 2.3000 | 0.0901 | 0.2445 |
| 2.4000 | 0.0817 | 0.2280 |
| 2.5000 | 0.0723 | 0.2094 |
| 2.6000 | 0.0618 | 0.1887 |
| 2.7000 | 0.0503 | 0.1659 |
| 2.8000 | 0.0378 | 0.1409 |
| 2.9000 | 0.0242 | 0.1137 |
| 3.0000 | 0.0095 | 0.0843 |
| 3.0636 | -0.0000 | 0.0644 |
| 3.0951 | 0.0314 | 0.0314 |

Table 9.4. Concluded.

** BLADE SECTION PROPERTIES OF STATOR NO. 1 FOLLOWING ROTOR NO. 1 **

NUMBER OF BLADES = 30.0 AXIAL LOCATION OF STACKING LINE IN COMPRESSOR = 6.460 IN.

| BLADE SECTION NO. | RAD. LOC. (IN.) | STACKING POINT COORDINATES L (IN.) | STACKING POINT COORDINATES H (IN.) | SECTION SETTING ANGLE (DEG.) | BLADE SECTION C.G. COORDINATES L (IN.) | BLADE SECTION C.G. COORDINATES H (IN.) | SECTION AREA (IN.)**2 | MOMENTS OF INERTIA THROUGH C.G. IMIN (IN.)**4 | MOMENTS OF INERTIA THROUGH C.G. IMAX (IN.)**4 | IMAX SETTING ANGLE (DEG.) | SECTION TORSION CONSTANT (IN.)**4 | SECTION TWIST STIFFNESS (IN.)**6 |
|---|---|---|---|---|---|---|---|---|---|---|---|---|
| 17 | 8.000 | 3.0961 | 0.0308 | 13.137 | 1.5615 | 0.2415 | 0.72073 | 0.000106 | -1.66722 | 8.103 | 0.016047 | 15.533062 |

SECTION NO. 17 COORDINATES

| L (IN.) | HP (IN.) | HS (IN.) |
|---|---|---|
| 0.0 | 0.0340 | 0.0340 |
| 0.0340 | 0.0 | 0.0730 |
| 0.1000 | 0.0146 | 0.1104 |
| 0.2000 | 0.0356 | 0.1623 |
| 0.3000 | 0.0545 | 0.2088 |
| 0.4000 | 0.0714 | 0.2505 |
| 0.5000 | 0.0863 | 0.2878 |
| 0.6000 | 0.0995 | 0.3209 |
| 0.7000 | 0.1111 | 0.3502 |
| 0.8000 | 0.1210 | 0.3757 |
| 0.9000 | 0.1293 | 0.3978 |
| 1.0000 | 0.1363 | 0.4164 |
| 1.1000 | 0.1417 | 0.4317 |
| 1.2000 | 0.1459 | 0.4438 |
| 1.3000 | 0.1487 | 0.4528 |
| 1.4000 | 0.1503 | 0.4586 |
| 1.5000 | 0.1505 | 0.4613 |
| 1.6000 | 0.1496 | 0.4610 |
| 1.7000 | 0.1474 | 0.4576 |
| 1.8000 | 0.1441 | 0.4511 |
| 1.9000 | 0.1397 | 0.4415 |
| 2.0000 | 0.1341 | 0.4288 |
| 2.1000 | 0.1273 | 0.4129 |
| 2.2000 | 0.1195 | 0.3938 |
| 2.3000 | 0.1105 | 0.3714 |
| 2.4000 | 0.1004 | 0.3456 |
| 2.5000 | 0.0892 | 0.3165 |
| 2.6000 | 0.0768 | 0.2838 |
| 2.7000 | 0.0634 | 0.2476 |
| 2.8000 | 0.0489 | 0.2076 |
| 2.9000 | 0.0333 | 0.1637 |
| 3.0000 | 0.0166 | 0.1158 |
| 3.0961 | -0.0000 | 0.0658 |
| 3.1000 | 0.0002 | 0.0637 |
| 3.1269 | 0.0308 | 0.0308 |

# 10. APPENDIX C: PARAMETER EQUATIONS

The equations used for computing the time-averaged flow quantities and performance parameters are presented in this appendix. Sign conventions are shown in Figure 10.1. Circumferential-mean and radial mass-average parameters were computed using a spline-fit integration scheme [3].

## 10.1. General Parameters

### 10.1.1. Basic Fluid Properties

Barometric pressure, $N/m^2$:

$$P_{atm} = h_{hg@t_{baro}} (1.0 - 0.00018 (t_{baro} - 273.15)) \gamma_{hg@273°K} \tag{10.1}$$

Density of air, $kg/m^3$:

$$\rho = \frac{P_{atm}}{R\ t} \tag{10.2}$$

Specific weight of water, $N/m^3$:

$$\gamma_{H_2O} = g\left(996.86224 + 0.1768124\left(\frac{9}{5}\ t - 459.67\right) - 2.64966 \times 10^{-3}\left(\frac{9}{5}\ t - 459.67\right)^2 + 5.00063 \times 10^{-6}\left(\frac{9}{5}\ t - 459.67\right)^3\right) \tag{10.3}$$

PREVIOUS PAGE IS BLANK

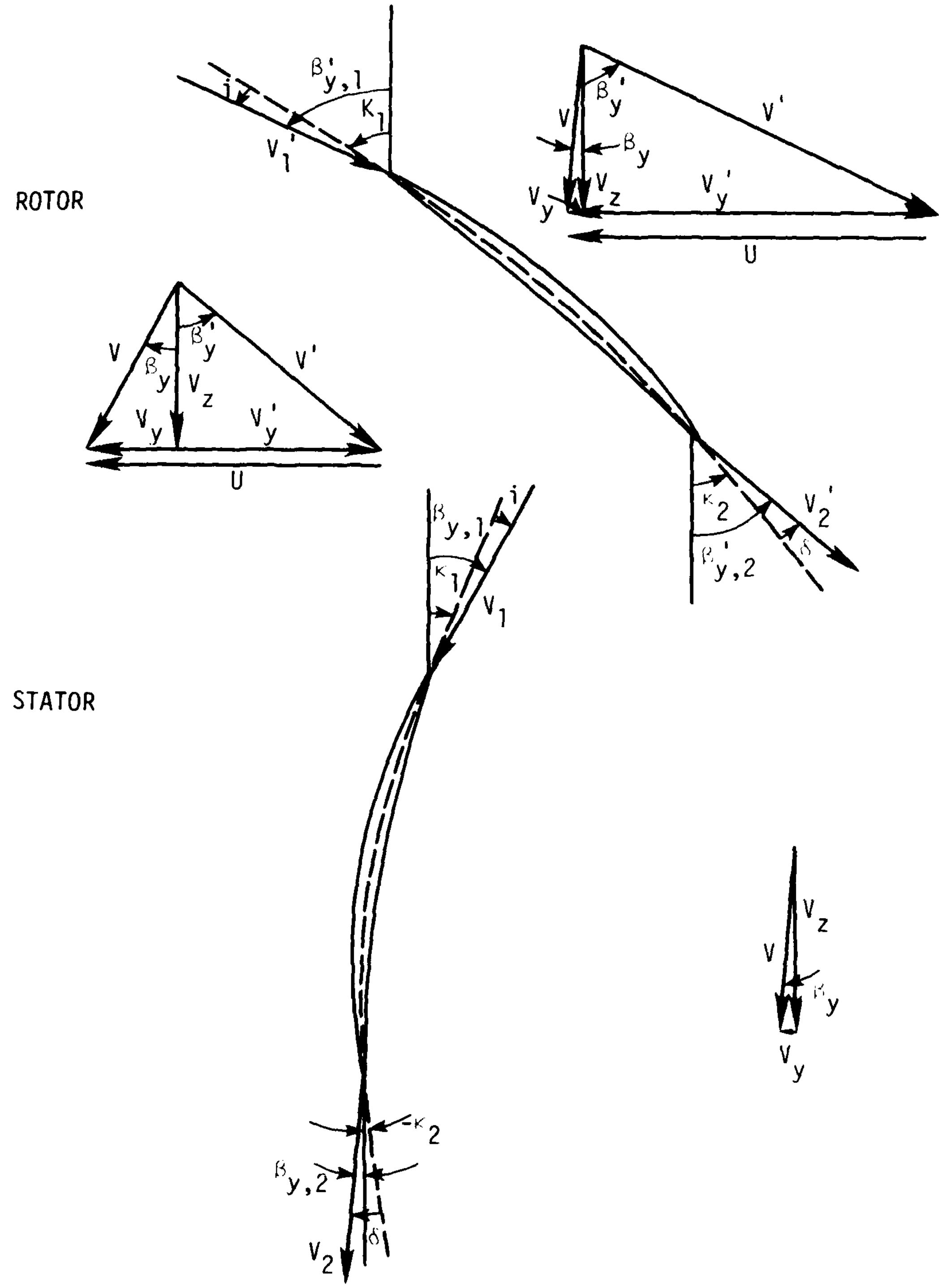


Figure 10.1. Notation and sign conventions (all positive except as noted) for flow-field parameters.

### 10.1.2. Spanwise Measurement Location

Percent passage height from hub:

$$PHH = \frac{r - 0.14224}{0.06096} \times 100 \qquad (10.4)$$

## 10.2. Flow-Field Parameters

### 10.2.1. Point and Circumferential-Mean Quantities

Total head, N-m/kg:

$$H = \frac{P_t \gamma_{H_2O}}{\rho} \qquad (10.5)$$

and

$$\bar{H} = \frac{1}{S_S} \int_0^{S_S} H \, dY \qquad (10.6)$$

Absolute flow angle behind rotors (see Figure 8.1 for sign convention), degrees:

$$\overline{\beta_y} = \frac{1}{S_S} \int_0^{S_S} \beta_y dY \qquad (10.7)$$

Absolute flow angle behind stators (see Figure 8.' 'or sign convention), degrees:

$$\bar{\beta}_y = \frac{1}{\Delta Y_{fs}} \int_{\substack{\text{across} \\ \Delta Y_{fs}}} \beta_y dY \qquad (10.8)$$

Casing static head, N-m/kg:

$$h_w = \frac{P_w \gamma_{H_2O}}{\rho} \tag{10.9}$$

and

$$\overline{h_w} = \frac{1}{S_S}\int_0^{S_S} h_w dY \tag{10.10}$$

Static head (radial equilibrium equation), N-m/kg:

$$\frac{d\bar{h}}{dr} = \frac{2 \sin^2 \bar{\beta}_y(\bar{H} - \bar{h})}{r} \tag{10.11}$$

Absolute fluid velocity, m/s:

$$V = \sqrt{2(H - \bar{h})} \tag{10.12}$$

and

$$\bar{V} = \frac{1}{S_S} \int_0^{S_S} V \, dY \tag{10.13}$$

Blade velocity, m/s:

$$U = \frac{\pi r(RPM)}{30.0} \tag{10.14}$$

Axial component of absolute fluid velocity, m/s:

$$V_z = V\cos \beta_y \tag{10.15}$$

and

$$\bar{V}_z = \bar{V}\cos\bar{\beta}_y \tag{10.16}$$

Tangential component of absolute fluid velocity (see Figure 8.1 for sign convention), m/s:

$$V_y = V\sin\beta_y \tag{10.17}$$

and

$$\bar{V}_y = \bar{V}\sin\bar{\beta}_y \tag{10.18}$$

Tangential component of relative fluid velocity (see Figure 8.1 for sign convention), m/s:

$$V_y' = U - V_y \tag{10.19}$$

and

$$\overline{V_y'} = U - \bar{V}_y \tag{10.20}$$

Relative fluid velocity, m/s:

$$V' = \sqrt{(V_y')^2 + (\bar{V}_z)^2} \tag{10.21}$$

and

$$\overline{V'} = \sqrt{(\overline{V_y'})^2 + (\bar{V}_z)^2} \tag{10.22}$$

Relative tangential flow angle (see Figure 8.1 for sign convention), degrees:

$$\beta_y' = \tan^{-1}\left(\frac{V_y'}{V_z}\right) \tag{10.23}$$

and

$$\overline{\beta_y'} = \tan^{-1}\left(\frac{\overline{V_y'}}{\overline{V_z}}\right) \tag{10.24}$$

Incidence angle for rotors (see Figure 8.1 for sign convention), degrees:

$$\bar{i}_R = \overline{\beta'}_{y,1,R} - \kappa_{1,R} \tag{10.25}$$

Deviation angle for rotors (see Figure 8.1 for sign convention), degrees:

$$\bar{\delta}_R = \overline{\beta'}_{y,2,R} - \kappa_{2,R} \tag{10.26}$$

Incidence angle for stators (see Figure 8.1 for sign convention), degrees:

$$\bar{i}_S = \bar{\beta}_{y,1,S} - \kappa_{1,S} \tag{10.27}$$

Deviation angle for stators (see Figure 10.1 for sign convention), degrees:

$$\bar{\delta} = \bar{\beta}_{y,2,S} - \kappa_{2,S} \tag{10.28}$$

Flow coefficient:

$$\bar{\phi} = \frac{\bar{V}_z}{U_t} \tag{10.29}$$

10.2.2. Global Parameters

Venturi volumetric flow rate, $m^3/s$:

$$Q_v = 0.05229 \sqrt{\frac{2\gamma_{H_2O}\Delta P_v}{\rho}} \tag{10.30}$$

Venturi flow coefficient:

$$\phi = \frac{Q_v}{A\ U_t} \tag{10.31}$$

Integrated volumetric flow rate at each axial measurement station, $m^3/s$:

$$Q_a = 2\pi \int_{r_h}^{r_t} \bar{V}_z\ r\ dr \tag{10.32}$$

Integrated flow coefficient at each axial measurement station:

$$\phi_a = \frac{Q_a}{A\ U_t} \tag{10.33}$$

Integrated and venturi flow-coefficient comparison, percent:

$$FCC = \frac{\phi_a - \phi}{\phi} \times 100 \tag{10.34}$$

General radial mass-average parameter equation (let $\xi$ be any general parameter):

$$\dot{\xi} = \frac{\int_{r_h}^{r_t} \xi \, \bar{V}_z \, r \, dr}{\int_{r_h}^{r_t} \bar{V}_z \, r \, dr} \tag{10.35}$$

10.2.3. Performance Parameters (Based on Kiel and Cobra Probe Data)

Actual total-head rise coefficient for rotor:

$$\psi_R = \frac{(\bar{H}_{2,R} - \bar{H}_{1,R})}{U_t^2} \tag{10.36}$$

Actual total-head rise coefficient for stage:

$$\psi_{stage} = \frac{(\bar{H}_{2,S} - \bar{H}_{1,R})}{U_t^2} \tag{10.37}$$

Actual total-head rise coefficient for overall compressor:

$$\psi_{overall} = \frac{(\bar{H}_{2,2S} - \bar{H}_{1,1R})}{U_t^2} \tag{10.38}$$

Ideal total-head rise (aerodynamic work-input) coefficient for rotor:

$$\psi_{i,R} = \frac{U(\bar{V}_{y,2,R} - \bar{V}_{y,1,R})}{U_t^2} \qquad (10.39)$$

Ideal total-head rise coefficient for stage:

$$\psi_{i,stage} = \psi_{i,R} \qquad (10.40)$$

Ideal total-head rise (aerodynamic work-input) coefficient for overall compressor:

$$\psi_{i,overall} = \psi_{i,1R} + \psi_{i,2R} \qquad (10.41)$$

Hydraulic efficiency for rotor:

$$\eta_R = \frac{\psi_R}{\psi_{i,R}} \qquad (10.42)$$

Hydraulic efficiency for stage:

$$\eta_{stage} = \frac{\psi_{stage}}{\psi_{i,stage}} \qquad (10.43)$$

Hydraulic efficiency for overall compressor:

$$\eta_{overall} = \frac{\psi_{overall}}{\psi_{i,overall}} \qquad (10.44)$$

Total-head loss coefficient for rotor:

$$\omega_R = 2(\psi_{i,R} - \psi_R) \frac{U_t^2}{(\overline{V'_{1,R}})^2} \tag{10.45}$$

Total-head loss coefficient for stator:

$$\omega_S = -2 \frac{(\bar{H}_{2,S} - \bar{H}_{1,S})}{(\bar{V}_{1,S})^2} \tag{10.46}$$

## 10.2.4. Overall Performance Parameters (Performance Map Parameters)

Cross-section average absolute velocity at the second stator exit assuming zero swirl, m/s:

$$\bar{\bar{V}}_{2,2S} = \frac{Q_v}{A} \tag{10.47}$$

Cross-section average absolute velocity at the venturi, m/s:

$$\bar{\bar{V}}_v = \frac{Q_v}{A_v} \tag{10.48}$$

Cross-section average total-head at the second stator exit assuming constant flow passage annulus static-head, N-m/kg:

$$\bar{\bar{H}}_{2,2S} = h_{w,2,2S} = \frac{\bar{\bar{V}}^2_{2,2S}}{2} \tag{10.49}$$

Cross-section average total-head at the venturi assuming constant venturi flow passage static-head, N-m/kg:

$$\bar{\bar{H}}_v = \frac{\gamma_{H_2O} P_v}{\rho} + \frac{\bar{\bar{V}}_v^2}{2} \tag{10.50}$$

Actual head-rise coefficient for overall compressor:

$$\psi_{overall,2,2S} = \frac{\bar{\bar{H}}_{2,2S}}{U_t^2} \tag{10.51}$$

Actual head-rise coefficent for overall compressor incuding losses between the second stator exit and the venturi:

$$\psi_{overall,v} = \frac{\bar{\bar{H}}_v}{U_t^2} \tag{10.52}$$

Work-input coefficient for overall compressor including mechanical losses:

$$\psi_{i,overall,m} = \frac{\pi T(RPM)}{(30)\rho Q_v U_t^2} \tag{10.53}$$

Efficiency for overall compressor including mechanical losses:

$$\eta_{m,overall,2,2S} = \frac{\psi_{overall,2,2S}}{\psi_{i,overall,m}} \tag{10.54}$$

# 11. APPENDIX D: TABULATION OF EXPERIMENTAL DATA

Circumferential-mean data for the four different compressor builds are tabulated in Tables 11.1 through 11.10 in this section. All data in the following tables pertain to compressor operation at the design shaft speed of 2400 rpm and the off-design flow coefficient of 0.500. The data for the Baseline 1 build at design point operation (flow coefficient = 0.587 and shaft speed = 2400 rpm) are tabulated in Appendix E of Reference 1. The column headings in Tables 11.1 through 11.4 are defined as follows:

- BETA R = Relative flow angle, $\beta_y'$
- BETA Y = Absolute flow angle, $\beta_y$
- FC = Flow coefficient, $\bar{\phi}$
- HS = Static head, h
- HT = Total head H
- PHH = Percent passage height from hub, PHH
- V = Absolute velocity, V
- VR = Relative velocity, V'
- VY = Tangential component of absolute velocity, $V_y$
- VZ = Axial component of absolute velocity, $V_z$
- VYR = Tangential component of relative velocity, $V_y'$
- Y/SS = Fraction of stator pitch, $Y/S_s$

Table 11.1 Circumferential-mean flow-field quantities for the baseline 1 compressor build ($\phi$ = 0.500).

STATION 1 : ROTOR 1 INLET

| PHH | HT N*M/KG | HS N*M/KG | BETA Y DEG. | V M/S | VZ M/S | VY M/S | BETA R DEG. | VR M/S | VYR M/S | FC |
|---|---|---|---|---|---|---|---|---|---|---|
| 5.00 | -1.409 | -372.234 | 1.480 | 27.233 | 27.224 | 0.703 | 52.758 | 44.985 | 35.811 | 0.533 |
| 10.00 | -0.494 | -372.226 | 1.640 | 27.266 | 27.255 | 0.780 | 53.251 | 45.554 | 36.501 | 0.534 |
| 30.00 | -0.254 | -372.185 | 1.350 | 27.274 | 27.266 | 0.643 | 55.520 | 48.164 | 39.702 | 0.534 |
| 50.00 | 0.019 | -372.161 | 1.190 | 27.283 | 27.277 | 0.567 | 57.516 | 50.789 | 42.843 | 0.534 |
| 70.00 | -0.113 | -372.146 | 0.760 | 27.277 | 27.275 | 0.362 | 59.396 | 53.574 | 46.112 | 0.534 |
| 80.00 | -0.245 | -372.144 | -0.340 | 27.273 | 27.272 | -0.162 | 60.482 | 55.352 | 48.167 | 0.534 |
| 90.00 | -2.449 | -372.143 | -0.330 | 27.192 | 27.191 | -0.157 | 61.314 | 56.647 | 49.694 | 0.532 |
| 95.00 | -7.508 | -372.143 | -0.510 | 27.005 | 27.004 | -0.240 | 61.886 | 57.305 | 50.544 | 0.529 |

STATION 2 : ROTOR 1 EXIT / STATOR 1 INLET

| PHH | HT N*M/KG | HS N*M/KG | BETA Y DEG. | V M/S | VZ M/S | VY M/S | BETA R DEG. | VR M/S | VYR M/S | FC |
|---|---|---|---|---|---|---|---|---|---|---|
| 5.00 | 594.832 | 77.270 | 34.310 | 32.173 | 26.575 | 18.135 | 34.669 | 32.312 | 18.380 | 0.520 |
| 10.00 | 585.442 | 84.411 | 33.170 | 31.655 | 26.497 | 17.319 | 36.993 | 33.175 | 19.962 | 0.519 |
| 30.00 | 594.488 | 106.947 | 31.820 | 31.226 | 26.533 | 16.464 | 41.989 | 35.697 | 23.881 | 0.520 |
| 50.00 | 611.740 | 126.055 | 30.070 | 31.167 | 26.972 | 15.616 | 45.859 | 38.729 | 27.793 | 0.528 |
| 70.00 | 635.336 | 142.071 | 27.810 | 31.409 | 27.781 | 14.654 | 48.876 | 42.241 | 31.820 | 0.544 |
| 80.00 | 658.262 | 148.907 | 26.390 | 31.917 | 28.591 | 14.186 | 49.788 | 44.285 | 33.819 | 0.560 |
| 90.00 | 644.064 | 155.372 | 30.640 | 31.263 | 26.898 | 15.933 | 51.325 | 43.044 | 33.605 | 0.527 |
| 95.00 | 541.040 | 158.941 | 37.110 | 27.644 | 22.045 | 16.679 | 56.750 | 40.207 | 33.625 | 0.432 |

Table 11.1 concluded.

STATION 3 : STATOR 1 EXIT / ROTOR 2 INLET

| PHH | HT N*M/KG | HS N*M/KG | BETA Y DEG. | V M/S | VZ M/S | VY M/S | BETA R DEG. | VR M/S | VYR M/S | FC |
|---|---|---|---|---|---|---|---|---|---|---|
| 5.00 | 497.470 | 205.571 | 4.280 | 24.078 | 24.010 | 1.797 | 55.333 | 42.212 | 34.718 | 0.470 |
| 10.00 | 552.993 | 205.705 | -0.650 | 26.265 | 26.264 | -0.298 | 55.050 | 45.847 | 37.579 | 0.514 |
| 30.00 | 564.111 | 205.877 | -0.320 | 26.673 | 26.672 | -0.149 | 56.628 | 48.489 | 40.494 | 0.522 |
| 50.00 | 577.833 | 205.890 | 0.550 | 27.166 | 27.164 | 0.261 | 57.807 | 50.987 | 43.148 | 0.532 |
| 70.00 | 592.276 | 205.904 | 2.130 | 27.632 | 27.613 | 1.027 | 58.718 | 53.177 | 45.446 | 0.541 |
| 80.00 | 600.512 | 205.939 | 4.000 | 27.844 | 27.776 | 1.942 | 58.910 | 53.790 | 46.063 | 0.544 |
| 90.00 | 546.118 | 206.035 | 4.260 | 25.830 | 25.759 | 1.919 | 61.590 | 54.139 | 47.619 | 0.504 |
| 95.00 | 485.554 | 206.088 | 0.300 | 23.477 | 23.477 | 0.123 | 64.928 | 55.401 | 50.181 | 0.460 |

STATION 4 : ROTOR 2 EXIT / STATOR 2 INLET

| PHH | HT N*M/KG | HS N*M/KG | BETA Y DEG. | V M/S | VZ M/S | VY M/S | BETA R DEG. | VR M/S | VYR M/S | FC |
|---|---|---|---|---|---|---|---|---|---|---|
| 5.00 | 1126.535 | 621.723 | 43.950 | 31.772 | 22.874 | 22.051 | 32.307 | 27.063 | 14.464 | 0.448 |
| 10.00 | 1115.447 | 634.703 | 32.770 | 31.002 | 26.068 | 16.780 | 38.182 | 33.163 | 20.501 | 0.510 |
| 30.00 | 1135.789 | 652.201 | 29.790 | 31.098 | 26.988 | 15.450 | 42.689 | 36.717 | 24.895 | 0.528 |
| 50.00 | 1160.897 | 668.311 | 28.070 | 31.386 | 27.694 | 14.769 | 45.962 | 39.840 | 28.641 | 0.542 |
| 70.00 | 1191.417 | 682.863 | 28.230 | 31.890 | 28.097 | 15.084 | 48.168 | 42.127 | 31.389 | 0.550 |
| 80.00 | 1219.137 | 690.127 | 29.570 | 32.524 | 28.288 | 16.050 | 48.484 | 42.677 | 31.955 | 0.554 |
| 90.00 | 1175.189 | 698.048 | 31.690 | 30.890 | 26.284 | 16.227 | 51.724 | 42.432 | 33.311 | 0.515 |
| 95.00 | 1076.326 | 702.117 | 36.910 | 27.351 | 21.870 | 16.426 | 57.156 | 40.323 | 33.878 | 0.428 |

STATION 5 : STATOR 2 EXIT

| PHH | HT N*M/KG | HS N*M/KG | BETA Y DEG. | V M/S | VZ M/S | VY M/S | BETA R DEG. | VR M/S | VYR M/S | FC |
|---|---|---|---|---|---|---|---|---|---|---|
| 5.00 | 980.943 | 747.531 | 3.390 | 21.232 | 21.195 | 1.255 | 58.989 | 41.139 | 35.259 | 0.415 |
| 10.00 | 1033.804 | 747.566 | 2.003 | 23.768 | 23.753 | 0.831 | 56.909 | 43.507 | 36.450 | 0.465 |
| 30.00 | 1082.361 | 747.592 | -1.190 | 25.758 | 25.753 | -0.535 | 57.791 | 48.315 | 40.880 | 0.504 |
| 50.00 | 1120.967 | 747.609 | 0.030 | 27.167 | 27.167 | 0.014 | 57.952 | 51.197 | 43.395 | 0.532 |
| 70.00 | 1140.072 | 747.622 | 2.734 | 27.793 | 27.761 | 1.325 | 58.413 | 53.000 | 45.148 | 0.544 |
| 80.00 | 1143.003 | 747.674 | 4.350 | 27.783 | 27.703 | 2.107 | 58.886 | 53.611 | 45.898 | 0.542 |
| 90.00 | 1097.334 | 747.783 | 3.193 | 26.023 | 25.983 | 1.450 | 61.617 | 54.659 | 48.088 | 0.509 |
| 95.00 | 1044.936 | 747.821 | -0.060 | 24.137 | 24.137 | -0.025 | 64.378 | 55.817 | 50.329 | 0.473 |

Table 11.2 Circumferential-mean flow-field quantities for the baseline 2 compressor build ($\phi = 0.500$).

STATION 3 : STATOR 1 EXIT / ROTOR 2 INLET

| PHH | HT N*M/KG | HS N*M/KG | BETA Y DEG. | V M/S | VZ M/S | VY M/S | BETA R DEG. | VR M/S | VYR M/S | FC |
|---|---|---|---|---|---|---|---|---|---|---|
| 5.00 | 490.805 | 205.550 | 4.280 | 23.778 | 23.712 | 1.775 | 55.685 | 42.061 | 34.740 | 0.464 |
| 10.00 | 546.940 | 205.682 | -0.650 | 26.029 | 26.027 | -0.295 | 55.291 | 45.710 | 37.576 | 0.510 |
| 30.00 | 562.609 | 205.851 | -0.320 | 26.604 | 26.603 | -0.149 | 56.696 | 48.451 | 40.494 | 0.521 |
| 50.00 | 575.090 | 205.865 | 0.550 | 27.059 | 27.058 | 0.260 | 57.909 | 50.931 | 43.149 | 0.530 |
| 70.00 | 593.734 | 205.879 | 2.130 | 27.694 | 27.674 | 1.029 | 58.659 | 53.208 | 45.444 | 0.542 |
| 80.00 | 595.792 | 205.913 | 4.000 | 27.630 | 27.563 | 1.927 | 59.113 | 53.693 | 46.078 | 0.540 |
| 90.00 | 553.782 | 206.009 | 4.260 | 26.132 | 26.060 | 1.941 | 61.299 | 54.263 | 47.596 | 0.510 |
| 95.00 | 497.289 | 206.062 | 0.300 | 23.995 | 23.995 | 0.126 | 64.443 | 55.620 | 50.178 | 0.470 |

STATION 4 : ROTOR 2 EXIT / STATOR 2 INLET

| PHH | HT N*M/KG | HS N*M/KG | BETA Y DEG. | V M/S | VZ M/S | VY M/S | BETA R DEG. | VR M/S | VYR M/S | FC |
|---|---|---|---|---|---|---|---|---|---|---|
| 5.00 | 1133.810 | 621.083 | 43.950 | 32.020 | 23.053 | 22.223 | 31.798 | 27.124 | 14.292 | 0.451 |
| 10.00 | 1120.490 | 634.247 | 32.770 | 31.180 | 26.218 | 16.877 | 37.892 | 33.222 | 20.404 | 0.513 |
| 30.00 | 1138.156 | 652.048 | 29.790 | 31.179 | 27.059 | 15.490 | 42.569 | 36.741 | 24.855 | 0.530 |
| 50.00 | 1162.882 | 668.219 | 28.070 | 31.451 | 27.752 | 14.799 | 45.872 | 39.858 | 28.610 | 0.543 |
| 70.00 | 1192.792 | 682.818 | 28.230 | 31.934 | 28.135 | 15.105 | 48.110 | 42.138 | 31.368 | 0.551 |
| 80.00 | 1219.412 | 690.098 | 29.570 | 32.532 | 28.295 | 16.054 | 48.473 | 42.679 | 31.951 | 0.554 |
| 90.00 | 1187.770 | 698.041 | 31.690 | 31.294 | 26.629 | 16.440 | 51.182 | 42.480 | 33.098 | 0.521 |
| 95.00 | 1080.189 | 702.174 | 36.910 | 27.488 | 21.979 | 16.508 | 56.962 | 40.314 | 33.795 | 0.430 |

STATION 5 : STATOR 2 EXIT

| PHH | HT N*M/KG | HS N*M/KG | BETA Y DEG. | V M/S | VZ M/S | VY M/S | BETA R DEG. | VR M/S | VYR M/S | FC |
|---|---|---|---|---|---|---|---|---|---|---|
| 5.00 | 1023.191 | 747.573 | 3.390 | 23.305 | 23.264 | 1.378 | 56.491 | 42.141 | 35.137 | 0.456 |
| 10.00 | 1057.305 | 747.617 | 2.003 | 24.637 | 24.622 | 0.861 | 55.938 | 43.962 | 36.420 | 0.482 |
| 30.00 | 1082.034 | 747.645 | -1.190 | 25.767 | 25.761 | -0.535 | 57.782 | 48.320 | 40.880 | 0.504 |
| 50.00 | 1120.536 | 747.662 | 0.030 | 27.187 | 27.187 | 0.014 | 57.933 | 51.208 | 43.395 | 0.532 |
| 70.00 | 1143.802 | 747.675 | 2.734 | 27.973 | 27.941 | 1.334 | 58.242 | 53.087 | 45.139 | 0.547 |
| 80.00 | 1141.375 | 747.728 | 4.350 | 27.689 | 27.610 | 2.100 | 58.975 | 53.569 | 45.905 | 0.541 |
| 90.00 | 1104.853 | 747.837 | 3.193 | 26.378 | 26.338 | 1.469 | 61.281 | 54.811 | 48.068 | 0.516 |
| 95.00 | 1048.241 | 747.875 | -0.060 | 24.200 | 24.200 | -0.025 | 64.320 | 55.845 | 50.329 | 0.474 |

Table 11.3 Circumferential-mean flow-field quantities for the modified 1 compressor build ($\phi$ = 0.500).

STATION 1 : ROTOR 1 INLET

| PHH | HT N*M/KG | HS N*M/KG | BETA Y DEG. | V M/S | VZ M/S | VY M/S | BETA R DEG. | VR M/S | VYR M/S | FC |
|---|---|---|---|---|---|---|---|---|---|---|
| 5.00 | -1.805 | -370.849 | 3.330 | 27.168 | 27.122 | 1.578 | 52.177 | 44.229 | 34.937 | 0.531 |
| 10.00 | -0.912 | -370.809 | 3.520 | 27.199 | 27.148 | 1.670 | 52.680 | 44.779 | 35.611 | 0.532 |
| 30.00 | -0.858 | -370.645 | 1.790 | 27.195 | 27.182 | 0.849 | 55.463 | 47.945 | 39.496 | 0.532 |
| 50.00 | 0.002 | -370.611 | 0.680 | 27.225 | 27.223 | 0.323 | 57.714 | 50.966 | 43.086 | 0.533 |
| 70.00 | -0.023 | -370.608 | -0.260 | 27.224 | 27.224 | -0.124 | 59.705 | 53.967 | 46.597 | 0.533 |
| 80.00 | -0.762 | -370.608 | -0.100 | 27.197 | 27.197 | -0.047 | 60.491 | 55.216 | 48.053 | 0.533 |
| 90.00 | -2.625 | -370.608 | -0.670 | 27.129 | 27.127 | -0.317 | 61.449 | 56.757 | 49.855 | 0.531 |
| 95.00 | -8.700 | -370.608 | -0.740 | 26.904 | 26.901 | -0.347 | 62.027 | 57.352 | 50.651 | 0.527 |

STATION 2 : ROTOR 1 EXIT / STATOR 1 INLET

| PHH | HT N*M/KG | HS N*M/KG | BETA Y DEG. | V M/S | VZ M/S | VY M/S | BETA R DEG. | VR M/S | VYR M/S | FC |
|---|---|---|---|---|---|---|---|---|---|---|
| 5.00 | 589.344 | 78.299 | 36.720 | 31.970 | 25.626 | 19.115 | 34.176 | 30.975 | 17.400 | 0.502 |
| 10.00 | 583.848 | 86.291 | 35.040 | 31.545 | 25.828 | 18.112 | 36.583 | 32.164 | 19.169 | 0.506 |
| 30.00 | 593.780 | 110.321 | 32.000 | 31.095 | 26.370 | 16.478 | 42.148 | 35.567 | 23.867 | 0.516 |
| 50.00 | 608.828 | 129.152 | 29.150 | 30.973 | 27.050 | 15.087 | 46.316 | 39.165 | 28.322 | 0.530 |
| 70.00 | 631.861 | 143.916 | 27.080 | 31.239 | 27.814 | 14.221 | 49.225 | 42.589 | 32.252 | 0.545 |
| 80.00 | 651.366 | 150.422 | 26.250 | 31.652 | 28.388 | 14.000 | 50.145 | 44.298 | 34.006 | 0.556 |
| 90.00 | 642.311 | 156.711 | 29.780 | 31.164 | 27.048 | 15.478 | 51.545 | 43.493 | 34.059 | 0.530 |
| 95.00 | 537.182 | 160.135 | 36.270 | 27.461 | 22.140 | 16.245 | 56.974 | 40.622 | 34.058 | 0.434 |

STATION 3 : STATOR 1 EXIT / ROTOR 2 INLET

| PHH | HT N*M/KG | HS N*M/KG | BETA Y DEG. | V M/S | VZ M/S | VY M/S | BETA R DEG. | VR M/S | VYR M/S | FC |
|---|---|---|---|---|---|---|---|---|---|---|
| 5.00 | 501.594 | 204.326 | 3.150 | 24.310 | 24.273 | 1.336 | 55.395 | 42.740 | 35.179 | 0.475 |
| 10.00 | 537.819 | 204.412 | -0.910 | 25.728 | 25.725 | -0.409 | 55.685 | 45.632 | 37.689 | 0.504 |
| 30.00 | 543.525 | 204.525 | 0.430 | 25.850 | 25.850 | 0.194 | 57.226 | 47.753 | 40.151 | 0.506 |
| 50.00 | 557.122 | 204.537 | 1.320 | 26.300 | 26.293 | 0.606 | 58.439 | 50.234 | 42.803 | 0.515 |
| 70.00 | 594.810 | 204.567 | 2.060 | 27.790 | 27.772 | 0.999 | 58.586 | 53.284 | 45.474 | 0.544 |
| 80.00 | 602.675 | 204.600 | 3.630 | 28.039 | 27.983 | 1.775 | 58.814 | 54.039 | 46.230 | 0.548 |
| 90.00 | 561.813 | 204.679 | 3.530 | 26.574 | 26.523 | 1.636 | 61.027 | 54.754 | 47.901 | 0.519 |
| 95.00 | 497.058 | 204.718 | 0.450 | 24.098 | 24.097 | 0.189 | 64.320 | 55.607 | 50.114 | 0.472 |

Table 11.3 concluded.

STATION 4 : ROTOR 2 EXIT / STATOR 2 INLET

| PHH | HT N*M/KG | HS N*M/KG | BETA Y DEG. | V M/S | VZ M/S | VY M/S | BETA R DEG. | VR M/S | VYR M/S | FC |
|---|---|---|---|---|---|---|---|---|---|---|
| 5.00 | 1125.282 | 621.825 | 43.860 | 31.728 | 22.877 | 21.984 | 32.423 | 27.101 | 14.531 | 0.448 |
| 10.00 | 1113.947 | 634.791 | 32.510 | 30.950 | 26.100 | 16.634 | 38.346 | 33.279 | 20.647 | 0.511 |
| 30.00 | 1129.481 | 652.168 | 31.120 | 30.894 | 26.448 | 15.967 | 42.667 | 35.969 | 24.378 | 0.518 |
| 50.00 | 1157.493 | 669.375 | 29.790 | 31.241 | 27.112 | 15.521 | 45.808 | 38.895 | 27.888 | 0.531 |
| 70.00 | 1190.043 | 685.428 | 28.200 | 31.766 | 27.995 | 15.011 | 48.337 | 42.114 | 31.463 | 0.548 |
| 80.00 | 1217.026 | 692.640 | 28.860 | 32.381 | 28.359 | 15.629 | 48.784 | 43.040 | 32.376 | 0.555 |
| 90.00 | 1181.857 | 700.069 | 30.900 | 31.039 | 26.634 | 15.940 | 51.595 | 42.874 | 33.598 | 0.522 |
| 95.00 | 1082.090 | 703.829 | 36.200 | 27.499 | 22.191 | 16.241 | 56.916 | 40.653 | 34.062 | 0.435 |

STATION 5 : STATOR 2 EXIT

| PHH | HT N*M/KG | HS N*M/KG | BETA Y DEG. | V M/S | VZ M/S | VY M/S | BETA R DEG. | VR M/S | VYR M/S | FC |
|---|---|---|---|---|---|---|---|---|---|---|
| 5.00 | 1009.314 | 759.842 | 2.010 | 22.097 | 22.084 | 0.775 | 58.288 | 42.012 | 35.740 | 0.432 |
| 10.00 | 1065.226 | 759.864 | 0.080 | 24.648 | 24.648 | 0.034 | 56.505 | 44.663 | 37.246 | 0.483 |
| 30.00 | 1081.969 | 759.883 | -0.220 | 25.253 | 25.253 | -0.097 | 58.018 | 47.679 | 40.442 | 0.494 |
| 50.00 | 1112.264 | 759.887 | 1.400 | 26.273 | 26.265 | 0.642 | 58.445 | 50.188 | 42.767 | 0.514 |
| 70.00 | 1149.449 | 759.928 | 2.600 | 27.711 | 27.682 | 1.257 | 58.524 | 53.017 | 45.216 | 0.542 |
| 80.00 | 1157.128 | 759.977 | 4.080 | 27.954 | 27.883 | 1.989 | 58.787 | 53.805 | 46.017 | 0.546 |
| 90.00 | 1122.771 | 760.074 | 3.190 | 26.768 | 26.726 | 1.490 | 60.915 | 54.981 | 48.048 | 0.523 |
| 95.00 | 1058.519 | 760.111 | 0.020 | 24.353 | 24.353 | 0.009 | 64.163 | 55.881 | 50.295 | 0.477 |

Table 11.4 Circumferential-mean flow-field quantities for the modified 2 compressor build ($\phi$ = 0.500).

STATION 3 : STATOR 1 EXIT / ROTOR 2 INLET

| PHH | HT N*M/KG | HS N*M/KG | BETA Y DEG. | V M/S | VZ M/S | VY M/S | BETA R DEG. | VR M/S | VYR M/S | FC |
|---|---|---|---|---|---|---|---|---|---|---|
| 5.00 | 501.800 | 204.278 | 2.330 | 24.321 | 24.301 | 0.989 | 55.626 | 43.042 | 35.526 | 0.476 |
| 10.00 | 537.711 | 204.340 | -1.630 | 25.726 | 25.716 | -0.732 | 55.921 | 45.894 | 38.013 | 0.504 |
| 30.00 | 545.536 | 204.497 | -0.120 | 25.935 | 25.935 | -0.054 | 57.301 | 48.008 | 40.399 | 0.508 |
| 50.00 | 558.048 | 204.508 | 1.090 | 26.337 | 26.333 | 0.501 | 58.463 | 50.344 | 42.908 | 0.516 |
| 70.00 | 593.404 | 204.532 | 1.910 | 27.736 | 27.721 | 0.924 | 58.676 | 53.321 | 45.549 | 0.543 |
| 80.00 | 599.742 | 204.560 | 3.500 | 27.944 | 27.892 | 1.706 | 58.934 | 54.052 | 46.300 | 0.546 |
| 90.00 | 567.253 | 204.634 | 3.540 | 26.784 | 26.733 | 1.654 | 60.825 | 54.841 | 47.884 | 0.523 |
| 95.00 | 500.171 | 204.673 | 0.160 | 24.235 | 24.235 | 0.068 | 64.246 | 55.776 | 50.236 | 0.475 |

STATION 4 : ROTOR 2 EXIT / STATOR 2 INLET

| PHH | HT N*M/KG | HS N*M/KG | BETA Y DEG. | V M/S | VZ M/S | VY M/S | BETA R DEG. | VR M/S | VYR M/S | FC |
|---|---|---|---|---|---|---|---|---|---|---|
| 5.00 | 1140.473 | 623.468 | 43.770 | 32.152 | 23.218 | 22.242 | 31.582 | 27.254 | 14.273 | 0.455 |
| 10.00 | 1121.970 | 636.873 | 32.680 | 31.142 | 26.212 | 16.815 | 37.982 | 33.256 | 20.466 | 0.513 |
| 30.00 | 1133.469 | 654.658 | 30.620 | 30.943 | 26.629 | 15.761 | 42.714 | 36.242 | 24.584 | 0.521 |
| 50.00 | 1161.029 | 671.370 | 28.890 | 31.290 | 27.396 | 15.117 | 45.922 | 39.382 | 28.292 | 0.536 |
| 70.00 | 1192.709 | 686.542 | 27.340 | 31.815 | 28.261 | 14.612 | 48.427 | 42.590 | 31.862 | 0.553 |
| 80.00 | 1223.407 | 693.444 | 28.220 | 32.553 | 28.684 | 15.393 | 48.668 | 43.432 | 32.613 | 0.562 |
| 90.00 | 1182.564 | 700.667 | 30.260 | 31.042 | 26.813 | 15.643 | 51.654 | 43.218 | 33.895 | 0.525 |
| 95.00 | 1076.089 | 704.319 | 35.120 | 27.261 | 22.298 | 15.683 | 57.215 | 41.180 | 34.620 | 0.437 |

STATION 5 : STATOR 2 EXIT

| PHH | HT N*M/KG | HS N*M/KG | BETA Y DEG. | V M/S | VZ M/S | VY M/S | BETA R DEG. | VR M/S | VYR M/S | FC |
|---|---|---|---|---|---|---|---|---|---|---|
| 5.00 | 1050.475 | 759.868 | 0.750 | 23.949 | 23.947 | 0.313 | 56.516 | 43.405 | 36.201 | 0.469 |
| 10.00 | 1072.131 | 759.874 | -0.480 | 24.859 | 24.858 | -0.208 | 56.452 | 44.982 | 37.489 | 0.487 |
| 30.00 | 1081.867 | 759.893 | -0.810 | 25.232 | 25.230 | -0.357 | 58.206 | 47.887 | 40.702 | 0.494 |
| 50.00 | 1112.710 | 759.899 | 0.890 | 26.310 | 26.307 | 0.409 | 58.542 | 50.409 | 43.001 | 0.515 |
| 70.00 | 1148.731 | 759.923 | 2.300 | 27.692 | 27.670 | 1.111 | 58.618 | 53.135 | 45.362 | 0.542 |
| 80.00 | 1158.303 | 759.962 | 3.850 | 27.988 | 27.925 | 1.879 | 58.809 | 53.921 | 46.126 | 0.547 |
| 90.00 | 1125.946 | 760.048 | 2.780 | 26.939 | 26.908 | 1.307 | 60.843 | 55.229 | 48.231 | 0.527 |
| 95.00 | 1060.663 | 760.078 | -0.270 | 24.451 | 24.451 | -0.115 | 64.129 | 56.035 | 50.419 | 0.479 |

Table 11.5 Circumferential-mean incidence angles (deg.) for the different compressor builds ($\phi$ = 0.500).

BASELINE 1 BUILD

| PHH | STATION 1 (ROTOR 1) | STATION 2 (STATOR 1) | STATION 3 (ROTOR 2) | STATION 4 (STATOR 2) |
|---|---|---|---|---|
| 5.00 | 3.668 | 9.480 | 6.243 | 19.120 |
| 10.00 | 3.501 | 8.750 | 5.300 | 8.350 |
| 30.00 | 3.350 | 8.910 | 4.458 | 6.880 |
| 50.00 | 3.206 | 8.490 | 3.497 | 6.490 |
| 70.00 | 3.116 | 7.450 | 2.438 | 7.870 |
| 80.00 | 3.232 | 6.440 | 1.660 | 9.620 |
| 90.00 | 2.724 | 8.830 | 3.000 | 9.880 |
| 95.00 | 1.976 | 11.020 | 5.018 | 10.820 |

MODIFIED 1 BUILD

| PHH | STATION 1 (ROTOR 1) | STATION 2 (STATOR 1) | STATION 3 (ROTOR 2) | STATION 4 (STATOR 2) |
|---|---|---|---|---|
| 5.00 | 3.087 | 13.720 | 6.305 | 20.860 |
| 10.00 | 2.930 | 12.200 | 5.935 | 9.670 |
| 30.00 | 3.293 | 9.930 | 5.056 | 9.050 |
| 50.00 | 3.404 | 8.130 | 4.129 | 8.770 |
| 70.00 | 3.425 | 7.460 | 2.306 | 8.580 |
| 80.00 | 3.241 | 7.350 | 1.564 | 9.960 |
| 90.00 | 2.859 | 8.910 | 2.437 | 10.030 |
| 95.00 | 2.117 | 10.500 | 4.410 | 10.430 |

MODIFIED 2 BUILD

| PHH | STATION 1 (ROTOR 1) | STATION 2 (STATOR 1) | STATION 3 (ROTOR 2) | STATION 4 (STATOR 2) |
|---|---|---|---|---|
| 5.00 | 3.087 | 13.720 | 6.536 | 20.770 |
| 10.00 | 2.930 | 12.200 | 6.171 | 9.840 |
| 30.00 | 3.293 | 9.930 | 5.131 | 8.550 |
| 50.00 | 3.404 | 8.130 | 4.153 | 7.870 |
| 70.00 | 3.425 | 7.460 | 2.396 | 7.720 |
| 80.00 | 3.241 | 7.350 | 1.684 | 9.320 |
| 90.00 | 2.859 | 8.910 | 2.235 | 9.390 |
| 95.00 | 2.117 | 10.500 | 4.336 | 9.350 |

Table 11.6 Circumferential-mean deviation angles (deg.) for the different compressor builds ($\phi$ = 0.500).

BASELINE 1 BUILD

| PHH | STATION 2 (ROTOR 1) | STATION 3 (STATOR 1) | STATION 4 (ROTOR 2) | STATION 5 (STATOR 2) |
|---|---|---|---|---|
| 5.00 | 3.999 | 9.140 | 1.637 | 8.250 |
| 10.00 | 4.863 | 4.180 | 6.052 | 6.833 |
| 30.00 | 4.679 | 4.400 | 5.379 | 3.530 |
| 50.00 | 4.209 | 5.180 | 4.312 | 4.660 |
| 70.00 | 3.566 | 6.660 | 2.858 | 7.264 |
| 80.00 | 2.929 | 8.520 | 1.624 | 8.870 |
| 90.00 | 4.005 | 9.250 | 4.404 | 8.183 |
| 95.00 | 10.700 | 6.470 | 11.106 | 6.110 |

MODIFIED 1 BUILD

| PHH | STATION 2 (ROTOR 1) | STATION 3 (STATOR 1) | STATION 4 (ROTOR 2) | STATION 5 (STATOR 2) |
|---|---|---|---|---|
| 5.00 | 3.506 | 7.090 | 1.753 | 5.950 |
| 10.00 | 4.453 | 3.150 | 6.216 | 4.140 |
| 30.00 | 4.838 | 4.850 | 5.357 | 4.200 |
| 50.00 | 4.666 | 5.830 | 4.158 | 5.910 |
| 70.00 | 3.915 | 6.320 | 3.027 | 6.860 |
| 80.00 | 3.285 | 7.670 | 1.924 | 8.120 |
| 90.00 | 4.225 | 7.740 | 4.275 | 7.400 |
| 95.00 | 10.924 | 5.690 | 10.866 | 5.260 |

MODIFIED 2 BUILD

| PHH | STATION 2 (ROTOR 1) | STATION 3 (STATOR 1) | STATION 4 (ROTOR 2) | STATION 5 (STATOR 2) |
|---|---|---|---|---|
| 5.00 | 3.506 | 6.270 | 0.912 | 4.690 |
| 10.00 | 4.453 | 2.430 | 5.852 | 3.580 |
| 30.00 | 4.838 | 4.300 | 5.404 | 3.610 |
| 50.00 | 4.666 | 5.600 | 4.272 | 5.400 |
| 70.00 | 3.915 | 6.170 | 3.117 | 6.560 |
| 80.00 | 3.285 | 7.540 | 1.808 | 7.890 |
| 90.00 | 4.225 | 7.750 | 4.334 | 6.990 |
| 95.00 | 10.924 | 5.400 | 11.165 | 4.970 |

Table 11.7 Circumferential-mean performance parameters for the baseline 1 compressor build ($\phi$ = 0.500).

*** FIRST STAGE ***

| PHH | HEAD RISE COEFFICIENT ROTOR | HEAD RISE COEFFICIENT STAGE | LOSS COEFFICIENT ROTOR | LOSS COEFFICIENT STATOR | EFFICIENCY ROTOR | EFFICIENCY STAGE |
|---|---|---|---|---|---|---|
| 5.00 | 0.2286 | 0.1913 | 0.0398 | 0.1881 | 0.9367 | 0.7838 |
| 10.00 | 0.2247 | 0.2122 | 0.0295 | 0.0648 | 0.9503 | 0.8977 |
| 30.00 | 0.2280 | 0.2164 | 0.0376 | 0.0623 | 0.9317 | 0.8841 |
| 50.00 | 0.2345 | 0.2215 | 0.0322 | 0.0698 | 0.9364 | 0.8845 |
| 70.00 | 0.2436 | 0.2271 | 0.0200 | 0.0873 | 0.9567 | 0.8919 |
| 80.00 | 0.2525 | 0.2303 | 0.0198 | 0.1134 | 0.9560 | 0.8722 |
| 90.00 | 0.2479 | 0.2103 | 0.0938 | 0.2004 | 0.8111 | 0.6883 |
| 95.00 | 0.2103 | 0.1890 | 0.1843 | 0.1452 | 0.6445 | 0.5793 |
| MASS AVERAGED | 0.2357 | 0.2188 | 0.0447 | 0.0905 | 0.9125 | 0.8470 |

*** SECOND STAGE ***

| PHH | HEAD RISE COEFFICIENT ROTOR | HEAD RISE COEFFICIENT STAGE | LOSS COEFFICIENT ROTOR | LOSS COEFFICIENT STATOR | EFFICIENCY ROTOR | EFFICIENCY STAGE |
|---|---|---|---|---|---|---|
| 5.00 | 0.2412 | 0.1854 | 0.1240 | 0.2885 | 0.8506 | 0.6537 |
| 10.00 | 0.2157 | 0.1844 | 0.0706 | 0.1699 | 0.8834 | 0.7552 |
| 30.00 | 0.2192 | 0.1987 | 0.0491 | 0.1105 | 0.9084 | 0.8235 |
| 50.00 | 0.2236 | 0.2082 | 0.0359 | 0.0811 | 0.9258 | 0.8624 |
| 70.00 | 0.2297 | 0.2100 | 0.0383 | 0.1010 | 0.9171 | 0.8385 |
| 80.00 | 0.2372 | 0.2080 | 0.0405 | 0.1439 | 0.9134 | 0.8010 |
| 90.00 | 0.2412 | 0.2113 | 0.0544 | 0.1632 | 0.8875 | 0.7777 |
| 95.00 | 0.2265 | 0.2145 | 0.1494 | 0.0839 | 0.7204 | 0.6821 |
| MASS AVERAGED | 0.2258 | 0.2041 | 0.0505 | 0.1157 | 0.8998 | 0.8134 |

*** OVERALL ***

| PHH | HEAD RISE COEFFICIENT | EFFICIENCY |
|---|---|---|
| 5.00 | 0.3767 | 0.7139 |
| 10.00 | 0.3966 | 0.8253 |
| 30.00 | 0.4151 | 0.8540 |
| 50.00 | 0.4298 | 0.8736 |
| 70.00 | 0.4372 | 0.8654 |
| 80.00 | 0.4383 | 0.8369 |
| 90.00 | 0.4217 | 0.7303 |
| 95.00 | 0.4035 | 0.6298 |
| MASS AVERAGED | 0.4229 | 0.8304 |

Table 11.8 Circumferential-mean performance parameters for the baseline 2 compressor build ($\phi$ = 0.500).

*** FIRST STAGE ***

| PHH | HEAD RISE ---COEFFICIENT---- ROTOR | STAGE | LOSS ---COEFFICIENT---- ROTOR | STATOR | ----EFFICIENCY---- ROTOR | STAGE |
|---|---|---|---|---|---|---|
| 5.00 | 0.2286 | 0.1887 | 0.0398 | 0.2010 | 0.9367 | 0.7733 |
| 10.00 | 0.2247 | 0.2099 | 0.0295 | 0.0768 | 0.9503 | 0.8878 |
| 30.00 | 0.2280 | 0.2158 | 0.0376 | 0.0654 | 0.9317 | 0.8818 |
| 50.00 | 0.2345 | 0.2205 | 0.0322 | 0.0755 | 0.9364 | 0.8803 |
| 70.00 | 0.2436 | 0.2277 | 0.0200 | 0.0843 | 0.9567 | 0.8941 |
| 80.00 | 0.2525 | 0.2285 | 0.0198 | 0.1226 | 0.9560 | 0.8653 |
| 90.00 | 0.2479 | 0.2133 | 0.0938 | 0.1847 | 0.8111 | 0.6979 |
| 95.00 | 0.2103 | 0.1935 | 0.1843 | 0.1145 | 0.6445 | 0.5931 |
| MASS AVERAGED | | | | | | |
| | 0.2357 | 0.2185 | 0.0447 | 0.0920 | 0.9125 | 0.8459 |

*** SECOND STAGE ***

| PHH | HEAD RISE ---COEFFICIENT---- ROTOR | STAGE | LOSS ---COEFFICIENT---- ROTOR | STATOR | ----EFFICIENCY---- ROTOR | STAGE |
|---|---|---|---|---|---|---|
| 5.00 | 0.2465 | 0.2041 | 0.1172 | 0.2158 | 0.8612 | 0.7130 |
| 10.00 | 0.2199 | 0.1957 | 0.0638 | 0.1300 | 0.8959 | 0.7972 |
| 30.00 | 0.2207 | 0.1992 | 0.0472 | 0.1155 | 0.9122 | 0.8232 |
| 50.00 | 0.2254 | 0.2091 | 0.0334 | 0.0856 | 0.9313 | 0.8642 |
| 70.00 | 0.2297 | 0.2109 | 0.0389 | 0.0961 | 0.9158 | 0.8409 |
| 80.00 | 0.2391 | 0.2092 | 0.0378 | 0.1475 | 0.9196 | 0.8045 |
| 90.00 | 0.2431 | 0.2113 | 0.0572 | 0.1693 | 0.8827 | 0.7673 |
| 95.00 | 0.2235 | 0.2112 | 0.1559 | 0.0846 | 0.7073 | 0.6686 |
| MASS AVERAGED | | | | | | |
| | 0.2273 | 0.2060 | 0.0492 | 0.1132 | 0.9026 | 0.8178 |

*** OVERALL ***

| PHH | HEAD RISE COEFFICIENT | EFFICIENCY |
|---|---|---|
| 5.00 | 0.3929 | 0.7408 |
| 10.00 | 0.4056 | 0.8417 |
| 30.00 | 0.4150 | 0.8527 |
| 50.00 | 0.4296 | 0.8724 |
| 70.00 | 0.4386 | 0.8677 |
| 80.00 | 0.4377 | 0.8352 |
| 90.00 | 0.4246 | 0.7308 |
| 95.00 | 0.4048 | 0.6302 |
| MASS AVERAGED | | |
| 0.0 | 0.4245 | 0.8320 |

Table 11.9 Circumferential-mean performance parameters for the modified 1 compressor build ($\phi$ = 0.500).

*** FIRST STAGE ***

| PHH | HEAD RISE ---COEFFICIENT---- ROTOR | STAGE | LOSS ---COEFFICIENT---- ROTOR | STATOR | ----EFFICIENCY---- ROTOR | STAGE |
|---|---|---|---|---|---|---|
| 5.00 | 0.2267 | 0.1930 | 0.0503 | 0.1717 | 0.9232 | 0.7861 |
| 10.00 | 0.2242 | 0.2066 | 0.0281 | 0.0925 | 0.9540 | 0.8789 |
| 30.00 | 0.2280 | 0.2087 | 0.0312 | 0.1040 | 0.9431 | 0.8634 |
| 50.00 | 0.2334 | 0.2136 | 0.0247 | 0.1078 | 0.9500 | 0.8693 |
| 70.00 | 0.2423 | 0.2281 | 0.0239 | 0.0759 | 0.9479 | 0.8923 |
| 80.00 | 0.2500 | 0.2314 | 0.0146 | 0.0972 | 0.9671 | 0.8949 |
| 90.00 | 0.2473 | 0.2164 | 0.0854 | 0.1658 | 0.8242 | 0.7214 |
| 95.00 | 0.2093 | 0.1939 | 0.1756 | 0.1064 | 0.6540 | 0.6059 |
| MASS AVERAGED | | | | | | |
| | 0.2349 | 0.2158 | 0.0403 | 0.1031 | 0.9202 | 0.8455 |

*** SECOND STAGE ***

| PHH | HEAD RISE ---COEFFICIENT---- ROTOR | STAGE | LOSS ---COEFFICIENT---- ROTOR | STATOR | ----EFFICIENCY---- ROTOR | STAGE |
|---|---|---|---|---|---|---|
| 5.00 | 0.2391 | 0.1947 | 0.1426 | 0.2304 | 0.8272 | 0.6734 |
| 10.00 | 0.2209 | 0.2022 | 0.0569 | 0.1017 | 0.9068 | 0.8301 |
| 30.00 | 0.2247 | 0.2064 | 0.0442 | 0.0996 | 0.9208 | 0.8461 |
| 50.00 | 0.2302 | 0.2129 | 0.0373 | 0.0927 | 0.9273 | 0.8574 |
| 70.00 | 0.2282 | 0.2127 | 0.0394 | 0.0805 | 0.9141 | 0.8517 |
| 80.00 | 0.2356 | 0.2126 | 0.0347 | 0.1143 | 0.9237 | 0.8337 |
| 90.00 | 0.2377 | 0.2151 | 0.0591 | 0.1227 | 0.8751 | 0.7917 |
| 95.00 | 0.2243 | 0.2153 | 0.1439 | 0.0623 | 0.7245 | 0.6953 |
| MASS AVERAGED | | | | | | |
| | 0.2282 | 0.2106 | 0.0480 | 0.0949 | 0.9058 | 0.8356 |

*** OVERALL ***

| PHH | HEAD RISE COEFFICIENT | EFFICIENCY |
|---|---|---|
| 5.00 | 0.3877 | 0.7252 |
| 10.00 | 0.4088 | 0.8541 |
| 30.00 | 0.4152 | 0.8547 |
| 50.00 | 0.4265 | 0.8633 |
| 70.00 | 0.4407 | 0.8722 |
| 80.00 | 0.4440 | 0.8645 |
| 90.00 | 0.4315 | 0.7548 |
| 95.00 | 0.4092 | 0.6499 |
| MASS AVERAGED | | |
| 0.0 | 0.4264 | 0.8406 |

Table 11.10 Circumferential-mean performance parameters for the modified 2 compressor build ($\phi = 0.500$).

*** FIRST STAGE ***

| | HEAD RISE ---COEFFICIENT---- | | LOSS ---COEFFICIENT---- | | ----EFFICIENCY---- | |
|---|---|---|---|---|---|---|
| PHH | ROTOR | STAGE | ROTOR | STATOR | ROTOR | STAGE |
| 5.00 | 0.2267 | 0.1931 | 0.0503 | 0.1713 | 0.9232 | 0.7864 |
| 10.00 | 0.2242 | 0.2065 | 0.0281 | 0.0927 | 0.9540 | 0.8787 |
| 30.00 | 0.2280 | 0.2095 | 0.0312 | 0.0998 | 0.9431 | 0.8666 |
| 50.00 | 0.2334 | 0.2140 | 0.0247 | 0.1059 | 0.9500 | 0.8707 |
| 70.00 | 0.2423 | 0.2275 | 0.0239 | 0.0788 | 0.9479 | 0.8902 |
| 80.00 | 0.2500 | 0.2302 | 0.0146 | 0.1031 | 0.9671 | 0.8905 |
| 90.00 | 0.2473 | 0.2185 | 0.0854 | 0.1546 | 0.8242 | 0.7283 |
| 95.00 | 0.2093 | 0.1951 | 0.1756 | 0.0982 | 0.6540 | 0.6097 |
| MASS AVERAGED | | | | | | |
| | 0.2349 | 0.2161 | 0.0403 | 0.1016 | 0.9202 | 0.8466 |

*** SECOND STAGE ***

| | HEAD RISE ---COEFFICIENT---- | | LOSS ---COEFFICIENT---- | | ----EFFICIENCY---- | |
|---|---|---|---|---|---|---|
| PHH | ROTOR | STAGE | ROTOR | STATOR | ROTOR | STAGE |
| 5.00 | 0.2449 | 0.2104 | 0.1483 | 0.1741 | 0.8230 | 0.7070 |
| 10.00 | 0.2240 | 0.2049 | 0.0664 | 0.1028 | 0.8931 | 0.8170 |
| 30.00 | 0.2254 | 0.2056 | 0.0435 | 0.1078 | 0.9214 | 0.8406 |
| 50.00 | 0.2312 | 0.2127 | 0.0248 | 0.0987 | 0.9504 | 0.8742 |
| 70.00 | 0.2298 | 0.2129 | 0.0259 | 0.0869 | 0.9422 | 0.8730 |
| 80.00 | 0.2391 | 0.2142 | 0.0229 | 0.1229 | 0.9492 | 0.8501 |
| 90.00 | 0.2359 | 0.2142 | 0.0517 | 0.1175 | 0.8879 | 0.8062 |
| 95.00 | 0.2208 | 0.2149 | 0.1347 | 0.0415 | 0.7332 | 0.7135 |
| MASS AVERAGED | | | | | | |
| | 0.2294 | 0.2107 | 0.0408 | 0.1000 | 0.9188 | 0.8439 |

*** OVERALL ***

| PHH | HEAD RISE COEFFICIENT | EFFICIENCY |
|---|---|---|
| 5.00 | 0.4035 | 0.7429 |
| 10.00 | 0.4114 | 0.8468 |
| 30.00 | 0.4151 | 0.8535 |
| 50.00 | 0.4266 | 0.8725 |
| 70.00 | 0.4405 | 0.8818 |
| 80.00 | 0.4444 | 0.8706 |
| 90.00 | 0.4327 | 0.7649 |
| 95.00 | 0.4100 | 0.6600 |
| MASS AVERAGED | | |
| 0.0 | 0.4268 | 0.8452 |

END

FILMED

DTIC